DYNAMIC STRATIGRAPHY

OF THE

TAHARA FORMATION, HAMADA BASIN,

WESTERN LIBYA

By

ISSAM ABDUL-HAMED AMSAAD HASSI

A thesis submitted in the fulfilment of the degree of Master of Science (by research) in the Faculty of Science

Department of Geology and Applied Geology
University of Glasgow

DEPARTMENT OF GEOLOGY AND APPLIED GEOLOGY
University of Glasgow
Scotland
September, 1993

ProQuest Number: 13815526

All rights reserved

INFORMATION TO ALL USERS
The quality of this reproduction is dependent upon the quality of the copy submitted.

In the unlikely event that the author did not send a complete manuscript
and there are missing pages, these will be noted. Also, if material had to be removed,
a note will indicate the deletion.

ProQuest 13815526

Published by ProQuest LLC (2018). Copyright of the Dissertation is held by the Author.

All rights reserved.
This work is protected against unauthorized copying under Title 17, United States Code
Microform Edition © ProQuest LLC.

ProQuest LLC.
789 East Eisenhower Parkway
P.O. Box 1346
Ann Arbor, MI 48106 – 1346

ACKNOWLEDGEMENTS

First and foremost I would like to thank Allah for providing me with this opportunity and for guiding me through all the problems and difficulties that I've met during the completion of this research work.

I would like to sincerely thank my supervisor Professor Brian J. Bluck who was a constant source of guidance and encouragement over the years of my study in the University of Glasgow.

Among the many staff members that discussed problems with me or guided me through their field of knowledge, I want to particularly thank Dr. C. Braithwite, Dr. A. Owen, Dr. C. Burton, Dr. M. Keen Dr. A. Hall, and Professor M. Russell

I would also like to express my thanks to Mr. R. Morrison, chief Technician, Mr. D. McLean for photography Mr. M. MacLeod for XRD analysis, Mrs. S. Hall for tracing and the technical staff of the department of Geology and Applied Geology

I am also grateful to the technical staff in the laboratory of the Arabian Gulf Oil Company for their help with the core material.

I gratefully acknowledge the management of the Arabian Gulf Oil Company, particularly the Exploration Department, who sponsored this research project.

Finally I wish to sincerely thank my parents, my wife, my children, and all my family for the help, support and encouragement they have given me.

ABSTRACT

The Hamada basin is little known with respect to tectonic evolution, depositional history, facies relationships and reservoir characteristics. The descriptive stratigraphy of the Hamada basin is however, mostly well established but the dynamic processes that control such intracratonic seas are far from being understood. Thus the scope of this study was to focus on a process oriented stratigraphy; an approach summarized by Matthews (1974, 1984) as Dynamic Stratigraphy, in order to reconstruct the dynamics of one of the several stratigraphic accumulations in the Hamada basin (The Tahara Formation). The sequence stratigraphic approach to dynamic stratigraphy, however, depends on the recognition of a hierarchy of stratal units including: lamina, lamina sets, beds, bedsets, parasequences, parasequence sets and sequences, bounded by chronostratigraphically significant surfaces of erosion, non deposition, or their correlative surfaces.

At the lowest level in the above hierarchy individual strata are analyzed as the smallest depositional units and as the basic building elements of sequence stratigraphy. Associations of stratal types are grouped into facies. Nine facies are classified, described and interpreted. Stratification and lithotypes, bio and ichnofabrics allow the reconstruction of depositional dynamics (eg. erosional / depositional processes, mode of transport, substrate changes, and colonisation patterns) over short time spans. Each facies is then given an environmental interpretation partly based on a general understanding of the sequence.

At an intermediate level (parasequences), vertical and lateral changes of facies over longer time spans are analysed. Such sequential analysis sheds light on parasequence dynamics (eg. progradation, retrogradation). For instance, it was found that the Tahara Formation consists of 16 siliciclastic shallowing upward parasequences stacked in a parasequence set. Each parasequence consists of an upward – shoaling

association of facies suggesting deposition in progressively shallower waters. Each parasequence is marked by an upward increase in grain size, bed thickness, and percentage of sand, and a decrease in bioturbation. This vertical pattern of upward coarsening and thickening suggests parasequence progradation (Van Wagoner, 1990).

At a higher level (parasequence set) the vertical stacking pattern of parasequences is analysed over still longer time spans. This stratal hierarchy sheds light on parasequence set dynamics (eg. Progradational, aggradational & retrogradational parasequence sets). It was found that younger parasequences tend to be thicker, more sandy and less bioturbated, consisting of a higher percentage of shallow marine facies than older parasequnces in the set. In addition younger parasequences were found to step farther into the basin suggesting a progradational parasequence set (Van Wagoner, 1990).

At still higher levels (sequences) the sequential and geometrical arrangement and packaging of parasquence sets within the whole depositional basin is analysed over still longer time spans. The hierarchy of these cycles and their regional distribution patterns give insights to the basin dynamics.

However, only the first three of the above four levels are of our concern, sinse the fourth level exceeds the limits of our formation boundary (parasequence set boundary) and is beyond the scope of the present study. The Tahara Formation is, however, interpreted as a silisiclastic shelf–shoreface sequence deposited in a storm dominated regime.

The stratigraphic sequence of the Tahara Formation was also analysed using the technique of the Markov chain. End results were similar to those obtained by the sequence stratigraphic technique.

DEDICATION

This thesis is dedicated to my parents
my wife, my son Hamed and
To my daughter Arwa

TABLE OF CONTENTS

TABLE OF CONTENTS

CHAPTER THREE: SEQUENCE STRATIGRAPIC ANALYSIS STATISTICAL TECHNIQUE

CHAPTER FOUR:

LIST OF FIGURES

Page

LIST OF TABLES

LIST OF PLATES

Page

LIST OF ENCLOSURES

CHAPTER 1

CHAPTER 1

INTRODUCTION

1.1 Definition:

The Tahara formation is believed to represent the basal transgressive unit of the last Paleozoic sedimentary cycle deposited in the Hamada basin. It is a predominantly sandy Formation known from bore-holes in the subsurface of the Hamada basin and from outcrops in the Fazzan region along the jabal Fazzan (Al-Qarqaf uplift) where the main Paleozoic formations are exposed.

The term Tahara Formation was first introduced as "Gres de Tahara" by Burollet *et al.*, (1967) and as the Tahara formation by Massa et al., (1974). It is defined in the CPT(L) well B1-49, located in wadi Tahara south of concession NC-7A from which it derives it's name. Massa *et al.*, (1976) gave the principle characteristics as follows: the facies is sandy-shaly; the sands are generally fine to very fine grained with feldspars and frequent ferruginous and hematitic levels.

In the north El-Gullebi area (study area) the Tahara is described (North El-Gullebi Project, internal company report) as a predominantly sandy formation:

- sands, light grey, white green, very fine grained, argillaceous, with some dolomitic cement, micaceous
- shale interbeds: dark grey-black, brownish or dark green, micaceous, platy, fissile
- siltstones and silty shales

- bioturbated layers with common worm burrows filled with very fine grained sandstones together with thin beds of pelleted dolomite
- ferruginous oolitic sandstone: grey or light brown to black, fine grained, well sorted with a dolomitic matrix
- hematitic oolitic sandstone: dark brick red, fine grained, well sorted, well cemented with dolomite.

Unfortunately this report give no indication of either proportions of lithofacies or of the general succession.

Based on palynological evidence Bellini *et al.*, (1980) suggested a basal Carboniferous Upper Devonian (Strunian) age for the Tahara Formation. According to Harland *et al.*, (1990), however, the problem of the Devonian–Carboniferous boundary is yet to be resolved. The argument is about where the boundary is to be placed with respect to the macrofossil and microfossil zones. It is likely to be placed close to the base of the Gattendorfia Goniatite zone. With respect to this zone the Strunian lies at the top of the Devonian (Tn1a) and, depending upon the ICS (International Commission of Stratigraphy) decision may be divided between the Famenian and Tournaisian. The Tahara Formation contains fossils, *Spelaeotriletes* and *Vallatisporites* (Bellini *et al.*, 1980) which cross the Devonian–Carboniferous boundary as defined for the Courceyan by George et al., (1976), and this suggests that the Tahara Formation it-self crosses the Devonian-Carboniferous boundary. The ICS decision seems likely to place the boundary within the Tahara Formation. Thus placing the formation totally in the Devonian or Carboniferous is unlikely to be correct. The Formation is conformably overlain by the transgressive Carboniferous Marrar Formation (middle Tournaisian–upper Visean)

and conformably overlies the Aouient Ouenine Formation (Couvinian–Famenian). A regional study of the Hamada Basin (internal company study) suggested an unconformity (Acedian) at the base of the Tahara Formation (Pers. comm.).

The regionally uniform thickness of the Tahara Formation (50–70m) (Bellini *et al.*, 1980) leads one to envisage a basin with little differential subsidence during the deposition of the Tahara Formation (Beicip, 1973, internal company report). The local trends of thickness are irregular and show no preferred orientation (Beicip, 1973, internal company report)). The average thickness of the Tahara at El–Gullebi area is about 47m. There is a higher percentages of sand in the south and southeastern parts of the basin (Beicip, 1973, internal company report), suggesting a source in that direction.

The Tahara depositional environment has been described as a low energy deltaic complex transgressed by the Marrar sea (Bellini *et al.*, 1980). The same environment is described in the north of the El-Gullebi area (North El-Gullebi Project, internal company report).

In some parts of the Hamada Basin the sandstones of the Tahara Formation are productive. Elsewhere, in spite of a good section and adequate structure, (and even high porosity) they are dry. However, from the experience obtained within the basin oil production is not confined to one particular sandstone facies. Production can be from different sandstone units at different depths in different localities. Hence, understanding the geometry, orientation and genetic origin of the sandstone bodies is of primary importance.

1. 2 Geographic and Tectonic Location:

Libya covers an area of about 1,757,000 km^2 extending 1925km in an east-west direction along the northern coast of Africa, and about 1450km. north-south to the borders with Chad and Niger. Tectonically Libya is divided into four large basins separated by intervening uplift arches (Fig. 1.1).

The Hamada basin (also known as the Rhadames, Ghadames and al-Hamara basin) is an intracratonic basin of Paleozoic to Mesozoic age located in the central part of western Libya (Fig. 1.1). It covers an area of about 330,000 km^2. It is deepest along the Tunisian border north of Gadamis. The basin extends westward into Algeria and forms one of the largest basement depressions in Africa. On the northern edge, the basin is bounded by the Gharyan Yifran uplift (also known as Nafusa uplift), and to the south by the Qarqaf uplift. In the east the basin is abruptly cut by the SSE-NNW trending Hon graben, related to the Sirte basin. To the west the Edjeleh uplift separates the western part of the Hamada basin from the Algerian part known as the Illizi basin.

The area studied shown in (Fig. 1.1), is named El-Gullebi, and is located in the south central part of the Hamada basin in concession NC–7A. It encompasses the only structural element in the area, known as the El-Gullebi structure, which trends NE-SW and has a length of 60km and a width of about 5km. In terms of latitudes and longitudes, the area is located between latitudes 29°30' and 30°00'N and between longitudes 11°30' and 12°00'E.

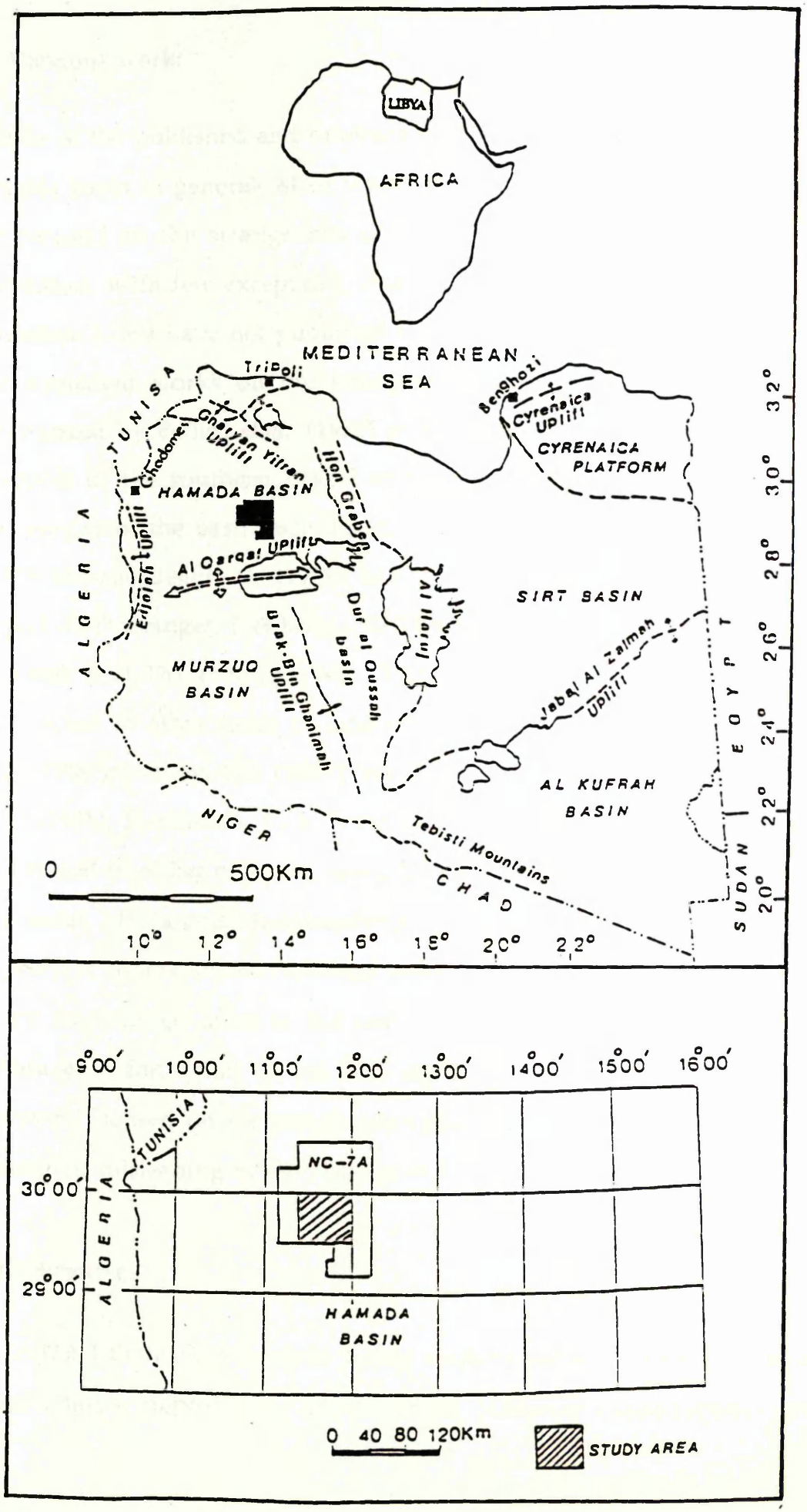

Fig. 1.1 Geographic and tectonic map of libya showing the studied area in the Hamada basin.

1.3 Previous work:

In spite of the published and unpublished data still little is known of the Hamada basin in general. Most work was carried out by oil companies, and focused on the stratigraphy of the basin which by now is solidly established. With few exceptions, most of the oil companies that worked in western Libya have not published the results obtained by drilling. The few published works on the stratigraphy of the basin are, however, summarized by Bellini *et al.*, (1980) in a stratigraphic contribution to the Paleozoic of the southern basins of Libya. Recent contributions to the stratigraphy of the basin includes the work of Loboziak, S. & Streel, M. (1989); Moreau-Benoit, A. (1988); Moreau-Benoit, A. & Massa, D. (1988); Coquel, R; Doubinger, J. & Massa, D. (1988); Buret, MB. & Moreau-Benoit, A. (1986); Said, FM. & Kanes, WH. (1985); Bless, MJM. & Massa, D. (1982). Other work in other fields of interest includes that of Salaj, J. & Nairn, AEM. (1987); Walley, CD. (1985); Whitbread, T. & Kelling, G. (1982); Vos, R. G. (1981); Hammuda, O. S. (1980). The Tahara Formation is even less understood in either company work or among the geological community in general. Massa and Moreaeu-Benoit (1976) described the formation in the general context of the Devonian stratigraphy of Libya, and to the best of my knowledge there is not one publication which deals with the Tahara as a formation on its own right. Internal company work has, however, focused on the petroleum aspects of the formation which are sometimes misleading in the absence of true sedimentological data.

1. 4 Objective:

Since the Tahara Formation is poorly understood with respect to facies relationships, depositional environment, reservoir characteristics and

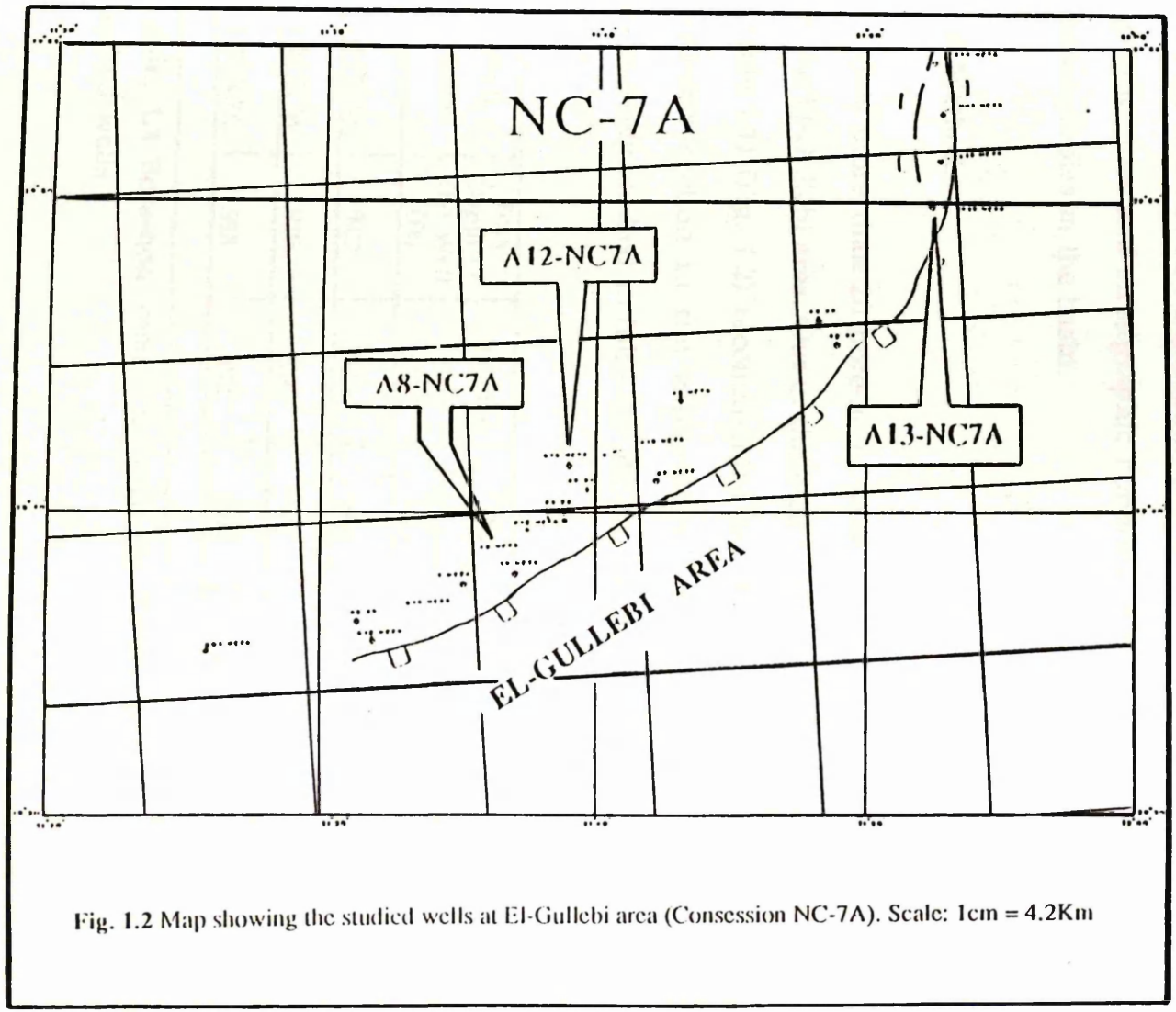

Fig. 1.2 Map showing the studied wells at El-Gullebi area (Consession NC-7A). Scale: 1cm = 4.2Km

tectonic history it merited closer study. The objective of this study is to construct a depositional model for the Tahara Formation which will serve as a key to understanding this formation; as a dynamic explanation for vertical and lateral changes in modes of deposition; as a predictive tool for hydrocarbon exploration that may guide exploratory activities to specific areas and stratigraphic horizons and finally as a framework for future studies in the basin.

1.5 Method:

To date more than 20 bore-holes have penetrated the Tahara formation in the El-Gullebi area. Out of these 20 cored bore-holes three were chosen (Table 1.1) (Fig. 1.2) recommended by Mr. S. Bushaala the head of the well-site section in the exploration department in (AGOCO) to be extensively studied to fulfil the above objective.

Well Name	Total Depth of The Well (ft)	Formation Top (ft)	Total Formation Thickness (ft)	Thickness of Cored Section (ft)	Thickness of Cored Section (m)	STATUS
A8-NC7A	5900	5679	169.9	150	45.7	OIL WELL
A12-NC7A	5905	5730	146	150	45.7	DRY WELL
A13-NC7A	6601	5622	109.9	96.7	29.5	GAS WELL

Table. 1.1 Bore-hole record through the Tahara formation in the three studied wells

Well A8-NC7A is chosen as the type well based on core coverage and a visual inspection of sand/shale ratios. The main source of data are detailed core description; representative slabbed core samples; a set of

photographs showing the complete cored interval in the three studied wells; core chips from which more than 100 thin sections are made, and a rock colour chart (The rock colour chart committee: The Geological Society of America, Boulder, Colorado, 1975). Selected samples of shales and certain mudrocks are analysed with the SEM and XRD for composition and mineral identification. The different modes of investigation are summarised as follow:

(1) Sequence stratigraphic technique for sequence analysis:

(a) Facies analysis (classification; description and interpretation of the rock under study).

(b) The identification of time significant stratal hierarchies (lamina; bed; bedset; parasequence and parasequence set) based on physical relationships of strata which include lateral continuity of the bounding surfaces and strata within these surfaces and vertical stacking patterns (Van Wagoner 1990). In addition, facies interpretations of strata on either sides of bounding surfaces are important particularly in parasequence and parasequence set identification (Van Wagoner 1990).

(c) Interpretation of facies associations (vertical facies analysis) on either side of these physical boundaries.

(d) Correlation of time and facies using these physical boundaries resulting in a high resolution litho-chronostratigraphical framework.

(2) For the statistical treatment work was carried out on thin-sections and photographs of known scale to determine vertical changes in the following parameters:

(a) Grain size (mm)

(c) Thickness of sandstone units (cm)

(d) Percentage of sand per meter of core

(e) Percentage of bioturbation per meter of core

(3) Markov chain technique for sequence analysis (explained in detail the relevant chapter)

1.6 Stratigraphy and Tectonic framework of Libya:

1.6.1 General: Libya is located on the Mediterranean foreland of the African shield. It comprises a platform with a number of cratonic basins. Several periods of earth movement affected the foreland and formed the present major structural and tectonic features (see Fig. 1.1). The major diastrophic disturbances include the Caledonian and Hercynian orogenies as well as disturbances during Late Cretaceous, Middle Tertiary (Oligocene through Miocene) and Holocene times (Conant et al., 1967). These events caused uplifts, subsidence, tilting, block faulting and differential depression of the Libyan part of the African foreland and resulted in repeated transgressions of the Tethyan sea. The effect of these diastrophic events were generally large scale, and extensional rather than compressional. East-west and North-south-trending faults are present but the major fault systems trend parallel to the Red Sea and other African rifts.

Libya has been a site of deposition since early Paleozoic times. Cambrian and Ordovician rocks are exposed at many places in southern Libya along the uplifted flanks of the Murzuq and Al-Kufrah basins and consist of a thick succession (600-900m) of mainly continental clastics. During the

middle Ordovician a minor marine transgression disturbed the continental conditions in western Libya crossing the southern border into Chad and depositing a thin unit of fine marine clastics. A major transgression of the sea took place during the Silurian, this time reaching the Chad and Niger Republics and depositing about 300m of Silurian graptolitic shale (exposed on the flanks of the Murzuq basin). Devonian, rocks, exposed in southeastern Libya, are chiefly continental sandstones as thick as 300m, though some marine beds are present on the eastern and western flanks of the Murzuq basin. As a result of the Hercynian (Variscan) tectonism a general regression took place over most of Libya during the Late Devonian and Early Carboniferous. In Permian and Triassic times most of the country was exposed and undergoing erosion, and only the Hamada basin and northern Cyrenaica were covered by the sea. The Jurassic sea extended further to the south over the Hamada basin and Cyrenaica where shallow marine sediments unconformably overlayie Paleozoic rocks. During the Lower Cretaceous the sea retreated from northwestern Libya, resulting in predominantly continental deposition in the Hamada basin, while Cyrenaica was still covered by a shallow sea. In the Upper Cretaceous (Cenomanian) the paleo-Sirte arch collapsed, resulting in the opening of the Sirte basin and the invasion of the sea over almost all the northern half of the country. As a result, a thick sequence of deep marine shales was deposited in the trough areas whilst shallow marine carbonates were deposited on the highs. Rocks of Tertiary age, chiefly carbonates, are widespread in northern Libya and in the northeast they form long high escarpments. In the Gulf of Sirte nearly 3000m of Oligocene to Miocene clastic sedimentary rocks is known to have been deposited along the axis of a deep trough. Laterally these clastics thin over the highs where they are replaced by carbonates and

evaporites. Abundant lava flows cover large areas of central and western parts of Libya as a result of extensive volcanic activity during Oligocene times. Quaternary deposits of northern Libya are principally continental deposits. Nearly one-fourth of the country is covered by Quaternary deposits.

1.6.2 Hamada Basin: The Hamada intracratonic basin of western Libya is an extension of the Saharan basin which stretches from Algeria eastward into Tunisia and Libya, covering an area of more than 3 million square kilometres. The tectonics and sedimentology of the region have been greatly influenced by the Caledonian and Hercynian orogenies. Northwest- and northeast-trending faults are characteristic of the broad shallow basin (Kirmani, K. U, 1988). The western (Edjeleh uplift) and southern (Al-Qarqaf uplift) parts of the Hamada basin were uplifted during the Caledonian orogeny (Goudarzi, 1980). The northern part of the basin was uplifted during Hercynian folding (Burollet, 1963b) but subsided again during the Early Mesozoic. It was uplifted once more near the end of the Cretaceous with uplift accompanied by NW trending faults. The old highs, in the south and north were reactivated during Late Cretaceous or Early Paleocene times (Goudarzi, 1980).

The Hamada basin is mainly a Paleozoic basin in which was deposited a thick succession of predominantly terrigeneous clastics ranging in age from Cambrian to Paleocene (Conant et al., 1967) (see enclosure I). The Cambrian Ordovician rocks are of fluvial to shallow marine origin. The Silurian constitutes a complete sedimentary cycle, ranging from deep marine shales to shallow marine and deltaic deposits. The Devonian occupies a unique position between two major orogenies. The

Carboniferous represents the last Paleozoic marine cycle and has a maximum thickness of 1300m. The Mesozoic strata are relatively thin: the Triassic consists of well developed continental sandstones, whereas the Jurassic and Cretaceous rocks are mainly lagoonal dolomites, evaporites and shales. A thin cover of Paleocene sediments is spread all over the Hamada basin (Beicip, 1973, internal company report).

The primary hydrocarbon source rocks for the Hamada basin are the Silurian shales and the deeper parts of the basin have shown a better source quality than the margins. Paleozoic rocks have the best hydrocarbon potential, with oil and gas being found in sandstones of Ordovician, Silurian, Devonian and Carboniferous. Hydrocarbons have also been encountered in Triassic rocks. The best known field is El-Hamra with estimated reserves of 155 million bbl, producing from the Devonian. Most of the producing structures in the basin are believed to be anticlines although several unconformities within the section probably influenced the hydrocarbon accumulation (Conant et al., 1967).

1. 7 Paleozoic Stratigraphy of The Hamada Basin:

1 - Mouizidie Formation (Cambrian):

Burollet et al., (1963b) proposed the name Mouizidie Formation for a sequence of red and violet sandstones, quartzitic arkoses and quartzites lying unconformably on the folded metamorphic Precambrian (Pharusian) basement on the south-eastern flanks of the Murzuq basin. The deepest wells in the Hamada basin have penetrated a formation with

lithological characteristics and stratigraphic position which compare with the Mouizidie Formation. This formation is conformably overlain by the unfossiliferous Hassaouna formation.

2 - *Hassaouna Formation (Cambrian):*

The term Hassaouna Formation was introduced by Massa et al., (1960) after Jabal Hassaouna, which is a local name for Jabal Qarqaf (the southern boundary of the Hamada basin) where the type section is located. It consists of 340m of brown to yellowish brown, massive, medium- to coarse-grained highly cross-bedded, predominantly continental, sandstone. This contains *Tigillites* in the upper few meters. The Hassouna represents sedimentation of an extensive sand blanket spread over the entire Saharan basin, with consistent paleocurrent patterns towards the north and north east. It is deltaic or perhaps fluvial in nature (Burollet et al., 1969). Although a producer in Algeria reservoir characteristics are poor in the Hamada Basin. The Hassaouna Formation is conformably overlain by the Haouaz Formation

3 - *Haouaz Formation: Ordovician (Ll anvirnian-Llandeilian):*

The term Haouaz Formation was introduced by Massa et al., (1960) after Jabal Haouaz in the western part of Jabal Gragaf (Al-Qarqaf uplift) on the south-western edge of the Hamada basin. The formation consists of thin to thick fine grained, slightly cross-bedded quartz sandstones with many *Tigillites* beds and abundant ripple marks. The Formation is about 280m thick in the area of Qarqaf. The Haouaz Formation was deposited in a shallow marine low energy environment. Reservoir characteristics are poor except for the coarse grained portion of the formation (Beicip 1973,

internal company report)) It is conformably overlain by the Melez Chograne Formation

4 - Melez Chograne Formation: Ordovician (Caradocian):

The term Melez Chograne Formation was introduced by Massa et al., (1960) after the Melez Chograne Mountain in the western part of Jabal Qarqaf (Qarqaf uplift) on the south-western edge of the Hamada basin. In the type section The Melez Chograne is a 10-60m thick sequence of argillaceous varicoloured green and purple, chloritic, thin bedded shale intercalated with angular and sub-angular fine grained micaceous sandstone and siltstone. Big blocks of granite gneiss, quartz, polished and striated pebbles showing glaciation and iceberg transportation are included in this formation.The upper boundary is erosive and discordant with the upper Ordovician Memouniat Formation. The formation is deposited in a marine environment somewhat restricted at times (Beicip, 1973, internal company report). Reservoir quality is still poor but show some porosity (Beicip, 1973, internal company report).

5 - Memouniat Formation: Ordovician (Caradocian):

The term Memouniat Formation was introduced by Massa et al., (1960) after Jabal al Memouniat in the south western part of the Hamada basin (Jabal Qarqaf in the Fazzan region). It consists of a 100-140m thick sequence mainly of sandstones. These are massive, cross-bedded medium-coarse grained, and partly conglomeratic. A preglacial facies is indicated on ecological grounds (Havlicek et al., 1973). The beds are usually unfossiliferous but sometimes contain *Tigillites* and badly preserved Brachiopod and bivalve shells. The upper boundary is

unconformable with the Silurian Tanezzuft Formation (Tanezzuft shale). The depositional environment is described as marine with fluvio-glacial influences. Reservoir characteristics are greatly dependent on facies (Beicip, 1973, internal company report).

6 - Tanezzuft Formation: Silurian (Lower Llandoverian):

The name was formally introduced by Desio, (1936b) after Wadi Tanezzuft about 65km northeast of Ghat (Murzuq basin) where the type section was described. Klitzsch, (1965) criticized Desio's type section and proposed a new section at Takarkhouri south of Ghat in wadi Tanezzuft. The Klitzsch, (1965) type section has a total thickness of 402m and consists of gray marine shale, partially silty with sandstone lenses and some thin sandstone beds in the lower part. The Tanezzuft shales are essentially a sequence of graptolitic shales with minor beds of fine grained sandstone and siltstone. The upper boundary is gradational and conformable with the overlaying Acacus Formation (Acacus sandstone). The Tanezzuft shales are thought to have been deposited in a pelagic environment (Beicip, 1973, internal company report).

7 - Acacus Formation: Silurian (Upper Llandoverian):

The term Acacus Formation is introduced by Desio (1936a) after Jabal Acacus in the Ghat area of southwest Libya. The Acacus Formation is predominantly sandy with shale and siltstone alternations. The Klitzsch, (1965) type section has approximately 345m of marine subcontinental sandstones, white, gray and brown, mainly fine grained, thinly-thickly bedded. They are quartizitic near the top and shaly in the lower part. Frequent trace fossils occur indicating shallow marine conditions. In the

subsurface of the Hamada basin the formation is progressively truncated from north to south by the unconformably overlying Tadrart Formation. An increase in the percentage of sand was also observed in the same direction suggesting a southern origin for the detritus (Beicip,1973). The Acacus sands are oil producers in the Hamada basin and are thus of interest in petroleum exploration.

8 - Tadrart Formation: Devonian (Siegenian):

The name Tadrart Formation was first published in the Stratigraphic Lexicon (Burollet, 1960) on the basis of unpublished oil company reports and is derived from Jabal Tadrart in south west Libya. The Tadrart type section (Klitzsch, 1970) is a 317m succession. The lower part is white to brown, sometimes ferruginous, thickly cross-bedded sandstones with plant remains. The upper part is thinly bedded sanstones with abundant trace fossils. The same facies are described from the subsurface of the Hamada Basin with a maximum thickness in excess of 150m in the Ghadamis area. The Formation is conformably overlain by the Ouan-Kasa Formation. The depositional environment changed from continental or subcontinental in the lower part to probably shallow marine to the upper part of the formation. The Tadrart Formation is an excellent reservoir and is a major oil producer in Algeria.

9 - Ouan-Kasa Formation: Devonian (Emsian-Couvinian):

The Ouan-Kasa Formation was first described by Borghi et al., (1940) from Wadi Wan-Kasa in southwest Libya. In the type section (Klitzsch, 1970) at Takarkhouri the formation consists of about 43m of gray, partly silty, shale interbedded with clayey siltstone and fine grained sandstone with

minor calcareous beds. The siltsone and sandstone beds contain numerous brachiopods, Tentaculitids, Styliolines and other marine fossils. In the subsurface of the Hamada Basin the Ouan-Kasa Formation is about 50-170m thick and contains a microflora indicating an Emsian age (Massa et al., 1976). In the northern Hamada basin and in southeast Tunisia the Ouan-Kasa Formation grades upwards into a bioclastic limestone that contains abundant skeletal debris of bryozons, echinoderms and brachiopods. The upper boundary is unconformable with the overlying Aouinet-Ouenine Formation. The Ouan-Kasa Formation is an oil producer in the Hamada basin and is the main reservoir in the eastern part of the Illizi basin in Algeria.

10 - Aouinet-Ouenine Formation: Devonian (Couvinian–Famenian):

The term Aouinet-Ouenine Formation was introduced by Lelubre (1946) and was named after a well in in the western part of Jabal Qagaf in the Fazzan region. Recently the formation has been raised to the rank of a Group by Massa et al., (1976) who subdivided the Aouinet-Ouenine into four informal formations. These are named the Aouinet-Ouenine I to IV, and range in age from Couvinian to Fammenian (on the basis of Palynological studied from boreholes in the Hamada basin). The formation in general consists of interbedded, varicoloured silty shales, siltstones and fine to medium grained yellow-brown locally cross-bedded sandstones containing fossils (mainly brachiopods). Litho- and biofacies suggest sedimentation in shallow water. Important iron-bearing formations occur in these Devonian rocks (L Frasnian-Strunian) in the Wadi Ash-Shatti area in a belt 160km long and 120km wide. About 3.5 billion metric tons of iron ores with an average Fe% content varying

between 35% and 52% are estimated in this belt. The upper boundary is conformable with the overlying Tahara Formation.

11 - Tahara Formation: Devonian- Carboniferous (Strunian):

The term Tahara Formation was introduced by Massa et al., (1974) for a sand-shale sequence laying beneath the marine Carboniferous and marking the transition between the Devonian and Carboniferous systems in the Hamada basin. The type section is from the CPTL well B1-49 (Massa et al., 1976). In the Hamada basin the thickness of the unit (70-50m) is relatively constant. It consists of white siliceous sandstone, medium grained and locally calcareous with argillaceous fine grained sandstones, siltstones (sometimes with Tigillites) and interbeds of black shale (Beicip, 1973, internal company report). Spirififerid brachiopod and Gastropod shells form a coquina and ferruginous beds are also known (Beicip, 1973, internal company report). The formation has been dated using playnological evidence. Bellini et al., (1980) noticed the presence of a microflora characteristic of the Strunian (Tn1a of Belgium). The Tahara Formation is conformably overlain by the Marar Formation (Marar shale). The depositional environment of the Tahara Formation is described as deltaic with continental influences and (plant remains). Reservoir quality is apparently not understood (Beicipe, 1973; North El-Gullebi Project).

12 - Marar Formation: Carboniferous (Tournaisian-Visean):

The name was introduced by Lelubre, (1948) after the hill Gara el marar in the Hamada basin. It comprises a sequence of alternating silty micaceous shales and micaceous, fine grained sandy and often ferruginous

sandstones with interbeds of siltstone and minor limestone. The thickness ranges from 760-790m in the Hamada basin. Klitzsch, (1963) divided the formation into two informal units, The Basal Shale (120m) (Middle Tournasian-Visean) and the Upper Marine Shale and Sandstone with plants (Visean). The basal shaly unit (Klitzsch, 1963) is greenish-gray, partly silty and partly bituminous containing numerous brachiopods (*Chonetes, Camarotoechia, Lingula* etc.) The Marar Formation is conformably overlain by the Assedjefar Formation. The depositional environment was shallow marine and a number of sandy possible reservoirs can be traced rather easily throughout the basin

13 - Assedjefar Formation: Carboniferous (U-Visean-L-Namurian):

Lelubre (1952a) introduced the term Assedjefar Formation after Adrar Uau Assedjefar. The formation crops out in the mountains of Acacus, Qarqaf and Jabal Ben Ghnema. It is composed of fine-coarse grained poorly consolidated cross-bedded feldspathic sandstones having sandy and silty green shale interbeds. Minor beds of ferruginous sandstones are noted, with locally petrified wood. The Assedjefar Formation is about 170m thick in the Hamada basin. The upper contact is conformable with the overlying Dembaba Formation.

14 - Dembaba Formation: carboniferous (Namurian-Moscovian):

The name for the upper most Carboniferous of southern Libya was introduced by Lelubre (1952a) after Hassi Dembaba well. No type section has been described. The formation occurs in a wide region in Acacus, Tadrart, Qarqaf and Jabal Ben-Ghanema. It is a marine calcareous shale and marl formation having three members (Burollet 1960):

- The Upper Limestone Member has a rich fauna of productids and gastropods.
- The Middle Shale Member has occasional sandy dolomitic beds and rare gypsum.
- The Lower Limestone-Marl Member is sometimes dolomitic with green shale alternations.

The Dembaba Formation passes progressively to the overlaying Tiguentourine Formation through a gradational contact. Deposition was in a shallow marine environment almost exclusively under littoral conditions.

15 - Tiguentourine Formation: Upper Carboniferous

The Paleozoic ends with the deposition of relatively homogeneous red-brown dolomitic shales, and distinctive beds of shaly dolomite and anhydrites. This formation has previously been described in Algeria, near the Algerian-Libyan border (De Lapparent & Lelubre, 1948). Following Fabre (1970a), the base is considered to be of Stephanian age and the top of Autunian age i.e., basal Permian. The formation has been recorded both in the surface and subsurface of the Hamada basin, and reaches a maximum thickness of about 250m

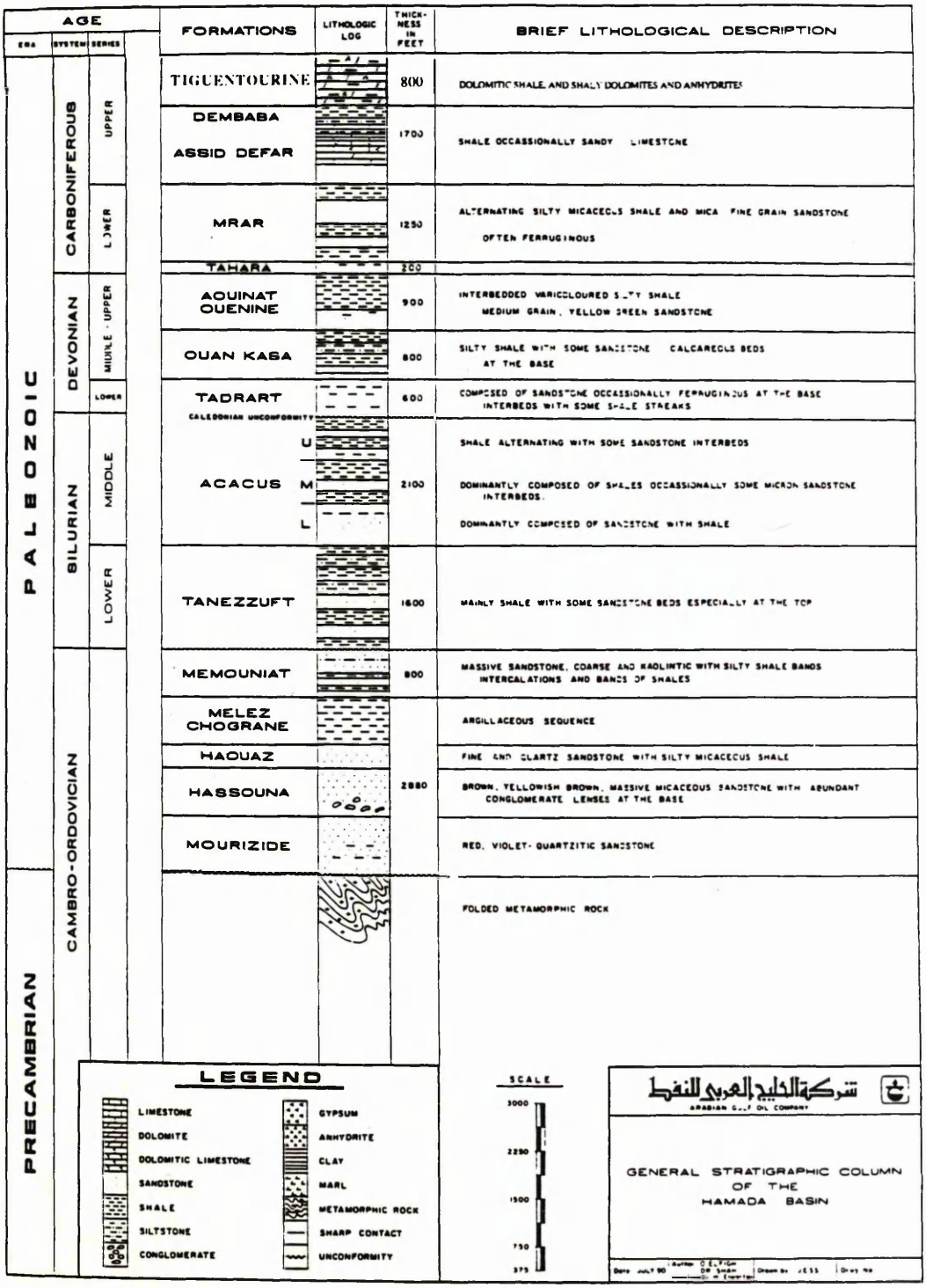

Fig.1.3 Precambrian-paleozoic stratigraphy of the Hamada basin (modified after Elfighi, Shah & Elwarfali, 1990 unpublished work). Not all unconformities are shown on section .

CHAPTER 2

CHAPTER 2

SEQUENCE STRATIGRAPHIC ANALYSIS

SEQUENCE STRATIGRAPHIC TECHNIQUE

2.1 Introduction:

Sequence stratigraphy is defined as the study of genetically related facies within a frame work of chronostratigraphically significant surfaces (Van Wagoner 1991). The application of sequence stratigraphic analysis depends on the recognition of a hierarchy of stratal units including lamina, lamina set, beds, bed set, parasequence, parasequence set and sequences (Table 2.1 & 2.2) bounded by chronostratigraphically significant surfaces of erosion, non-deposition or their correlative surfaces (Van Wagoner 1991). With the exception of the lamina each stratal unit in the above hierarchy is a genetically related succession bounded by chronostratigraphically significant surfaces; and each bounding surface is a physical boundary which everywhere separates all of the strata above from all of the strata below along the extent of the surface (Van Wagoner 1991). Correlation of these bounding surfaces results in a high resolution chronostratigraphic frame work for facies analysis. Walther's concept of facies relationships does not apply to successions with major breaks, as Middleton (1973) has pointed out, and since parasequence, parasequence set, and sequence boundaries are significant depositional discontinuities, vertical facies analysis should thus only be done within the context of parasequences, parasequence sets, and sequences to accurately interpret lateral facies relationships (Van Wagoner 1991). The fundamental stratal unit in the sequence stratigraphic analysis is the sequence, which is defined as a relatively conformable genetically related succession of strata

STRATAL UNIT	DEFINITION	CHARACTERISTICS OF CONSTITUENT STRATAL UNITS	DEPOSITIONAL PROCESSES	CHARACTERISTICS OF BOUNDING SURFACES
BEDSET	A RELATIVELY CONFORMABLE SUCCESSION OF GENETICALLY RELATED BEDS BOUNDED BY SURFACES (CALLED BEDSET SURFACES) OF EROSION, NON-DEPOSITION, OR THEIR CORRELATIVE CONFORMITIES	BEDS ABOVE AND BELOW BEDSET ALWAYS DIFFER IN COMPOSITION, TEXTURE, OR SEDIMENTARY STRUCTURE FROM THOSE COMPOSING THE BEDSET	EPISODIC OR PERIODIC. (SAME AS BED BELOW)	(SAME AS BED BELOW) PLUS • BEDSETS AND BEDSET SURFACES FORM OVER A LONGER PERIOD OF TIME THAN BEDS • COMMONLY HAVE A GREATER LATERAL EXTENT THAN BEDDING SURFACES
BED	A RELATIVELY CONFORMABLE SUCCESSION OF GENETICALLY RELATED LAMINAE OR LAMINASETS BOUNDED BY SURFACES (CALLED BEDDING SURFACES) OF EROSION, NON-DEPOSITION OR THEIR CORRELATIVE CONFORMITIES	NOT ALL BEDS CONTAIN LAMINASETS	EPISODIC OR PERIODIC EPISODIC DEPOSITION INCLUDES DEPOSITION FROM STORMS, FLOODS, DEBRIS FLOWS, TURBIDITY CURRENTS PERIODIC DEPOSITION INCLUDES DEPOSITION FROM SEASONAL OR CLIMATIC CHANGES	• FORM RAPIDLY, MINUTES TO YEARS • SEPARATE ALL YOUNGER STRATA FROM ALL OLDER STRATA OVER THE EXTENT OF THE SURFACES • FACIES CHANGES ARE BOUNDED BY BEDDING SURFACES • USEFUL FOR CHRONOSTRATIGRAPHY UNDER CERTAIN CIRCUMSTANCES • TIME REPRESENTED BY BEDDING SURFACES PROBABLY GREATER THAN TIME REPRESENTED BY BEDS • AREAL EXTENTS VARY WIDELY FROM SQUARE FEET TO 1000's SQUARE MILES
LAMINASET	A RELATIVELY CONFORMABLE SUCCESSION OF GENETICALLY RELATED LAMINAE BOUNDED BY SURFACES (CALLED LAMINASET SURFACE) OF EROSION, NON-DEPOSITION OR THEIR CORRELATIVE CONFORMITIES	CONSISTS OF A GROUP OR SET OF CONFORMABLE LAMINAE THAT COMPOSE DISTINCTIVE STRUCTURES IN A BED	EPISODIC, COMMONLY FOUND IN WAVE- OR CURRENT-RIPPLED BEDS, TURBIDITES, WAVE-RIPPLED INTERVALS IN HUMMOCKY BEDSETS, OR CROSS BEDS AS REVERSE FLOW RIPPLES OR RIPPLED TOES OF FORESETS	• FORM RAPIDLY, MINUTES TO DAYS. • SMALLER AREAL EXTENT THAN ENCOMPASSING BED
LAMINA	THE SMALLEST MEGASCOPIC LAYER	UNIFORM IN COMPOSITION/TEXTURE NEVER INTERNALLY LAYERED	EPISODIC	• FORMS VERY RAPIDLY, MINUTES TO HOURS • SMALLER AREAL EXTENT THAN ENCOMPASSING BED

Table: 2.1 Detailed characteristics of lamina, lamina set, bed, and bedset (from Campbell, 1967) see Van Wagoner, 1991.

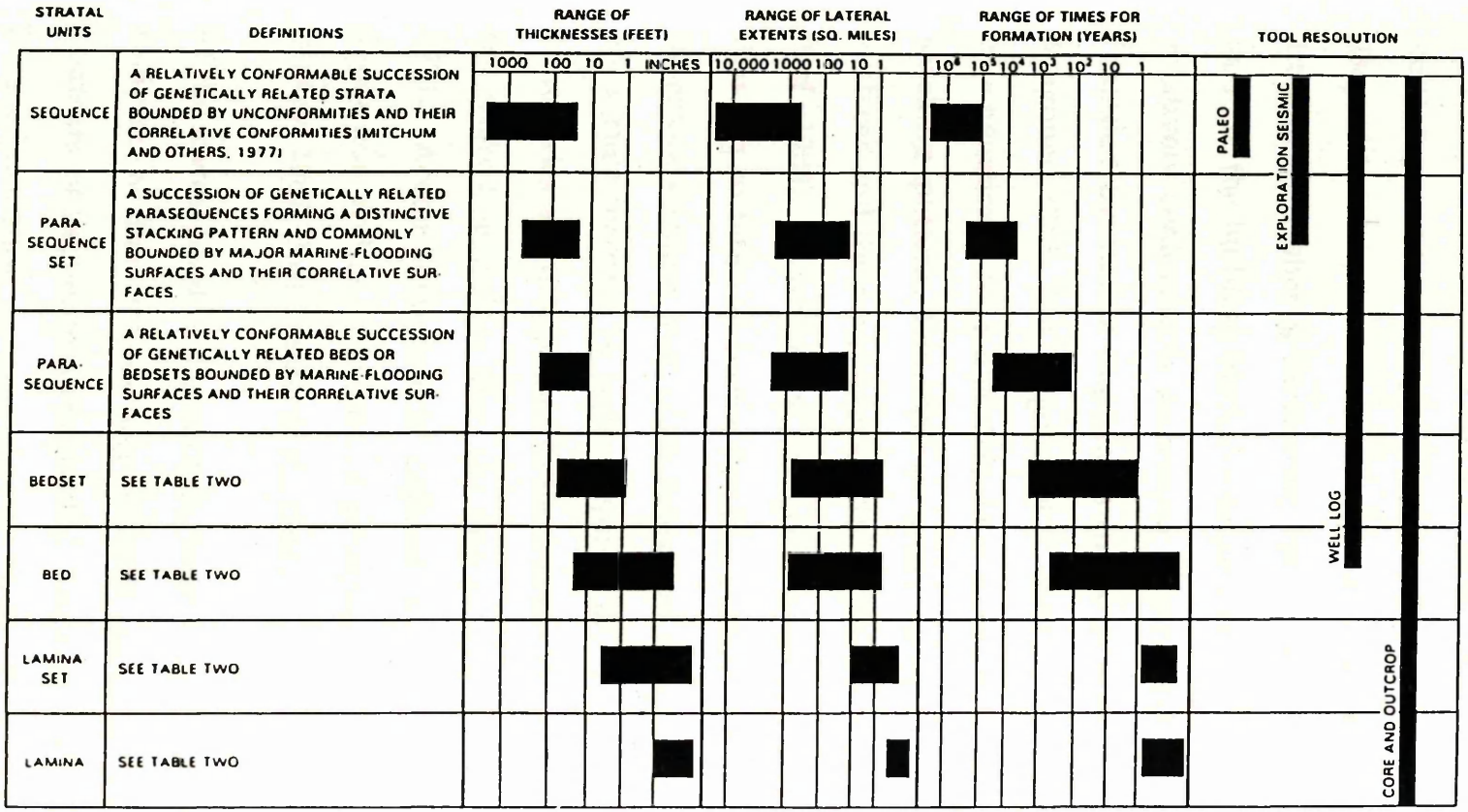

Table: 2.2 Stratal units in hierarchy: Definitions and characteristics (from Van Wagoner,1991)

bounded by unconformities or their correlative conformities (Mitchum, 1977). A sequence can be divided into systems tracts (Van Wagoner *et al.*, 1988; Posamentier *et al.*, 1988). Systems tracts are defined as a linkage of contemporaneous depositional systems (Brown & Fisher, 1977). Depositional systems are defined as three dimensional assemblages of lithofacies (Fisher & McGowen, 1967). Parasequences and parasequence sets are the building blocks of sequences. A parasequence is defined as a relatively conformable succession of genetically related beds or bedsets bounded by marine flooding surfaces or their correlative surfaces (Van Wagoner, 1985; Van Wagoner *et al.*, 1988). A parasequence set is defined as a genetically related succession of parasequences that form a distinctive stacking pattern, bounded in many cases by major marine flooding surfaces and their correlative surfaces (Van Wagoner, 1985; Van Wagoner *et al.*, 1988). Parasequence and parasequence set boundaries are marine flooding surfaces. A marine flooding surface is defined as a surface which separates younger from older strata and along which there is evidence of an abrupt increase in water depth (Van Wagoner, 1991). Parasequence boundaries are interpreted to form when the rate of sediment supply at the shore-line is less than the rate of accommodation (Van Wagoner, 1991). Accommodation is defined as the new space available for deposition and is a function of subsidence and eustatic sea level change (Jervey, 1988; Posamentier *et al.*, 1988).

At the lowest level in the analysis, lamina, lamina set, beds and bedset are analysed as the smallest depositional units and as the basic building elements of sequence stratigraphy. Associations of stratal types in the Tahara Formation are grouped into facies and nine facies are recognized (A, B, C, D, E, F, G, H & I) based on the physical and biological

characteristics of the rocks. Each facies is then described and discussed in detail, and every aspect of the facies which can be deduced on parameters such as flow conditions; variation of flow with time; sediment transport mechanisms; environmental significance of body and trace fossils, stratification and lithology types etc. is recorded. Finally each facies is given an environmental interpretation partially in isolation from adjacent sediments.

At an intermediate level in the analysis, vertical and lateral changes in the previously deduced processes are analysed over longer time spans, to examine departures from the vertical sequence (Parasequence set). To determine how these processes have changed through time at every point on the earth,s surface represented by our cored section. Such a sequential analyses have revealed cyclic processes in which sixteen siliciclastic progradational parasequences are stacked in a parasequence set separated by minor marine flooding surfaces.

At even longer time spans the lateral geometry and the vertical stacking pattern of parasequences are analysed to determine the type of parasequence set present. This resulted in the identification of the Tahara Formation as a progradational parasequence set in which the rate of deposition was greater than the rate of subsidence during the overall regressive movement of the formation.

The stacking pattern of parasequences in the Tahara Formation is terminated by a major marine transgression (Marar Shale) which flooded the Hamada basin resulting in the formation of a parasequence set boundary.

DESCRIPTION AND INTERPRETATION OF FACIES

NINE FACIES ARE RECOGNIZED WITHIN THE TAHARA FORMATION.

- A - SHALE-SILTSTONE INTERLAMINATED FACIES.
- B - HUMMOCKY CROSS-STRATIFIED SANDSTONE FACIES.
- C - CHONDRITES MUDSTONE FACIES.
- D - PARALLEL LAMINATED SANDSTONE FACIES.
- E - SHALE AND SANDSTONE INTERLAMINATED FACIES.
- F - WAVY BEDDED SANDSTONE FACIES.
- G - OOLITIC IRONSTONE FACIES
- H - RIPPLED SANDSTONE FACIES
- I - FOSILIFEROUS SANDSTONE FACIES

2.2 DESCRIPTION AND INTERPRETATION OF FACIES:

2.2.1 Facies (A) Shale-siltstone interlaminated facies:

This facies represents a total thickness of 9m, which is 7.5% of the total core section. It is confined to the basal part of the succession and consists of shale-siltstone alternations (Plate. 2.1). The facies occurs as continuous and vertically persistent units 0.7–8cm thick with an average bed thickness of 2.5cm (Fig. 2.1). The shale is made up of mainly kaolinite [$Al_2 Si_2 O_5 (OH)_4$] and quartz as shown by X.R.D. analysis (Fig. 2.2). It is very dusky red (10R2/2) and generally homogeneous, less commonly parallel laminated with moderate fissility, and remarkably free from intense bioturbation (estimated to be 10% or less of the total thickness) probably indicating very low oxygen conditions.

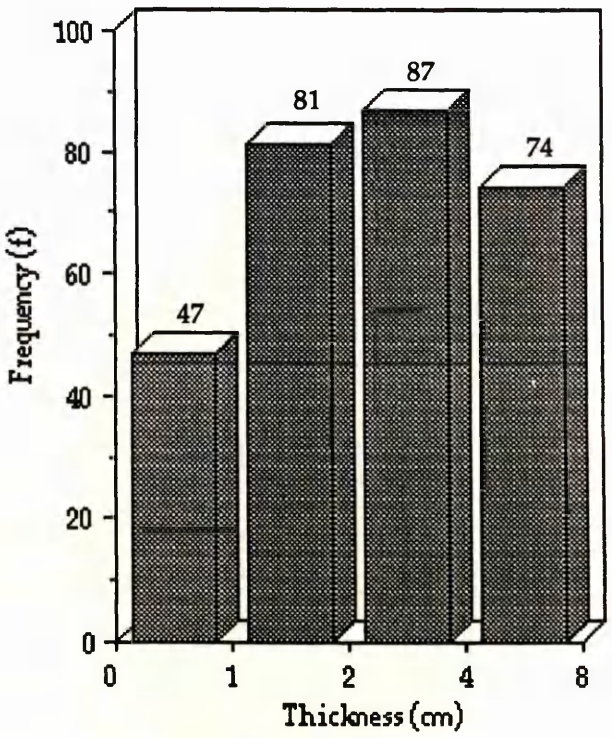

Figure 2.1 Histogram showing thickness frequency distribution of shale beds of facies (A). N.B. The programe used to generate this graph presents classes as isolated columns. In reality data form a continuous series.

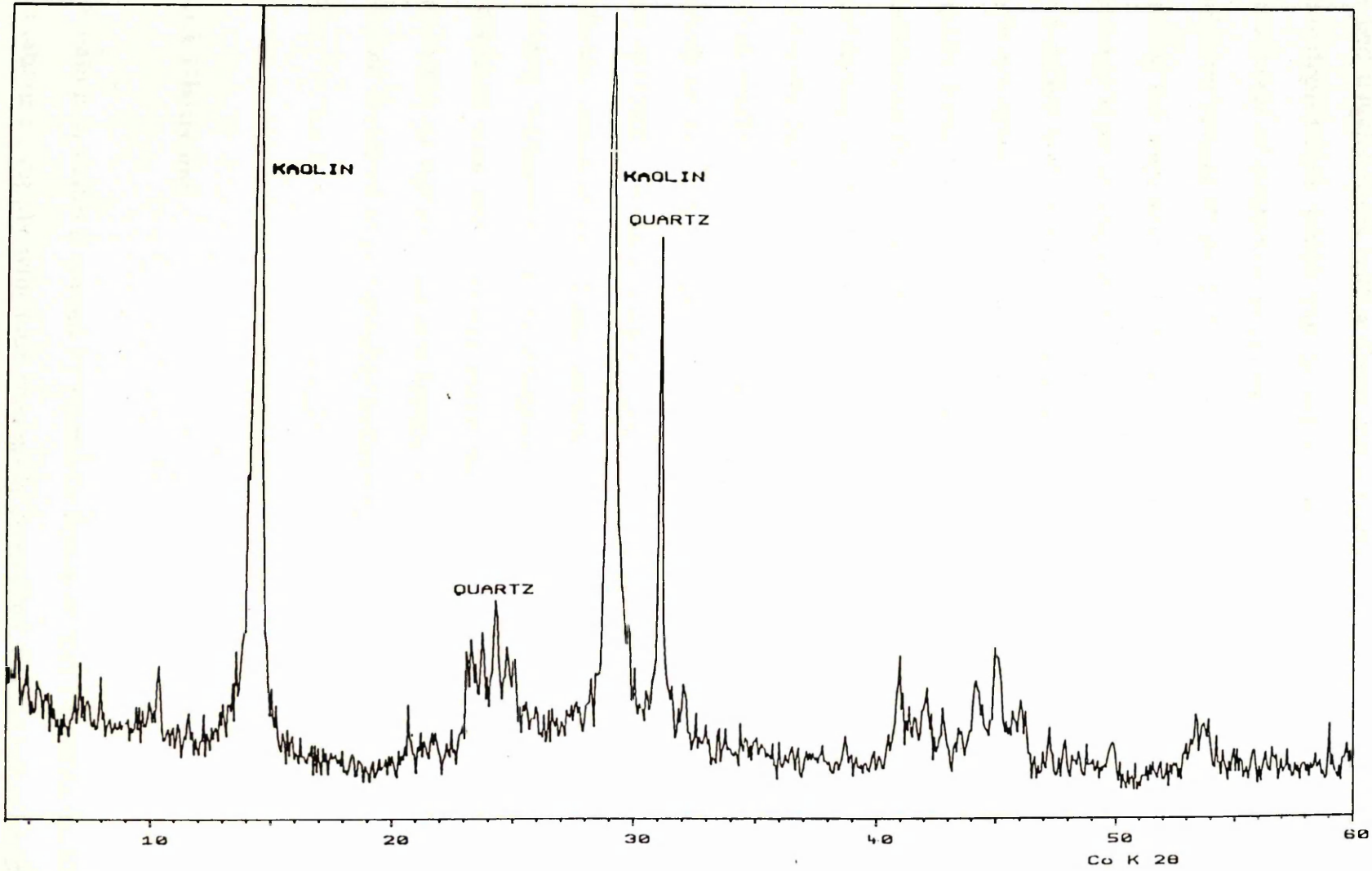

Fig. 2.2 X-ray diffraction pattern showing minerals kaolinite and quartz (facies A)

Grading is a common feature throughout the siltstone beds of the facies. A bed usually starts with a sharp contact which consists of small scour-like depressions which can be either produced by erosion or by the movement of benthonic organisms, grazing, crawling or resting on the sediment surface (Plate. 2.1). These scour-like depressions are filled by silt during the deposition of the succeeding cross-bedded relatively light coloured layer of silt, which when traced vertically decreases in grain size to a darker layer of mud forming normal grading (Plate. 2.1). The graded beds are siltstone-mudstone and are devoid of trace fossils or they are slightly bioturbated, and are sharply overlain by darker relatively more bioturbated shaly beds (Plate 2.1). They form the high energy deposits of this facies, probably introduced by storms capable of transporting sediments into distal areas of the shelf. The darker more bioturbated shales overlying the graded beds are probably deposited during longer periods of time. The facies is partly interbedded with 0.7–2cm thick very dark red (5R2/6) to dark reddish brown (10R3/4) sideritic beds (Fig. 2.3). At different levels in this basal section the facies is intersected by beds showing hummocky cross-stratification suggesting periods where deposition was above storm wave base. In general the facies is an alternation of lighter coloured layers of silt (graded beds) and darker coloured layers of shale probably indicating fast and slow sedimentation rats.

2.2.1.1 Discussion:

Lamination in shales is caused by storms or floods or may be attributed to fluctuations in supply which are seasonally controlled. On the other hand

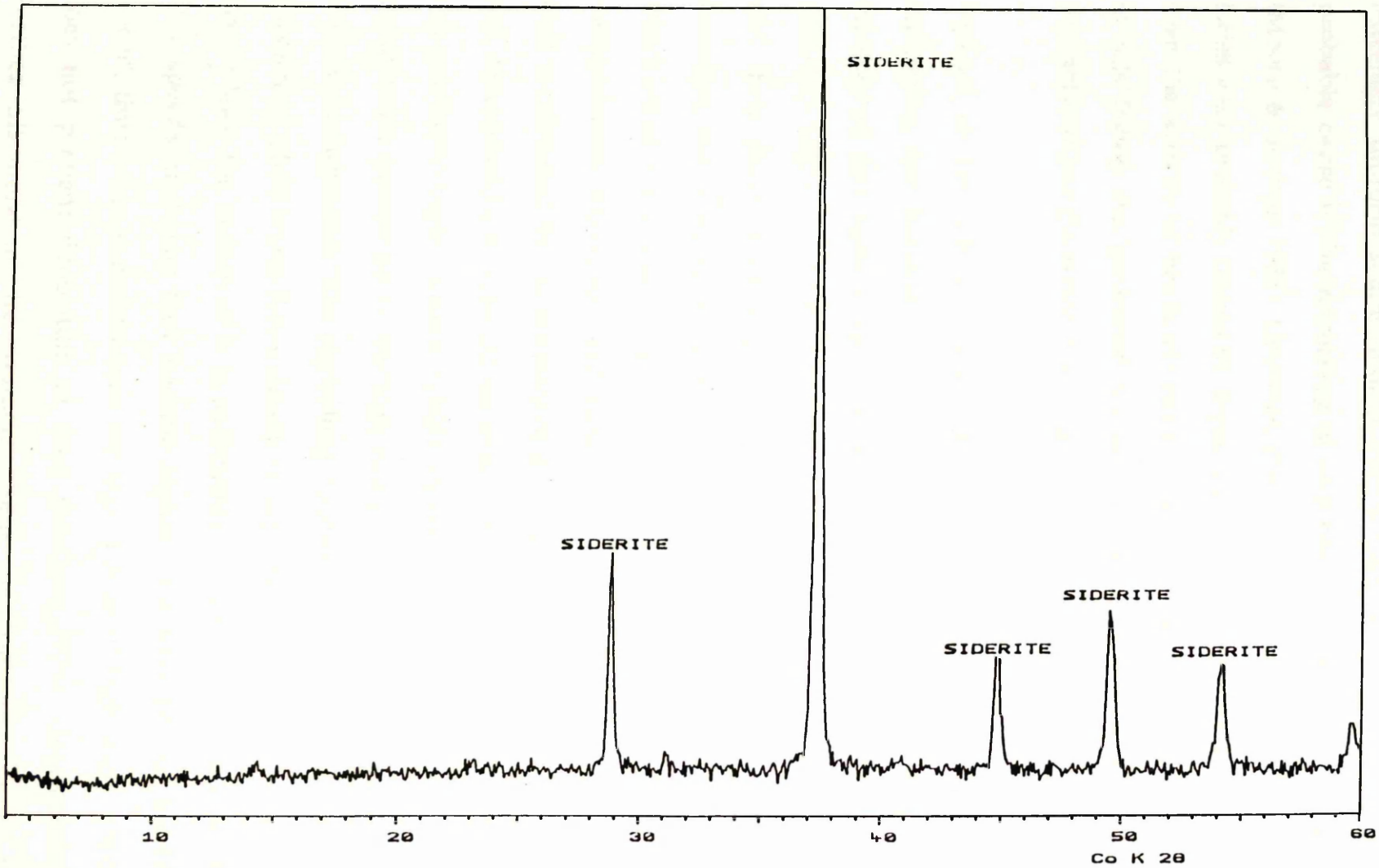

Fig. 2.3 X-ray diffraction pattern showing a pure state of the mineral siderite (facies A)

the absence of lamination, which is rather common, can be caused by extremely uniform sedimentation over a long period of time; a more probable cause is the reworking of sediments by benthonic organisms (Moore & Scruton 1975). However, the homogeneous shaly units of this facies were probably caused by deposition over long periods of time rather than the activity of benthonic organisms which was obviously minimal in this facies; the laminated portion of the facies on the other hand probably reflects the action of storms.

Because of the difficulty encountered in the study of muddy shelf sediments, and because of the idea that sandstones are more easily interpreted and have a higher economic value, mud rocks have been relatively neglected. As a result of this the conditions of their formation and their characteristics are not fully understood (McCave, 1985). However, the major source of shelf mud is the suspended load of rivers which escapes the coastal barrier leaving behind coarse sediments. The transportation, deposition, and accumulation of mud on the continental shelf is controlled by the intensity of the hydraulic regime and by the rate and concentration of external sediment supply (Johnson *et al.*, 1986). In the southern Bight, Eisma (1968) shows that mud (<50μ) form a considerable proportion of the high energy near shore bottom sediments (20% in some places); "The controlling condition is that sufficient mud be deposited, while water flows slowly to provide a layer thick enough so that at least the bottom of it is sufficiently compacted to withstand the flow speeds next time they become higher,– the next tide or the next storm", thus when concentrations are high a zone of high wave activity does not prevent deposition of mud (McCave 1971a). Nevertheless, Further off-shore in the southern Bight the concentration of the

suspended matter decreases and as a result the bottom sediments also decrease. In this zone weak wave and current activity are sufficient to counteract slow mud deposition (McCave, 1971a). Moving north over the Texel spur and further onto the shelf, mud is abruptly found below 30m water depth. "The controlling factor appears to be depth related and is most reasonably attributed to the low wave effectiveness below depths of 30m"(McCave, 1971a). Mud deposition in facies A is also thought to be depth related, with deposition probably below depths of storm wave base (see interpretation).

Kulm *et al.*, (1975) recognised three water layers on the Oregon Washington shelf in which fine sediments are transported to the off-shore areas.

(a) The surface turbid layer which occurs at the level of the seasonal thermocline. In this layer sediments move seaward in response to large waves or high river discharge. The intensity of the layer decreases with increasing depth away from the source.

(b) The mid water layer coincides with the permanent pycnocline and occurs at the level of the permanent thermocline. The sediments received from the surface layer and the surf zone move towards the shelf edge where the layer becomes thicker and more diffuse. However, west of the Columbia river the intensity of the layer is maintained to the limit of the outer shelf (Bourgeois 1980).

(c) The bottom turbid layer receives sediments from the bottom through re-suspension by waves and currents, in addition to the supply from the surf-zone and overlaying layers. High concentrations of suspended matter in this bottom layer may develop into a low density

bottom current near the middle or the outer part of the shelf. (Komar *et al.*, 1974). These operate in addition to storm generated turbidity currents, which are thought to be the major cause of the graded beds in this facies (Hamblin & Walker, 1979; Leckie & Walker, 1982),

Shelf muds may form shore-parallel belts in near-shore, mid-and outer shelf settings, or may extend across the full width of the shelf. The last case is found adjacent to major river mouths such as the Amazon, where huge amounts of suspended sediments are delivered to the shelf, covering it with a blanket of mud. Such deposition of mud is due to the high concentration of fine sediment in the water column (hundreds of grams per cubic meter) (McCave, 1985). In areas of lower concentration a near shore belt is formed eg. the Gulf of Geata Italy (McCave, 1985). However, McCave (1985) showed that relative to the wave and current energy the seaward limit of the mud belt is controlled by the drop in concentration of the suspended matter and thus deposition rate. Thus, in high wave energy settings the near shore mud belt migrates seaward and forms a mid-shelf mud belt, with a wider zone of near shore sands. Further off-shore the concentration of suspended matter dramatically decreases (<1gm-3) (McCave, 1985) so that in most cases there is no outer-shelf mud belt. Nevertheless, an exception occurs in the Gulf of Mexico (Curray, 1960), where the outer shelf is covered with a mud blanket. In the Tahara Formation the stratigraphic position of facies A within the sequence and the interpretation of sedimentological data in the light of the overall section, suggest that facies A represents an outer shelf mud belt (see interpretation).

The rate of deposition of mud on the Oregon Washington shelf is estimated to be 6cm/1000Years, and is explained as the result of re-suspension and off-shore transport during winter ((Johnson *et al.*, 1986). In the North sea southeast of Heligoland shelf mud is estimated to be deposited at a rate of 20–50cm/100Years (Reineck *et al.*, 1980)

2.2.1.2 Interpretation:

The presence of graded rhythms and absence of oscillatory flow indicators combined with the lack of coarse sediments, erosion surfaces, shell or pebble lag deposits and the presence of weak bioturbation, suggest that deposition of facies (A) was mainly in an outer shelf mud zone below storm wave base, and under oxygen depleted conditions. The rare presence of hummocky beds interbedded with this facies suggests either powerful storms or periods of shallowing during which storm sands were capable of reaching such distal settings of the shelf. Below storm wave base, however, one would expect low rates of sedimentation, resulting in bioturbation being the dominant feature of shelf muds, reflecting the lower intensity and frequency of storms. However, the situation depends on the level of the hydraulic regime which dominates in an area; for example in a high wave energy California beach face, shelf deposits are frequently influenced by storms and are composed of bioturbated silts with only a few remnants of storm generated parallel lamination (Clifton et al. 1971; Howard & Reineck 1981). In contrast, lower wave energy shore-lines show lower intensity and frequency of storms, reflected in a decrease in storm generated beds and an increase in bioturbation eg. in the Gulf of Geata in the Mediterranean sea (Reineck & Singh 1971, 1972). The deposition of shelf muds is highly episodic with the maximum rate

following storms and the minimum during prolonged fair-weather periods (Jonson *et al.*, 1986). In facies A storms seems to have played an important role in deposition. The abundance of graded bedding throughout the facies suggests relatively high rates of deposition and as a result bioturbation is minimal. These graded beds are interpreted as reflecting storm generated turbidity currents which are capable of depositing sediments beyond the influence of storm waves (Hamblin & Walker, 1979; Leckie & Walker, 1982). The cross-bedded siltstone zone accompanying these beds is interpreted as forming as a result of unidirectional flows. The darker relatively more bioturbated layers of shale underlying such beds are interpreted as representing the slow fair-weather suspension sedimentation; the relatively weak bioturbation in such beds is probably due to the oxygen deficient conditions prevailing under such depositional environments. Thus this facies reflects an alternation of low and relatively high energy conditions. The high energy deposits (graded beds) probably represent what Aigner *et al.*, (1982) described as distal tempestites. The nature of the sharp contacts at the bases of these beds is not clear, however, Aigner *et al.*, (1982) stated that the bases of distal storm layers are mostly erosional, although in some cases they may appear non erosional. The above interpretation is partially based on a general understanding of the sequence.

2.2.2 Facies (B) Hummocky cross-stratified sandstone facies:

This facies (13.4m thick) comprises 10.2% of the total core section and consists of distinctive hummocky cross-stratified sandstone beds. The sandstones are light olive gray in colour, very fine-grained (0.070-

0.110mm in grain size), with an average grain diameter of 0.090mm; moderately-poorly-sorted and have subrounded-rounded grains (visual-estimation). Hummocky bed-sets vary in thickness from 16-55cm and average 42cm but single beds may range from 1.5-23cm in thickness with an average of 5cm, (Fig. 2.4). Bioturbation is minimal (5% of the total thickness) and present only in a top mud layer or as vertical burrows in some beds (Plate. 2.2 & 2.3). Sandstone is the major lithology and forms 90% (by thickness) of the facies.

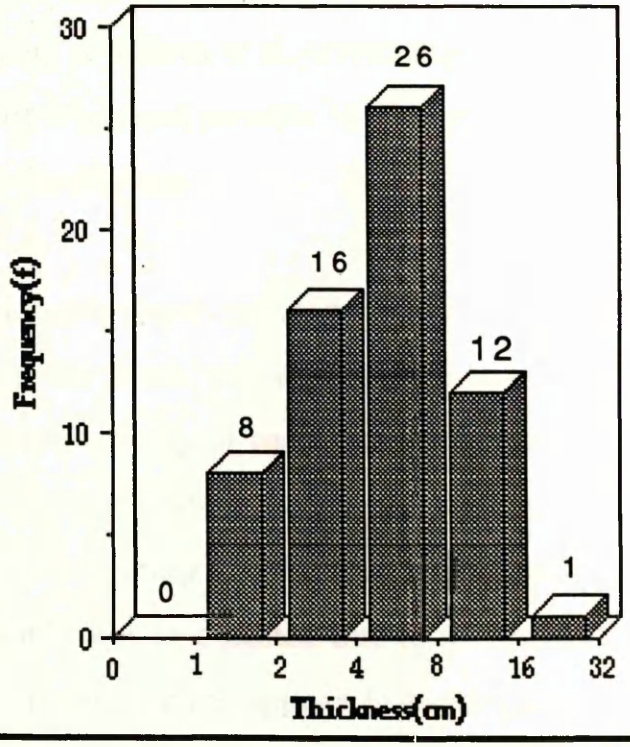

Fig. 2.4 Histogram showing thickness frequency distribution of the sandstone beds of facies (B). N.B. The programe used to generate this graph presents classes as isolated columns. In reality data form a continuous series.

The identification of hummocky cross-stratification in drill cores is a difficult problem, primarily because cores may not wide enough to

sample the whole structure. Where hummocky beds are small they are easily identified in the cores by their form and internal structure (Plates. 2.4 & 2.5). When the size of hummocks are larger, it is difficult or even impossible to identify them in core section. Some of these may be mistakenly identified as parallel lamination but where the large-scale hummocky beds have fine internal stratification it is possible to recognize discordant dips and therefore suggest them to be of hummocky bed origin (Fig. 2.5). However, the majority of hummocky beds of this facies seem to occur on a relatively small scale and thus antiformal hummocks and synformal swales can be identified within the limits of the core (Plates.2.4 & 2.5). According to Harms *et al.*, (1975) dip directions of laminae should be scattered but it was not possible to determine this in the drill cores due to their small dimensions.

The beds commonly have scoured bases, showing some relief, but in some instances the bases are sharp and nearly flat. Dott & Bourgeois (1982) termed such erosional bases first-order boundaries. However, it is very difficult to determine the nature of such boundaries in cores because what appears to be a sharp and flat base could possibly be a part of a large scour which could not be detected due to the the small width of the core sample (Fig 2.5). Most beds appear to be single depositional units, but internal bioturbation horizons and thin mudstones indicate breaks in sedimentation and show that amalgamated beds occur. Basal lag deposits are not a common feature but pebbles of sideritic mudstone are observed at the bases of some beds. Lamination within the hummocky bedding is well defined by the alternations of lighter coloured sand and darker silt laminae, but some beds show additional faint lamination. The absence of mud partings or sharp grain breaks within single beds suggests deposition

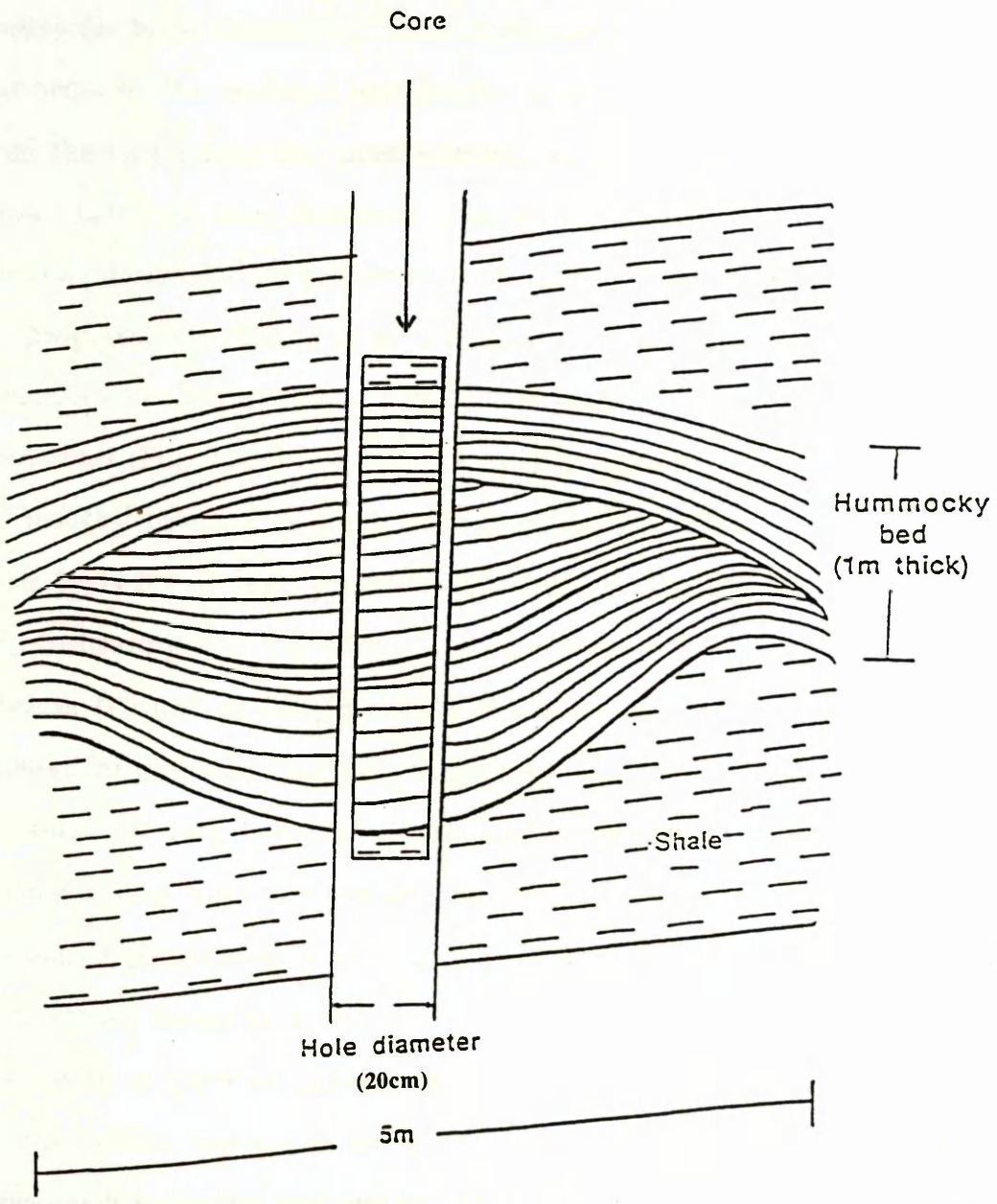

Fig. 2.5 Diagram illustrating hummocky cross-bed structure in core and possible relationship to complete structure In this case the core diameter is small compared with that of the complete structure. Curved surfaces appear as flat, slightly inclined laminae in the core. Note the large scour in the shale and how it appears as a flat slightly inclined surface.

in a single flow event. Most probably hummocky cross-stratification resulted from the filling of scours within or at the base of the hummocky sandstone beds (Brenchley 1985). Lamination in the fill approximately conforms to the scoured topography and single laminae can be traced from the swale onto and over adjacent hummocks as much as core limits allow. Laminae, may however, overlap up the sides of the hummocks. Laminae generally thicken from crests into adjacent swales so that scours are progressively filled and stratification flattens towards the top until the hummocky morphology is almost lost and the stratification is almost horizontal (Fig. 2.6). Thus, the presence of parallel lamination above the hummocky interval of some beds is explained (Plate 2.4). However, in some beds it has been observed that laminae thicken onto crests (Plate. 2.4), indicating that the hummocks have formed by accretion and not by erosion, (Hunter & Clifton, 1982). However, their close association with normal hummocky bedding suggests that they also developed in response to large storm waves under conditions of high rates of sedimentation from suspension. An oscillatory movement of particles is envisaged (Brenchley *et. al.* 1982). However, Brenchley, (1985) regarded accretionary forms of hummocky bedding as rare phenomena. Beds that start with a parallel laminated interval are interpreted as reflecting storms which were not severe enough to scour the bottom into an irregular hummocky surface; and thus the laminae draped a flat surface. Alternatively, unidirectional storm, rip, or wind-driven currents may have deposited the structure under unidirectional upper flow regime conditions (Dott & Bourgeois 1982). However, parting lineation if present is not visible in the core samples so it is not possible to verify this statement. Brenchley (1985) showed that current lineations was almost always absent from such intervals suggesting that

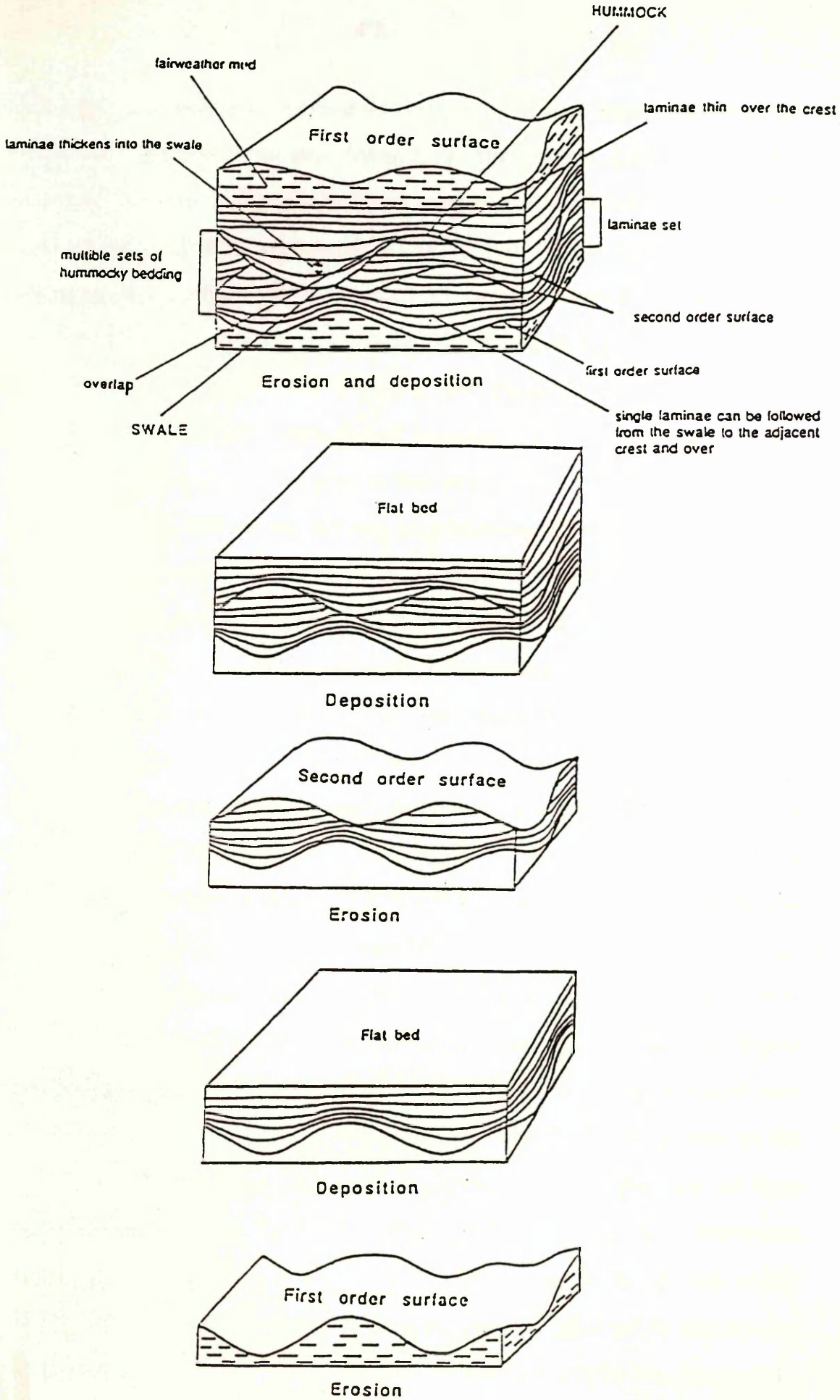

Fig. 2.6 Schematic diagram showing the creation of a hummocky bed with multiple set formed in a single flow event.

although depositional velocities might of been high the parallel laminated interval was not formed in the higher flow regime but probably by rapid deposition from suspension. Internal second order surfaces are common and most probably represent fluctuations in the intensity of a single storm event, producing alternating periods of deposition and erosion (Dott & Bourgeois 1982) (see Fig. 2.6 and compare with Plate. 2.2, 2.4 & 2.5). Positive bed forms (hummocks) are less abundant than swales, presumably because they would be selectively eroded. The presence of ripples at the top of hummocky beds is a rare phenomenon in this facies but can be observed (Plate. 2.5), indicating a return to lower flow regime conditions. The boundary between the top of a bed and the overlying muds may be sharp and planar or sharp and erosional (Plate. 2.3). However, such sharp contacts indicate that either the flow waned very quickly, or that there was some erosional event after the hummocky bed was laid-down. The overlying mud interval is commonly homogeneous but may be totally or partly bioturbated or show some remnants of stratification. In general it is not known whether the mud zone represents pelagic fall-out of mud, a late stage in the deposition of the storm bed (Dott & Bourgeois 1982), or a separate storm event not related to the initial storm cycle. In the latter case, however, storm erosion unaccompanied by sand deposition may result in the scouring of the bottom (a muddy bottom or the sandy bottom of a former hummocky bed) and in the deposition of a mud layer. This could be related to the event (deposited rapidly by fast suspension and redeposition of local muds or brought in by storm currents or both) or may represent subsequent filling of mud (fair-weather fall-out of mud). In any case a layer of mud is deposited, but differences may be reflected in the amount of bioturbation which would be less intense or absent in the rapidly

deposited layer of mud Plate 2.3, might show such a relationship. The thickness of the mud zone of this facies varies from 0.5–8cm with an average of 3cm. Referring to the ideal hummocky bed sequence model of Walker *et al.*, (1983) (fig.2.7) the following transition variations are recognised arranged in a decreasing order of abundance: (HM = 72%), (HFM = 13.5%) , (BHM = 8.4%), (HFXM = 3%) (PHFM = 2.7%) (see fig. 2.7 for terminology and explanation). The importance of such variability is briefly discussed below.

2.2.2.1 Discussion:

A considerable volume of literature has in recent years addressed the problem of the nature, origin and significance of hummocky cross stratification (HCS). Gilbert (1899), was the first to discover the sedimentary structure, now known as hummocky cross-stratification, while working on the Silurian Medina Formation. Duke, (1982b) re-examined the Medina in New York and Ontario and confirmed that the undulatory bedforms to which Gilbert referred were indeed examples of hummocky cross-stratification. Gilbert's interpretation of the structure as a shallow-marine indicator generated by large storm waves was criticized by Fairchild, (1901). And the structure went unnoticed for over half a century until it was re-discovered by (Campbell, 1966; 1971). He regarded the structure as large scale truncated wave ripple laminae. The term hummocky bedding (strictly hummocky cross-stratification) was introduced by Harms et al. (1975) after which it became widely recognised as a very significant storm-influenced sedimentary structure.

Subsequently this structure has been recognised and defined from many ancient sedimentary sequences where it typically occurs between near-

shore and outer-shelf facies. It has also been reported in coastal sediments, namely in beach and tidal flat environments, (Greenwood 1984 & Bartsch, Winkler & Schmoll, 1984). Although it forms in a wide range of environments the common occurrence is between fair-weather and storm wave base due to the high preservation potential of that zone (Dott & Bourgeois, 1982). Because of their scale, complete sets of hummocky bedding cannot be recognised in vibracores or even in box cores (Hunter & Clifton, 1982). However, scuba divers have reported hummocky beds immediately following winter storms (Hunter & Clifton, 1982). The problem is that the structures have never been seen forming in the natural environment. However, several experiments have produced smaller structures of similar morphology (Caarstens et al. 1969; , Southard et al. 1990; Arnott & Southard 1990)

Harms *et al.*, 1975, characterised hummocky cross-stratification as follow:

(1) Lower bounding surfaces of sets are erosional and commonly dip at angles less than 10°, though dips can reach 15.°

(2) Laminae above these erosion set boundaries are parallel to that surface or nearly so.

(3) Laminae can systematically thicken laterally in a set, so that their traces on a vertical surface are fanlike and dip diminishes regularly.

(4) The dip directions of erosion set boundaries and of the overlying laminae are scattered.

The thickness of a single bed varies from a few cms. to 5 or 6m; bed sets on the other hand may be tens of meters thick (Dott & Bourgeois, 1982). Hummocks may reach a wave length of 4m or more and height (swell to hummock) may be tens of cm's, or they can be very small with ripple

dimensions (Bourgeois, 1985). A distinguishing characteristic of HCS storm beds is that they commonly display a preferred internal arrangement of primary structures. Several papers have described ideal sequences for such storm beds (e.g ., Dott & Bourgeois 1982; Walker *et al.*, 1983; Duke 1985; Leckie & Krystinik 1989). Brenchley (1985) described the ideal sequence of structures in an ascending order following the model of Walker *et al.*, (1983) as follows (fig. 2.7):

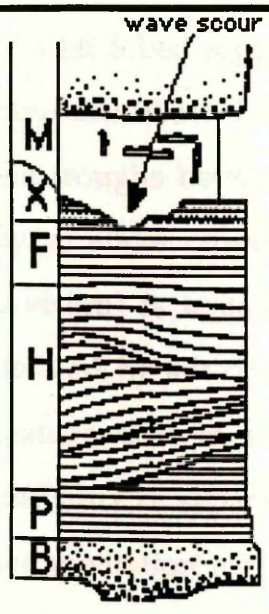

OBSERVATION	INTERPRETATION
Bioturbation	Fairweather sedimentation
Wave ripples	Moderate wave action
Hummocky topography becomes subdued	Deposition from suspension
Hummocky surface	Wave erosion
Mantling laminae flatten topography	Deposition from suspension
Hummocky surface	Erosion by periodic large waves
Parallel lamination	Deposition from sediment laden
Erosion + sole marks	Current and / or wave scour

Figure. 2.7 An idealised hummocky bed sequence (after Walker *et al.*, 1983) with interpretation of the successive phases of deposition

They begin with a sharp base, referred to as a first-order boundary by Dott & Bourgeois (1982) to distinguish it from the second order truncations within the sequence. Commonly such surfaces are nearly flat but may be deeply scoured and may show channel-like or hummocky morphology. A basal lag (B-division) of coarse-grained sediments such as coarse sand, granules, pebbles, shell & mudstone interaclasts follows (Walker *et al.*, 1983; Dott & Bourgeois 1982). This may be overlain or replaced by a unit

of parallel lamination (P-division) in which primary current lineation is almost always absent. A unit of hummocky cross-stratification (H-division) commonly succeeds the parallel laminated unit with a second-order surface cutting into P-division. The scoured surface is progressively filled through a laminae set until the hummocky morphology almost vanishes. A new second-order hummocky surface might then be initiated to form a new lamina set and so forth until eventually multiple lamina sets are formed in a single bed (see Fig. 2.6). A late stage in the deposition of a HCS bed sequence is represented by an interval of flat lamination (F-division) (Plate. 2.4). This represents deposition on a flat surface created as the troughs between hummocks are progressively filled; this is followed by a wave rippled (X-division) interval. The upper mud zone (M-division) is usually homogeneous but may show very fine lamination defined by silt or very fine sand streaks. Bioturbation is such a common feature that in many cases it obliterates the original structure. The difficulty in separating the storm waning phase from normal fair weather sedimentation makes this zone difficult to treat. It may be part of the ideal hummocky sequence or it may be a distinct bed (Dott & Bourgeois, 1982). Where the upper mud zones become thicker and more frequent and are associated with thin hummocky units they are believed to indicate more distal settings (Dott & Bourgeois, 1982).

Amalgamated hummocky beds can succeed one another for as much as 40m in a vertical sequence (Bourgeois, 1980). To differentiate between first and second order surfaces in such a succession is a difficult task. However, Dott & Bourgeois (1982) suggested several clues for such a distinction. These are:

(a) truncated burrowed zones in an otherwise homogeneous bioturbated sequence

(b) truncated contoured zones

(c) lateral cutting out of mudstone layers from between hummocky units. Amalgamation might be taken as evidence of either frequent storms or violent events which eroded all fair weather deposits prior to any deposition (Dott & Bourgeois, 1982). In either case amalgamation provides evidence of proximity to the source (Dott & Bourgeois, 1982).

As with other sedimentary models the idealized hummocky stratigraphic sequence provides a conceptual model to which variations can be referred and interpreted, in terms of factors such as proximity to shore-line, depth of water, magnitude and duration of storm, position relative to the track of a storm, magnitude of sand supply, steepness of the slope, and configuration of the coast (Brenchley, 1985; Dott & Bourgeois 1982). Brenchley (1985) has summarised the common variations amongst beds with hummocky cross-stratification and differences from the model as follows:

(1) The depth and steepness of the basal erosion surface is variable and it may have a channel-like or hummocky morphology.

(2) The basal lag unit (B) is commonly missing.

(3) The thickness of the parallel laminated unit (P) is variable it can be absent or form the whole bed.

(4) The interval with hummocky cross-stratification (H) shows variation in wave length (<4m) and height (<1m) of the hummocky 2nd order surfaces and the steepness of dip of those surfaces and their overlying lamina (0 >40°) there is a wide variation in the number of

laminae-sets in a bed. The hummocky cross-stratification can either be erosional or accretionary.

(5) The upper horizontal interval (F) is commonly absent

(6) Wave ripples (x) are very variable in their morphology. They may be absent. Combined-flow and unidirectional ripples may occasionally be present.

(7) The upper surface of beds may be bioturbated to different degrees, and there may be a distinctive suite of trace fossils in the fair weather facies.

(8) Scour of the upper surface of beds may be rare or common, shallow or deep (see Plate. 2.3).

The emplacement of sand on the continental shelf and its reworking into hummocky cross-stratification is still a matter of controversy. Studies of both ancient (Walker *et al.*, 1983) and recent sediments (Nelson, 1982) show that depositional currents are capable of transporting large volumes of sand more than 100km off-shore."The almost universal fine grain of hummocky bedding must reflect efficient selective sorting of sand by suspension transport to the site of deposition" (Dott & Bourgeois, 1982) Sediments introduced to the shelf by river-mouth flooding and storm erosion can be dispersed on the shelf by a variety of mechanisms. Oceanographers, and marine geologists prefer wind forced currents or storm surge ebb currents as mechanisms of transport but others favour the mechanism proposed by (Walker 1979) in which storm initiated turbidity currents transport and deposit sediments well below wave base. The controversy concerning the development of hummocky bedding is whether oscillatory or combined (oscillatory & unidirectional) currents are capable of forming the hummocky erosion surfaces and draping them

with sand. Several workers (eg. Walker *et al.*, 1983; Brenchley, 1985; Krystinik, 1989) considered unidirectional currents as the predominant component which eroded the bottom and transported material off-shore, and that the ideal sequence of structures was generated under predominantly oscillatory flows as the unidirectional component diminished. In contrast, Duke, (1990) suggested that the initial erosive flows are oscillatory-dominant and that HCS is only deposited when the unidirectional component becomes vanishingly small. Others (eg. Dott & Bourgeois, 1982; Swift *et al.*, 1983; Allen & Underhill, 1989) suggested combined (oscillatory \ unidirectional) flows for the deposition of the HCS storm-bed sequence excluding the wave rippled zone. In support to this interpretation a recent study Cheel (1991) suggested deposition of hummocky beds from waning combined (oscillatory\unidirectional) flows.

Hummocky cross-stratification can easily be mistaken for other structures. The low angle truncations and low angle inclined laminae are similar to swash-zone lamination. Abundant mica and plant flakes may help to distinguish hummocky from swash-zone laminae which are normally devoid of such grains because of surf agitation (Dott & Bourgeois 1982). The synformal swales resemble both trough cross-stratification and ordinary scour and fill structure. The synforms are less regularly spaced and less oriented than trough sets, and dip angles are statistically smaller (Dott & Bourgeois, 1982). Although both structures have erosional base, upward-diminishing inclination is more characteristic of hummocky stratification (Dott & Bourgeois 1982). Regardless of orientation vertical cross-sections look the same suggesting a circular plan-form. This unique characteristic of hummocky cross-

stratification can be particularly helpful in recognizing hummocky stratification in drill cores (Dott & Bourgeois 1982). Beside the several features characterizing hummocky stratification, its presence in very fine sand with very low angle truncations; nearly horizontal to low angle undulating lamination, and association with parallel lamination and rippled tops; basal lag; burrowed zones, and stratigraphic position within a vertical sequence helps to identify hummocky stratification (Dott & Bourgeois 1982).

Based on the assumption that first order surfaces reflect major storm events they could be separated in time by weeks, months, or years. In contrast, if second-order surfaces represent pulses within a single storm event or season, they would be separated by hours, days or weeks (Dott & Bourgeois, 1982). Individual laminae similarly would represent seconds or minutes, i.e the period of individual wave oscillations or pulsations of wave trains (Harms *et al.*, 1975; Harms, 1979). The geological point of view of storm deposits is however, different from that of oceanographers and marine geologists. Simply because such events are rare in the geological record and are measured at the scale of hundreds or thousands of years. They could not have been seen by oceanographers. Several studies have suggested a storm frequency of 400-15000 years per bed (eg. Brenchley *et al.*, 1985; Kreisa, 1981; Aigner, 1982).

2.2.2.2 Interpretation:

From the above discussion the hummocky bedding of facies B is interpreted to be a storm feature formed in an environment which was sufficiently near shore for the deposition of relatively thick sand beds and for the floor to be frequently reworked by wave and wind induced

currents. However, the relative abundance of this facies in the sequence and its association with most of the facies described, suggests that it may be deposited in a wide range of environments, which probably extend along the beach face profile to include shelf muds and lower shore-face environments. Nevertheless, most deposition of facies (B) is believed to be between the offshore-transiton and lower shore-face environment. This interpretation however, is based on the following points:

(a) The general agreement that the structure is a storm feature produced under combined (oscillatory & unidirectional) currents.

(b) The common stratigraphic occurrence of the structure in units between fair-weather and storm wave base deposits.

(c) The sharp bases of the deposits cutting into underlying muddy substrate's suggest sudden input of sand in an otherwise quite environment.

(d) Normally bioturbation and mud deposition are favoured in sites of low energy conditions below effective wave base. Thus, the presence of hummocky bedded sandstones interbedded with mudstones with burrowed zones indicates that the hummocky beds have interrupted the quiet conditions of these environments.

(e) The occurrence of relatively thick amalgamated hummocky beds suggests proximity to source and deposition in relatively shallow waters (Dott & Bourgeois, 1982), probably in a lower shore-face environment

where evidence of storm activity is more often preserved than in middle or upper shore-face facies (Brenchley, 1985).

2.2.3 Facies (C) Chondrites mudstone facies:

This facies represents a total thickness of 12m and comprises 9.1% of the total core section. It consists of dark reddish brown (10R3/4) beds of mudstone ranging in thickness from 1.5-30cm with an average thickness of 10cm (Fig. 2.8); bedsets, however, may reach a thickness of 1m.

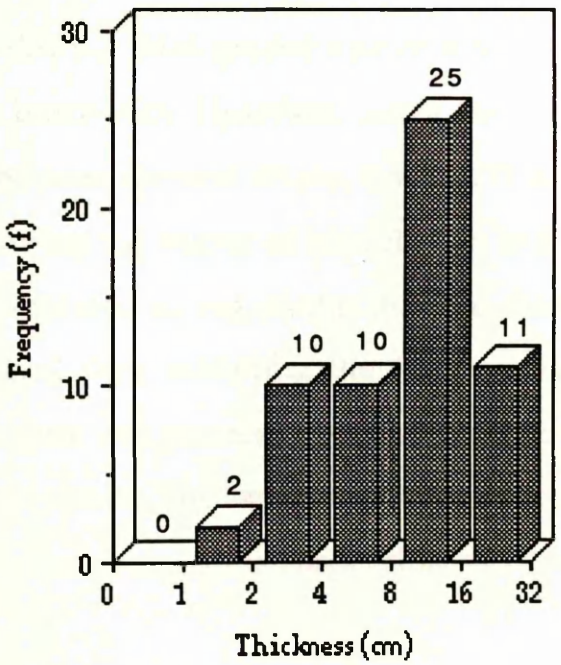

Figure 2. 8 Histogram showing thickness frequency distribution of mudstone beds of facies (C). N.B. The programe used to generate this graph presents classes as isolated columns. In reality data form a continuous series.

Bioturbation is the prevalent feature of this facies being estimated to occupy 70% of the total thickness. It was produced by deposit feeders. The traces belong to the ichnogenus *Chondrites* which is thought to have been adapted to feeding in sediments with little oxygen in the interstitial

waters below the sea floor (Bromley *et al.*, 1991)). Mudstone is the predominant constituent, being estimated to form 90% of the facies. The facies consists of completely homogenised sandy silty mudstones (Plate 2.6) except for remnants of thin, sharply based, partially bioturbated sandstone beds. In addition, where there are few or no sandstones, shales showing fine lamination and vertical grading; and with only slight or no bioturbation are scattered throughout the facies as units 1 - 8 cm thick (Plate. 2.6 & 2.7). These are most likely to have been deposited either during periods of lower oxygen or by higher sedimentation rate, probably by the rapid suspension and redeposition of local muds which obliterated traces and laid down a thick graded unit of mud which later could not be penetrated by burrowers. However, when beds of sandstone appear, bioturbation becomes obvious (Plate. 2.6 & 2.7) and so there is a clear relationship between the degree of bioturbation and the presence of sand. This can be interpreted as suggesting that the shale bed was originally devoid of oxygen, thus inhibiting the feeding organisms; When sand entered this regime oxygenated waters were also brought in and the stagnant bottoms stirred. The sandstone beds are normally weakly graded reflecting deposition from dilute suspension-currents.

2.2.3.1 Discussion:

Following the classic work of Simpson (1957) *Chondrites* has been considered the trace of a deposit-feeding organism of unknown taxonomic affinity. *Chondrites* is a regularly branched burrow system characterised by a root like structure (Fig. 2.9). It occurs in a variety of rocks from the Ordovician onwards and in a wide range of

environments, ranging from littoral to abyssal (Collinson 1987). *Chondrites* belongs to the Zoophycos ichnofacies which characterises the

Figure 2.9 Reconstruction of the *Chondrites* burrow system (after Simpson 1957)

off-shore area (Seilacher 1964). Recent occurrences are however, restricted to deep sea sediments, and they are believed to be the product of infaunal abyssal nematodes (Bromley *et al.*, 1984). Oxygen plays an important role in the distribution of *Chondrites*-producing organisms, and bathymetry seems to be a minor factor (Bromley *et al.*, 1984). It was originally thought that *Chondrites* occurred below the sediment water-interface beneath oxygen starved sea floors (Bromley et al 1984). More recently, however, Bromley *et al.*, (1991) have stated that in totally bioturbated sediments *Chondrites* on no account indicates sea floors deficient in oxygen as has been suggested before. Burrowers were able to penetrate beneath the sediment water interface being adapted to utilize oxygen-deffcient pore-waters. Thus, they are are taken to indicate low oxygen in the interstitial waters within the sediment.

Seilacher (1964) proposed four ichnofacies namely Skolithos, Cruziana, Zoophycos and Nereites, for recurring trace fossil assemblages, each having paleoenvironmental significance. His concept primarily focussed

on bathymetry as the limiting factor in the ichnofossil distribution, with the above four ichnofacies reflecting increasing water depth. His marine bathymetric paradigm has however, been criticised by several workers (eg. Ekdale 1988), and recently Frey *et al.*, (1990) showed that marine ichnofacies are based on recurring ichnocenoses which were rarely if ever depth controlled but reflect other factors which might be depth related. Such factors include oxygen and salinity levels, substrate consistency, hydraulic energy, rates of deposition, turbidity and the quality and quantity of available food (Frey *et al.*, 1990). The Zoophycos ichnofacies, to which the trace fossil *Chondrites* belongs, is found in environments ranging from "circumlittoral to bathyal, quiet-water conditions, or protected intracoastal to epeiric sites with poor water circulation; typified by muds or muddy sands rich in organic matter but somewhat deficient in oxygen. Off-shore sites are below storm wave base to deep water, in areas free of turbidity flows or significant bottom currents, this ichnocoenose may be omitted in the transition from infralittoral to abyssal environments. Infracoastal to epeiric sites include such features as silled basins and restricted lagoons" (Frey *et al.*, 1990). These conditions and the consequent lithologies resemble the facies described here .

2.2.3.2 Interpretation:

The highly bioturbated nature of this facies might suggest deposition under well-oxygenated bottom conditions. However, *Chondrites* is an opportunistic ichnogenus which takes advantage of the inability of other organisms to survive in a severely oxygen-depleted environment where it may occur alone (Ekdale 1985, see also Bromley *et al.*, 1991)). Vossler *et al.*, (1988) suggested that superabundant *Chondrites* indicates the presence

of organic rich layers in dysaerobic conditions. Furthermore Bromley *et al.*, (1984) stated that oxygen plays an important role in the distribution of *Chondrites*-producing organisms, and that bathymetry seems to be a minor factor. The relation between bioturbation and oxygen in this facies is in favour of the latter statement. Nevertheless the relatively thick homogeneous units of bioturbated mud in this facies suggests a very slow and continuous rate of deposition probably during a prolonged period of fair-weather caused by a temporary climatic change. However, the preservation of some thin sandstone beds in this facies reflects the influence of severe storms, and the inability of benthonic organisms to rework the thickness of the rapidly deposited layer. The rare presence of weak graded bedding probably indicates the effect of much weaker storms. Thus, this facies is interpreted as having been deposited above storm wave base but below fair-weather wave base in an environment which was far removed from the area of storm activity.

2.2.4 Facies (D) Parallel laminated sandstone facies:

This facies represents a total thickness of 10.2m which is 7.6% of the total core section. It consists of light olive gray (8Y/8/1), occasionally pale red (5R6/2) or moderate brown (5YR4/4) sandstone. Grain size is very fine to fine grained, ranging from 0.076–0.143mm with an average grain diameter of 0.100mm; grains are moderately–sorted to well sorted and subrounded–subangular (visual estimation). Single beds average 10cm thick and range from 2–87cm (Fig. 2.8). A bedset can reach a thickness of 160cm. Bioturbation is minimal, estimated to be 5% of the total thickness of the facies. Sandstone is the predominated lithology forming 90% by thickness of the facies.

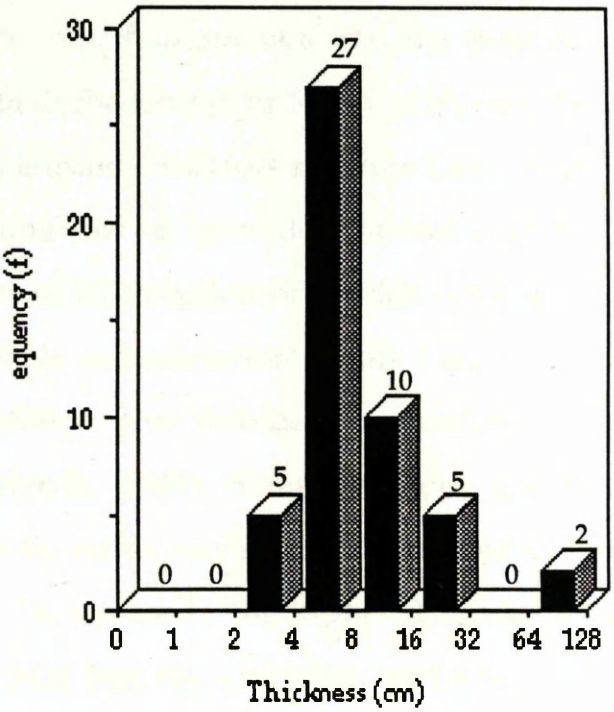

Figure 2. 10 Histogram showing thickness frequency distribution of sandstone beds of facies (D). N.B. The programe used to generate this graph presents classes as isolated columns. In reality data form a continuous series.

The sandstone beds contains thin, indistinct parallel lamination. The lamination is marked by the alternation of fine sandstone and mudstone, with transitional or non-erosion boundaries between them (Plate. 2.8 & 2.9). Less commonly lamination can be very distinctive with a clear separation into fine sandstone and mudstone. However, thicker mudstone laminae occur and these are bioturbated. These beds are thus thought to be the result of a pause in sedimentation; the clays representing suspended load which accumulated over sufficient time to permit the fauna to bioturbate the sediment. Where such beds are massive they are thought to be the result of storm sedimentation, in which a thick layer of mud is rapidly deposited from suspension in the later stages of a storm. It is assumed that such layers could not be penetrated by benthonic organisms. However, if the rapidly deposited

mud layer was not thick enough and the time of exposure was long enough then bioturbation might totally obliterate the layer. The presence of bioturbated erosional surfaces suggests that the bed is an amalgamated unit representing two or more depositional events. The laminated beds between layers of bioturbation or erosion surfaces are thought to be the deposits of single sedimentation events (storm events), produced as a result of deposition from turbulent suspension (Reineck & Singh, 1972; Aigner & Reineck, 1982). Some bed tops are reworked, indicating deposition above storm wave base. Lower bedset boundaries are sharp and erosive. In contrast, the upper boundaries either sharply or gradationally pass into the overlying mudstones. Individual beds either behave the same or when present within bedsets are separated by surfaces of erosion non deposition or abrupt change in lithology. Although it is not always possible to determine the nature of such boundaries in the core because of core damage, it is always possible to recognise that such beds are sharply emplaced over these boundaries. One case is reported where winnowed granule lag of reworked siderite nodules is concentrated as pebbles on the top of a bed, indicating in-situ reworking which involves the removal of sand and redepostion elsewhere (Plate. 2. 9).

2.2.4.1 Discussion:

Parallel laminae may be the product of two different flow regimes: upper and lower. On beaches the swash of a wave brings in a sand layer which is deposited by the unidirectional backwash in the form of a reverse graded lamina (Clifton, 1969). Large waves beyond the surf zone can produce such beds (Lindholm, 1987). The most common type of parallel lamination is that produced by bed load segregation in upper plane bed

phase of the high flow regime (Fig. 2.11). Under such conditions sediment moves continuously along the bottom resulting in a poorly defined parallel lamination which commonly shows flow lineation. This is shown by streaks or small stripes of slightly coarser sediments or aligned elongate grains (Fritz and Moore, 1988). Because such flows are achieved in shallow high energy environments mud is usually absent from such deposits. However, parallel laminated sands in turbidite sequences are deposited under the same conditions (Collinson *et al.*, 1987). At lower velocities (below the critical velocity of ripple formation) and in sands coarser than 0.6mm, a less common type of plane bed occurs, formed under lower flow regime conditions (lower plane bed). Such bedding is difficult to distinguish from upper flow regime plane bed. However, these beds show better developed stratification, due to the slow movement of the flow, which gives more chance for grain types and grain sizes to differentiate as they move along the bed. Flow lineation is totally absent under this type of flow regime and stratification is rather recognised by grain size changes (Fig. 2.11). An important mode of genesis of parallel laminated sand which is of prime importance in this discussion is that produced through the deposition of suspension clouds. Such sands have been experimentally produced by sieving sand into a slowly moving water, creating suspension clouds which, when deposited, result in parallel lamination (Reineck & Singh 1972). In nature storm sand layers in the shelf muds are formed as a result of similar processes. Under such conditions and different from those of upper and lower flow regime, one would expect thin mud laminae to be deposited between successive pulses of sand, indicating short pauses in sedimentation in a muddy environment giving the facies its laminated appearance (Fig. 2.11).

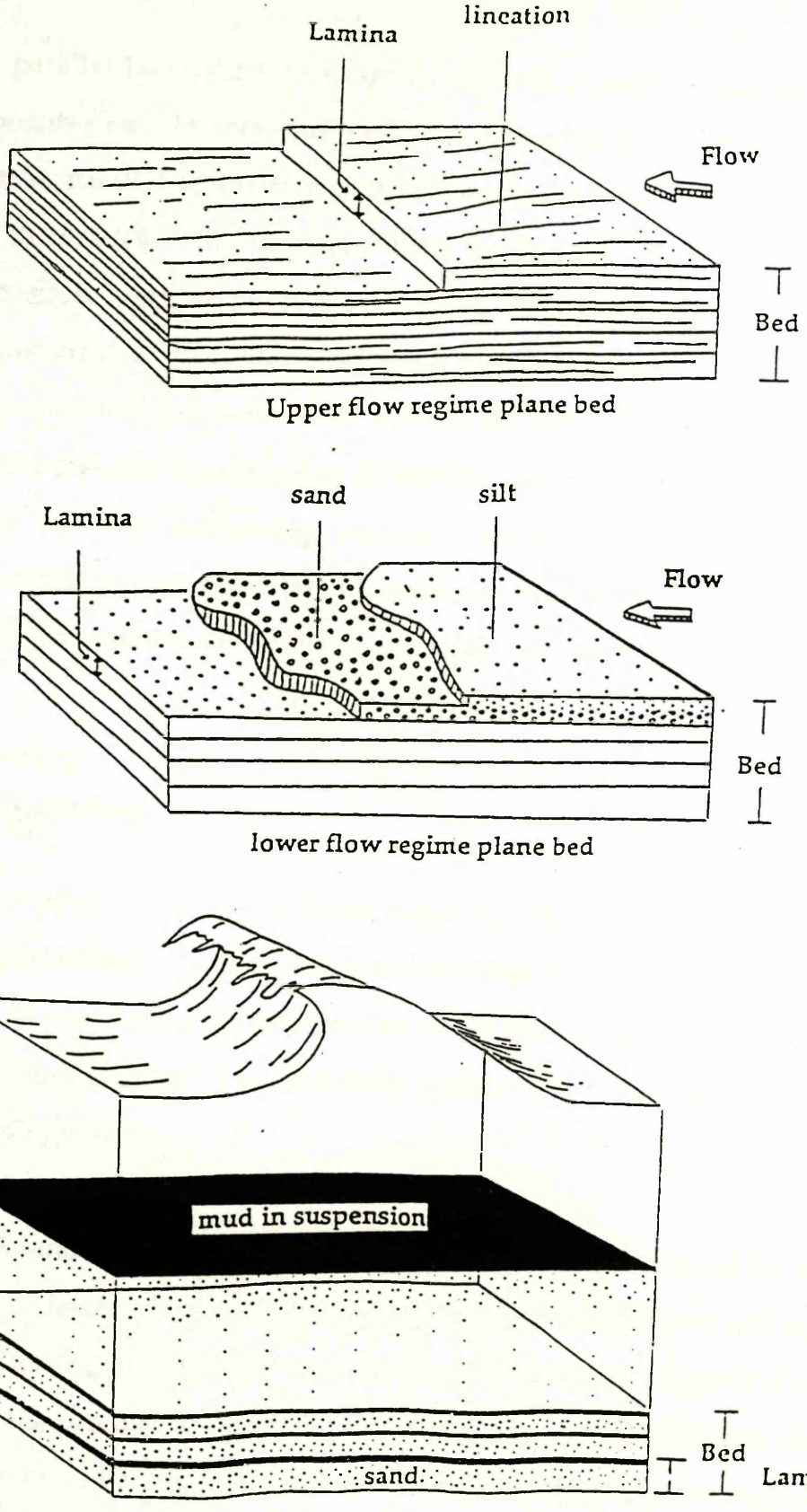

Fig. 2.11 Block diagram showing the different ways of producing parallel lamination.

Referring parallel lamination to a certain origin is a difficult and sometimes impossible task. In some cases it is not even possible to differentiate between true parallel lamination and low angle (inclined) stratification especially in core (eg. HCS; Lindholm 1987; see Fig. 2.5). Hummocky bed forms can grow very large both in height and width. The distance between the crest of two hummocks can reach 10m and their height (swale to hummock) can reach 0.6m (Dott *et al.*, 1982). Thus we have to bear in mind that the identification of parallel lamination based on core observation could be misleading because what appears to be parallel lamination could be a part of a large hummocky bedform which we failed to identify in the small width of the core sample (see Fig. 2.5).

2.2.4.2 Interpretation:

The origin of parallel lamination in this facies is attributed to the effect of storms which eroded, transported and deposited sand from turbulent suspension. It was deposited between the lower shore-face and off-shore transitional environment. The following points are in support of the above interpretation:

(1) The sandstone in this facies is too uniformly fine grained to be the product of lower plane bed conditions and the mud laminae are not likely to reflect tractive currents. The absence of lineations suggests that they are not the product of upper flow regime conditions required for the development of upper regime plane bed. Thus the simple flow regime concept cannot be applied in this facies. However, parallel laminated sand can occur at considerable water depths below the effect of normal wave

influence, in areas with low sedimentation rates. In the North sea, parallel laminated sands are reported from shelf muds of the Busum region 30km from the shore-line and in water depths ranging from 15–40m (Reineck *et al.*, 1980). During storms the resulting turbulence renders much sand into suspension. This is transported to off-shore areas by the returning water currents after a hurricane or a storm, and redeposited as parallel laminated sand from suspension clouds (Reineck & Singh, 1972). Aigner & Reineck (1982) suggested off-shore directed gradient currents as a depositing mechanism of the parallel laminated sands, in which sands are carried and deposited from suspension clouds below fair weather wave base. Such currents are produced by the hydraulic gradient developed in response to the water piled along the coastline during storms (Allen, 1982b).

(2) The sharp erosive bases to sandstones cutting into underlying muds and bioturbated horizons indicate rapid deposition of sand in a quiet muddy environment. The scarcity of bioturbation in an otherwise biologically active environment also supports the idea of rapid deposition. However, time and thickness are other controlling factors. Howard,(1975) stated that the chance of an organism to penetrate a newly deposited unit is inversely related to the thickness of that unit. He suggested a limit of 30cm above which little bioturbation is seen except in the upper few cm of the bed and below which bioturbation might destroy the rapidly deposited unit by the re-establishment of organisms on the surface or their movement upwards from below. However, if not enough time is given such a process will be ineffective.

(3) The presence of parallel lamination in the vicinity of (HCS), and in some instance in association with it, supports the idea of a storm affinity and thus deposition from suspension.

(4) The common presence of relatively thick amalgamated sections of parallel laminated sand throughout the sequence, suggests that most deposition of facies (D) was probably in the lower shore-face environment where such deposition is common (Brenchley, 1985; Aigner, 1985) .

(5) The interpretation of the facies is consistent with the shoreface origin of related facies

2.2.5 Facies (E) Shale and sandstone interlaminated facies:

This facies is absent in the northeastern part of the area (well A13). It represents a total thickness of 7.5m and comprises 5.3% of the total core section and consists of interstratified shale and sandstone (Plate 2.10). The shaly beds are very dusky red (10R2/2) in colour; moderately fissile and bed thickness averages 2cm and ranging from 0.4-8cm (Fig. 2.12). X.R.D analysis shows the shale to consist of the minerals kaolinite, mica, quartz and siderite (Fig. 2.13), mica being visible to the naked eye. The sandstones are very light gray; wavy bedded; very fine grained, ranging from 0.086–0.112mm with an average grain diameter of 0.100mm. They are moderately to well sorted, grains are subrounded (visual estimation) and bed thickness averages 0.6cm ranging from 0.5-4cm (Fig. 2.12). Sandstone is a minor constituent of the facies forming 20% by thickness, and sand to mud ratio is 1: 4. Generally bioturbation is sparse, and mainly concentrated in the sandy parts of the facies, being estimated to be 20% or less of the total facies thickness. The shale beds are generally massive but

graded bedding and very fine stringers of silt are also present. Bioturbation is mainly restricted to the uppermost parts of some beds.

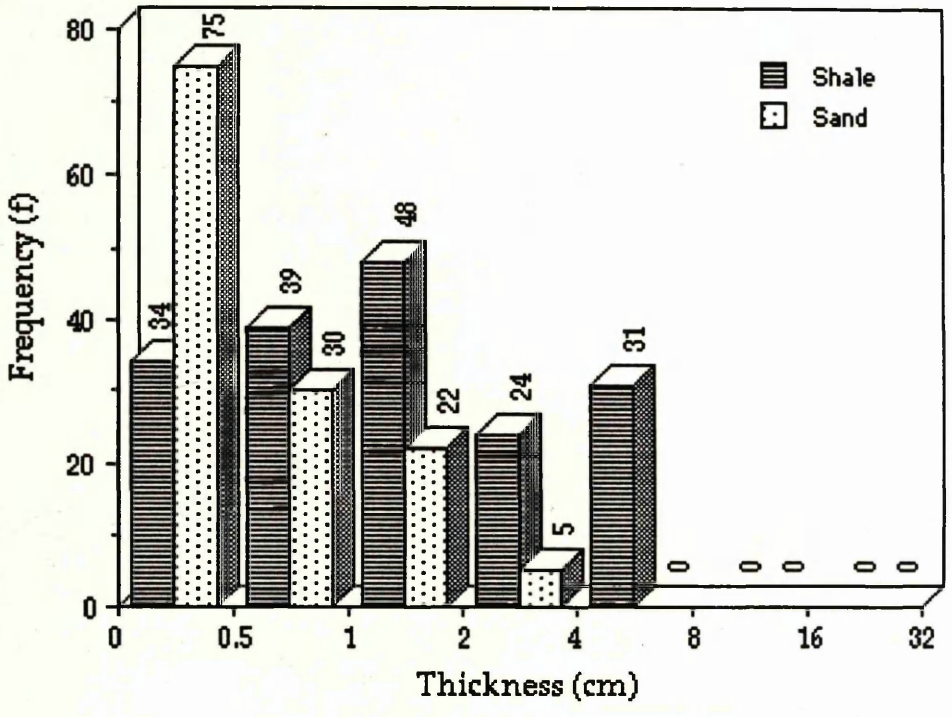

Figure 2.12 Histogram showing thickness frequency distribution of shale and sandstone beds of facies (E). N.B. The programe used to generate this graph presents classes as isolated columns. In reality data form a continuous series.

The associated sandstones are slightly to moderately bioturbated and either massive, suggesting rapid deposition from a decelerating current, or ripple laminated, indicating wave and current reworking. The lower boundaries of the sandstone units are sharp and load structures are observed at the bases of some beds, suggesting sudden input of sand on a semi consolidated muddy substrate and supporting the view that their massive structure could be related to rapid deposition. However, load structures are also observed at the bases of some rippled beds. This is due either to rapid deposition from rippled phase flow or to reworking of an originally massive bed.

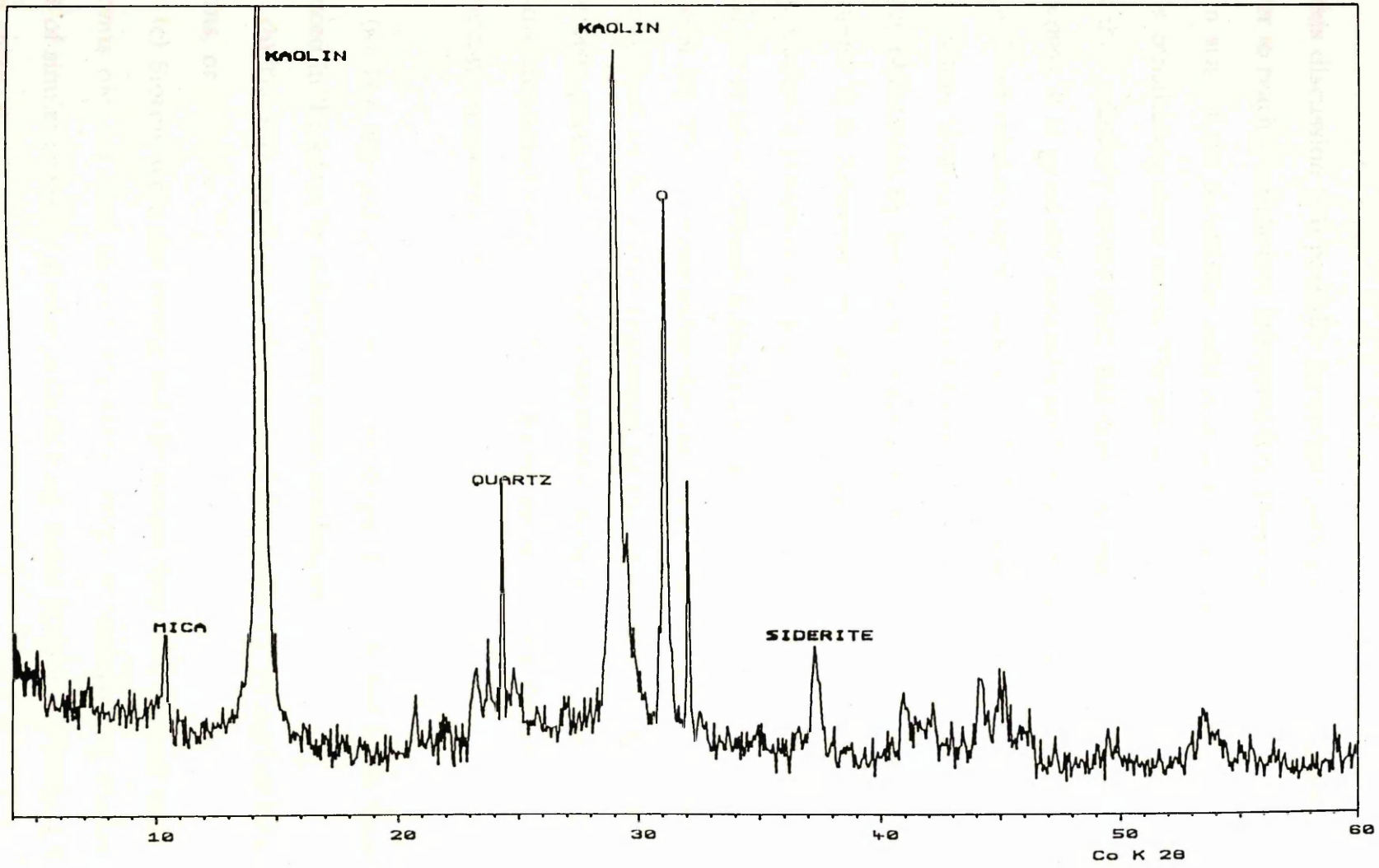

Fig. 2.13 X-ray diffraction pattern showing minerals kaolinite mica and quartz (facies E)

2.2.5.1 Discussion:

In this discussion two partially dependent points must be considered in-order to reach a satisfactory interpretation. These are: the thickness and grain size of the sandstone units and lack of bioturbation in the shaly units constituting these sands. The peculiar thing about the sandstones is that their relatively coarse grain size does not seem to fit with their small thickness. It is generally noticed elsewhere in the section that grain size has a direct relationship to thickness (Fig. 2.14; see also Figs. 30, 33 & 39). In addition, although the sandstone beds are thin enough to have been totally obliterated by benthonic organisms little bioturbation is observed in them. It is however, characteristic elsewhere in the section that bioturbation is inversely related to bed thickness and that wherever the thickness of beds increases bioturbation decreases (Fig. 2.15; see also Fig,s. 30, 33 & 39). This suggests either that the environment was not suitable to be inhabited by benthonic organisms or that the thin sandstone units have been protected from bioturbation by a thick unit of mud which was rapidly deposited on top of them. Based on the above discussion the following suggestions are made.

(a) The thin sandstone beds were originally thick but have been reduced in thickness by subsequent storm erosion, or

(b) The thin sandstone beds represent deposition by strong but brief storms, or

(c) Storms were not strong but the source was near so that storm currents did not need to exert the same energy in transporting thicker beds of similar or nearly similar grain size (eg. facies B & D) (see Table. 2.5 for a comparison), or

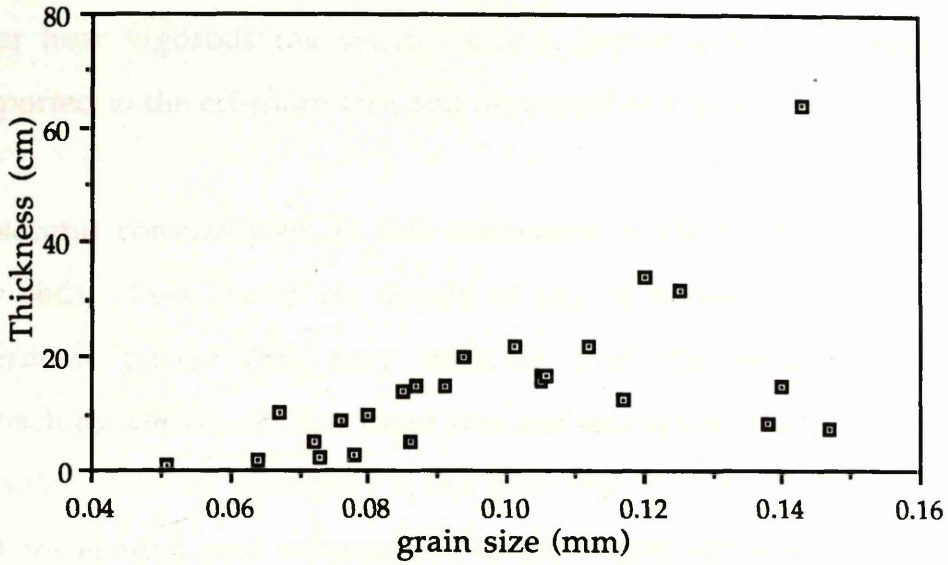

Figure: 2.14 Diagram showing the relationship between grain size and thickness of the sandstone units in facies E in the type well A8–NC7A. Sandstone units of this facies and subfacies F2 are not plotted on this diagram (see description of subfacies F2)

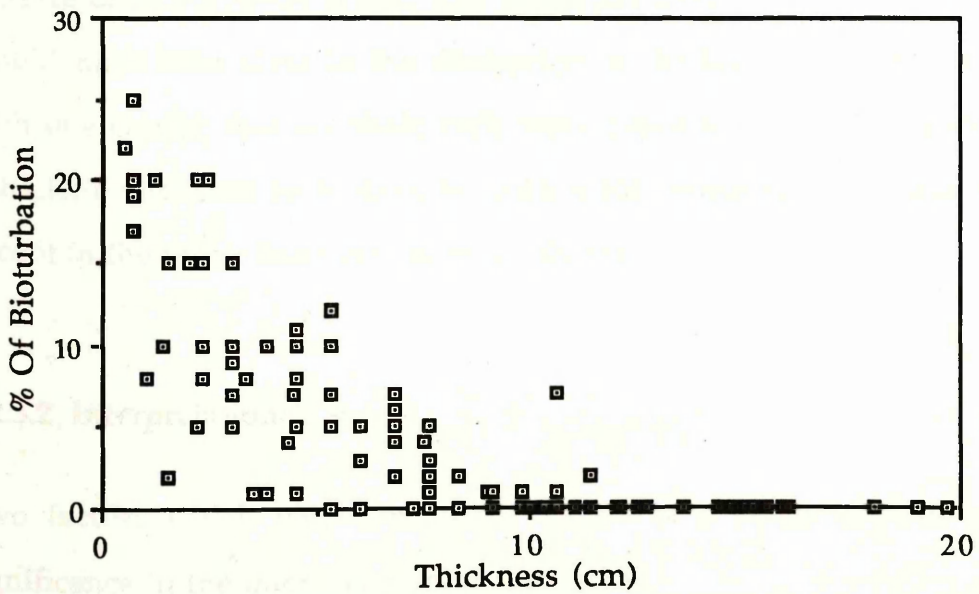

Figure: 2.15 Diagram showing the relationship between thickness of sandstone units and percentage of bioturbation in facies E in the type well A8–NC7A. For the sake of simplicity, beds less than 3cm thick are not all included

(d) The coastal area was dominated by mud deposition so that no matter how vigorous the storms only a limited amount of sand was transported to the off-shore area and deposited as a thin layer.

The second consideration in this discussion is the slightly bioturbated shaly beds. These shales are devoid of any bioturbation except at their uppermost parts. This may indicate that the environment was approaching anoxia, or that there was not enough time for bioturbation to develop. Another possibility is that bioturbation did take place but very rapid re- erosion and redeposition of sediments obliterated traces and deposited layers which were too thick to be later re-reworked by benthonic organisms. The idea of anoxia can be ruled out because the relatively coarse grain size of the associated sands suggests that they were unlikely to have been transported to such distal areas of the shelf. The absence of bioturbation is real. The shales are laminated and bioturbation would have been clear in the disruption of the laminae. This leaves us with one choice, that the shale beds were deposited so rapidly and with sufficient thickness as to give no chance for bioturbation to take place except in the upper few centimetres of the bed.

2.2.5.2 Interpretation:

Two factors which may control the nature of a storm deposit are of significance in the interpretation of this facies:

(a) The direction of storm generated currents with respect to the shore-line. The dispersal path of sediment need not lie perpendicular to the trend of the shore-line. It may lie at some angle to it.

(b) The storm may affect an area off-shore more than an area on-shore. As a result a sediment source for storm deposits may lie some distance from the shore-line.

With respect to facies E the thick mudstone storm layers may have been re-sedimented from an area well off-shore, or at least if onshore, from an area dominated by mud; sand was only a minor constituent. The following points suggest that deposition was probably in a shallow marine near-shore environment in which storms were frequently striking a muddy shore-line carrying lots of mud in suspension and that sand was only a minor component of the coastal area:

(a) The presence of coarse mica flakes visible to the naked eye (less than 1mm) within the shaly beds. These suggest that the mud was not part of the normal background sediment but was probably brought from near-shore areas by storm currents capable of carrying them to off-shore areas. Fine sediments in other facies are thought to have been made-up of background mud.

(b) The coarse grain size of the sandstone units relative to their thickness, and the associated thicker units of mud, suggests proximity to a muddy shore-line in which sand was a minor component of coastal sediments. therefore no matter how severe storms were only a limited amount of sand could be carried to the off-shore area and deposited as thin relatively coarse grained units of sand, probably succeeded by the deposition of a thicker unit of mud. The relatively weak bioturbation of

the sandstone units suggests that either immediately or shortly after deposition a thicker mud unit was rapidly deposited on top of the sand.

(c) The absence of intense bioturbation in an environment which seems to have been suitable for such biogenic reworking also suggests a near shore relatively high energy environment.

(d) The presence of bioturbation in the upper most parts of shaly units suggests rapid deposition of a thick unit of mud in which benthonic organisms were only capable of reworking the tops of beds. There was little time between deposition of successive beds, indicating a frequently reworked sea floor and hence inhibition of benthonic organisms.

(e) The common presence of ripple lamination suggests an environment which was shallow enough to be frequently reworked by waves and currents.

(f) The absence of facies E in the presumed basinal area (wellA13) (see lateral facies relationships in parasequence sets) also supports the idea of a shallow marine near shore environment.

2.2.6 Facies (F) Wavy bedded sandstone facies:

This facies consists of interstratified siltstones, sandstones, bioturbated sandstones, and mudstones. It is the volumetrically predominant facies of the Tahara Formation and forms almost the entire formation in the northeastern part of the the area (well A13). It represents a total thickness of 38m and comprises 30.6 % of the total core section studied. Average

grain size is 0.074 mm, ranging from 0.064-0.071mm. Sandstone beds range in thickness from 0.5 - 20cm with an average of 2cm (Fig. 2.16). In contrast, mudstone beds are thinner and range in thickness from 0.2 - 15cm with an average of 1.5cm. Sandstones are the major constituent and comprise 56% by thickness of the facies, sand to mud ratio is 1 : 0.7. Body fossils are absent and bioturbation is estimated to affect 35% of the total facies thickness. Physical structures include ripple lamination, horizontal lamination, and hummocky cross-stratification. There is, however, a variability in this facies related to bed thickness, percent of bioturbation, grain size, percentage of sand, and sand to mud ratio. The facies is subdivided into three subfacies, F1, F2 & F3. The nature of the contact and the number of times these subfacies are in vertical contact with each other is shown in table. 2.3.

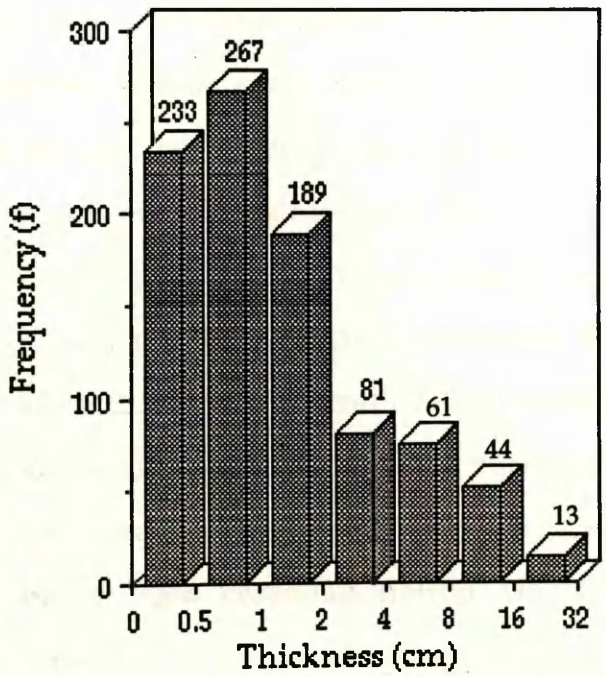

Figure. 2.16 Histogram showing thickness frequency distribution of the sandstone units of facies. (F). N.B. The programe used to generate this graph presents classes as isolated columns. In reality data form a continuous series.

2.2.6.1 Subfacies (F1):

Subfacies F1 consists of 9.7m of thinly bedded and interlaminated siltstones, sandstones, and mudstones. The sandstones are light olive gray to light gray in colour, very fine-grained (0.071mm), moderately-poorly sorted, with rounded-subrounded grains (visual estimation). Bed thickness is commonly 0.5 - 4cm with an average of 2cm (Fig.2. 17). Bioturbation is estimated at 10–15% of the section and both vertical and horizontal burrows are present with the last being less common. Sandstone is the major constituent and forms 70% by thickness of the facies, the sand to mud ratio is 2: 1. Internally the sandstones and siltstones consists of single or multiple sets of nearly horizontal to low angle, gently undulating, laminae and sets of small scale ripple cross lamination; parallel lamination is also present but is the less common (Plate.2.11 a & b). The sets of undulating laminae are commonly thicker and are characterized by low angle intersections between laminae, and erosive bases. Upper surfaces are either sharp or gradational (Plate. 2.11a). Thin layers of silt and mud often drape over the hummocks extend down to the swales where they commonly become thicker and more abundant (Plate. 2.11a). Sets are normally graded, indicating deposition from a waning current (Plate. 2.11a). A thin unit of mud usually mantles the top of such beds, probably deposited quickly from suspension. This structure is similar to the structure described by Harms et al. (1975) as hummocky cross-stratification. Ripple cross-lamination (Plate. 2.11a & b) is characterized by irregular, slightly undulating, lower set boundaries and foreset laminae tangential to lower bounding surfaces, probably indicating a wave origin (Boersma, 1970). Mud drapes are common and in some cases where full ripple morphologies are preserved extend over

the full width of the ripple, indicating a pause in sedimentation. The lower boundaries are sharp and beds grade from lighter (coarser) to darker (finer) upwards, indicating deposition from suspension followed by wave and possibly current ripple migration; sharp tops are also present. The flat beds are evenly laminated and show both reverse and normal grading (Plate. 2.11a). The sandstone beds are generally separated by thin wavy units (0.2-4cm, with an average thickness of 1cm) of very dusky red(10R2/2) to dark reddish brown (10R3/4) slightly bioturbated mud which undulate to conform with the upper surface of the under lying bed forms.

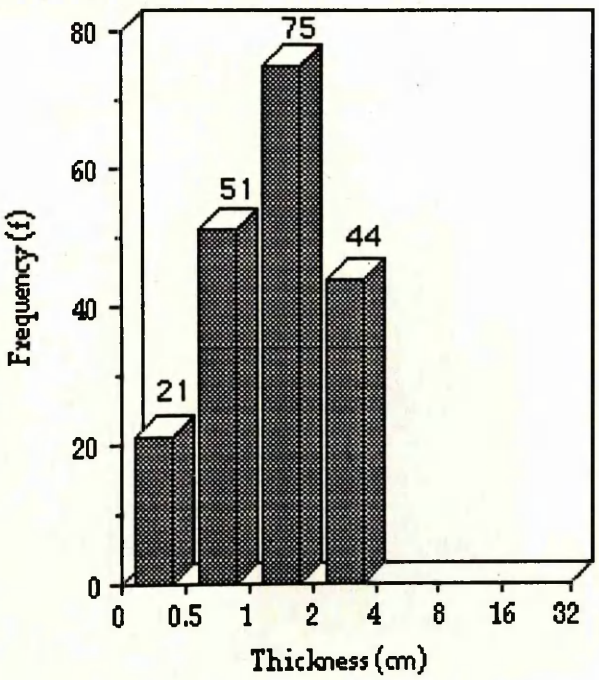

Figure 2.17 Histogram showing thickness frequency distribution of the sandstone beds of subfacies F1. N.B. The programe used to generate this graph presents classes as isolated columns. In reality data form a continuous series.

2.2.6.2 Subfacies (F2):

This subfacies (11.7m thick) can be identified by the lack of bedding structures, and heterogeneous mixing of mud and sand resulting from intense biogenic reworking (Plate 2.12a & b). The sandstone is light gray in colour, very fine grained, 0.087mm, moderately to poorly sorted, with subrounded-subangular grains (visual estimation). Bed thickness averages 5cm, and ranges from 0.7-20cm (Fig.2.18). However, the measurements of thickness in this facies are not precise due to bioturbation which mixes and obliterates stratification thus making it difficult to recognise individual beds. As a result, several thin homogenised beds are measured as one thick unit and the figure given here for thickness is probably much higher than the original. A few thin isolated mudstone beds occur between the bioturbated muddy sandstones.

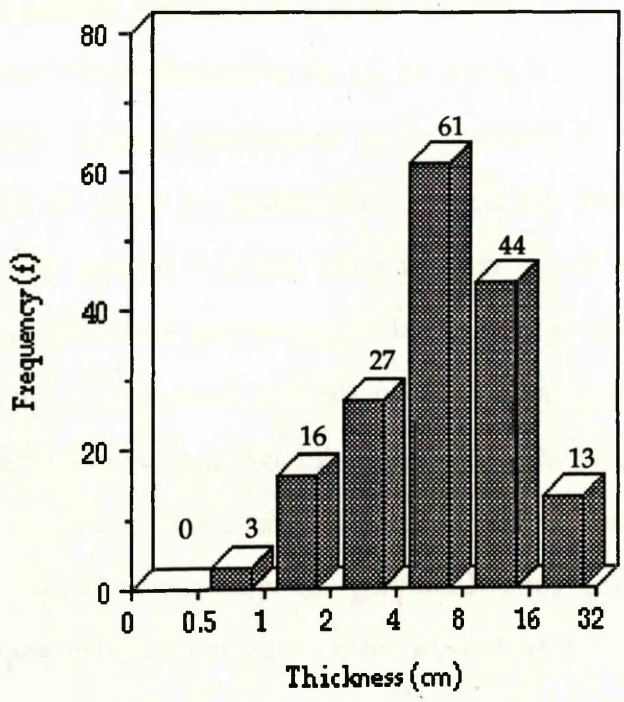

Figure 2.18 Histogram showing thickness frequency distribution of the sandstone beds of subfacies F2. N.B. The programe used to generate this graph presents classes as isolated columns. In reality data form a continuous series.

Although not always the case commonly each cycle of biogenic reworking starts with a bioturbated slightly sandy mudstone and increases upwards in sandstone content. The sandstone content then decreases and the cycle ends up with mud as it began. The mud units range in thickness from 0.5 – 15cm, with an average of 3cm. Bioturbation is the most characterizing feature of this subfacies, estimated to affect 80% of the total thickness of the facies (mostly of the deformative type). Sandstone comprises 65% by thickness of the facies. Some stratification remains visible within the bioturbated muddy sandstones. This remnant stratification commonly occurs as 2-3cm, thick sets of (probably) hummocky cross-stratification.

2.2.6.3 Subfacies (F3):

This subfacies resembles subfacies (F1) in both bedding style and sedimentary structures (Plate. 2.13 a & b). It represents a total thickness of 15.5m and differs from subfacies F1 by its finer grain size, 0.064mm as against 0.071mm, thinner sandstone units 0.2-4cm as against 0.5-4-cm, with an average of 0.6cm as against 2cm, (Fig.2.19). Mudstone units, are thicker 0.2-6cm as against 0.2-4cm with an average of 1.5cm rather than 1cm. There is an increased percentage of bioturbation 25-30% as compared with 10-15%, and a decreased percent of sand 35% compared with 70%. The sand to mud ratio is reversed 1:2 against 2:1. The reduced thickness of sandstone units and increased bioturbation of this subfacies have affected the definition and continuity of physical sedimentary structures. Hummocky types of structure are almost absent and ripple lamination is less in abundance (dominated mainly by starving ripples). In contrast, parallel laminated sandstones with graded rhythmites are relatively more common (Plate. 2.13a). In many parts, this subfacies is better described as a

sandy mud rather than an alternation of sand and shale, due to the increased amount of mud and bioturbation.

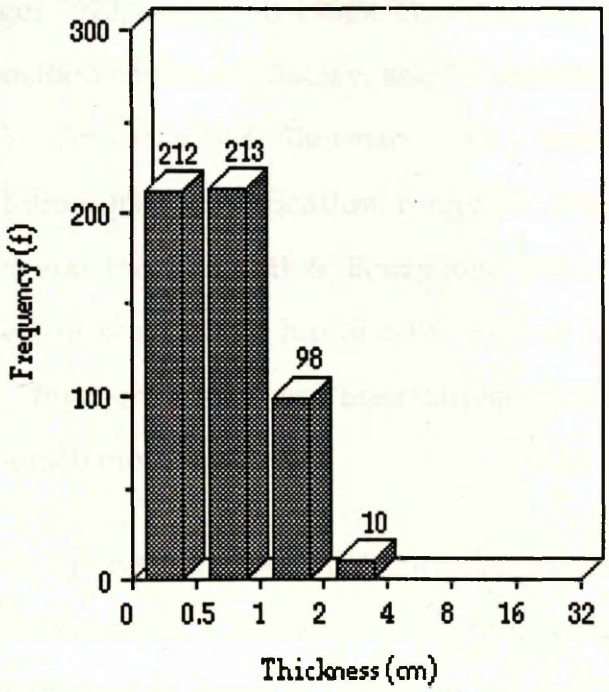

Figure 2.19 Histogram showing thickness frequency distribution of the sandstone beds of subfacies F3. N.B. The programe used to generate this graph presents classes as isolated columns. In reality data form a continuous series.

2.2.6.4 Discussion:

Rhythmic alternations of sandstone and mudstone are characteristic of a number of dissimilar environments including deep water turbidite fans, storm-dominated shelves, subaerial alluvial plains, and tidal flats. However, subaerial exposure indicators such as erosional surfaces, root structures, desiccation cracks and coal beds are absent. Hummocky cross stratification and wave ripples, indicate a relatively shallow, wave-agitated environment.

Hummocky bedding commonly occurs between off-shore laminated and burrowed siltstones and upper shore-face coarse sands. This suggests that it occurs in near-shore storm affected shelf environments, (Howard 1972; Goldring & Bridges 1973; Bourgeois 1980). This structure represents upper flow regime deposition under oscillatory, and/or combined-flow currents (Swift *et al.*, 1983 ; Greenwood & Sherman, 1986 ; Arnott and Southard 1990). Beds of hummocky stratification range in thickness from few centimetres to several metres (Dott & Bourgeois, 1982). The hummocky beds of this facies differ from the hummocky beds of facies (B) by their smaller thickness, finer grain size, and the relatively increased percentage of mud and of bioturbation.

Symmetrical wave ripples are reported from depth's exceeding 200m on the Oregon continental shelf. Calculated current velocities during storms are found to be sufficient to produce ripples in up to 100m of water and occasionally 200m (Komar et al., 1972). Wave ripples can also be the result of reworking during fair weather conditions, waning storm, or minor storm conditions (Simonson, 1984).

The normally graded sandstone beds with parallel lamination were probably deposited from suspension clouds in a waning storm flow at current velocities below those necessarly for the genesis of ripples (Reineck et al. 1972). The occurrence of reverse grading is due to "rapid rates of mud deposition in conditions of low bed shear and high concentration of mud before the arrival of the peak flood"(Reineck *et al.*, 1980)

The intense bioturbation of subfacies (F3) probably had more to do with the time available for biogenic activity per unit of accumulated sediment

than with the animal density (Howard. 1975). In the Gulf of Gaeta, Italy the animal population in the shelf mud is very sparse. However, the degree of bioturbation is extreme. In contrast, shelf muds of the North Sea (south of Heligoland) have an animal population which is very high but the degree of bioturbation is only moderate (Reineck *et al.*, 1980). Several factors including oxygen concentration, substrate continuity, and bathymetry may control the type and extent of bioturbation. For instance as dissolved oxygen decreases, the benthos becomes less diverse, less abundant, smaller in size, and dominated by endobenthos (Bromley. 1990). Substrate is another important controlling factor. It determines why and how animals burrow and is thus a limiting factor on the species present in the community (Bromley 1990). Some trace fossils have bathymetric significance. The aftermath of storms may provide a substrate which favours higher energy, Skolithos-type, tracemakers in a zone otherwise characterized by lower energy, Cruziana-type tracemakers (Pemberton et al. 1984a). Thus bathymetric interpretations cannot be made independently of associated physical and biological evidence. Generally bioturbation decreases with increasing wave and current energy which in contrast physical sedimentary structures increase (Purdy 1964).

2.2.6.5 Interpretation:

From the above discussion the main deposition of facies (F) was probably in an off-shore transitional environment between fair-weather and storm wave base, where normal sedimentation was from suspension but where the bottom was frequently affected by waves and currents. The high percentage of sand, the relatively increased bed thickness, the abundance

of wave generated structures with sharp bases, the presence of escape structures, and the minimal amount of bioturbation in subfacies (F1) suggest that this was deposited in a relatively high energy environment compared to the other two subfacies. This was an environment which probably between the lower shore-face and upper offshore-transition (Fig. 2.20). Sand was frequently brought in by storms of variable strength (Fig.2.17) and moulded into a series of sedimentary structures by a combination of processes including:

-1- storm induced currents which deposited hummocky bedding and parallel laminated sand

-2- gentler (fair-weather) mild storms which formed ripple bedding. Mud was deposited from suspension either as background suspension sedimentation and/or very rapidly during the waning stages of storms.

The decreased abundance of sedimentary structures (HCS is almost absent), the increased percent of bioturbation, the finer grain size and pronounced decrease in sandstone percent (30%), together with the presence of thin graded and sharp based beds also suggest a storm origin for subfacies (F3). However, this was in a sea ward environment with respect to subfacies (F1) (Fig. 2.20) where sand rarely invaded the depth barrier. This subfacies could be analogous to the distal tempestites of Aigner & Reineck (1982).

Subfacies (F2) was probably deposited in an environment intermediate between the deeper less oxygenated and biologically less productive environment of subfacies F3 and the more highly energetic environment of subfacies F1 (Fig. 2.20), an environment which was prone to intense biogenic reworking. The few preserved occurrences of hummocky cross-stratification in this subfacies suggest that sandstones

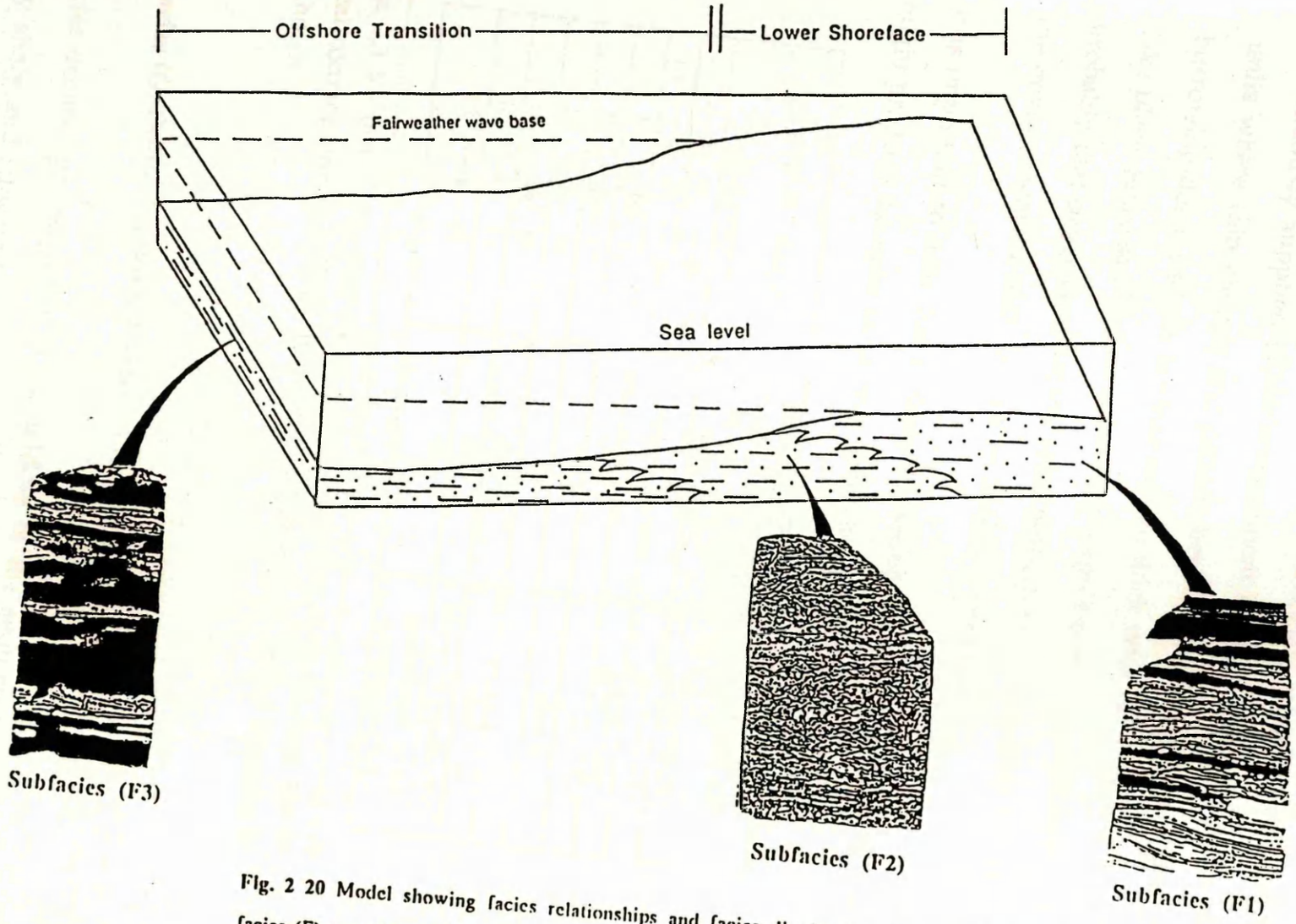

Fig. 2 20 Model showing facies relationships and facies distribution of the three subdivisions of facies (F) namely subfacies F1, F2 & F3.

which have been bioturbated by organisms were originally emplaced by storms. The scarcity of thick mudstones between the bioturbated muddy sandstones and the complete biogenic reworking, suggest that sand was continuously supplied to the environment in such a way that the sand units where thin enough and periods between storms long enough that burrowing destroyed the laminae and no thick mud accumulations could take place. Since sand was continuously supplied to the environment it is probably that oxygenated waters were brought simultaneously in making the environment suitable for intense biogenic reworking.

It is important to note that a change in sediment supply and/or climate might produce the same facies in a different position on the shelf.

VERTICAL FACIES TRANSITIONS	PERCENTAGE OF TIMES THE FACIES ARE IN VERTICAL CONTACT	NATURE OF CONTACT
F1 → F2 → F3	8	gradational
F3 → F2 → F1	10	gradational
F1 → F2	0	---
F1 → F3	15.7	sharp
F2 → F1	0	---
F2 → F3	26.3	sharp
F3 → F1	10.5	sharp or gradational
F3 → F2	13.5	gradational or less commonly sharp

Table 2.3 Vertical facies transitions and the number of times they are in vertical contact (converted to a percentage). The nature of the contacts is also shown.

2.2.7 Facies (G) Oolitic ironstone facies:

This facies occurs approximately in the middle of the sequence from a generally shaly and silty unit bellow to a clean and sandier unit above.

However, in the north-east of the area (well A13) there is no sandstone overlying the oolitic ironstone facies. The facies represents a total thickness of 3m which is 2.5% of the total core section. It consists of massive very dark red (5R2/6) beds (Plate 2.14 a & b) 0.5-5cm thick, (Fig. 2.21) consisting of kaolinitic siderite identified by (XRD) (Fig. 2.22) with scattered elliptical berthierine ooids (Plate 2.15) and elongate poorly sorted quartz grains.

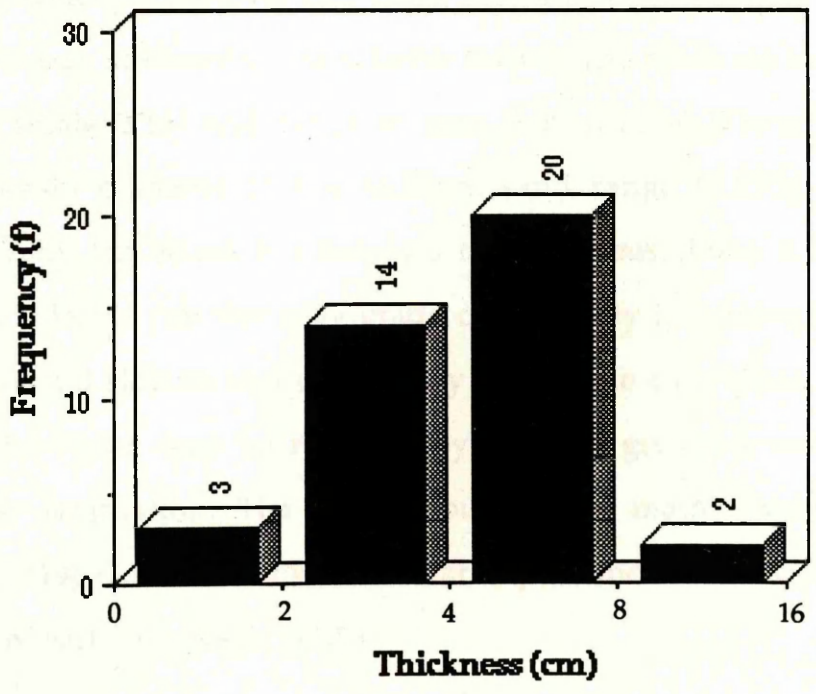

Figure 2.21 Histogram showing thickness frequency distribution of the sideritic beds of facies (G). N.B. The programe used to generate this graph presents classes as isolated columns. In reality data form a continuous series.

The facies is extensively bioturbated with vertical burrows 2-8cm long and 0.5-1.5cm wide probably made by *Skolithos*-type trace makers (see Plate 2.14 a & b). Articulated brachiopod shells (Plate. 2.16) are also recorded in this facies indicating marine conditions, since they occupy relatively narrow normal marine salinities (Johnson *et al* ., 1986). In the SW of the area (well A8) the facies is interbedded with a few, relatively

thin, sharply based, hummocky cross-stratified sandstone beds (Plate 2.14b). Many mudstones have scoured bases, in some instances with basal lags overlain by mud deposition. These suggest that storms have activated areas where sand was probably absent.

Observations on the nature of the ooids is derived from scanning electron microscopy, microscopic and macroscopic examination. Ooids are concentrated in burrows and along the surfaces of sideritic beds and are less densely scattered in the sideritic matrix. The ooids are well-sorted, elliptical (Plate 2.15) and range in size from 0.125-0.275mm, with an average grain diameter in the medium sand range (0.250). They are concentrically laminated but have no clear nucleus (Plate 2.15). Ooids contain a sideritic rim that may grade centripetally into mixed layers of berthierine and siderite or a dominantly berthierine core (plate 2.17). The entire ooid cortex may be replaced by siderite, giving a well defined concentric lamination. The ooid population is mainly siderite rich. Kearsley, (1989) showed for a similar replacement that siderite was probably of early diagenetic origin.

2.2.7.1 Discussion:

Phanerozoic ironstones have been studied for the past 125 years but there is no consensus regarding the mode of formation of the ooids which is essential for a thorough understanding of the origin of the oolitic ironstones (Bhattachrayya *et al.*, 1982). The majority of Phanerozoic oolitic ironstones were formed in shallow marine or brackish environments but pedogenic, reworked, and residual, oolitic ironstones are also described (Siehl *et al.*, 1989). Most oolitic ironstones formed in

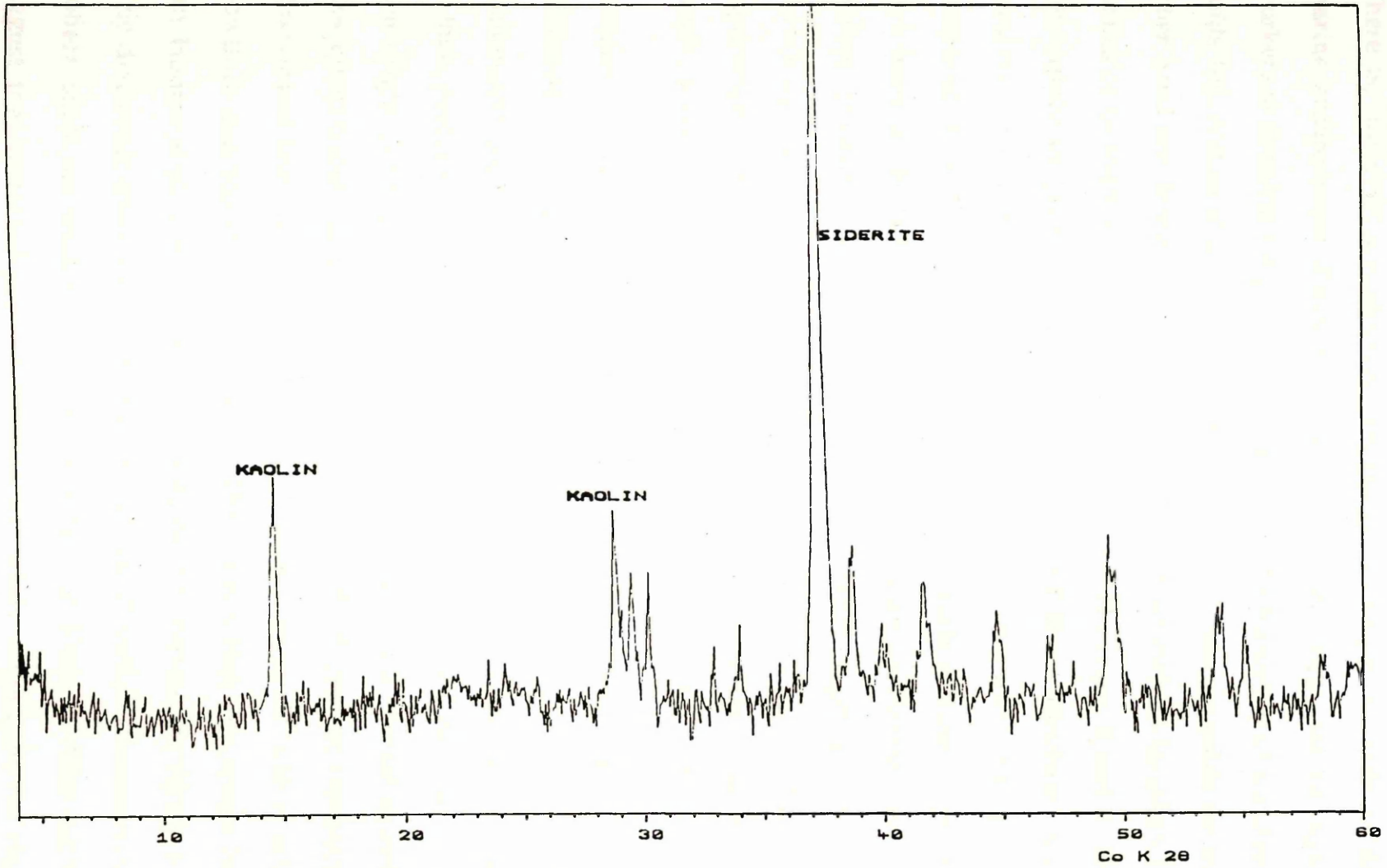

Fig. 2.22 X-ray diffraction pattern showing minerals siderite and kaolinite in the sideritic beds of facies (G).

tropical or subtropical settings (Van Houten & Bhattachrayya, 1982). There is, however, a controversy regarding the origin of ooids in the marine environment. Pedogenic ooids have been suggested by some workers as forming the precursor granules for the formation of ironstone ooids (eg. Nahen *et al.*, 1980; Siehl & Thein, 1989). Marine ooids on the other hand are thought to form on sediment starved shelves; in off-shore swales or in restricted lagoons (see Young 1989). However, it seems that the supply of both chemical components and final allochems was involved in the formation of some marine ironstones. These are composed in part of reworked terrestrial ferruginous allochems and in part from ooids generated from ferruginous granules formed in the marine environment from chemical components supplied by the reworking of terrestrial weathering products (Young, 1989). The requirements for formation include a pronounced reduction in sediment supply; adequate iron supply and physical reworking (Young, 1989).

Berthierine [$(Fe_{10}\ Al_2)\ (Si_6\ lA_2)\ O_{20}\ (OH)_{16}$] A. Hall (Pers. Comm.) and chamosite [$(Fe^{2+}{}_5Al)\ (Si_3\ Al)\ O_{10}\ (OH)_8$] are common constituents of Phanerozoic oolitic ironstones and have received much attention because of their problematic origin. Many hypotheses have been proposed for their origin. Among these are mechanical accretion of clay particles with subsequent transformation to iron rich phases, early diagenetic alteration of reworked lateritic ooids, replacement of calcareous ooids, and in situ growth of microconcretions (see Young, 1989). According to a review by Van Houten *et al.*, (1984) most workers agree that berthierine forms by early diagenetic alteration of a precursor material. Recent observations on modern shelf sea sediments in tropical areas (eg. Rude & Aller 1989) suggest that reworked lateritic particles are likely candidates for this

precursor. Chamosite on the other hand is believed to originate in the deep burial diagenetic environment (at a depth of 3Km) by the transformation of berthierine at temperatures of 150–160 °C (Iijima *et al.*, 1982; Curtis, 1985). In the wells studied however, depths range from 6601 – 5900ft (2.01 – 1.8Km) (see Table 1.1), this is above the depth required for berthierine transformation and thus the mineral incorporated here is probably berthierine and not chamosite. Differentiation between the two minerals is not possible by chemical means and a pure mineral could not be extracted for XRD analysis.

2.2.7.2 Interpretation:

The essential condition for the growth of ironstone ooids is the absence of terrigenous sediment supply so that the accumulation of iron is not swamped by other sediments. In the present example a reduction in the volume of terregenous sediments might have been brought about by a sea level rise or a shift in the sediment source. The latter is more likely accepted because of the abundance of *Skolithos* which is characteristic of moderately to relatively high energy conditions (lower littoral to infra-littoral) (Frey *et al.*, 1990). Although isolated Skolithos may occur in the proximal parts of deep sea fans (Frey *et al.*, 1990) the abundance seen here suggests that the water was fairly shallow at that time. The presence of ooids concentrated in vertical burrows and along the surfaces of sideritic beds with both flat erosional and scoured bases suggests varying degrees of either reworking of in situ formed microconcretional ooids (see Young, 1989) or that ooids were transported by storms from a near by source, or both. If reworked ooids were transported did they form in the marine environment or were they derived from land?. With the

available data this question cannot be answered. However, the elongate angular poorly-sorted quartz grains associated with the ooids have been suggested by (Madon Mazlan, 1992) in a similar facies description as probably representing first–cycle fluvial sediments derived from land and hence hinting at a similar source for the associated ooids. Lateritic soil profiles were a possible source for the ooids on land. Under humid tropical conditions intense lateritic weathering results in the formation of ooids which are later incorporated in the marine sediments during the subsequent transgression (Madon Mazlan, 1992). The Tahara Formation was probably undergoing a similar or nearly similar transgression during the subtropical climatic period of the Late Devonian andearly Carboniferous (Stanley, 1986) at the time of the deposition of this facies.

2.2.8 Facies (H) Rippled sandstone facies:

Facies H represents a total thickness of 20.9m which is 16.4% of the total core section. It forms the main reservoir in the type well A8-NC7A. The facies is predominantly composed of sand (95% by thickness). It is confined to the upper part of the sequence and consists of continuous and vertically persistent rippled sandstone units separated by thin (0.1-1cm thick) layers of mudstone. In the NE of the area (well A13) the facies consists of cross bedded sandstone with superimposed small ripples at the top. The contact with the overlying facies is sharp and erosional, the lower contact is also sharp but the nature of the contact could not be determined because of core damage. The sandstone is light olive gray (5Y6/1), fine grained (0.08–0.144mm) with an average grain size of 0.111mm. It is moderately sorted to well sorted, with subrounded grains

(visual estimation). Single beds are commonly 0.5-24cm thick with an average of 7cm (Fig.2.23), bed sets can reach a thickness of 10m. Body fossils and bioturbation are absent. The sandstone units consist entirely of faintly preserved ripples and ripple lamination. Multiple sets of ripple bedding are stacked to form beds of variable thickness. Each single bed is separated from the next by a sharp surface draped by a thin layer of mudstone (Plate. 2.18). The time gap represented by these contacts cannot be determined. They may represent hours, days, months or even years. However, these contacts or surfaces present a problem. It is not known if the thin mud lamina overlying them is draping a rippled surface produced by accretion, or an irregular surface (which may occasionally resemble a rippled surface) produced by erosion. This problem arises from the fact that the sandstone units below these surfaces are almost strucurless probably produced by the rapid deposition of well-sorted sands in a mud free environment. Nevertheless, it seems that both types of surfaces occur and in some beds obviously mudstone laminae drape a rippled surface. However, the identification of ripple bedding in this facies is often based on the recognition of flaser bedding in which fine material (siltstone & mudstone) is deposited in the troughs of ripples (Plate. 2.18). Ripples seem to be bidirectional and form concordant. The presence of mudstone rip up clasts overlying the erosional surface probably indicates that these muddy layers were cohesive and were eroded. It is not clear whether current or wave action was the predominant process responsible for the formation of the ripples. However, the continuous stacking of ripples and ripple lamination throughout the facies suggests a predominance of waves over currents. The cross bedded portion of this facies consists of friable slightly coarser grained sandstone. The thickness of individual beds could not be

measured because of core damage (due to the friable nature of the sand). The distinctive bedding (Plate.2.19) was probably produced through megaripple migration.

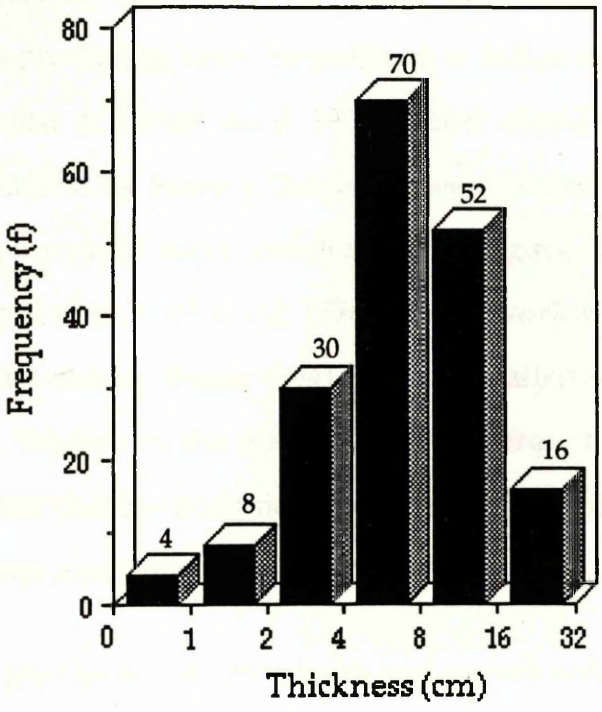

Figure 2.23 Histogram showing thickness frequency distribution of the sandstone beds of facies (H). N.B. The programe used to generate this graph presents classes as isolated columns. In reality data form a continuous series.

The small ripples superimposed on top of these beds are similar to those earlier described in this facies. The absence of storm features is probably due to the subsequent physical reworking by fair-weather wave action.

2.2.8.1 Discussion:

Bedforms and structures have been studied from a wide range of depositional environments including rivers, aeolian dunes, turbidity currents and coastal areas. There is a large volume of literature dealing with field, laboratory and theoretical studies, particularly concerning bed

forms generated by unidirectional currents (Davidson-Arnott & Greenwood 1976). There are however, comparatively few studies of bedforms produced under oscillatory flow conditions. This is probably due to the greater complexity of wave generated currents and the difficulty of reproducing such currents on a full scale in the laboratory (Davidson-Arnott & Greenwood 1976). Most studies of bedforms and structures produced by wave action have been carried out either seaward of the area where rapid wave transformation begins, or on the beach face (Davidson-Arnott & Greenwood 1976). Early work on the lower shoreface was carried out by Evans (1941) and a detailed study was made by Inman (1957). Studies in the inner near-shore area, have however, been very limited, the notable exceptions being those of Clifton *et al.*, (1971) on the Oregon coast and Reineck & Singh (1973) on the Mediterranean coast.

Ripple marks are the result of currents and waves acting on the sediment surface. Their genesis is controlled by the hydraulic regime which dominates in an area or by exceptional hydraulic conditions such as storms. Other factors influencing their nature include grain size, current velocity, water depth and sedimentation rate. Wavelengths can reach 60cm and wave height ranges from 0.5-5cm (Lindholm 1987). Above these values ripples are given different names (eg. megaripples and giant ripples). Ripples are mostly classified on their mode of origin, shape, and size. They can occur in a variety of shapes in response to different sedimentary processes, and hence shape can be used as an indicator of the conditions of deposition. The size of a ripple is mainly controlled by the current speed and wave period, and grain size; generally large ripples occur in coarser sand and small ripples in fine sand (Reineck *et al.*, 1980). However, ripples are most common in fine to medium sand but can also

be found in coarse sand (Reineck *et al.*, 1980). Wave ripples are distinguished from current ripples by the symmetrical shape of their crests. However, asymmetrical wave ripples are very similar to small current ripples and a distinction between the two is difficult and sometimes impossible. Nevertheless Boersma (1970) attempted to make such a distinction by characterising the features of wave ripples. Regardless of their external shape (symmetrical or asymmetrical), wave ripples usually contain unidirectional cross-lamination. Ripples are most abundant on beaches, intertidal flats, and in foreshore settings, with common occurrences in lakes, lagoons, upper shore-face, lower shore-face, and the off-shore transition zone (Reineck *et al.*, 1980). Megaripples, also known as dunes are dynamically different from small ripples, although they are similar in shape. Megaripples range in wave length from 0.6-30m and in height from 60cm-1.5m (Reineck et al.,1980). However, as stated by Sundbarg (1965) no definite forms intermediate between megaripples and small ripples exists. Furthermore Reineck *et al.*, (1980) showed that small ripples from a tidal flat environment were always less than 30cm amplitud and megaripples more than 60cm. Small ripples can be found superimposed on megaripples, as in the facies described here. Megaripples without such features are thought to be produced at higher energy (Reineck *et al.*, 1980). In sand of the same grain size megaripples are produced at higher energies than are required for the formation of small ripples (Reineck *et al.*, 1980). Thus, the cross-bedding of this facies was probably produced under higher velocities or energy conditions, than those forming small ripple bedding since the grain size of both is almost identical. Megaripples are most abundant in rivers, tidal channels and tidal inlets (Reineck *et al.*, 1980). Clifton (1972) and Davidson-Arnott *et al.*, (1974) showed that seaward-facing megaripples

are common structures in rip channels. Rip currents are competent enough to erode channels in very shallow water (<5m) and transport sand in suspension seaward of the breaker zone (Ingle 1966). McKenzie (1958) reported large rip currents in Australia flowing seaward to distance of 1.0-1.5km. Reimnitz and others (1976) proposed a rip current origin for the wave-rippled band, of coarse sand reported from the inner shelf off the Rio Balsas delta, Mexico. The bands were oriented normal to the shore-line and extended 1.5km off-shore to a depth of 30m. On the shore-face of Rhode Island and in water depths less than 10m Morang and McMaster (1980) reported the presence of shore-normal, wave-rippled sand strips and concluded that either rip currents or shore-parallel bottom currents were responsible. However, the main effect of rip currents is most probably the removal of sediment from the breaker zone to the upper shore-face (10m), where it is temporarily stored until transported seaward by other bottom currents (Field *et al.*, 1984). Rip currents are more effective during storms and hence are important in moving larger volumes of sediment during such periods .

In all sandy shore-face environments ripples are ubiquitous from just seaward of the breaker zone to the depth of fair-weather wave base. In a traverse off Virginia made in 1961, divers showed that the abrupt outer limit of active ripples coincides with the fair-weather wave base. Such ripple laminae have also been recognized and described in many ancient near-shore sedimentary sequences (eg. Cambell 1966). Nevertheless, ripples are most abundant in shallow water sandy environments (Reineck *et al.*, 1980). During fair-weather conditions oscillatory and shoaling wave processes operate on the lower part of the shore-face and breaker and surf zone processes on the upper part of the shore-face.

During such periods the resultant bottom current flow and orbital motion cannot move sediments beyond the shore-face, thus sand transport is probably limited to the shore-face region. Rip-currents and long-shore currents may operate on the upper shore-face but will be relatively weak during fair-weather unless the beach face is barred. Long-shore currents flow parallel to the coast in response to waves obliquely incident to the coast. Often, surf-zone processes entrain sediment and long-shore currents then transport it along shore (Komar & Inman 1970). The currents are strongest inshore from the breaker zone and are best developed in the troughs of long-shore bars if such exist. Long-shore currents commonly become rip- currents at breaks in such bars. During storm conditions shoaling waves, wind-driven currents, storm surge currents and enhanced rip currents erode the shore-face particularly the upper shore-face, and sediment eroded from it is either redeposited on the lower shore-face and beyond or carried landward into a lagoon.

2.2.8.2 Interpretation:

Facies H is interpreted to represent a high energy shore-face environment in which a near-shore bar is dissected by a rip channel (Fig. 2.24). The above interpretation is based on the following points:

(a) The abundance of wave ripple lamination throughout the facies probably indicates persistent wave action in the background, fair-weather facies, which is a characteristic of shore-face environments (Elliott, 1986)

(b) The relative increase in grain size of this facies in relation to the rest of the section can be taken as a criterion for the recognition of a shore-face environment ((Elliott, 1986)

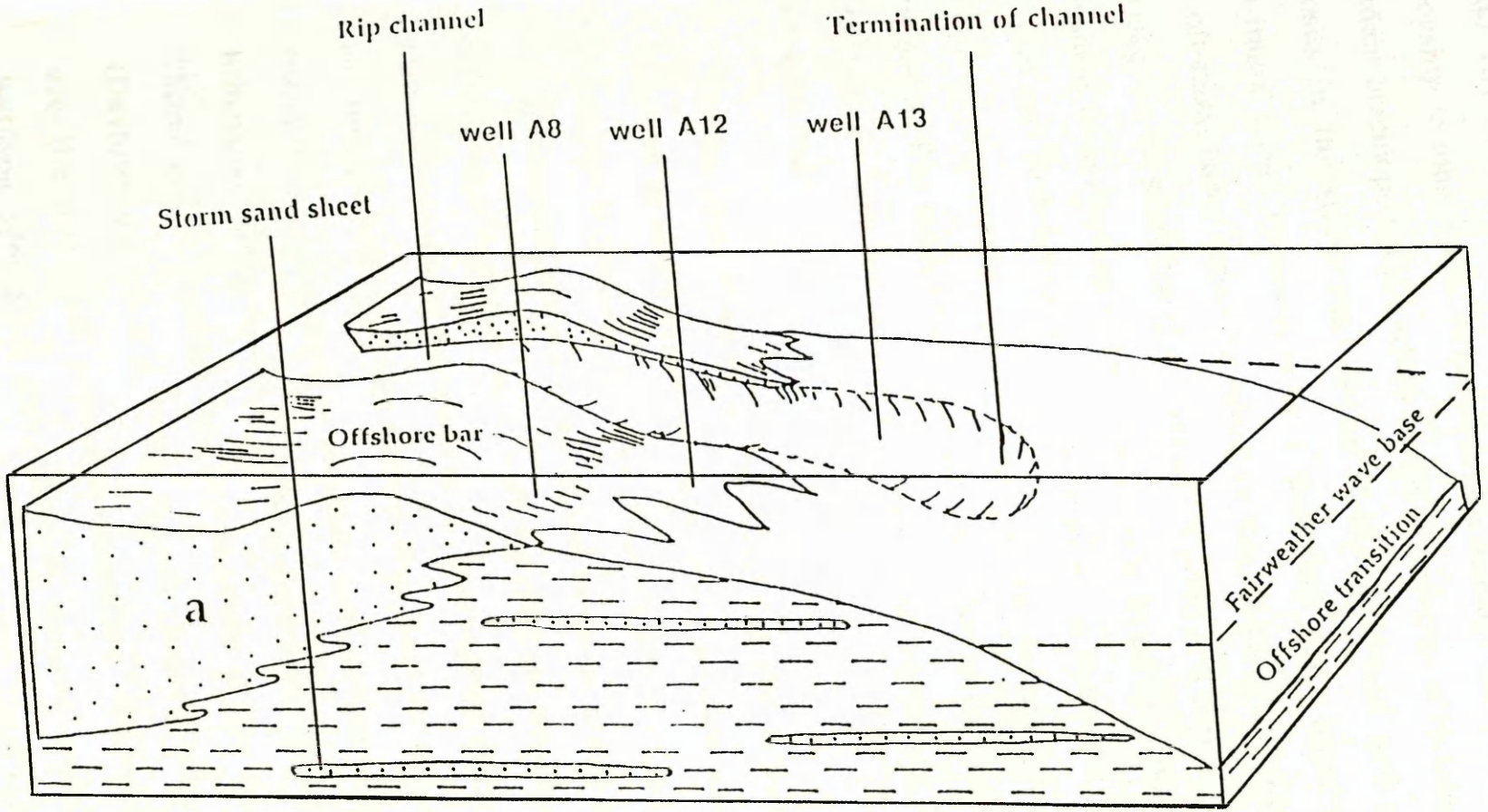

a=Shoreface– either sloping into the basin or forming an offshore bar (as in Figure)

Fig. 2.24 Block diagram showing the probable depositional environment of facies (H). See text for discussion.

(c) The interpretation of this facies is partly dependent on its relationship to other facies. Facies (I) which overlays this facies contains abundant brachiopod shells which would be expected to be found as lag deposits in the storm sand layers of the shelf-mud and off-shore transitional facies. However, none of these shell lags is found in any of the off-shore facies earlier described in this chapter. This leads one to envisage an off-shore bar (Fig. 2.24) which acted as a barrier, preventing the shells from reaching to the off-shore area. In addition the percentage of mud and bioturbation almost totally absent in facies (H), increases in the overlying coarser grained facies (I) (see description of facies I) suggesting that facies (I) was probably deposited in the relatively deeper waters of the back bar near-shore area and again supporting the idea of an off-shore bar.

(d) The series of wells A8, A12 & A13 (NE–SW) is thought to reflect a transition to an increasing off-shore (distal) position (see lateral facies relationships in parasequence sets). Thus one would expect an increase in the mud content and a decrease in bed thickness and grain size of sand from A8 to A13. However, in well A13 (NE) the lithofacies is relatively coarse grained and is characterized by cross bedding (Table 2.4).These facts led me to envisage a rip channel (Fig. 2.15) in which unidirectional currents are competent to transport sand further onto the shelf and achieve velocities capable of forming dune bedding. Velocities exceeding 75cm/sec are reported from rip channels of the Kouchibouguac Bay (Davidson-Arnott *et al.*, 1976). In such channels unidirectional currents are the dominant processes controlling sediment movement and bedform generation and oscillatory currents seems to be of limited significance (Davidson-Arnott *et al.*, 1976). Tidal features are absent in

this facies indicating that tidal effect were probably minor during the deposition of this formation. Consequently tidal channels or tidal inlets would be absent (as in the present Mediterranean) and thus a rip channel is most likely the environment of deposition.

Facies characteristics	Well A8	Well A12	Well A13
Thickness of Sandstone beds	10.7m	6.6	20cm?
Grain size	0.127mm	0.102mm	0.131mm
% of mud	3%	10%	0.5%
Sedimentary structure	ripple lamination	ripple lamination	Cross bedding

Table 2.4 Facies characteristics as they change from well A8 to well A13 in a probable offshore direction (see fig. 2.42).

The above interpretation leads to a further conclusion. Since the largest rip channels known extend seawards for distances not more than 1–1.5 Km (MeKenzie, 1958), and since the distance between well A8 and well A13 were the rip channel is intersected is 33.3Km, we conclude that the series of studied wells are not perpendicular to the shore-line and are thus oriented at some angle to it (see Fig. 2.24; see also Fig. 4.1). Consequently, the shoreline must have been oriented in an ENEWSW direction with respect to the NE-SW orientation of the wells

2.2.9 Facies (I) Fossiliferous sandstone facies:

This facies is restricted to the southwestern part of the area where it forms the uppermost part of the sequence in well A8. It is absent in wells A12 & A13. It overlies facies (H) through an erosional contact and represents a

total thickness of 3.9m, comprising 3.2% of the total core section. It consists of light gray to yellowish gray (5Y7/2) sandstone, fine to very fine-grained (0.120–0.140mm) with an average grain size of 0.135mm. It is moderately sorted with subrounded grains (visual estimation). Individual beds vary in thickness from 1.5–20cm with an average of 6cm, (Fig.2.25). Bioturbation is minimal, estimated to be 5% of the total thickness. Sand is the dominant constituent forming 90% (by thickness) of the facies.

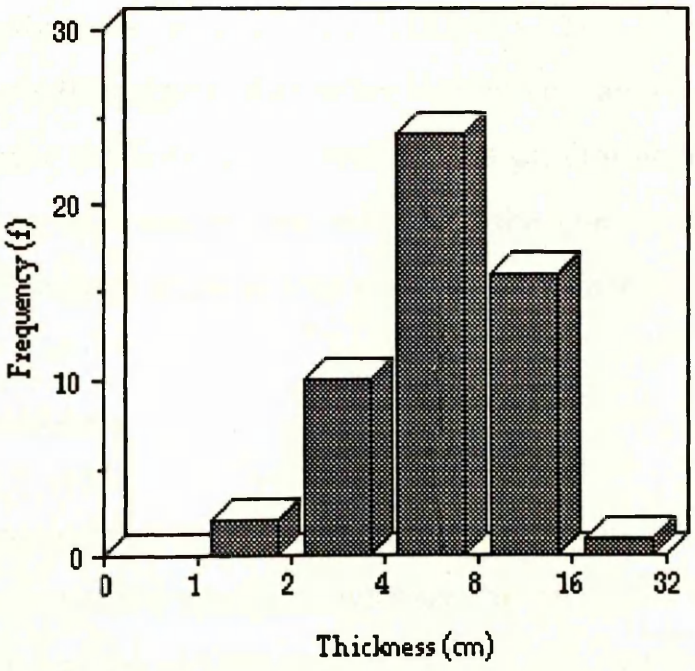

Figure 2.25 Histogram showing thickness frequency distribution of the sandstone beds of facies (I). N.B. The programe used to generate this graph presents classes as isolated columns. In reality data form a continuous series.

The sandstones consist of a basal lag of brachiopod valves and an upper laminated interval occasionally cross-laminated (Plate. 2.20 &2.21). Massive and ripple bedding are also present. Shells are also found scattered within beds. Lamination can either be very distinctive with a relatively clear separation into lighter (coarser) and darker (finer) layers,

or indistinctive showing very faint internal lamination (Plate. 2.20 &2.21). The lower boundaries to shell beds may appear gradational but the two units of sediment showing this boundary cannot be interpreted as the result of a single event. The shell bed may have produced sufficient turbulence in the current where it was emplaced to incorporate sediment from the underlying bed, so producing a gradational contact (Plate. 2.20 &2.21) Most brachiopod valves are disarticulated but unbroken and have a relatively high degree of sorting, with convex up preferred orientation of shells suggesting sorting by currents. The absence of broken shells, however, suggests insignificant transport. The predominance of brachiopod shells suggests that either storms activated a particular area (source) for the shells or we are looking at a general environment where only brachiopods lived, so that whatever the storms they could only transport brachiopod shells as they were the only ones around.

2.2.9.1 Discussion:

When making a paleoenvironmental interpretation based on body fossils it is very important to recognise whether the preserved fauna is in situ (reflecting the actual environment they lived in); transported to a new environment, or in a situation intermediate between the two representing in situ reworking of macrobenthonic organisms which are present in the area where they lived. "Repeated episodes of accretion and winnowing may however, result in the physical mixing of shells from different periods of accumulation" (Pickerill *et al.*, 1991). It is unusual to find an in situ fauna preserved within marine siliciclastic sediments, particularly siltstones and sandstones; instead, sedimentological and biological processes commonly transport and mix the macrobenthic fauna

to varying degrees (Pickerill *et al.*, 1991). However, significant transport and mixing of shells occurs predominantly in the near-shore zone (Aigner 1985). Fossils occur as sedimentary accumulations, which originate as a result of either biological and hydrodynamic processes (Pickerill *et al.*, 1991). The interpretive value of a fossil concentration can be defined by a range of preservational features, these are: (1) orientation (2) degree of articulation (3) degree of fragmentation (4) proportion of different elements of a skeleton (5) convex up to convex down ratio of shells (6) degree of abrasion, corrosion or bioerosion (7) type of shell-filling or coating (8) evidence of early dissolution of skeletons, and (9) any unusual features of preservation (Brett & Speyer 1990). Using four of the above preservational features (disarticulation ratio, re-orientation & sorting, fragmentation, and corrosion/ abrasion) Speyer and Brett (1988) have defined seven taphofacies on the bases of turbulence, sedimentation rate, and oxygen levels (a taphofacies consists of suites of sedimentary strata characterized by particular combinations of preservational features of the contained fossils (Brett & Baird 1986). They found that under conditions of extremely high turbulence, low sedimentation rate, and high oxygen levels, the four parameters (disarticulation ratio, re-orientation & sorting, fragmentation, and corrosion/ abrasion) where at their highest level (Tahpofacies 1) (Fig.2.26). In contrast the low turbulence, relatively low oxygen levels and higher sedimentation rates that characterize tahpofacies 7 are reflected in the low level of the four parameters (fig. 2.26). Between these two end members there exists a variable range of the four parameters. In the case of rapid transportation and deposition the concept of tahpofacies should be applied with caution because the several aspects of shell preservation (such as dissolution, breakage, and abrasion) are more a reflection of the original environment

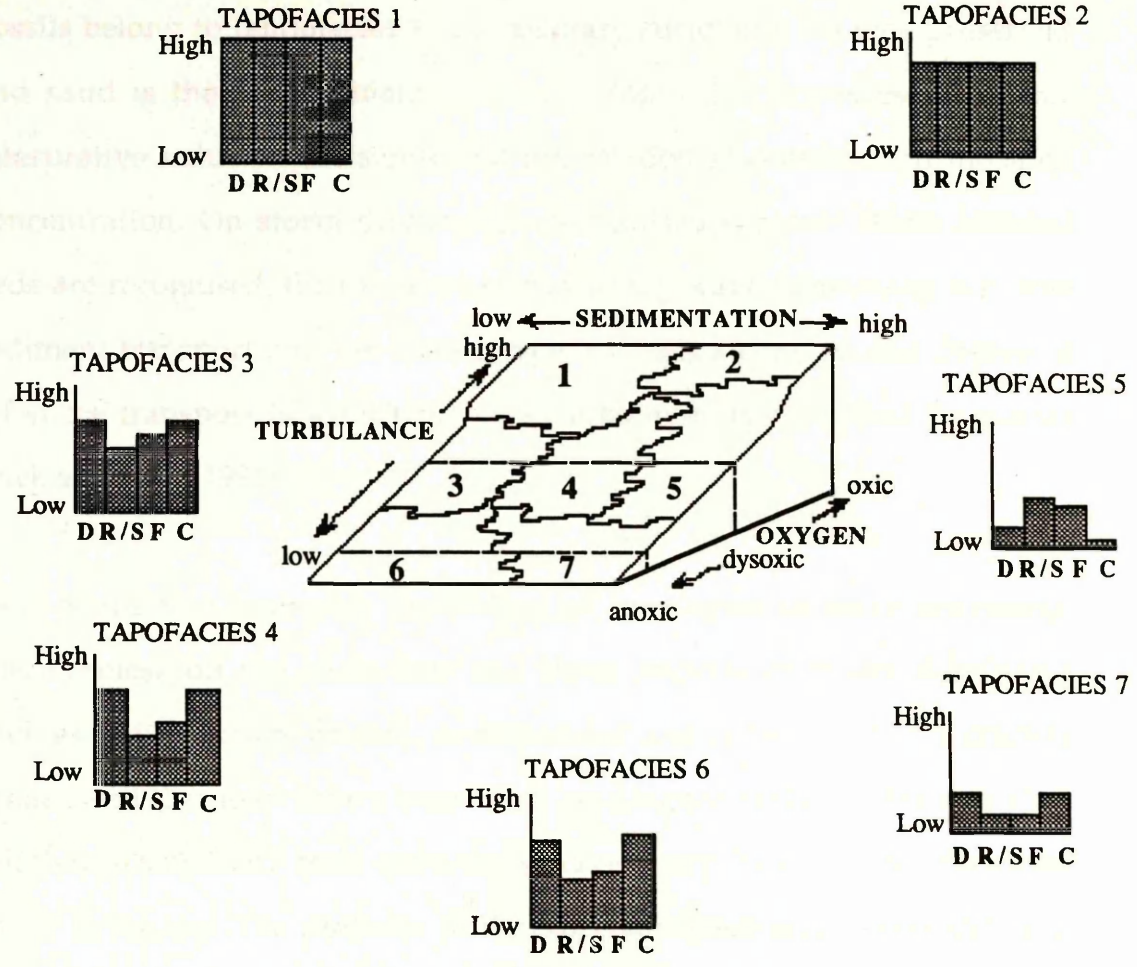

Figure 2.26 Diagram showing seven distinct tahpofacies differentiated on the bases of the following parameters: shell disarticulation (D) re-orientaion and sorting (R/S) fragmentation (F) and corrasion = Corrosion/abrasion (C). (Modified from speyer and Bertt, 1988; Brett and speyer, 1990)

of accumulation than of their final environment of deposition. The latter process is probably reflected in the size sorting, fabric and orientation of the shells (Davies, 1989). Norris (1986) defined three zones approximately corresponding to the shore-face, offshore-transtion and the offshore-shelf mud zone in which the relationship between the nature of the shell concentration and the hydrodynamics of the environment are clearly seen. In the near-shore zone (zone 1) the shells are repeatedly reworked.

Fossils belong to tahpofacies 1. Sedimentary structures are well preserved and sand is the predominant lithology. Zones 2 & 3 possess a greater interpretive value where significant information is contained in the shell concentration. On storm dominated shelves two types of storm affected beds are recognised: the first type shows strong wave winnowing but little sediment transport and the second type involves a considerable degree of off-shore transport of sand which was subsequently reworked by storms (Pickerill *et al.*, 1991).

Beds of the first type vary depending on the degree of wave reworking. Nevertheless on the shore-face and inner regions of storm dominated shelves sediments are eroded, re-suspended and redeposited as a crudely graded bed that may have a basal shell lag (Aigner 1982). On the mid shelf (offshore-transition) beds commonly have sharp bases with articulated shells at the top. The presence of thin discontinuous mud layers indicates repeated episodes of winnowing and sedimentation (Pickerill *et al.*, 1991). Still further off-shore shell beds become simpler, however, the bases are still sharp and are covered by a thin layer of finely comminuted shell debris commonly followed by an articulated shell layer and finally by a rapidly deposited (several cm's thick) layer of mud (Pickerill *et al.*, 1991). In deeper waters (shelf mud) the fossil concentrations are away from the reach of vigorous waves, thus the shell beds consist of pavements with commonly articulated shells which are thought to represent ecological beds which have been little modified by deep water storm waves (Pickerill *et al.*, 1991).

In the second type of storm influenced beds the shell concentrations usually occur as basal lags followed by sandstones of typically

characterized by hummocky cross-bedding, reflecting vigorous wave action. The taxonomic composition of the shell lag may be similar to that of the adjacent muds (Brenchley *et al.*, 1991), indicating a nearby sediment source, or may be of different taxonomic composition (Pickerill *et al.*, 1983), suggesting considerable transport.

2.2.9.2 Interpretation:

The predominance of sand and the presence of reworked shells with a relatively high degree of sorting re-orientation and disarticulation suggest that facies (I) was probably deposited in the near-shore zone of Norris (1986) and probably belongs to tahpofacies 1 of Speyer and Brett (1988). Although the stratigraphic position and coarser grain size of this facies suggest it to be environmentally the shallowest facies in the whole sequence the relative increase in the percentage of mud and bioturbation which were almost absent in the underlying facies (H) implies evidence of shallow and quiet water conditions in this facies. In order to explain this an origin on the landward side of a large off-shore bar is envisaged. The shells are then considered to have been derived from shallower water and the muds deposited in the shelter of the shore-ward facing bar margin.

2.2.10 Black shale:

At the end of deposition of the Tahara formation a wide spread marine transgression flooded the Hamada basin and resulted in the deposition of the Marar shale (Beicip, 1973, internal company report). Part of this shale

is recognised in well A12 in the interval 5732'–5726' (Fig 2.27) where it forms the upper limit of the core. The absence of the Marar shale in cores from wells A8 & A13 is simply because the formation was not cored in these two wells (Fig.2.27). The cored portion of this shale is a black fissile nonbioturbated shale, lacking any type of coarse sediment input and suggesting that deposition took place under severely oxygen depleted conditions below storm wave base. The latter environment was reached through a series of transitional facies before the deposition of black muds. This can be further explained as follows. After the deposition of the rippled sandstone facies (facies H) the sea gradually transgressed, shifting the position of the shore-line further landwards, and resulting in the reduction of clastic sediment supply and deepening of the basin. This resulted in the repetition of a series of off-shore facies, namely facies C, & F particularly subfacies F2 & F3. As the sea level continued to rise water depth increased, resulting in a reduction of oxygen and thus the deposition of black muds.

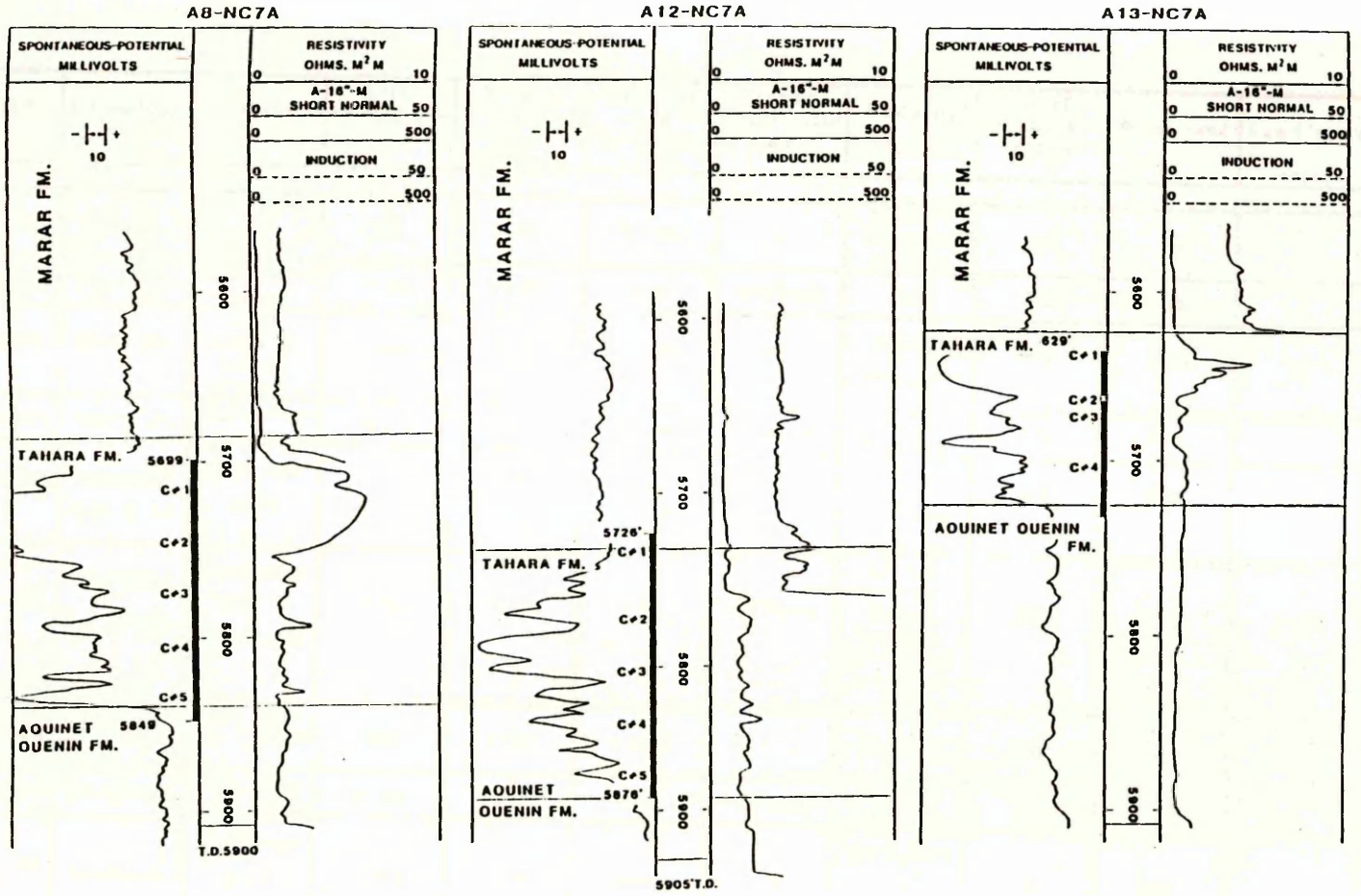

Fig. 2.27 Diagram showing the cored intervals and formation boundaries in the three studied wells (**A8, A12 & A13**). Formation boundaries are taken from (**AGOCO** Reports), but on the basis of sequence sytratigraphic analysis the lower boundaries should be lowered to the base of the shale unit underlying the Tahara Formation.

FACIES	Lithology	Colour	Total thickness (m)	% from total cored section	Average bed thickness (cm)	Average grain size (mm)	Bedding type	% of Bioturb-ation	% of sand	Sand/shae ratio
Facies(A)	Shale	Very dusky red (10R2/2)	9m	7.5%	2.5cm	–	Massive &/graded bedding	10%	5%	-
Facies(B)	Sandstone	Light olive gray	13.4m	10.2%	5cm	0.090mm	HCS	5%	90%	-
Facies(C)	Mudstone	Dark reddish brown (10R3/4)	12m	9.1%	10cm	--	Totally bioturbated	70%	10%	-
Facies(D)	Sandstone	Light olive gray	10.2m	7.6%	10cm	0.100mm	Horizontal bedding	5%	90%	-
facies(E)	Interbedded Shale & Sst.	Very light gray	7.5m	5.3%	0.6cm	0.100mm	Massive and ripple bedding	20%	20%	1: 4
Facies(F)	Interbedded Sst. & Shale	Light olive gray to light gray	38m	30.6%	2cm	0.074mm	graded bedding; Ripple bedding; Horizontal bedding & HCS	35%	56%	1: 0.7
Facies(G)	Mudstone	Very dark red (5R2/6)	3m	2.5%	10cm	-	Massive	30%	4%	-
facies(H)	Sandstone	Light olive gray (5Y6)	20.9m	16.4%	7cm	0.111mm	Ripple bedding	0%	95%	-
Facies (I)	Sandstone	Yellowish gray (5Y7/2)	3.9m	3.2%	6cm	0.135	Horizontal cross bedding & ripple lamination	5%	90%	-

Table. 2.5 Showing in a quantitative and qualitative way facies characteristics derived from core data in wells A8, A12 & A13.

FACIES (F)			
Features	**Subfacies F1**	**Subfacies F2**	**Subfacies F3**
Lithology	Interstratified sandstone and shale	Muddy Sandstone	Interstratified sandstone and shale
colour	Light gray to Light olive gray	Light gray	Light gray to Light olive gray
Total thickness (m)	9.7m	11.7m	16.6m
% From total core section	8%	9.6%	12.9%
Average bed thickness (cm)	2cm	5cm (?)	0.6cm
Average grain size (mm)	0.071mm	0.087	0.064
Sedimentary structures	Ripple bedding ; hummocky x-stratification and horizontal bedding	Totally bioturbated with remnant stratification of hummocky bedding	Horizontal bedding; graded rhythmites and ripple lamination
% of bioturbation	10-15%	80%	30-25%
% of sand	70%	65%	35%
Sand/Mud ratio	2 : 1	--	1 : 2

Table. 2.6 Showing in a quantitative and qualitative way characteristics of the three subdivisions of facies (F)

BORE HOLES	QUANTITATIVE CHARACTER-ESTICS	FACIES								
		A	B	C	D	E	F	G	H	I
WELL A8	TOTAL THICKNESS OF FACIES IN (cm)	316.9	662.9	405	507.1	186.7	886.2	117	1075.5	391.4
WELL A12		174.8	504.9	505.7	33.9	466.9	1617.9	25.8	668.9	---
WELL A13		415.6	77	457.3	85.9	---	1393.9	163.4	247.8	---
WELL A8	% FROM TOTAL CORE SECTION	6.9	14.5	8.8	11	4	19.3	3.5	23.5	8.5
WELL A12		3.8	11	11	7.3	10.2	35.3	0.5	14.6	---
WELL A13		14	2.6	15.5	3.9	---	47.2	5.5	8.3	---

Table. 2.7 Total thickness and percentage of facies in the three wells studied.

Well Name	Quantitative facies characteristics	FACIES (F)		
		SUBFACIES (F 1)	SUBFACIES (F 2)	SUBFACIES (F 3)
A8	TOTAL THICKNESS OF SUBFACIES IN (cm)	545.1	147	193.8
A12		230.1	653.4	733.8
A13		202.1	370.7	624
A8	% FROM CORED SECTION	11.9 %	3.2 %	4.2 %
A12		5 %	14.3 %	16 %
A13		6.8 %	12.5 %	21%

Table. 2.8 Total thickness and percentage of subfacies F1, F2 & F3 in the three wells studied.

FACIES RELATIONSHIPS IN PARASEQUENCES AND PARASEQUENCE SETS

-1- VERTICAL FACIES RELATIONSHIP IN PARASEQUENCES

-2- LATERAL FACIES RELATIONSHIPS IN PARASEQUENCES

-3- VERTICAL FACIES RELATIONSHIPS IN PARASEQUENCE SETS

-4- LATERAL FACIES RELATIONSHIPS IN PARASEQUENCE SETS

2.3 FACIES RELATIONSHIPS IN PARASEQUENCES AND PARASEQUENCE SETS

2.3.1 Vertical facies relationships in parasequences:

A detailed study of the cored-section in the type well A8-NC7A has revealed fifteen coarsening-upward parasequences (cycles), stacked in a parasequence set separated by minor marine flooding surfaces. Each parasequence is found to display the following characteristics.

(a) An upward increase in grain size

(b) An upward increase in the percentage of sand

(c) An upward decrease in the percentage of bioturbation

(d) Amalgamation increases upwards

(e) Facies gradually shoal towards the top.

This vertical pattern of upward coarsening , thickening , and shallowing suggests parasequence progradation (Van Wagoner, 1990). The sequence boundary in each parasequence is marked by:

(a) A sharp change in the environment across the boundary, from generally shoreface sands below the boundary to bioturbated offshore–transitional muds above.

(b) A sharp lithological change from sandstone below the boundary to mudstone above the boundary.

Basically sand and shale are the two main lithologies forming the parasequences, mixed to varying degrees by physical and biological processes resulting in nine different facies (A,B,C,D,E,F,G,H,I). However, the deposition and distribution of these facies within the parasequence set, which comprises the entire Tahara Formation is controlled by several interrelated factors; including sediment supply, rate of subsidence, rate of sea level change, oxygen circulation, slope, local compaction and time.

These factors interacted at different rates and magnitudes producing several cycles of deposition (parasequences) each with its own complicated faces patterns and different facies association (Table 2.9). An ideal coarsening upward parasequence is constructed (Fig.2.28) based on an understanding of facies and their vertical and lateral relationships and distribution in the parasequence set. Assuming a constant and continuous supply of sediments over a slowly to moderately subsiding basin, and stable sea level, the ideal parasequence progressively coarsens and thickens upwards via a series of shoaling facies reflecting increasing wave power. At the base, the ideal parasequence begins with the shale/siltstone interlamination of facies (A), deposited in the shelf mud zone below the effect of storm waves under oxygen depleted conditions. The graded rhythmites present in this facies represent the most distal storm deposits (Aigner & Reineck 1982) in the ideal parasequence. The relative scarcity of biogenic structures is attributed to the relatively high rate of deposition and low frequency of benthonic organisms as a result of oxygen deficiency. This facies gradually passes above storm wave base to the lower offshore–transition into subfacies (F3). This shows a similar pattern of deposition to facies (A) with the following main differences:

(a) The percentage of sand increased remarkably from 5% in facies (A) to about 35% in subfacies (F3) suggesting progressive shallowing

(b) The percentage of bioturbation increased from 10% in facies (A) to about 25% in subfacies (F3), suggesting a relative increase in the amount of oxygen circulation and

(c) The presence of oscillatory flow indicators such as hummocky cross–stratification interbedded with this subfacies suggests deposition above storm wave base.

WELL A8 - NC7A							
PARASEQUENCS	INTERVAL (ft)	THICKNESS (cm)	% OF SAND	% OF BIOTURBA-TION	AVERAGE BED THICKNESS (cm)	FACIES ASSOCIATIONS	ENVIRONMENT
15	5749.4-5699	1536.2	90	5	10	F3-H-I	LLSF-UMSF
14	5759.8-5749.4	316.9	85	11.7	11	C-[F1-B-F1]-B-[D-B]	LUOST-UUOST-MLSF-ULSF
13	5762.2-5759.8	73.1	88.2	16	4	C-D-[F1-F3]	UMOST-MLSF-UUOST
12	5765-5762.2	85.3	74.8	25	7	C-[D-B]	UMOST-MLSF
11	5774-5765	274.3	44.7	47.3	5.3	C-F1-D-F2	ULOST-UUOST-MLSF-UUOST
10	5786-5774	365.7	49.2	37.5	2	[F2-F3-F1-F3-F2-F1]-[B-F1]-B	UMOST-UUOST-LLSF
9	5789-5786	91.4	31.5	52	1.6	F3- F2-[F1-B]	LMOST-UMOST-LLSF
8	5801.5-5789	381	58	7.2	4.6	[F3-B]-[G-F1-G]-B-D	UOST-ULSF-LMSF-UMSF
7	5809-5801.5	228	49.3	21	2	C-F1-[B-F1]	UMOST-LUOST-LLSF
6	5816.25-5809	220.9	37.5	50.9	4.3	C-F2-B	UMOST-UOST-MLSF
5	5819.4-5816.25	96	25.3	23	4.2	C-E-B	UOST-LLSF-MLSF
4	5827-5819	231.6	46.7	7.5	9	E-B	LLSF-ULSF
3	5830.25-5827	99	42.9	27.6	9.3	C-B	UMOST-ULSF
2	5838.4-5830	248	57	29.1	8.4	C-B-D	UMOST-MLSF-ULSF
1	5849-5838.4	323	9	10	4	A-B-A-B	SHM-UOST

Table. 2.9 shows quantitative characteristics of parasequences with facies associations and environmental interpretations in the type well A8–NC7A. SHM = shelf mud; OST = offshore transition; SF = shoreface; L = lower; M = middle; U = upper.

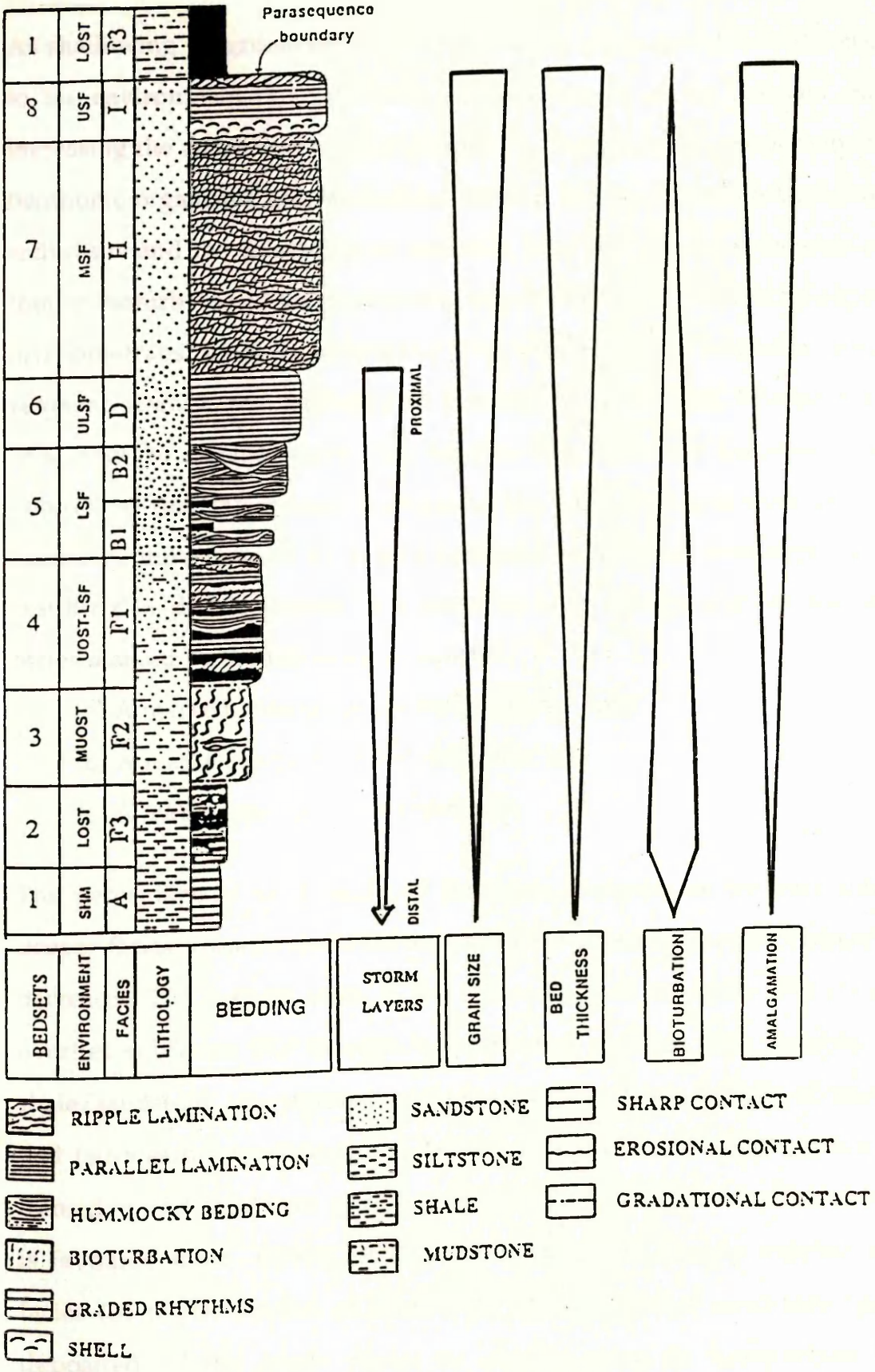

Fig. 2.28 An idealised coarsening-thickening- and shallowing-upward parasequence, with environmental interpretation and vertical changes in distal to proximal storm layers. [**SHM** = shelf mud; **LOST** = lower offshore-transition; **MUOST** = middle-upper offshore-transition; **UOST** = upper offshore-transition; **LSF** = lower shoreface; **MSF** = middle shoreface; **USF** = upper shoreface].

As shallowing progressively increases relatively more sands are delivered to the environment during storms, causing stirring of the bottoms and increasing the amount of oxygen circulation. Consequently, the activity of benthonic organisms also increases, resulting in the total bioturbation of sediments and the deposition of subfacies (F2). This subfacies consists of totally bioturbated muddy sandstone deposited in the middle to upper offshore–transitional environment. The subfacies also includes some remnant stratification probably of hummocky bed origin. However, at this stage of parasequence progradation the shoreline becomes near enough so that the marked increase in the frequency and thickness of sandstone units exceeds the rate of biological activity and mud deposition resulting in the deposition of a series of high energy shallow marine facies marked by the following criteria:

(a) A marked increase in the percentage of sand

(b) A marked increase in bed thickness, and

(c) A marked decrease in bioturbation

The percentage of sand, and bed thickness increases as we pass from deeper facies towards shallower ones and the percentage of bioturbation decreases. The deepest facies in the above series is subfacies (F1) which overlies subfacies (F2) through a gradational contact. This consists of shale/sandstone interlaminations typical of alternating periods of storm and fair-weather conditions and deposited between the upper offshore–transition and the lower shoreface environment where such deposition is favoured most (Elliott, 1986). This subfacies is sharply overlain by facies (B) which consists of hummocky cross–stratified sandstone beds deposited in the lower shoreface environment. In comparison to proximality trend models of storm sedimentation (eg. Aigner & Reineck,

1982; Aigner, 1985; Dott & Bourgeois 1982) the hummocky beds of facies (B) can be divided into lower (distal: B1) and and upper (proximal: B2) parts. The lower distal part consists of individual hummocky beds separated by mud zones and bioturbated horizons, suggesting more distal settings (Dott et al., 1982). Each hummocky bed in the lower part represents a single storm event (Dott et al., 1982). The upper proximal part consists of an amalgamated sequence of hummocky beds. In such a sequence vigorous events erode all or most of the fair-weather muds and immediately lay new hummocky beds over former ones until eventually a thick amalgamated sequence is formed. However, frequent events might produce the same sequence. Facies (B) is sharply overlain by facies (D) which consists of a thicker amalgamated sequence of parallel laminated sands deposited in the upper-lower shoreface environment. This facies is complicated and might not truly represent what it apparently shows; large hummocky bed-forms might appear as parallel laminated sands in the small width of the core sample and hence could be mistaken with true parallel lamination (see Fig. 1.5). The structure might however, truly represent parallel laminated sand deposited from turbulent suspension during foul–weather conditions. Brenchley (1985) showed that during such conditions the lower shoreface facies is commonly thickly bedded and parallel laminated. One might then ask the question why are these beds not reworked into hummocky cross-stratification under the high energy conditions of foul-weather. The answer to this question is that these beds were probably not deposited in the direct path of the storm and that deposition may have taken place some distance to the east or west of the storm path, assuming a N–S storm direction. In such areas the currents and waves become so weak that they are not capable of eroding a hummocky surface, and the

subsequent weak waves could not rework the resultant parallel laminated interval into hummocky cross–stratification. Thus, beds could be parallel laminated throughout (Brenchley, 1985). Facies (D) represents the most proximal storm deposits in the ideal parasequence, above which storm deposits are no longer preserved. Facies (H) which sharply overlies facies (D) comprises the main reservoir in the ideal parasequence and is interpreted as representing a prograding offshore bar, deposited in the middle to upper shoreface environment. The facies consists entirely of ripple laminated sands and no record of storm action is preserved. The absence of a storm record is attributed to the subsequent physical reworking of storm beds and their transformation into small ripples by fair-weather wave action. The erosional contact at the base of the overlying facies (I) is probably limited in time and space, resulting from the excessive growth of the bar crest, probably in response to an increase in the rate of sediment supply. Facies (I), however, consists of parallel laminated and ripple laminated sands, and can be interpreted in the context of facies (H) as deposited in the relatively deeper waters of the back bar area (upper shoreface environment) since facies (I) showed a relative increase in the percentage of mud and bioturbation which are almost totally absent in facies (H). The parallel laminated portion of facies (I) consists of a basal concentration of disarticulated, unbroken and convex-up oriented brachiopod shells, suggesting insignificant transport and sorting by relatively weak currents, supporting the idea of a restricted environment. Although the direct contact between some facies (eg. facies B & D) is sharp the overall relationships between facies are gradational and for this reason the parasequence is considered to be a genetically related succession.

Facies C, E & G are absent from the ideal parasequence because, it is thought, under the set of conditions given here, these facies would not form. They are thus considered to be deposited under exceptional conditions (see facies C, E & G). A complete sequence such as the one described above is not found in any of the cored sections. Variations to the ideal parasequence are shown in table 2.9 with environmental interpretations and quantitative parasequence characteristics. Such variations are related to factors discussed later in the thesis (see chapter geological history).

2.3.2 Lateral facies relationships in parasequences:

The ideal parasequence in Figure 2.28 is converted into a three dimensional model (Fig.2.29) to visualise the lateral relationships between facies. The model shows a shoreface bar prograding over a muddy shelf (Facies A) in which the various laterally migrating facies belts are finely stacked one above the other in a vertical sequence such as that shown in Fig. 2.28. In the light of sequence stratigraphy, facies (A) probably represents marine muds which were deposited on top of a parasequence set boundary (Aouient Ouenine Formation) during or shortly after a major marine flooding event (see chapter on geologic history). The ideal parasequence is composed of several bedsets which possess laterally persistent chronostratigraphically significant surfaces along which the various facies transitions (I to A) are observed. Each bedset, when followed laterally, shows the same sequence of facies as Figure 2.28. Correlating single beds was not possible for most of the studied section, partially because of the rapid lateral changes in their

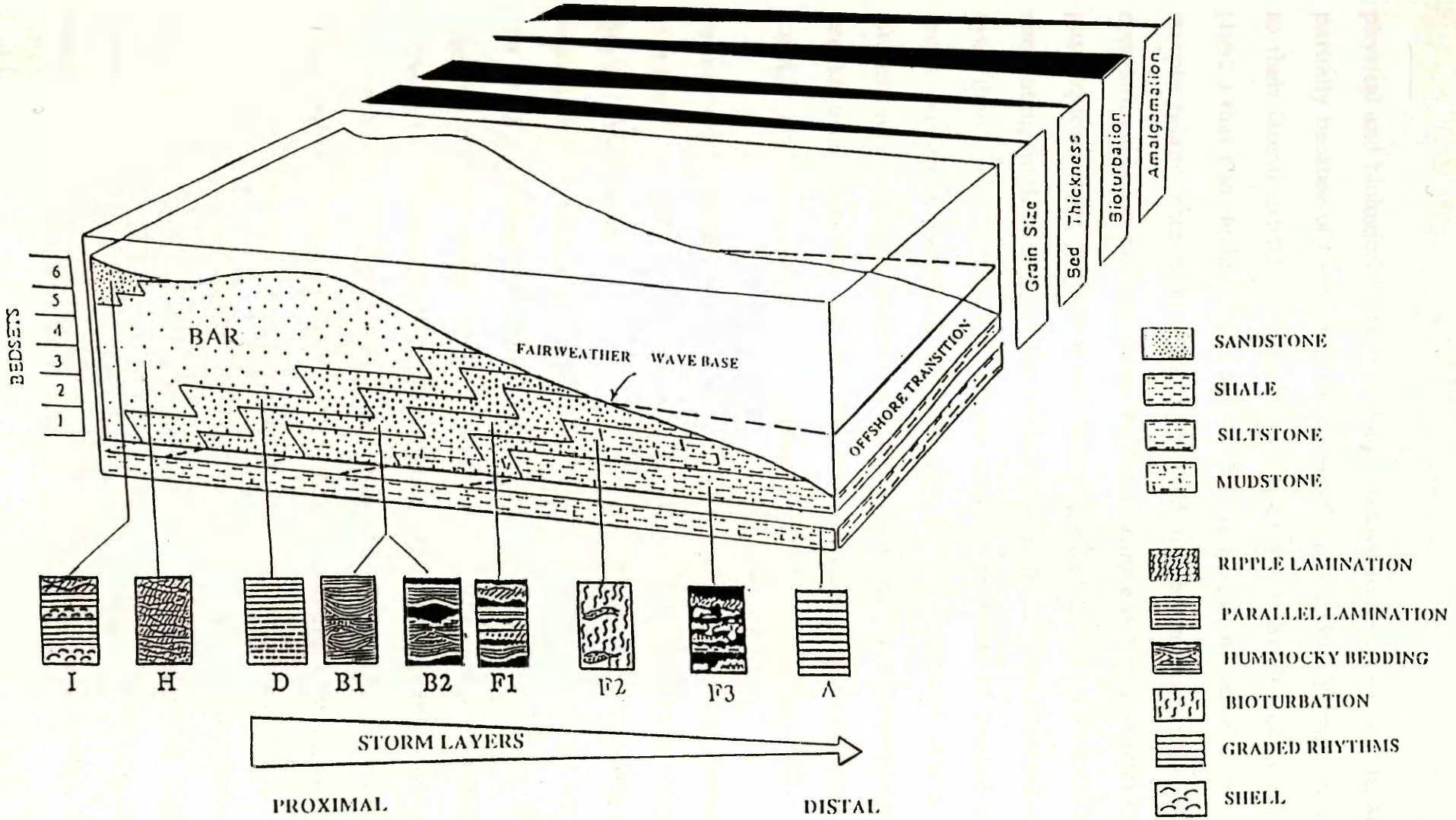

Fig.2 29 A three dimensional representation of the ideal sequence in fig.(2.28) showing lateral facies relationships and their inferred depositional environments, with lateral changes in proximal to distal storm layers.

physical and biological characters along the shelf to shoreface profile, and partially because of their small thickness which is probably proportional to their lateral extent. However, it has been found by Brenchley *et al.*, (1992) that bed thickness and bed continuity do not necessarily have a simple relationship (i.e., thick beds need not be continuous). Thus, correlating a bedset is much easier than correlating a bed and correlating a parasequence is much easier than correlating a bedset and so forth. When correlating single beds a number of closely spaced wells are required and even then one cannot be sure unless correlations relate to surface outcrops. Nevertheless, lateral facies change in each bedset is similar in successively younger bedsets and no significant chronostratigraphic breaks occur between bedsets. For these reasons a parasequence is considered to be a genetically related succession (Van Wagoner, 1990).

Stratification patterns systematically shift from upper shore-face (facies I) to middle and lower shore-face (facies H, D, & B) and finally to the offshore transition (subfacies F1, F2, facies C & subfacies F3). This down dip succession of structures and bedforms, with the exception of facies I & H, can be explained in the context of the proximality trend concept. This suggests that the effects of storm waves and storm generated currents decrease in a basinward direction with increasing water depth. Aigner *et al.*, (1982) and Aigner (1985) described proximal storm facies as relatively thickly bedded, coarse grained, weakly bioturbated and characterized by multiple events of storm reworking. In contrast, distal facies are dominated by single event storm beds separated by fair-weather muds, in addition to a finer grain size, thinner beds and relatively higher percentage of bioturbation (Aigner *et al.*, 1982 & Aigner, 1985). Fig. 2.29 shows a similar progressive change in bed thickness, grain size,

bioturbation and amalgamation from a proximal to a distal position along the shelf–shore-face profile. Most storm beds of the distal facies were the products of single storm events that were relatively infrequent and show reworking under low energy conditions. Event deposits associated with the lowest energy levels are the graded silty mud layers of facies A and subfacies F3. These are similar to the mud tempestites described by Aigner *et al.*, (1982). Subfacies F2 and F1 are viewed as relatively distal expressions of storm currents which interrupted muddy fair-weather sedimentation. In contrast, proximal facies B and D are dominated by multiple episodes of storm reworking which were the products of separate events. This is evident in the truncated rippled and burrowed zones in the presence of mud rip up clasts, the absence of thick mud layers, and the presence of larger bedforms of hummocky cross-stratification suggesting a high energy near shore environment. The absence of a storm record in the zone of facies I & H is probably due to the low preservation potential of that zone. Storm facies deposited during foul-weather were probably latter reworked under fair-weather conditions.

The high energy shallow marine facies, particularly facies I, H, D, and the upper proximal part of facies B, in the ideal parasequence are found to be potential hydrocarbon reservoirs. Oil production in the type well A8-NC7A is mainly restricted to the interval 5700'-5759' which consist mainly of these facies (see Fig. 1.30, and enclosure II).

Lateral differences to the ideal parasequence are shown in table 2.10 and are probably a reflection of the interaction of several variables including sediment supply, differential subsidence, water depth, local compaction, and the orientation of the studied wells with respect to the

WELL NAME	PARASEQUENCES	INTERVAL (ft)	FACIES ASSOCIATIONS	ENVIRONMENT
WELL A 8-NC7A	8	5810.5-5789	[F3-B]-[G-F1-G]-B-D	UOST-ULSF-LMSF-UMSF
WELL A12-NC7A		5825-5819.6	F3-G-[F1-D]	MOST-MLSF-ULSF-MSF
WELL A13-NC7A		5688.1-5676	F3-G-F2-B	LMOST-LLSF-MLSF
WELL A 8-NC7A	7	5809-5810.5	C-F1-B-F1	UMOST-UUOST-LLSF
WELL A12-NC7A		5839.6-5825	C-D-[F2-B-F3-B-F1-F3-F1-F3]-B	LMOST-UMOST-UUOST
WELL A13-NC7A		5699-5688.1	F3-B-F3-D	LOST-ULOST-MOST
WELL A 8-NC7A	6	5816.25-5809	C-F2-B	UMOST-UOST-MLSF
WELL A12-NC7A		5842-5839.6	C-F2	LMOST-UMOST
WELL A13-NC7A		5702-5699	F3-F2	LOST-LMOST
WELL A 8-NC7A	5	5819.4-5816.25	C-E-B	UOST-LLSF-MLSF
WELL A12-NC7A		5845-5842.7	C-E-B	MOST-UUOST-LLSF
WELL A13-NC7A		5705-5702	F3-F2	LOST-MOST
WELL A 8-NC7A	4	5827-5819.4	E-B	LLSF-ULSF
WELL A12-NC7A		5852-5845	[E-D-E]-B	UUOST-LLSF
WELL A13-NC7A		5711-5705	F3-F2	LOST-UMOST
WELL A 8-NC7A	3	5830.25-5827	C-B	UMOST-ULSF
WELL A12-NC7A		5853.8-5852	C-B	LMOST-UUOST
WELL A13-NC7A		5714.8-5711	C-F2-B	LOST-UMOST-LOST
WELL A 8-NC7A	2	5838.4-5830	C-B-D	UMOST-MLSF-ULSF
WELL A12-NC7A		5865-5853.8	C-B	LMOST-[UOST-LLSF]
WELL A13-NC7A		5717-5714.8	C-D	LOST-LUOST
WELL A 8-NC7A	1	5849-5838.4	[A-B-A]-B	SHM-UOST
WELL A12-NC7A		5876-5865	[A-B-A]-B-F1	SHM-MOST
WELL A13-NC7A		5732-5717	A-B-F2-B-F2-B	SHM-LOST-MOST

Table. 2.10 shows facies associations and environmental interpretation of parasequences in the three studied wells. [SHM = shelf mud; OST = offshore transition; SF = shoreface; L = lower; M = middle; U = upper].

WELL A8 - NC7A	16	---	---	---
WELL A12-NC7A		5753-5726	F2-[B-F2]-F3-F2-F3	LOST-MOST-LOST-MOST-LOST
WELL A13-NC7A		---	---	---

WELL A8 - NC7A	15	5749.4-5699	F3-H-I	LLSF-UMSF
WELL A12-NC7A		5787.1-5753	F3-H-E-H-E-H-F2	MLSF-LMSF-LLSF-LMSF-LLSF-MLSF-UUOST
WELL A13-NC7A		5646-5635	F3-H	LOST-ULSF

WELL A8 - NC7A	14	5759.8-5749.4	C-[F1-B-F1]-B-[D-B]	LUOST-UUOST-LSF-MSF
WELL A12-NC7A		5796.6-5787	C-[D-B-F2]-[D-F1]-D	ULOST-UUOST-ULSF-LMSF
WELL A13-NC7A		AS BELOW	AS BELOW	AS BELOW

WELL A8 - NC7A	13	5762.2-5759.8	C-D-[F1-F3]	UMOST-MLSF-UUOST
WELL A12-NC7A		5797-5796.6	C-D	ULOST-UMOST
WELL A13-NC7A		AS BELOW	AS BELOW	AS BELOW

WELL A8 - NC7A	12	5765-5762.2	C-[D-B]	UMOST-MLSF
WELL A12-NC7A		5799-5797.5	C-F1-D	ULOST-UMOST-MUOST
WELL A13-NC7A		AS BELOW	AS BELOW	AS BELOW

WELL A8 - NC7A	11	5774-5765	C-F1-D-F2	ULOST-UUOST-MLSF-UUOST
WELL A12-NC7A		5804-5799	C-F2-B	MLOST-UMOST-LUOST
WELL A13-NC7A		5653-5646	C-[D-F1]	LLOST-LMOST

WELL A8 - NC7A	10	5786-5774	[F2-F3-F1-F3-F2-F1]-[B-F1]-B	UMOST-UUOST-LLSF
WELL A12-NC7A		5816-5804	[F3-D-F3]-[F2-B-F2]-B	LMOST-LUOST-UUOST
WELL A13-NC7A		5672-5653	F3-[F1-F2-B-F2-B-F2]-D-F2	LOST-MOST-LUOST

WELL A8 - NC7A	9	5789-5786	F3-F2-[F1-B]	LMOST-UMOST-LLSF
WELL A12-NC7A		5819-5816	F3-F2-B	ULOST-LMOST-UUOST
WELL A13-NC7A		5676-5672	F3-D	LLOST-UMOST

shore-line. These operated during the overall regressive history of the Tahara Fm. (see chapter on geological history).

2.3.3 Vertical facies relationships in parasequence sets:

Based on the ratio of depositional rate to accommodation rate Van Wagoner (1985) classified parasequence sets into progradational (RATE OF DEPOSITION / RATE OF ACCOMMODATION > 1); retrogradational (RATE OF DEPOSITION / RATE OF ACCOMMODATION < 1) and aggradational (RATE OF DEPOSITION / RATE OF ACCOMMODATION = 1). Accommodation is defined as the space available for deposition (Jervey, 1988; Pasamentier *et al.*, 1988). In a progradational parasequence set the overall rate of deposition is greater than the overall rate of subsidence; in such a parasequence set Van Wagoner (1990) showed that:

(a) The highest percentages of rocks deposited in shallow marine to coastal environments and the greatest depositional porosities are found in successively younger parasequences.

(b) The youngest parasequence in a parasequence set may consist entirely of rocks deposited in a coastal plain area.

(c) Younger parasequences in a parasequences set are generally thicker

We believe for these reasons that the stratigraphic sequence represented by the Tahara Formation (Fig.2.30; see also enclosure II) represents a progradational parasequence set; we found that:

(a) The percentage of shallow marine facies such as facies H and facies I increases upwards in the set (Fig. 2.31).

STRATIGRAPHIC SECTION

OF TAHARA FORMATION

IN THE TYPE WELL A8—NC7A

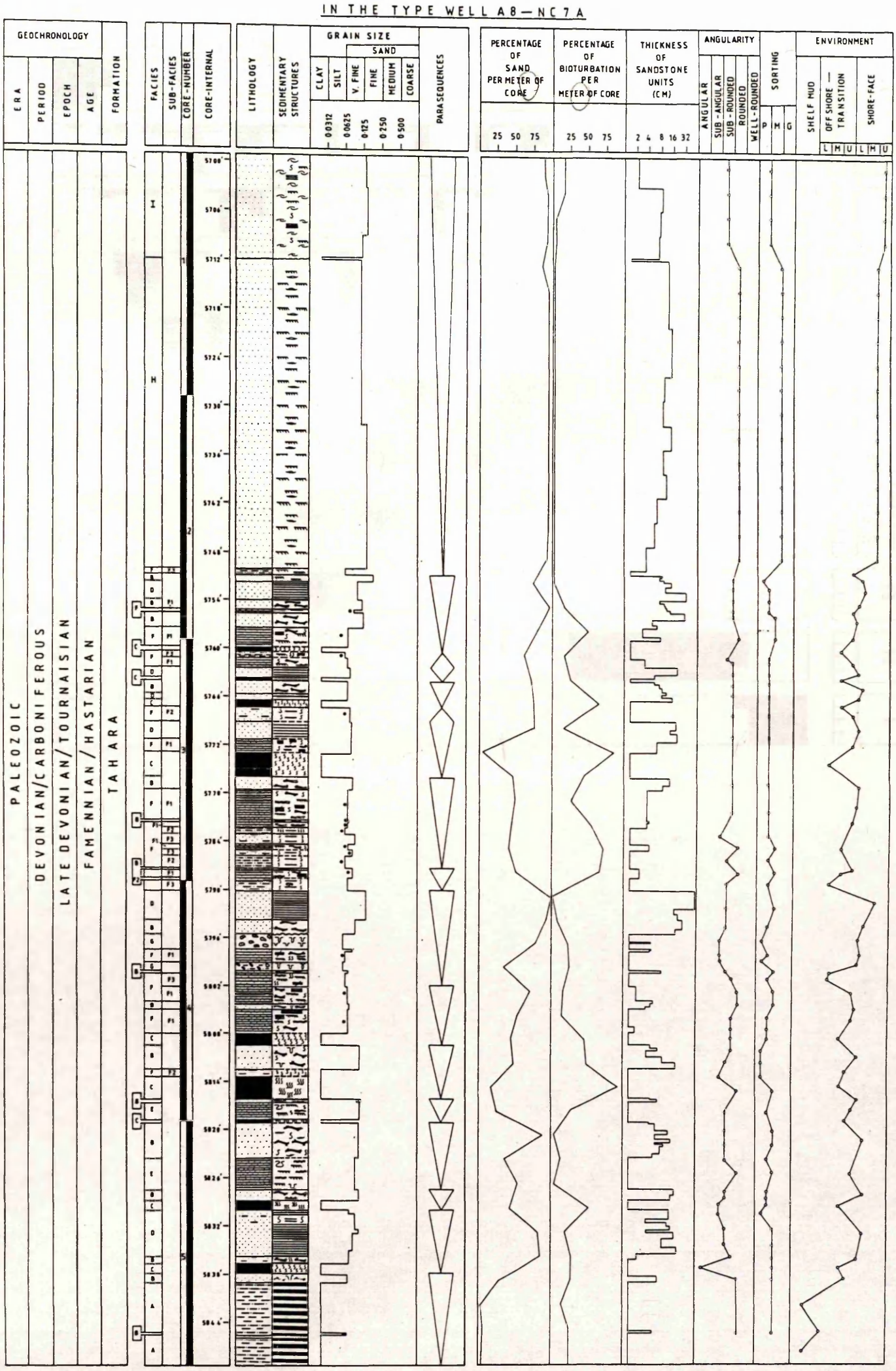

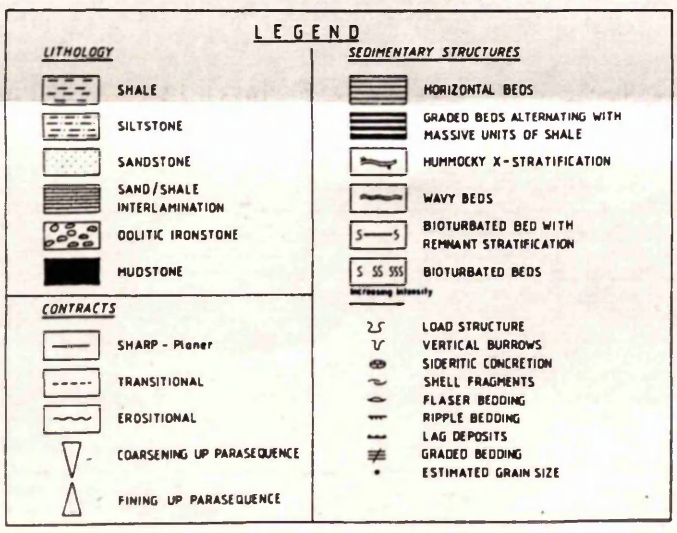

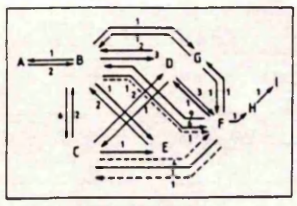

FACIES RELATIONSHIP DIAGRAM

Fig. 2.30 Detailed stratigraphic -section through the Tahara formation in the type well A8-NC7A

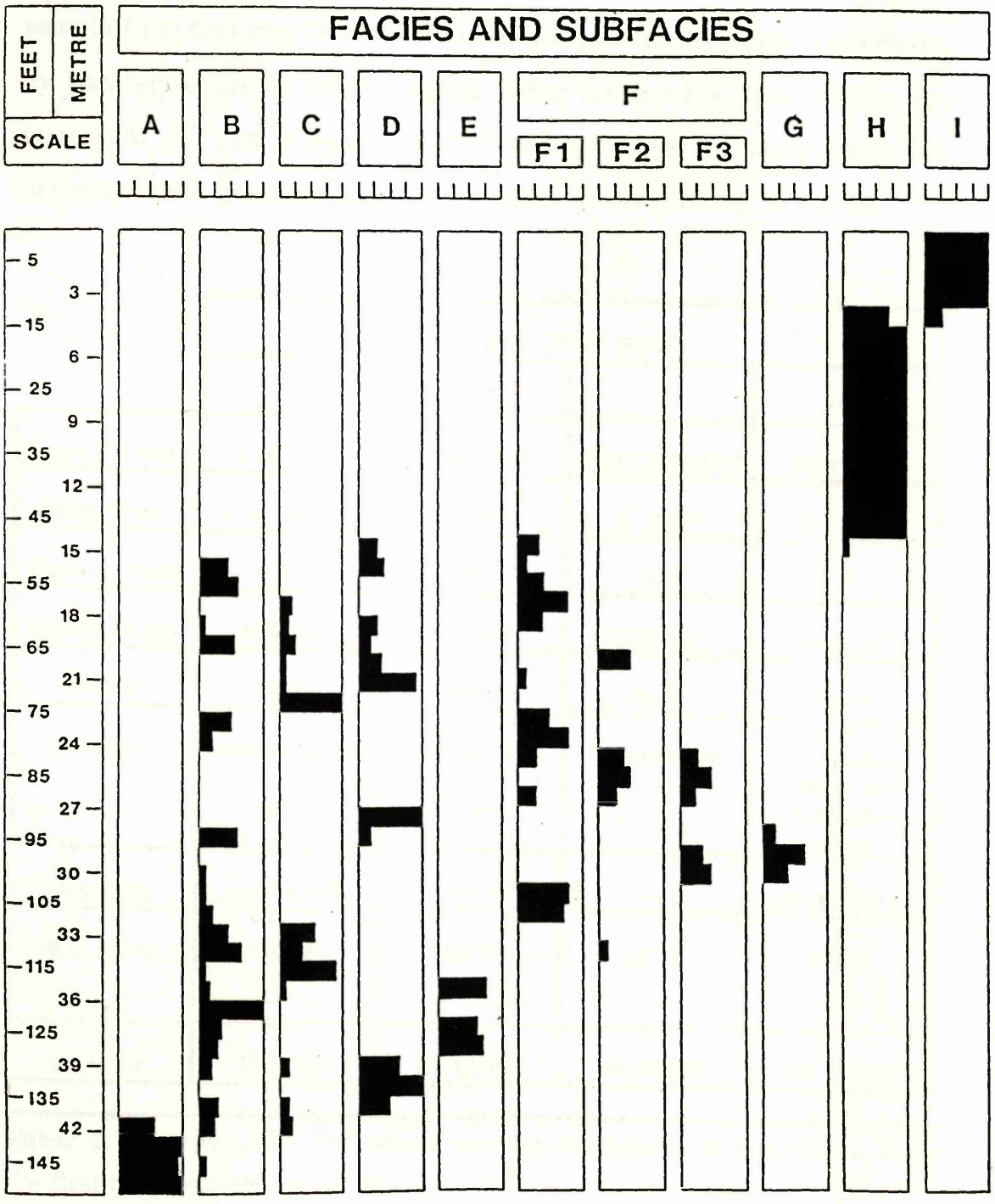

Fig. 2.31 Diagram showing the vertical distribution of facies in the type well A8-NC7A expressed as a percentage per meter of core. The scale is from 0 - 100%.

(b) Four drill stem tests were run in the type well A8–NC7A and only the first two tests recovered oil (Table 2.11). However, the interval tested of the first two D.S.T's almost coincides with the interval covered by parasequences 14 &15 (compare Table 2.9 & 2.11). This verifies the statement of Van Wagoner (1990) that younger parasequences are deposited with greater porosities than older parasequences in the set.

	DRILL STEM TEST			
	1	2	3	4
Interval Tested	5700'-5729'	5729'-5759'	5758'.44"-5789'	5808'-5849'
Hole Size	8 5"/8"	8 5"/8"	8 5"/8"	8 5"/8"
Surface Choke	1"	1"	1"	1"
Packer Depth	5700'.46"	5728'.44"	5758'.44"	5808'.44"
Cushion	None	None	None	None
Recovery	1200' oil + 4500' gases	1684' oil + 4045 gases	No recovery	2 Stands D/C Mud &25 Stands D/C Formation water
Analysis	A. P. I 42^{0}	A. P. I 42^{0}	—	110.000 P.P.M
Bott. Hole Temp	150^{0}F	152^{0}F	153^{0}F	154^{0}F
Duration	35 mins	40 mins	40 mins	40 mins

Table 2.11 Shows four drill steam tests in the type well A8-NC7A. Only the first two tests recovered oil

(c) The youngest parasequence in the set (parasequence 15) consists almost entirely of facies H and facies I which are the shallowest marine deposits in the parasequences set (see Fig. 2.30; and enclosure II).

(d) Although parasequences do not systematically thicken upward in the set, there is a general trend of thickness towards the top of the parasequence set (Fig. 2.32).

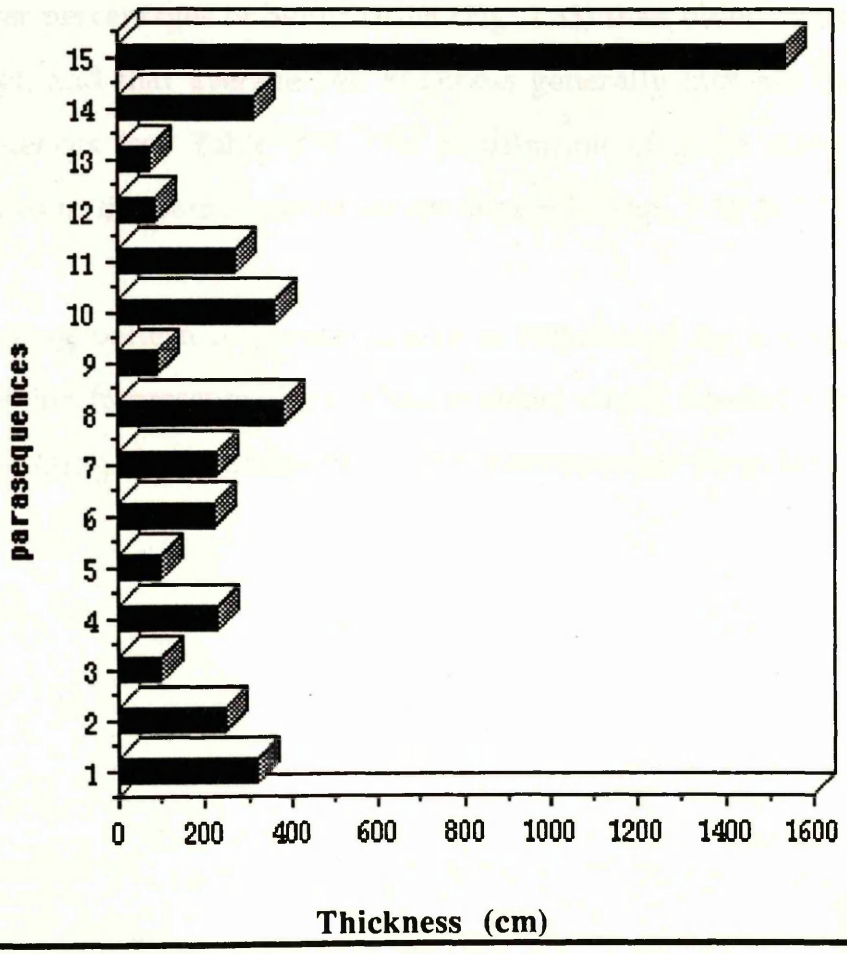

Figure 2.32 Histogram showing a general upward increase in thickness of parasequences in the type well A8-NC7A. N.B. The programe used to generate this graph presents classes as isolated columns. In reality data form a continuous series.

In addition grain size, thickness and percentage of sand also increase upwards in the set while the percentage of bioturbation decreases, suggesting parasequence set progradation (Fig. 2.33). Such parameters would show reverse trends in a retrogradational parasequence set and almost no trend at all in an aggradational parasequence set (Van

Wagoner 1990). In even more detail the percentage of sand, bed thickness, and percentage of bioturbation are calculated for each parasequence in the set in Table 2.9. The results of these calculations show that younger parasequences generally consist of higher percentages of sand (Fig. 1.34) and lower percentages of bioturbation (Fig. 2.35) than older parasequences in the set, and that average bed thickness generally increase in younger parasequences (see Table 2.9). The distribution of grain sizes and bed thicknesses in the parasequence set are shown in Figs. 2.36 & 2.37.

The stacking pattern of parasequences is terminated by a major marine transgression (represented by the Marar shale) which flooded the Hamada basin, resulting in the formation of a parasequence set boundary.

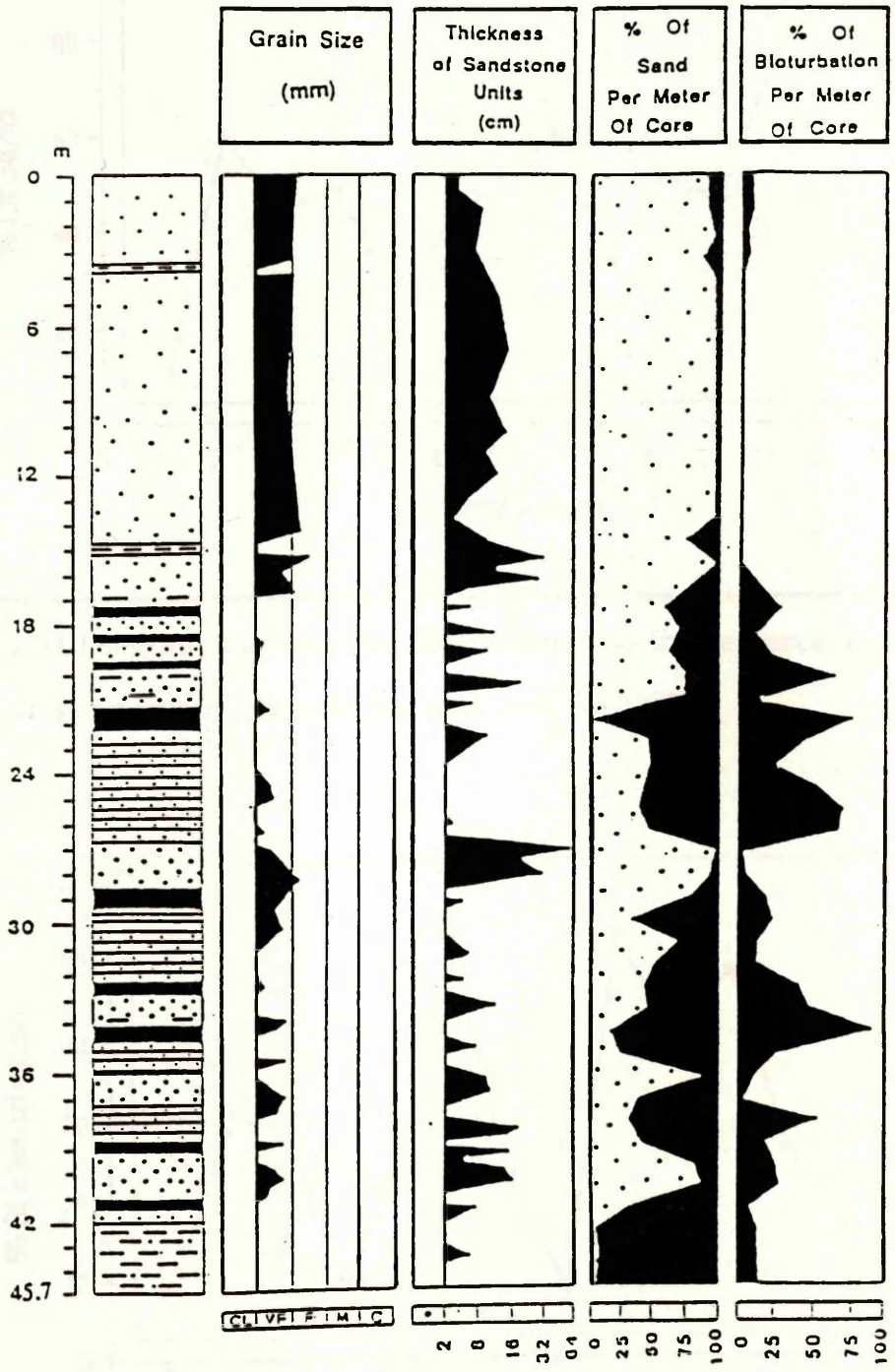

Fig. 2.33 Diagram showing vertical changes in grain size, bed thickness, percentage of sand and percentage of bioturbation, represented by means of vertical curves associated with a lithological column in the type well A8-NC7A. [· = sandstone beds less than 2cm thick; shale and mud zones and totally bioturbated sands]. [CL = clay; VF = very fine sand; F = fine sand; M = medium sand; C = coarse sand]. Legend for log on **fig. 2.39.**

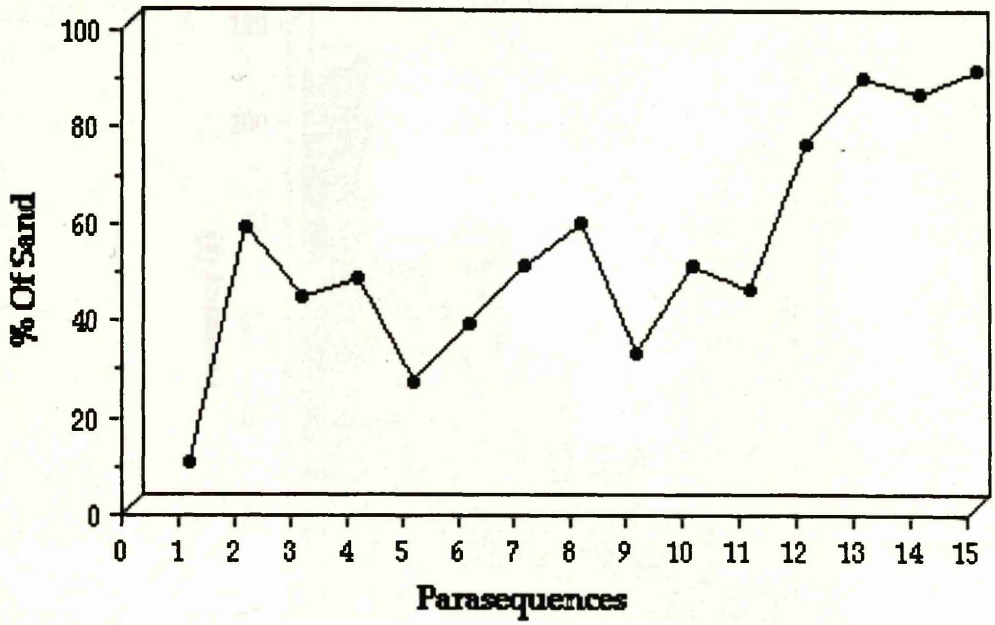

Fig. 2.34 Diagram showing the relative increase in the percentage of sand in younger parasequences in the type well A8-NC7A

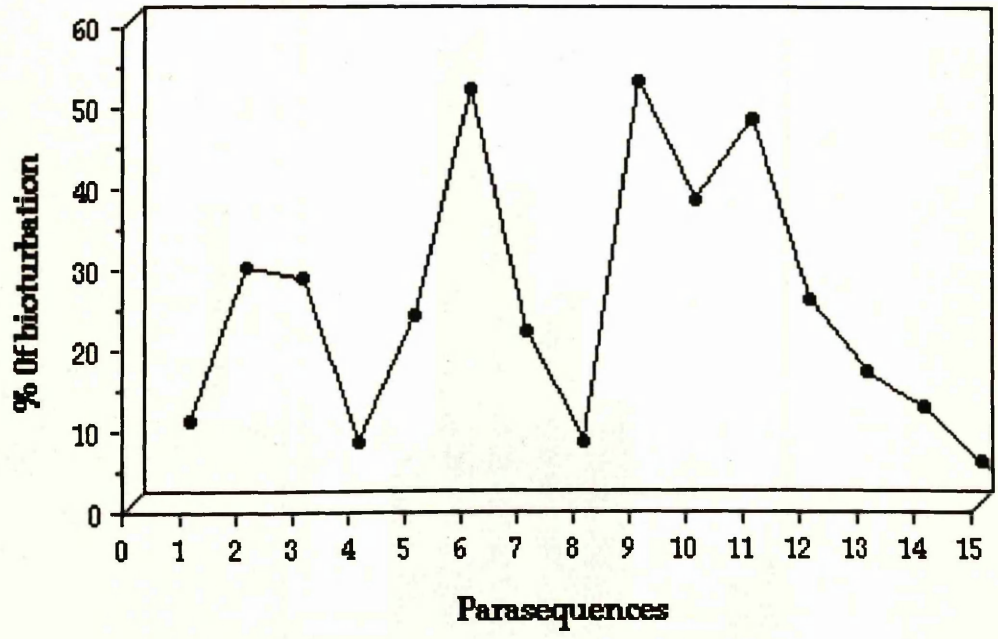

Fig. 2.35 Diagram showing the relative decrease in the percentage of bioturbation in younger parasequences in the type well A8-NC7A.

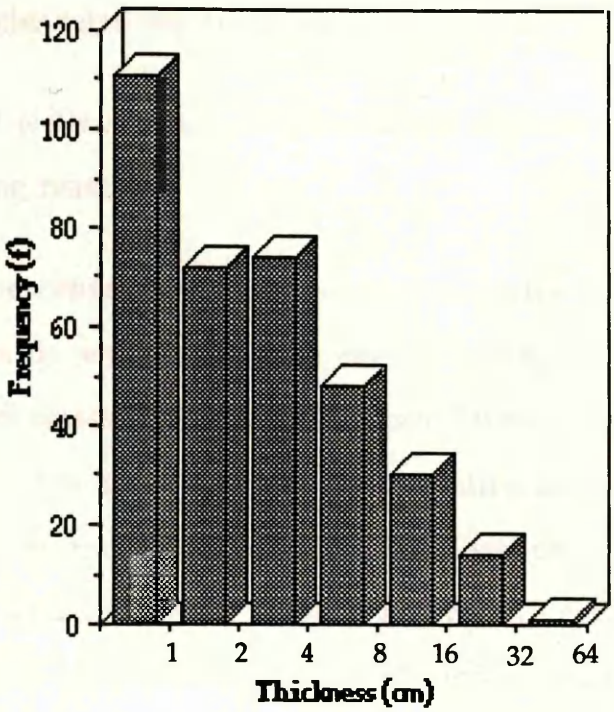

Figure 2.36 Histogram showing general thickness distribution of sandstone units in the type well A8-NC7A. N.B. The programe used to generate this graph presents classes as isolated columns. In reality data form a continuous series.

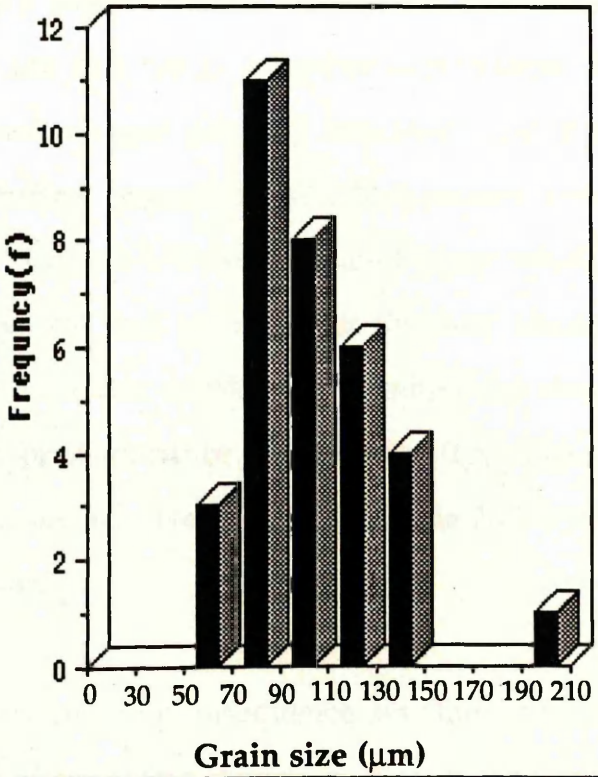

Figure 2.37 Histogram showing general grain size distribution in the type well A8-NC7A. N.B. The programe used to generate this graph presents classes as isolated columns. In reality data form a continuous series.

2.3.4 Lateral facies relationships in parasequence sets:

We believe that wells A12 and A13 are located offshore with respect to A8 for the following reasons:

(a) The percentage of shallow marine facies per meter of core decreases towards well A13 while the percentage of relatively deep marine facies increases (Fig. 2.38). The storm sands of facies B and D, for example, decreases in percentage in the direction of A13. This is characteristic of increasing water depth and distance from shore (Aigner, 1985). Facies I which is absent in wells A12 & A13 contains the coarsest grain size and is environmentally the shallowest marine facies in the parasequence set (the Tahara Formation). Similarly facies H and subfacies F1 decrease in the direction of well A13, while relatively deep marine facies, such as subfacies F3 & F2, dominate well A13. Although facies C is considered to be a relatively deep water facies it is virtually absent in well A13 (Fig. 2.38) and this needs a further explanation. As Bromley et al., (1984) have shown, oxygen plays an important rule in the distribution of *Chondrites*-producing organisms, and bathymetry seems to be a minor factor. However, oxygen is a depth related factor which can be correlated with bathymetry. We thus assume that the near absence of facies (C) in well A13 is due to water depth which limited the circulation of oxygen, resulting in the predominance of subfacies (F3). The low occurrence of facies (C) in well A8 relative to A12 (see Table 2.7) is due to the relatively higher energy level.

(b) Generally in the parasequence set (the Tahara Formation) grain size, percentage of sand, and thickness of sandstone units, decrease in the direction of well A13 and in contrast, the percentage of bioturbation

increases (Fig 2.39 & Table 2.12). The lateral distribution of grain size and bed thickness in the set are shown in Figures. 2.40 & 2.41

Well Name	Average Grain Size (mm)	Average Bed Thickness (cm)	% Of sand	% Of Bioturbation
A8-NC7A	0.100	13	66.4	21
A12-NC7A	0.093	6.5	50.6	30.5
A13-NC7A	0.067	5	31.4	34

Table 2.12 Lateral changes in quantitative characteristics in the three wells studied.

(c) In the parasequence set represented by the Tahara Formation we have found that younger parasequences step towards well A13 which we belive is in a basin-ward direction (Fig 2.42; see also enclosure III). This is consistent with the view of Van Wagoner (1990) who stated that in a prograding parasequence set successively younger parasequences step farther into the basin.

(d) Four parasequences, 11, 12, 13 & 14 (Fig.2.43; see also enclosure IV) loose their identity completely in well A13 where they become one parasequence (parasequence 11). Generally parasequences are difficult to identify in well A13 where their recognition is based more on their correlation with wells A8 & A12. It can be said that if wells A8 & A12 were not available for picking parasequences their identification in well A13 would be a difficult and sometimes impossible task. This loss of identity of the parasequences in a basin-ward direction accords with the work of Van Wagoner (1990).

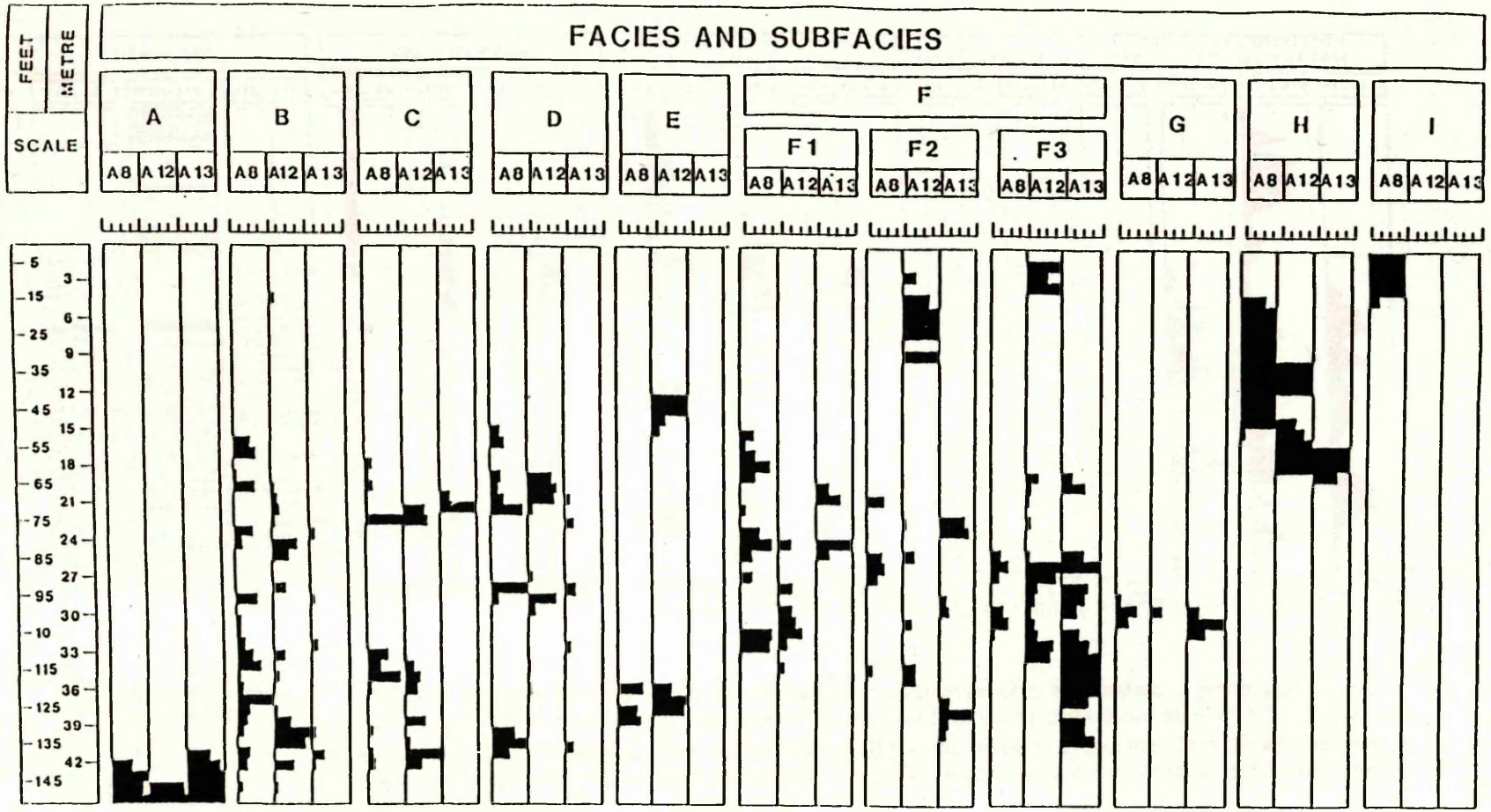

Fig. 2.38 Diagram showing the vertical and lateral distribution of facies in the three studied wells (A8, A12 & A13) expressed as a percentage per meter of core. The above scale is from 0 - 100% for each well in each facies.

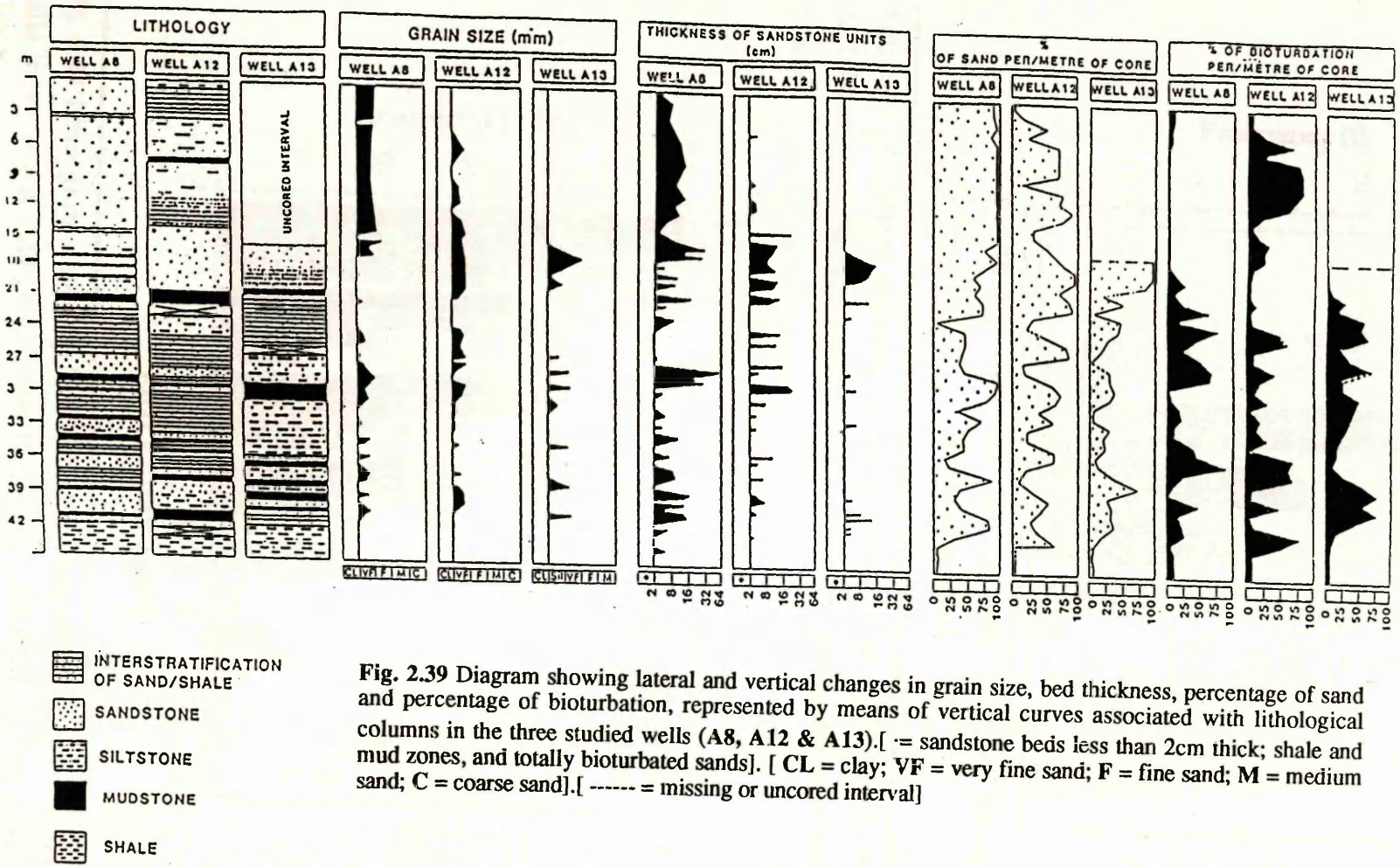

Fig. 2.39 Diagram showing lateral and vertical changes in grain size, bed thickness, percentage of sand and percentage of bioturbation, represented by means of vertical curves associated with lithological columns in the three studied wells (**A8, A12 & A13**).[· = sandstone beds less than 2cm thick; shale and mud zones, and totally bioturbated sands]. [**CL** = clay; **VF** = very fine sand; **F** = fine sand; **M** = medium sand; **C** = coarse sand].[------ = missing or uncored interval]

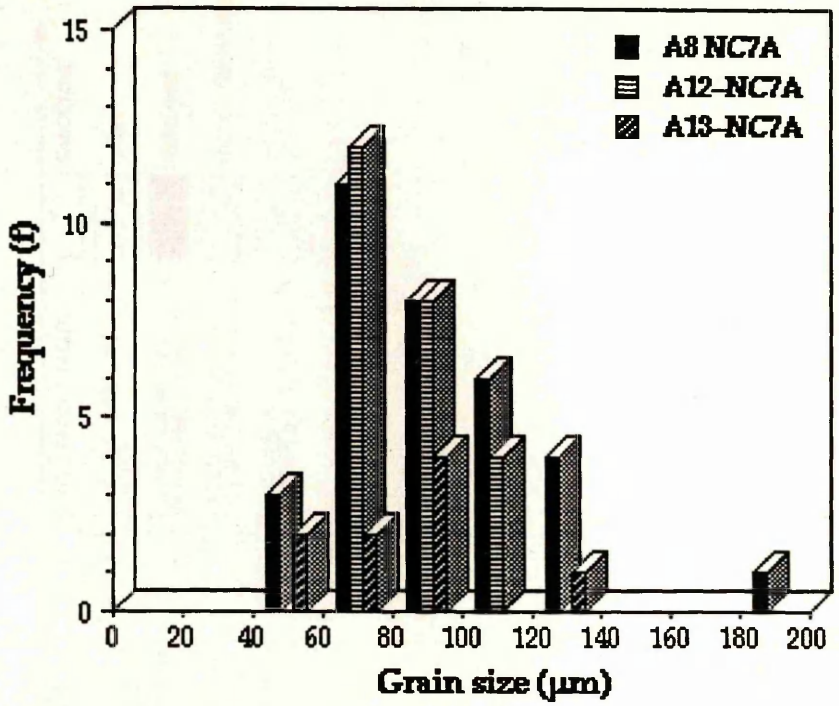

Fig. 2.40 Histogram showing lateral distribution of grain size in wells A8, A12 & A13. N.B. The programe used to generate this graph presents classes as isolated columns. In reality data form a continuous series.

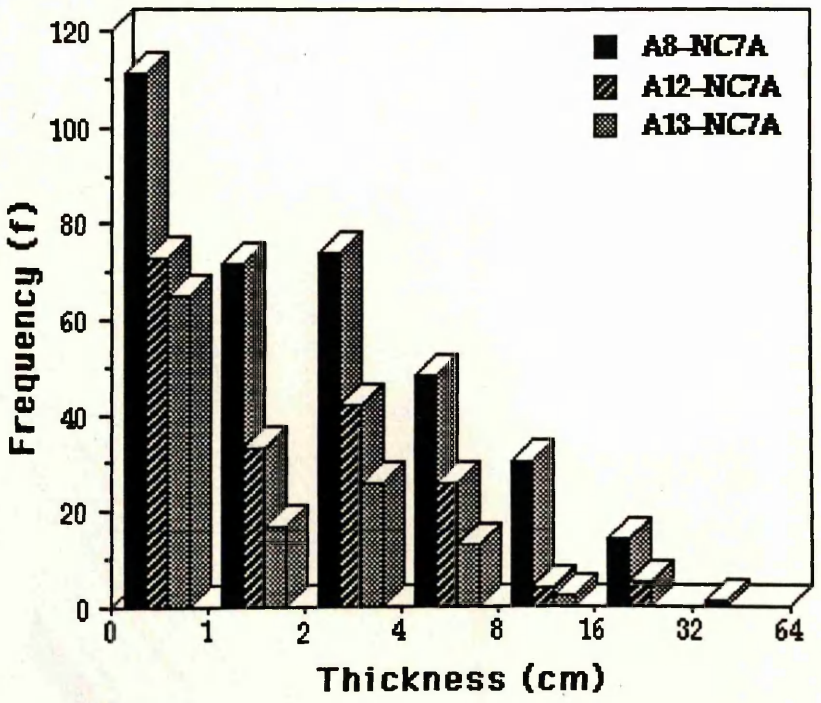

Fig. 2.41 Histogram showing lateral distribution of thickness of sandstone units in wells A8, A12 & A13. N.B. The programe used to generate this graph presents classes as isolated columns. In reality data form a continuous series.

SW

STRATIGRAPHIC CROSS — SECTION

NE

WELL A8-NC7A — 6·3 KM — WELL A12-NC7A — 27 KM — WELL A13-NC7A

DATUM: PARASEQUENCE SET BOUNDARY
(THE BASE OF THE MARAR SHALE)

UNCORED INTERVAL

UNCORED INTERVAL

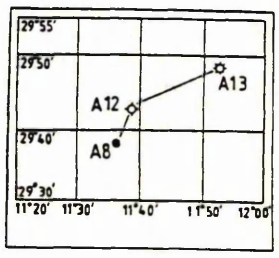

parasequence 14

parasequence 6

parasequence 1

VERTICAL SCALE
0
1
2
3
4m

HORIZONTAL SCALE
ARBITRARY

LEGEND

- A — SHALE SILTSTONE INTERLAMINATED FACIES
- B — HUMMOCKY CROSS STRATIFIED SANDSTONE FACIES
- C — CHONDRITIC MUDSTONE FACIES
- D — PARALLEL LAMINATED SANDSTONE FACIES
- E — SHALE SANDSTONE INTERLAMINATED FACIES
- F — WAVY BEDDED FACIES
- G — OOLITIC IRONSTONE FACIES
- H — RIPPLE LAMINATED SANDSTONE FACIES
- I — FOSSILEFEROUS SANDSTONE FACIES
- MISSING OR UNCORED INTERVAL
- SANDSTONE
- SHALE
- MUDSTONE
- OOLITIC IRONSTONE
- INTERFINGERING BOUNDARY
- CHANNEL

Fig. 2.42 Stratigraphic cross-section through the Tahara Formation with selected time lines taken from enclosure (V).

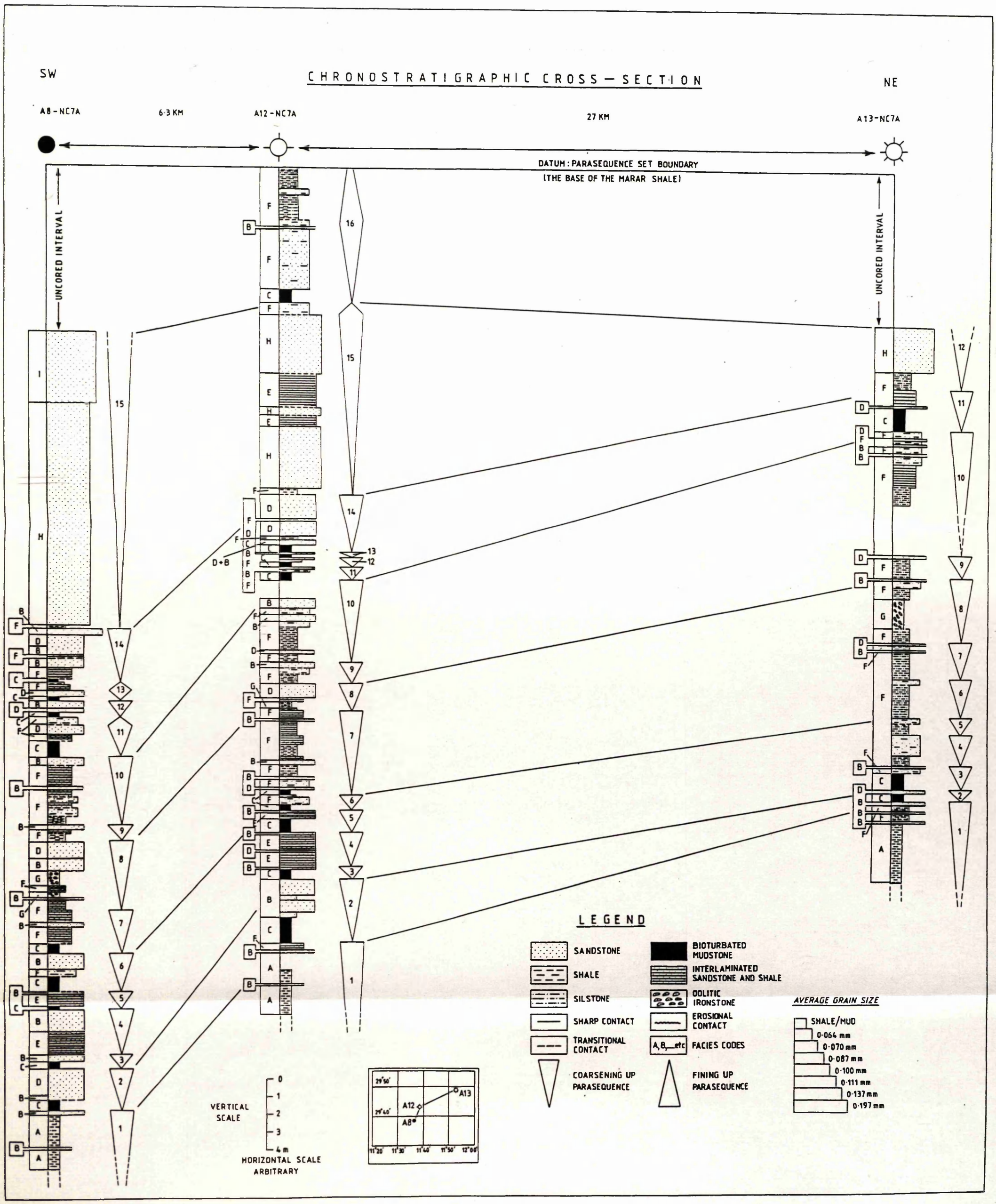

Fig.2.43 Chronostratigraphy of the Tahara Formation. Chronostratigraphy is based on an interpretation of the sequence stratigraphy and does not refer to absolute time or biostratigraphy.

PLATES

Plate. 2.1 Slabbed core sample from bore hole A8–NC7A, depth (5841.8-5842.2) showing shale-siltstone alternations of facies A. Note the presence of dark layers of bioturbated shale overlain by lighter coloured, less bioturbated, normally graded, sharply based layers of silt. Note the cross-lamination at the base of such beds. Scale: 2cm.

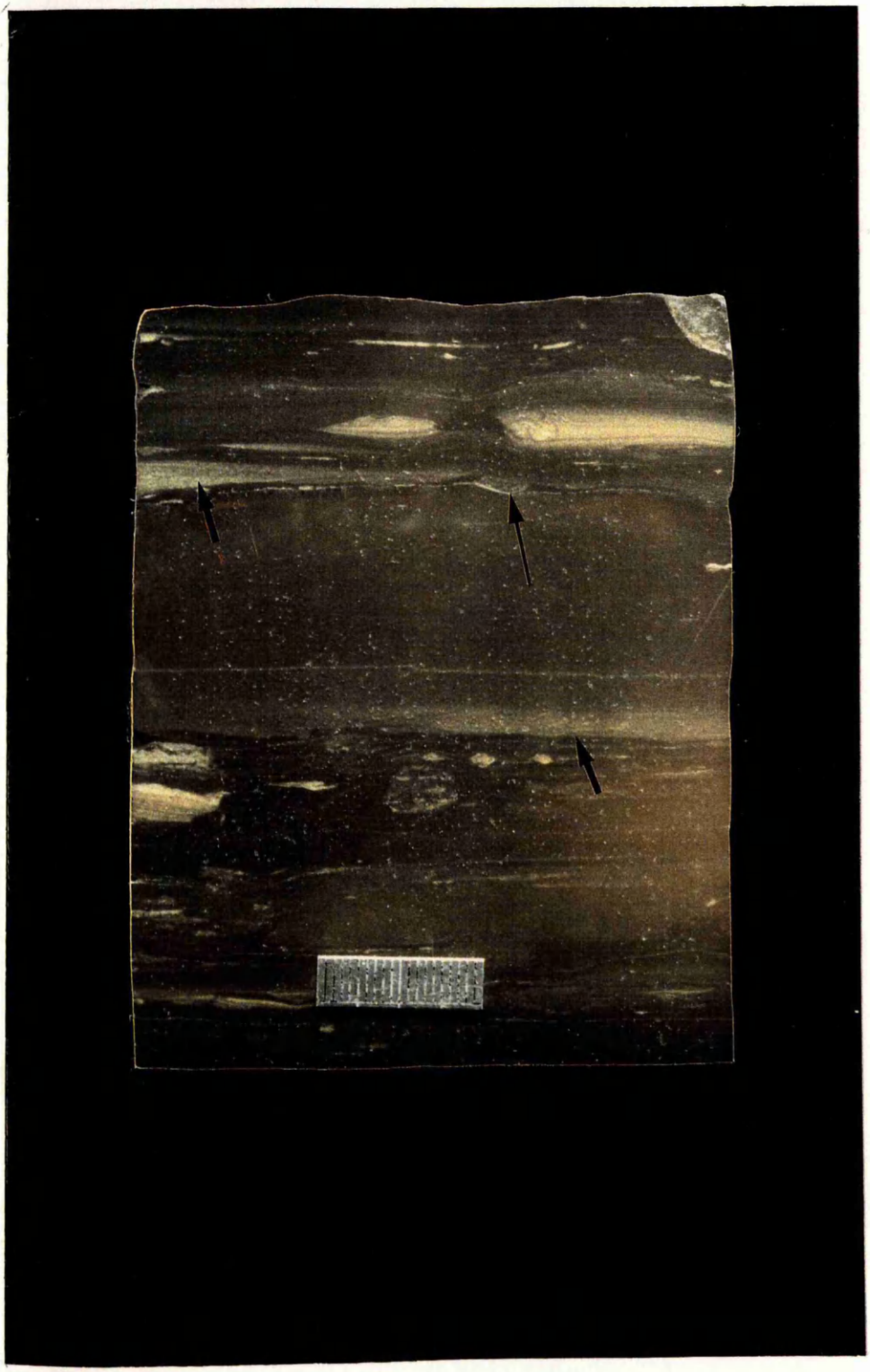

Plate. 2.2 Slabbed core sample from well A8–NC7A, deth (5804.55-5804.85) showing hummocky cross-stratification of facies B. Note the scoured second order surface within the sandstone bed (arrow), and the bioturbation at the top and bottom of the hummocky bed. What seem to be vertical burrows could possibly be escape structures or dewatering structures. Scale: 2cm.

Plate. 2.3 Slabbed core sample from well A8–NC7A, depth (5811.5-5811.77) showing (probably) three separate events: (a) hummocky sandstone bed with vertical burrows (may be escape structures) and slightly scoured top; (b) a 2cm thick sideritized slightly bioturbated mudstone bed sharply overlying the scoured surface. This indicates either a late stage in the deposition of the underlying storm bed in which it is common for such scoured tops to be followed by a mud fill or, probably a separate event related to the scoured surface. In either case the unit is a rapidly deposited layer of mud with rapid deposition reflected in the slight bioturbation; (c) shows relatively intense bioturbation suggesting slow fair-weather sedimentation. Scale: 2cm.

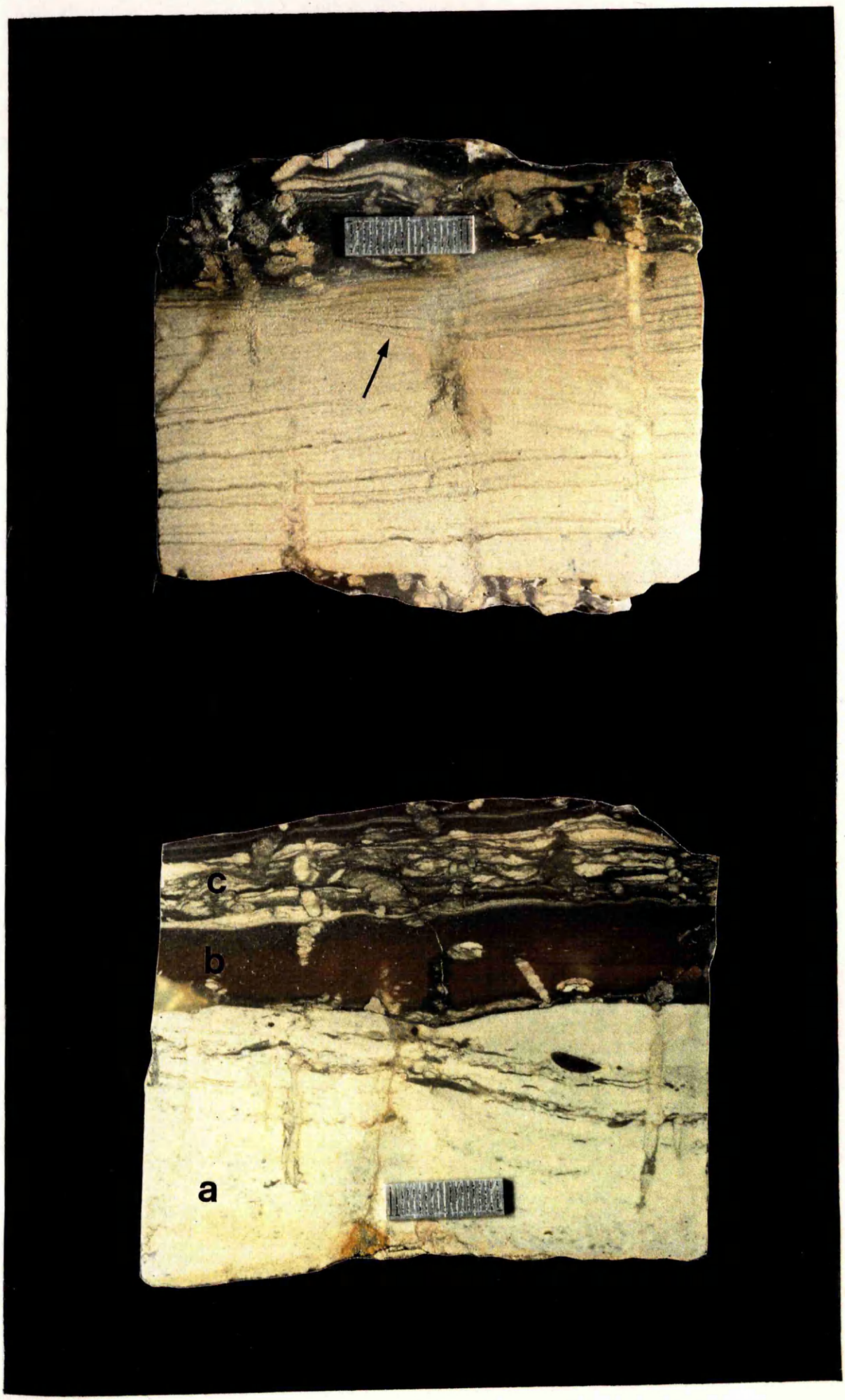
c
b
a

Plate. 2.4 Slabbed core sample from well A8–NC7A, depth (5762.75-5763) showing multiple sets of hummocky bedding separated by second order surfaces. Hummocks and swales can be recognised in this sample. Note the flattened topography and vertical grading at the upper few cms of the bed. Accretionary forms of hummocky bedding also exist in this sample (arrow). Scale: 2cm.

Plate. 2.5 Slabbed core sample from well A8–NC7A, depth (5828.3-5828.6) showing amalgamation of two successive beds : (a) a former hummocky bed with ripples at the top (arrow) truncated by probably a first order surface related to the erosional phase of the succeeding bed. Note the mud deposited in the swale of the hummocky bedform (arrow); (b) a hummocky bed showing the swale and part of a hummock of a hummocky cross-stratified bed, note the reverse grading and slight thickening of laminae into the swale. Scale: 2cm.

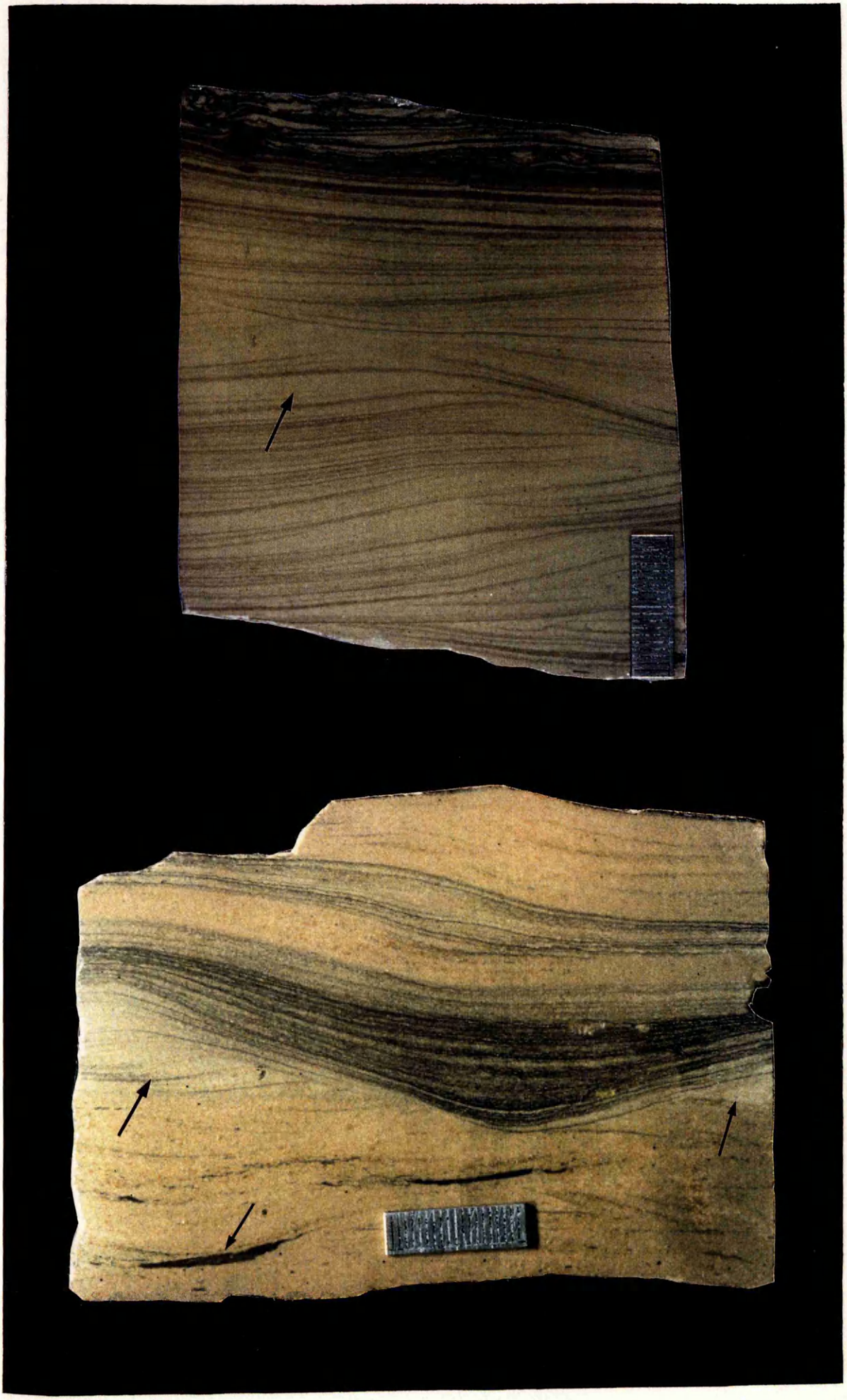

Plate. 2. 6 Slabbed core sample from well A12-NC7A depth (5867.7-5868.1) showing the trace fossil *Chondrites*. Note the relative lack of burrowing in the mud layer at the bottom and the increased amount of bioturbation and sand towards the top. Scale: 2cm.

Plate. 2.7 Slabbed core sample from borehole A8–NC7A, depth (5830-5830.47) showing the trace fossil *Chondrites*. Note the weakly graded, slightly bioturbated mudstone layer at the bottom. Scale: 2cm.

Plate. 2.8 Slabbed core sample from bore hole A8–NC7A, depth (5833-5833.55) showing distinctive parallel lamination of facies (D) produced by the deposition of sand from suspension clouds in relatively deep water. Note the thin mud laminae deposited between sandstone units, indicating short pauses in sedimentation in what was probably a single depositional event. Scale: 2cm.

Plate. 2.9 Slabbed core sample from bore hole A8–NC7A, depth (5830.42-5831.04) showing indistinct parallel lamination of facies (D), probably produced by rapid deposition from suspension. Note the reworked sideriteic lithoclasts at the top of the sandstone bed, and the intense bioturbation at the bottom. Scale: 2cm

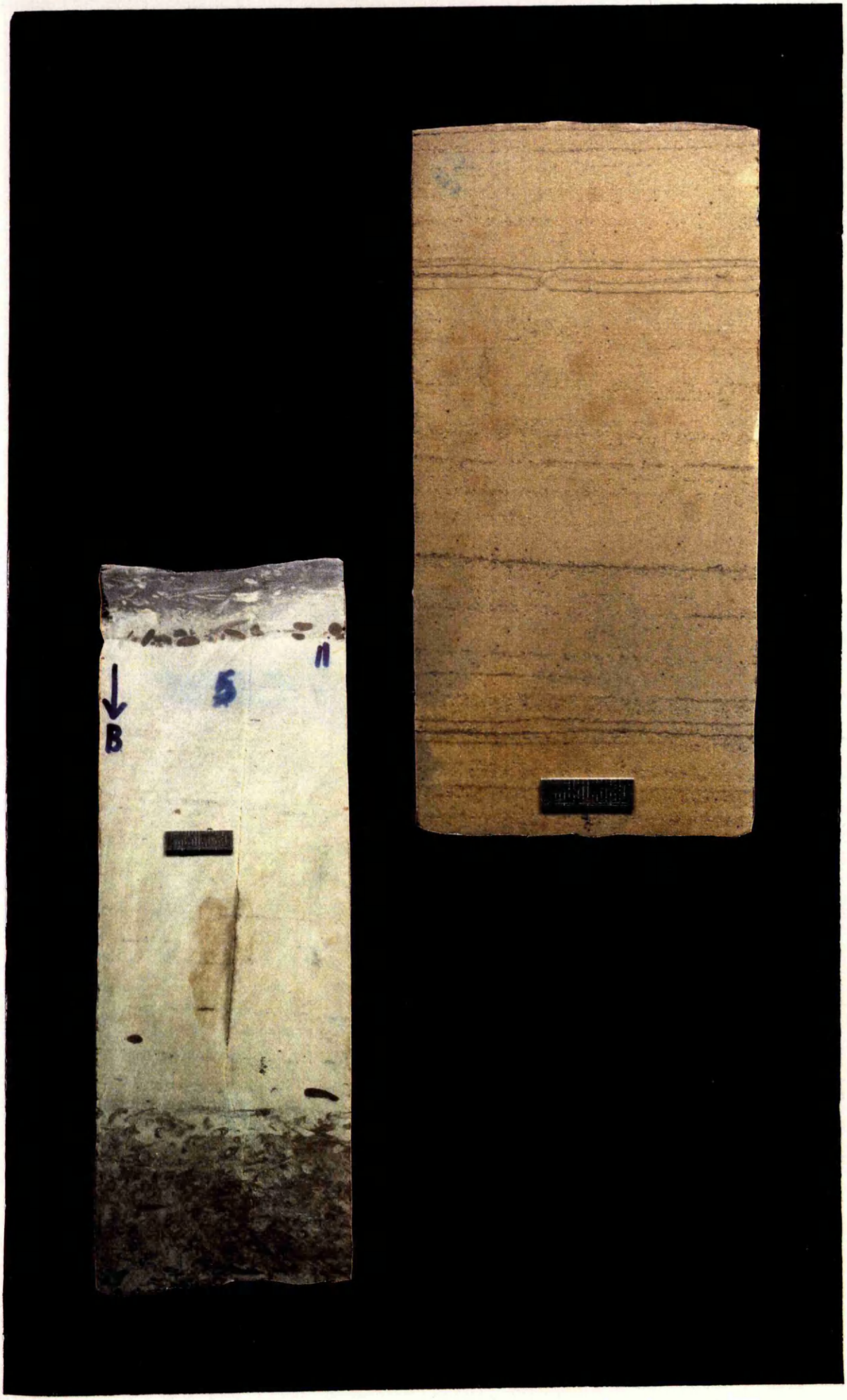
B
5
11

Plate. 2.10 Slabbed core sample from bore hole A8–NC7A, depth (5823.27-5823.47) showing shale sandstone interlamination. Note the massive and ripple laminated nature of the sand and the presence of load structures (arrow). Note the bioturbation at the upper part of shale beds filled with sand during the deposition of the succeeding sandstone bed. Scale: 2cm

Plate. 2.11a Slabbed core sample from bore hole A8–NC7A, depth (5806-5806.42) showing interlamination of sandstone and mudstone with multiple sets of hummocky bedding at the bottom and ripple lamination at the top. Note the vertical grading from sand to silt to mud. Scale is 2cm.

Plate. 2.11b Slabbed core sample from bore hole A8–NC7A, depth (5757.25-5757.6) showing interlamination of sandstone and mudstone with ripples and ripple lamination. Note the presence of parallel lamination with reverse grading and the traces of benthonic organisms trying to escape through a ripple bed at the top (spreite are convex downwards indicating an upward movement). Scale is 2cm.

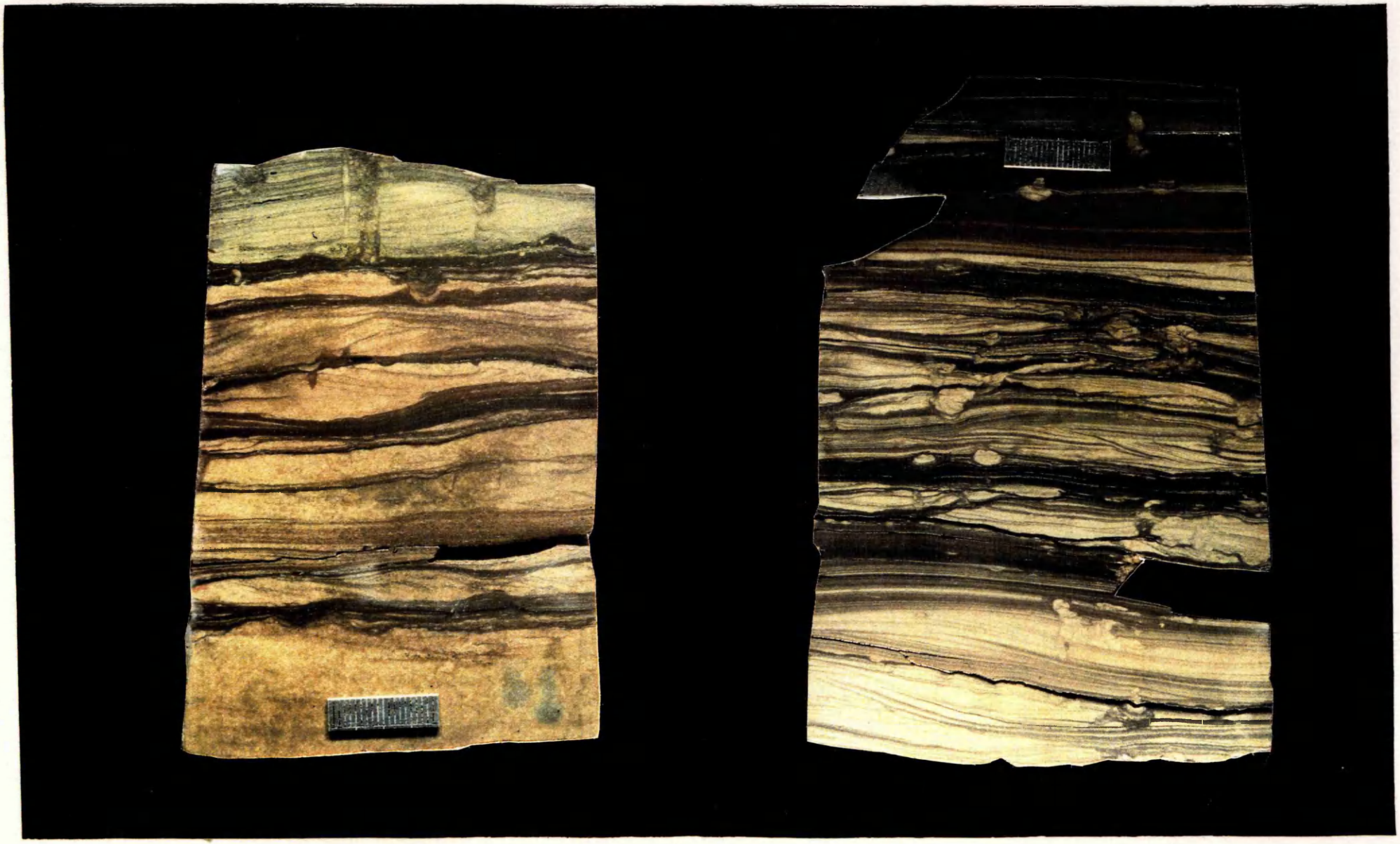

Plate. 2.12a Slabbed core sample from bore hole A12–NC7A, depth (5745.87-5746.27) showing intense biogenic reworking by benthonic organisms. Scale is 2cm.

Plate. 2.12b Slabbed core sample from bore hole A13–NC7A, depth (5708.87-5709.39) showing preserved mudstone beds between intensely bioturbated muddy sandstone units. Scale is 2cm.

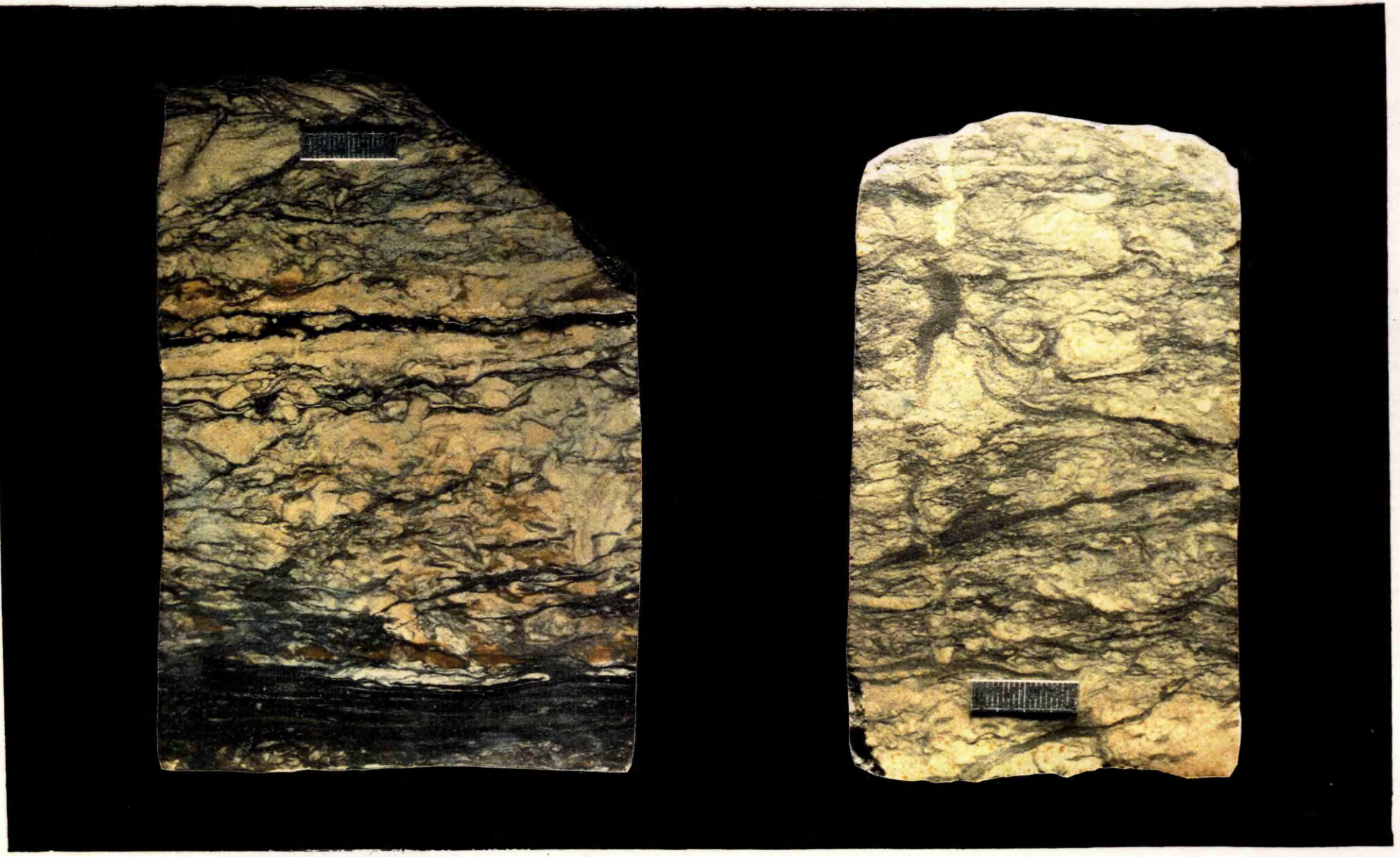

Plate. 2.13a Slabbed core sample from bore hole A8–NC7A, depth (5801-5801.37) showing ripple lamination and parallel lamination with normal and reverse grading. Note the sharp bases and slightly bioturbated tops of the sandstone beds. Scale is 2cm.

Plate. 2.13b Slabbed core sample from bore hole A13–NC7A, depth (5611.8-5612.25) showing possibly hummocky cross-stratification at the bottom with (probably) a resting trace (arrow). Note the erosional base and weak grading at the top (arrow). Scale is 2cm.

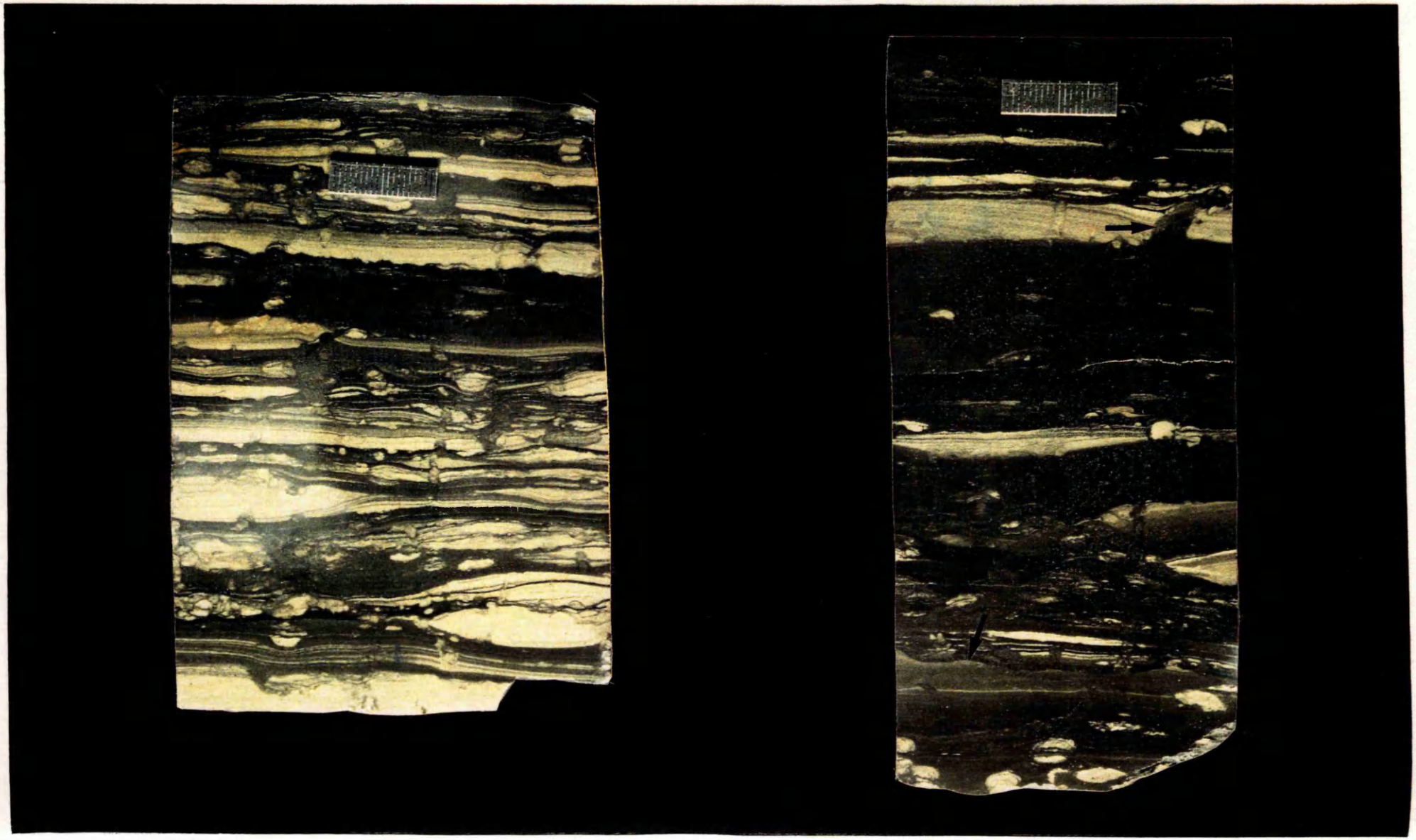

Plate. 2.14a Slabbed core sample from bore hole A13–NC7A, depth (5682.45-5682.97) showing massive sideritized beds with vertical burrows (*Skolithos*). Note the whitish material (ooids) filling the vertical burrows (arrow) and the different lengths and widths of the tunnels. Scale: 2cm

Plate. 2.14b Slabbed core sample from bore hole A8–NC7A, depth (5799.8-5800.1) showing a massive sideritized bed overlain by a thin sharply-based hummocky cross-stratified sandstone bed. Note the vertical burrow in the siderite bed. Scale: 2cm

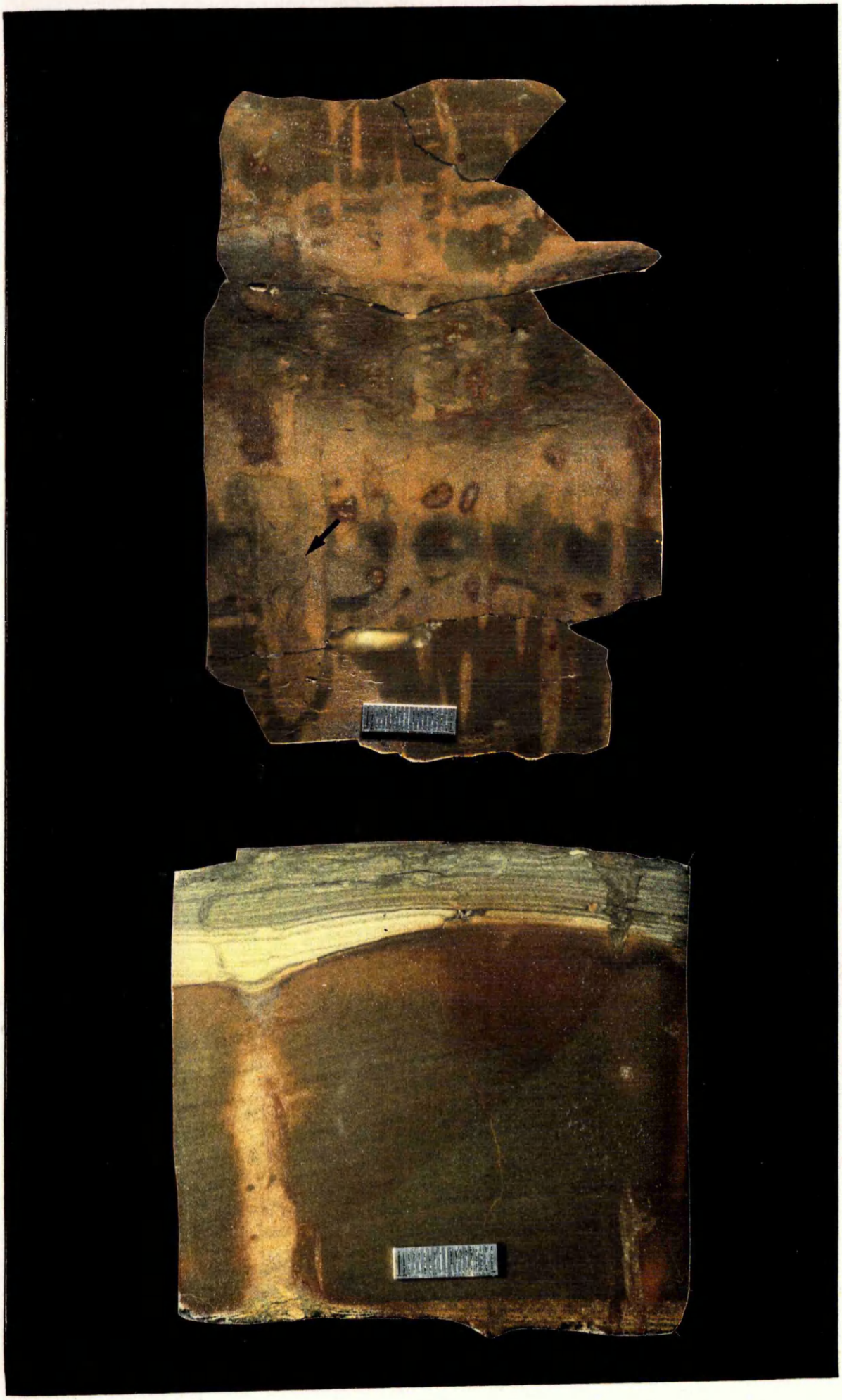

Plate. 2.15 Photomicrograph showing concentric elliptical berthierine ooids (A) partially replaced by siderite (B) in a koalinitic sideritic matrix. (X 25)

Plate. 2.16 Photomicrograph showing articulated brachiopod shells imbedded in a sideritic matrix. Note the dark reddish brown sideritic ooids (left). (X10).

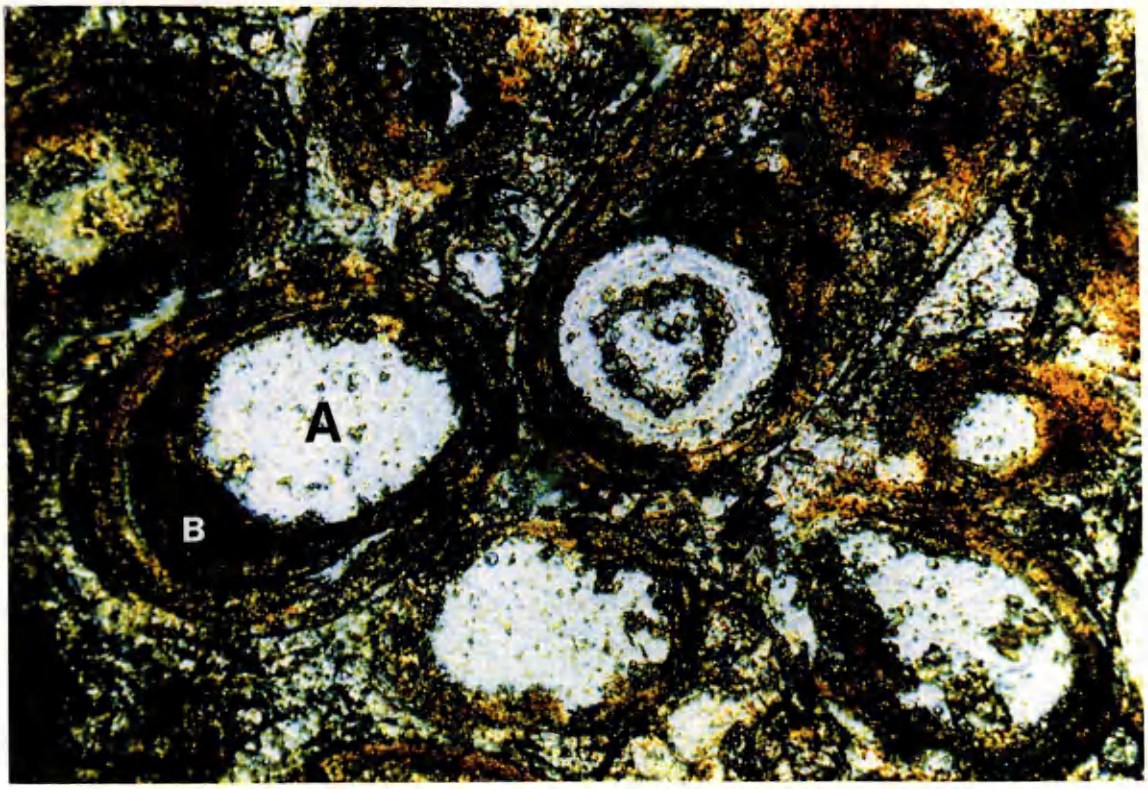
A
B

Plate. 2.17 This is a (Back-scattered) SEM Photomicrograph showing the composition of an ironstone ooid. (C) berthierine core (D) siderite replaced cortex (B) siderite (A) kaolinite.

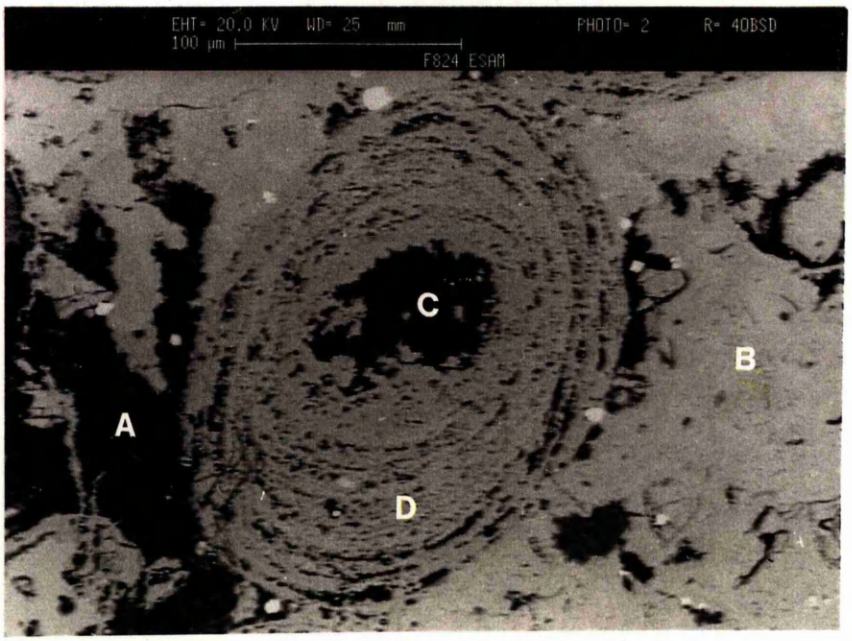
EHT= 20.0 KV WD= 25 mm
PHOTO= 2 R= 40BSD
100 µm
F824 ESAM
A
B
C
D

Plate. 2.18 Slabbed core sample from bore hole A8–NC7A, depth (5740.07-5740.5) showing ripple bedded sandstone units separated by thin layers of mud, note the ripple at the top draped by a thin layer of mud. The deposition of mud in the troughs of some beds (arrow) forms flaser bedding. Scale: 2cm

Plate. 2.19 Slabbed core sample from bore hole A13–NC7A, depth (5640.6-5640.98) showing cross stratification. Scale: 2cm.

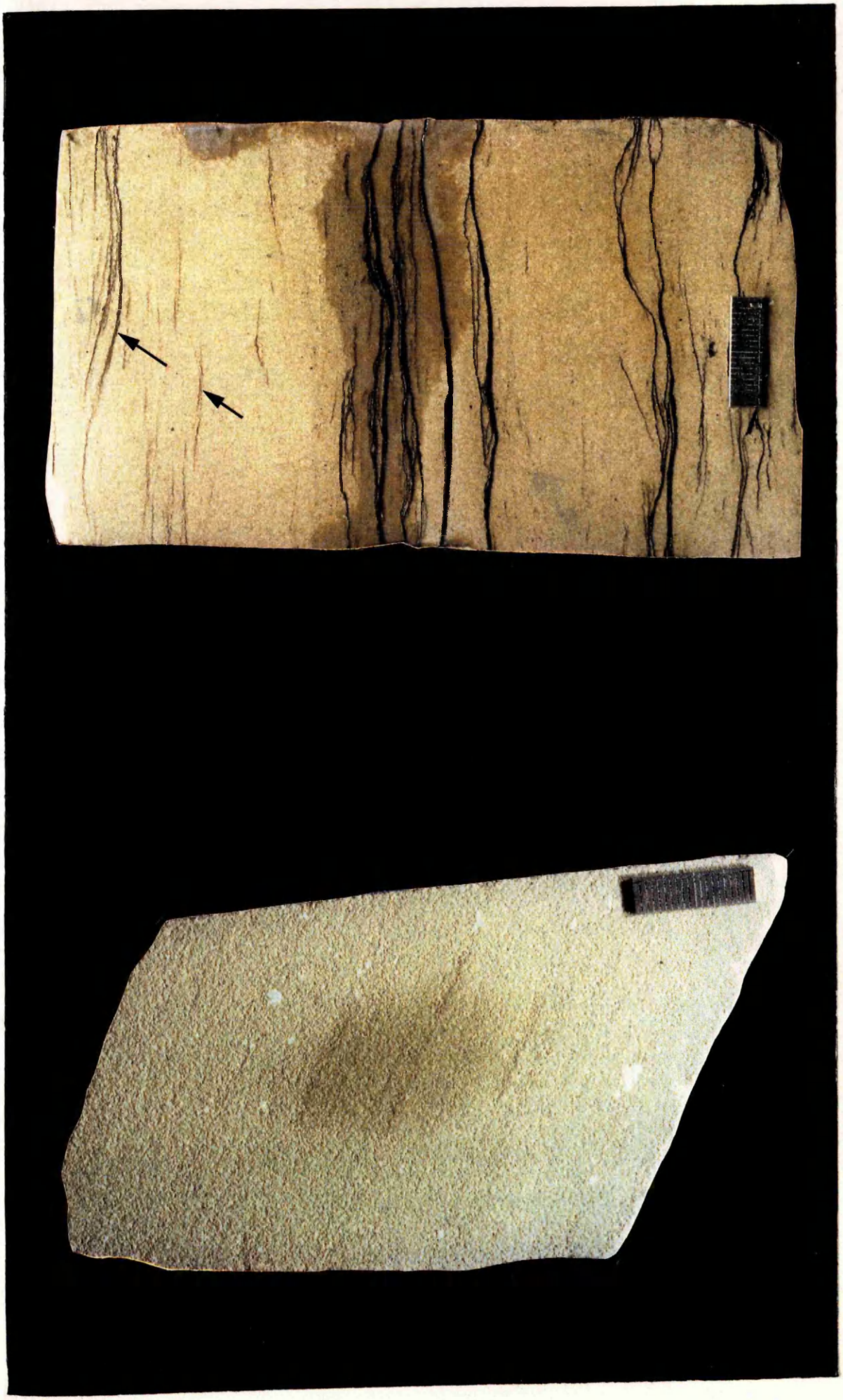

Plate. 2.20 Slabbed core sample from bore hole A8–NC7A, depth (5707.25-5707.66) showing a sandstone with repeated shell lags (coquina) of well sorted disarticulated convex up brachiopod valves (arrow). Note the indistinctive laminated nature of the sandstone units. Scale: 2cm

Plate. 2.21 Slabbed core sample from bore hole A8–NC7A, depth (5699.5-5699.79) showing a sandstone with shell lags (coquina) of mainly disarticulated convex up brachiopod valves. Note the indistinctive nature of the boundary between the sandstone bed and the overlaying shell bed (arrow). Scale: 2cm


32
33

CHAPTER 3

CHAPTER 3

SEQUENCE STRATIGRAPHIC ANALYSIS

STATISTICAL TECHNIQUE

3. 1 Introduction:

Statistical techniques are valuable where there is a large amount of data and when visual inspection of logs is impossible. They can be used as an objective test for sequential or non-sequential facies relationships. Quantitative relationships between facies were first described by de Raaf *et al.* (1965) in a diagram resembling the web of a demented spider, now termed a facies relationship diagram (F.R.D). It is a simple visual method to show the number of times the facies in a vertical succession are in vertical contact with each other. It is often possible to recognise a repeated pattern of facies by simple inspection of such diagrams. However, recognition of sequences is sometimes subjective: and quantification brings a level of objectivity. It may thus be necessary to determine whether a particular facies tends to pass into another more often than one would expect into a naturally random arrangement. As geologists have become more concerned with facies transitions, they have sought methods of simplifying the facies relationship diagram. Statistical analysis using the Markov chain has gained popularity in recent years, although this has been with some controversy. Reading (1986), cited three problems: (a) the type of contact is frequently ignored; (b) the data are oversimplified to facilitate statistical analysis and; (c) minor facies which might be statistically insignificant but geologically important are subordinated or eliminated. However, these criticisms can be largely

circumvented by returning to the row or semi– processed data after completing the analysis. The statistical method described below is based on Selly's (1970) method as discussed by Walker (1976, 1984)

3. 2 Method:

The following method is a simple statistical technique for the detection of repetitive processes in space or time.

(1) The cored sections are coded using letters (Figs. 3.1A, 3.1B &3.1C) and symbols to facilitate tabulation of transitions from one facies to another.

(2) The observed number of transitions can either be shown by arrows in a facies relationship diagram (Figs. 3.2A, 3.2B and 3.2C)) which at this stage is too complicated to be of much help, or they can be tabulated and put in a transition count matrix (Table 3.1A, 3.1B and 3.1C). This is a two-dimensional array which tabulates the number of times that all possible critical facies transitions occur in a given stratigraphic succession. The lower bed of each transition couplet is given by the row number of the matrix, and the upper bed by the column number. Elements in the transition count matrix are hereafter referred to by the symbol rij where i=row number and j= column number. It will be noted that where i=j zeros are present, ie., transitions have only been recorded where the facies shows an abrupt change in character, regardless of its thickness.The type of boundary between facies is indicated in the coded sequence and in the F. R. D (facies relationship diagram) but not necessarily in the transition count matrix.

(3) The tabulated number of transitions from one facies to another in step (2) are converted to observed probability of transitions (Table. 3.2A, 3.2B and 3.2C). Each row in this probability matrix must be a total of 1. This is done by dividing the number of transitions in each cell by the total number of transitions for the row containing the cell (row total) in the transition count matrix. For example in row one you will find tat facies (A) passes upwards into facies (B) twice. The observed transition probability is (2/2) = (1).

(4) A second matrix is calculated (Table. 3.3A, 3.3B and 3.3C) assuming the same abundance of facies but in a random sequence. Thus, the probability of transition from facies A to any other facies depends only upon the observed relative abundance of the other facies and is given by:-

$$r_{ij} = n_j/N\text{-}n_i$$

where rij is the random probability of transition from facies i to facies j, nj is the number of occurrences of facies j (column total for facies j) N is the total number of transitions for all facies, and ni is the number of occurrences of facies i (row total for facies i). To illustrate this let us evaluate the transition in type well A8- NC7A of facies (A) upwards into facies (B):

$$r_{ij} = n_j/N\text{-}n_i$$

where i = A and j =B

the row total (ni) for facies (A) = 2

The column total (nj) for facies (B) = 18

and the total for all transitions N = 54

using these values the random probability of transition (rij) from A to B is:

$$r_{AB} = n_B / N - n_A = 18 / 54 - 2 = 0.346$$

(5) A difference matrix is then calculated (observed probability of transition minus random probability of transition) which highlights those transitions which have a higher or lower probability of occurring than if the sequence were random. It has been argued that those transitions which occur more commonly than random must have some geological significance. The result is shown in tables (3.4A, 3.4B and 3.4C).

(6) We enter the stage of understanding what the difference matrix tells us. It is noted that some values are high-positive (transition much more common than if facies were random) and some are high negative (transitions much less common than random). We can now reconstruct a facies relationship diagram showing the transitions which occur more frequently than random (Figs. 3.3A, 3.3B and 3.3C) i.e., transitions with high positive values (heavy arrows). Lighter arrows can be drawn on the F.R.D showing transitions only a little more common than random (random being those transitions with values close to zero). what is included in the "high" category will depend on the range of numbers in the difference matrix. A reasonable amount of simplification occurs if only the entries in the different matrix greater than + 0.050 are shown in Figs 3.3A, 3.3B & 3.3C. lower +ve values are arbitrary rejected for the purpose of simplification and are thus not shown in Figs (3.3A, 3.3B & 3.3C).

3. 3 Facies sequence interpretation:

At some stage in the analysis of a complex facies sequence, simplification is essential to understand what previously appeared to be a random

succession. The previously described method was applied to the complex facies sequence in Figs. 3.1A, 3.1B & 3.1C to provide such a simplification. The result was a simplified facies relationship diagram (Figs 3.3A, 3.3B & 3.3C) which can be used as a basis for overall interpretation. Before we come to the interpretation of the facies relationship diagram, a few points are to be cleared in the following discussion.

The interpretation of the Tahara Formation is initially based on a tentatively adopted hypothesis, suggesting that the Tahara Formation is a storm dominated shelf to shoreface sequence in which the series of studied wells (A8, A12 & A13) are thought to reflect a transition to an increasingly offshore (distal) position. The hypothesis is based on preliminary examination of the sequence in terms of lithology, stratification types, grain size, sand/shale ratios and well log responses. Further testing of the hypothesis, using the sequence stratigraphic technique described earlier in chapter 2, have proven its validity. We thus consider the method described here as a further test to the validity of the hypothesis and as an alternative technique to sequence stratigraphic analyses.

Interpretations will be carried out on the type well, A8–NC7A and any lateral variations in the other two wells will be referred to it.

Based on previous facies descriptions and individual facies interpretations, together with our hypothesis, we can now interpret the facies relationship diagram in Figure 3.3A by comparing it with particular modern analogs and ancient examples. In comparison with modern (eg. Clifton, Hunter & Phillips, 1971; Howard & Reineck, 1981) and ancient (eg. Hamblin & Walker, 1979; Leckie & Walker, 1982; Reading, 1986) shelf

to shoreface profiles. The simplified facies relationship diagram in Figure 3.3A is interpreted as a storm dominated shelf to shoreface sequence in which three subenvironments of the beach face are recognised, shelf mud, offshore-transition & shoreface, with transitional facies linking them together. Each subenvironment is characterised by a unique facies association which serves as an indicator of that particular environment. Lateral variations in Figures 3.3B & 3.3C are interpreted in terms of sediment supply, subsidence, water depth and local compaction. In addition, the orientation of the wells with respect to the shoreline also has an effect on the distribution and relative abundance of facies (see chapter on geologic history). To avoid repetition we refer the reader to the beginning of chapter 2 for facies descriptions and interpretations.

This however, confirms our understanding of the sequence and provides supportive evidence in the interpretation of the Tahara formation as a whole.

A, B, A, B, C,B, D, C, B, E, B, C, E, B, C. F2, B, C. F1, B, [F1, F3], B, G, F1, G, B, D, [F3. F2. F1] , B, [F2. F3. F1, F3, F2, F1] , B, F1, B, C. F1, D. F2, C, D, B, C, D, [F1. F3]. C. F1, B. F1, B, D, B, F3, H, I

Figure. 3.1A Observed sequence of facies in well A8–NC7A. From stratigraphic base upward the sequence reads A, B, A, etc. [, = Sharp contact . = Transitional contact]

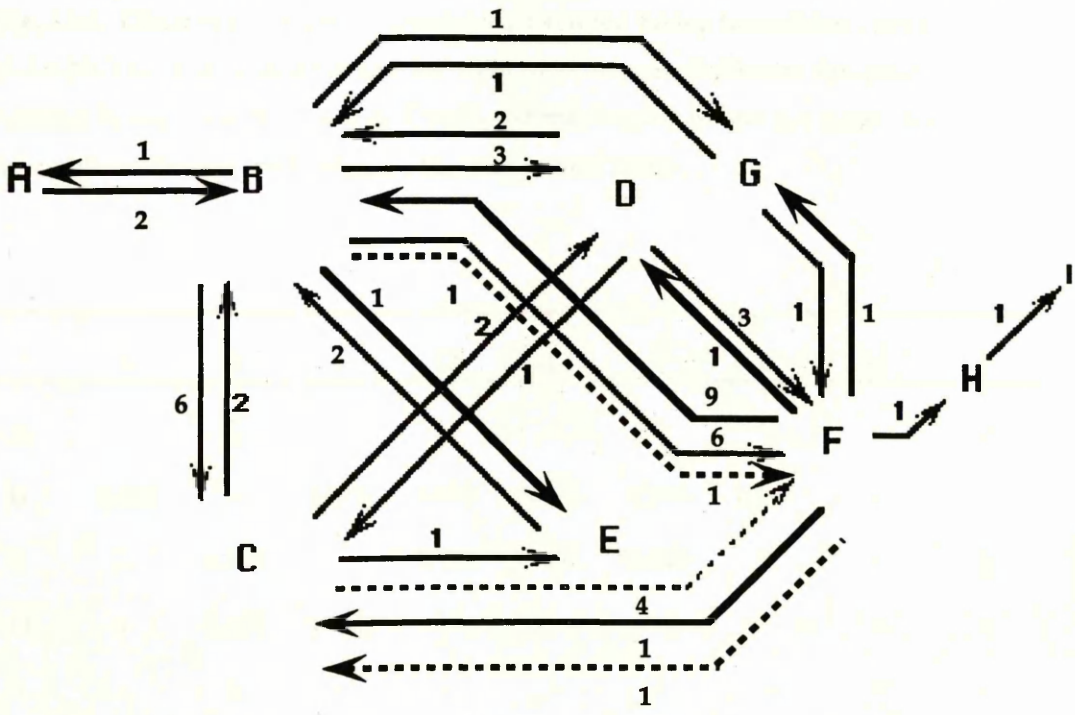

Figure. 3.2A Facies relationship diagram of the facies sequence in well A8 – NC7A. Numbers indicate how many times a particular upward transition occurs. Solid lines indicate sharp transitions between facies and dotted lines indicate gradational transitions.

	A	B	C	D	E	F	G	H	I	R-T
A	-	2	-	-	-	-	-	-	-	2
B	1	-	6	3	1	6	1	-	-	18
C	-	2	-	2	1	4	-	-	-	9
D	-	2	1	-	-	3	-	-	-	6
E	-	2	-	-	-	-	-		-	2
F	-	9	2	1	-	-	1	1	-	14
G	-	1	-	-	-	1	-	-	-	2
H	-	-	-	-	-	-	-	-	1	1
I	-	-	-	-	-	-	-	-	-	0
CL-T	1	18	9	6	2	14	2	1	1	54

Table. 3.1A Observed number of transitions between facies (transition count matrix) in well A8-NC7A. The number to the the right of the matrix indicates the total number of transitions in each row (R - T = Row Total); and the number below the matrix indicates the number of transitions in each column (CL-T = Column Total)

	A	B	C	D	E	F	G	H	I
A	-	1	--	–	–	–	–	–	–
B	0.055	-	0.333	0.166	0.055	0.333	0.055	–	–
C	–	0.222	-	0.222	0.111	0.444	–	–	–
D	–	0.333	0.166	-	–	0.5	–	–	–
E	–	1	–	–	-	–	–	–	–
F	–	0.643	0.143	0.071	–	-	0.071	0.071	–
G	–	0.5	–	–	–	0.5	-	–	–
H	–	–	–	–	–	–	–	-	1
I	–	–	–	–	–	–	–	–	-

Table. 3.2A Observed transition probabilities matrix in well A8-NC7A.

	A	B	C	D	E	F	G	H	I
A	0	0.346	0.173	0.115	0.038	0.269	0.038	0.019	0.019
B	0.027	0	0.25	0.166	0.055	0.388	0.055	0.027	0.027
C	0.022	0.400	0	0.133	0.044	0.311	0.044	0.022	0.022
D	0.166	0.375	0.187	0	0.042	0.292	0.042	0.021	0.021
E	0.019	0.346	0.173	0.115	0	0.269	0.038	0.019	0.019
F	0.025	0.450	0.225	0.150	0.050	0	0.050	0.025	0.025
G	0.019	0.346	0.173	0.115	0.038	0.269	0	0.019	0.019
H	0.018	0.339	0.169	0.113	0.037	0.264	0.037	0	0.018
I	0.018	0.333	0.166	0.111	0.037	0.259	0.037	0.018	0

Table. 3.3A Transition probabilities for random sequence matrix in well A8-NC7A.

	A	B	C	D	E	F	G	H	I
A	0	+0.64	- 0.173	- 0.115	- 0.038	- 0.269	- 0.038	- 0.019	- 0.019
B	+ 0.028	0	+ 0.083	0	0	- 0.055	0	- 0.027	- 0.027
C	- 0.022	- 0.178	0	+ 0.089	+ 0.067	+ 0.133	- 0.044	- 0.022	- 0.022
D	- 0.166	- 0.042	- 0.021	0	- 0.042	+ 0.208	- 0.042	- 0.021	- 0.021
E	- 0.019	+ 0.654	- 0.173	- 0.115	0	- 0.269	- 0.038	- 0.019	- 0.019
F	- 0.025	+ 0.193	- 0.082	- 0.079	- 0.050	0	+ 0.021	+ 0.05	- 0.025
G	- 0.019	+ 0.154	- 0.173	- 0.115	- 0.038	+ 0.231	0	- 0.019	- 0.019
H	- 0.018	- 0.339	- 0.169	- 0.113	- 0.037	- 0.264	- 0.037	0	+ 0.980
I	- 0.018	- 0.333	- 0.166	- 0.111	- 0.037	- 0.259	- 0.037	- 0.018	0

Table. 3.4A Observed minus random transition probabilities matrix in well A8-NC7A.

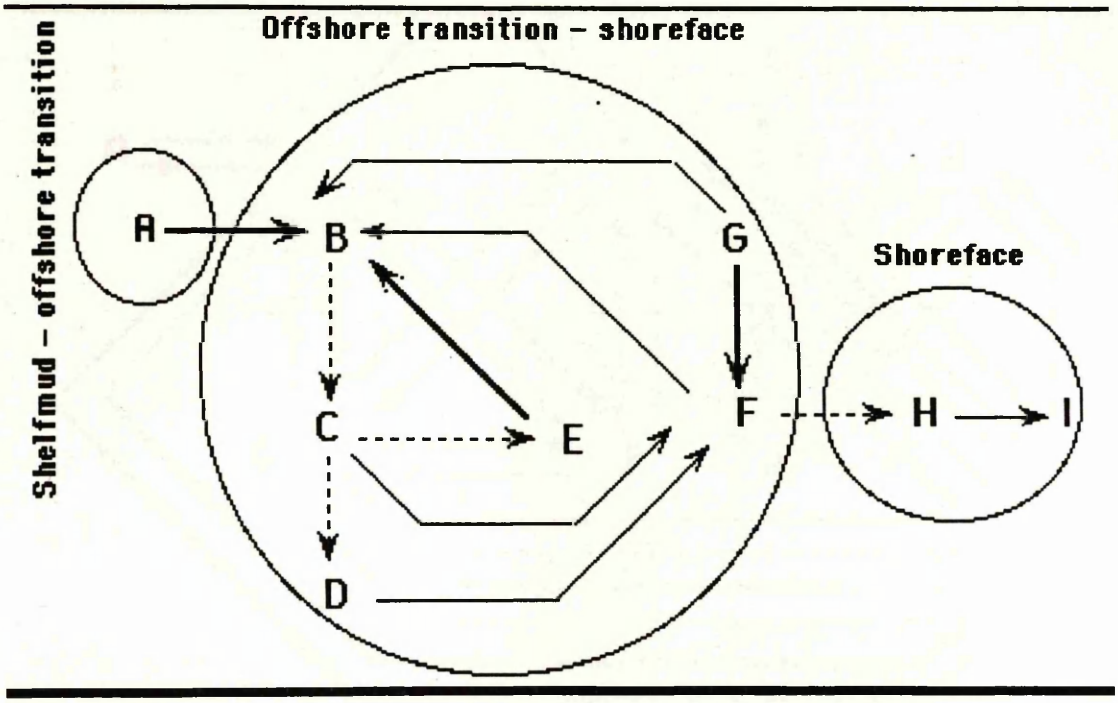

Figure 3.3A Facies relationship diagram showing facies transitions that occur more commonly than random in well A8-NC7A. The diagram is derived from data in Figure 1E, and only shows transitions whose observed random transition probability exceeds 0.050; dotted arrows show probability between 0.050 and & 0.1, light solid arrows 0.10 to 0. 20; heavy solid arrows probabilities > 0. 20 . Three interpreted facies associations are shown on the diagram.

A, B, A ** B, F1, C, B, C, B, E, D, E, B, C, E, B, C. F2. C, D, F2, B, F3, B, [F1, F3, F1, F3], B, F3, G, F1, D, [F3. F2] , B, F3, D, [F3. F2] , B, F2, B ** C, F2, B, C, F1, D, C, D, C, D, B, F2, D, F1, D. F3, H, E, H. E. H. F2, C, F2, B, [F2, F3, F2, F3]

Figure. 3.1B Observed sequence of facies in well A12–NC7A. From stratigraphic base upward the sequence reads A, B, A, etc. [, = Sharp contact . = Transitional contact ** = Missing or uncored interval]

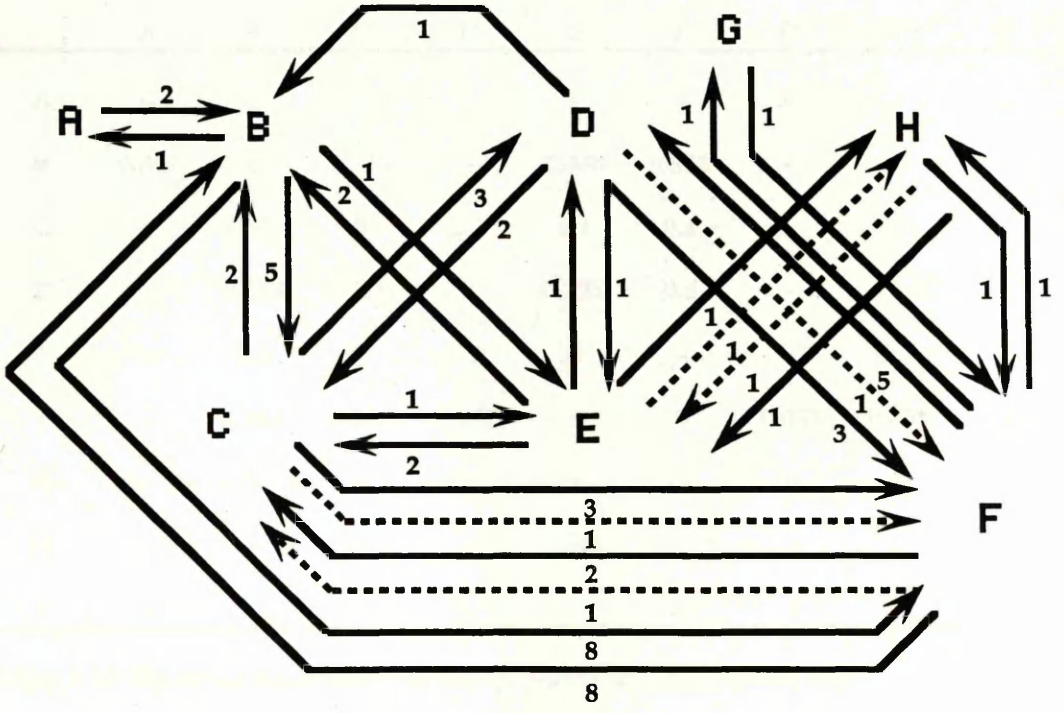

Figure. 3.2B Facies relationship diagram of the facies sequence in well A12 – NC7A. Numbers indicate how many times a particular upward transition occurs. Solid lines indicate sharp transitions between facies and dotted lines indicate gradational transitions.

	A	B	C	D	E	F	G	H	I	R-T
A	-	2	-	-	-	-	-	-	-	2
B	1	-	5	-	1	8	-	-	-	15
C	-	2	-	3	1	4	--	--	--	10
D	-	1	2	-	1	4	-	-	-	8
E	-	2	-	1	-	-	-	2	-	5
F	-	8	3	5	-	-	1	1	-	18
G	-	-	-	-	-	1	-	-	-	1
H	-	-	-	-	2	1	-	-	-	3
I	-	-	-	-	-	-	-	-	-	0
CL-T	1	15	10	9	5	18	1	3	0	62

Table. 3.1B observed number of transitions between facies (transition count matrix) in well A12–NC7A. The numbers to the the right of the matrix indicate the total number of transitions in each row (R - T = Row Total); and those below the matrix indicate the number of transitions in each column (CL-T = Column Total)

	A	B	C	D	E	F	G	H	I
A	0	1	-	-	-	-	-	-	-
B	0.066	0	0.333	-	0.066	0.533	-	-	-
C	-	0.2	0	0.3	0.1	0.4	-	-	-
D	-	0.125	0.25	0	0.125	0.5	-	-	-
E	-	0.4	-	0.2	0	-	-	0.4	-
F	-	0.444	0.166	0.277	-	0	0.055	0.055	-
G	-	-	-	-	-	1	0	-	-
H	-	-	-	-	0.666	0.333	-	0	-
I	-	-	-	-	-	-	-	-	0

Table. 3.2B Observed transition probability matrix in well A12–NC7A.

	A	B	C	D	E	F	G	H	I
A	0	0.250	0.166	0.15	0.083	0.3	0.016	0.05	-
B	0.021	0	0.212	0.191	0.106	0.382	0.021	0.63	-
C	0.019	0.288	0	0.173	0.096	0.346	0.019	0.057	-
D	0.018	0.277	0.185	0	0.092	0.333	0.018	0.055	-
E	0.017	0.263	0.175	0.157	0	0.315	0.017	0.052	-
F	0.022	0.340	0.227	0.204	0.113	0	0.022	0.068	-
G	0.016	0.245	0.163	0.147	0.081	0.295	0	0.049	-
H	0.016	0.254	0.169	0.152	0.084	0.305	0.016	0	-
I	-	-	-	-	-	-	-	-	0

Table. 3.3B Transition probabilities from random sequence matrix in well A12–NC7A.

	A	B	C	D	E	F	G	H	I
A	0	+0.75	-0.166	-0.15	-0.083	-0.3	-0.016	-0.05	-
B	+0.045	0	+0.121	-0.191	-0.04	+0.151	-0.021	-0.63	-
C	-0.019	-0.088	0	+0.127	-0.004	+0.054	-0.019	-0.057	-
D	-0.018	-0.152	+0.065	0	-0.033	+0.167	-0.018	-0.055	-
E	-0.017	+0.137	-0.175	+0.043	0	-0.315	-0.017	+0.348	-
F	-0.022	+0.104	-0.061	+0.073	-0.113	0	+0.033	-0.013	-
G	-0.016	-0.245	-0.163	-0.147	-0.081	+0.705	0	-0.049	-
H	-0.016	-0.254	-0.169	-0.152	+0.582	+0.028	-0.016	0	-
I	-	-	-	-	-	-	-	-	-

Table. 3.4B Observed minus random transition probabilities matrix in well A12–NC7A.

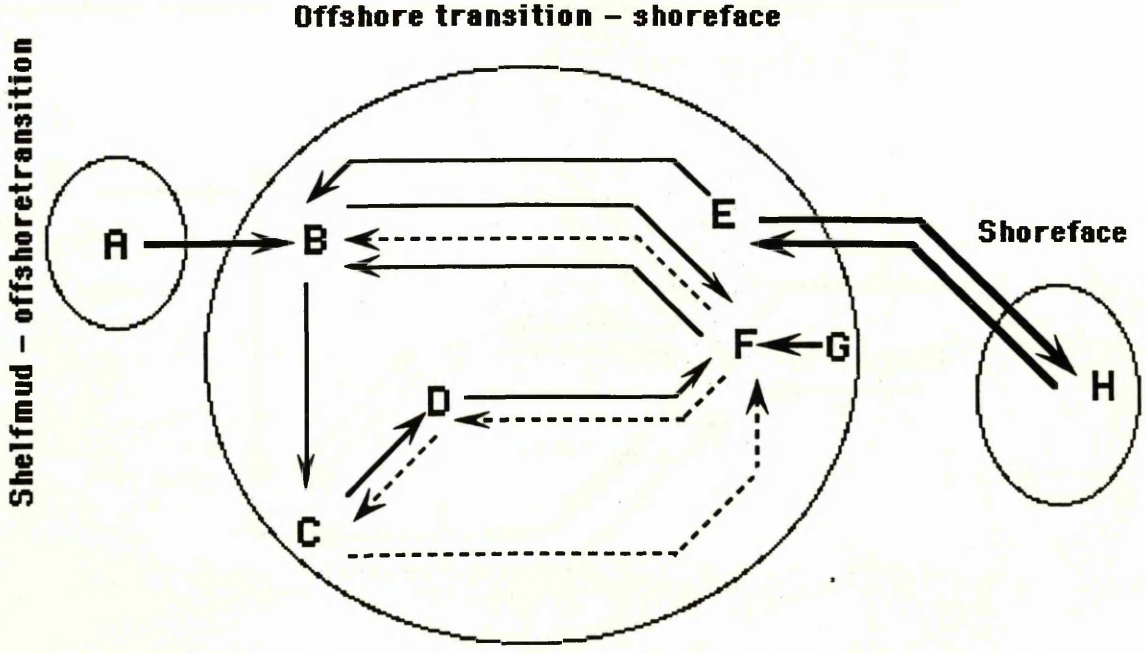

Figure 3.3B Facies relationship diagram showing facies transitions which occur more commonly than random in well A12–NC7A. The diagram is derived from data in Figure 2E , and only shows transitions whose observed - random transition probability exceeds 0.050 ; dotted arrows show probability between 0.050 & 0.1; light solid arrows 0.10 to 0. 20; heavy solid arrows probabilities > 0. 20 . Three interpreted facies associations are shown on the diagram.

A, B, F2, B, F2, B, C, D, C. F2, B, [F3, F2, F3. F2, F3. F2, F3] , B, F3, D, F3, G, F2, B, F3, D ** [F3. F1, F2] , B, F2, B, F2, D, F2, C, D, [F1, F3] ,H

Figure. 3.1C Observed sequence of facies in well A13–NC7A. From stratigraphic base upward the sequence reads A, B,F2, etc. [, = Sharp contact . = Transitional contact ** = Missing or uncored interval]

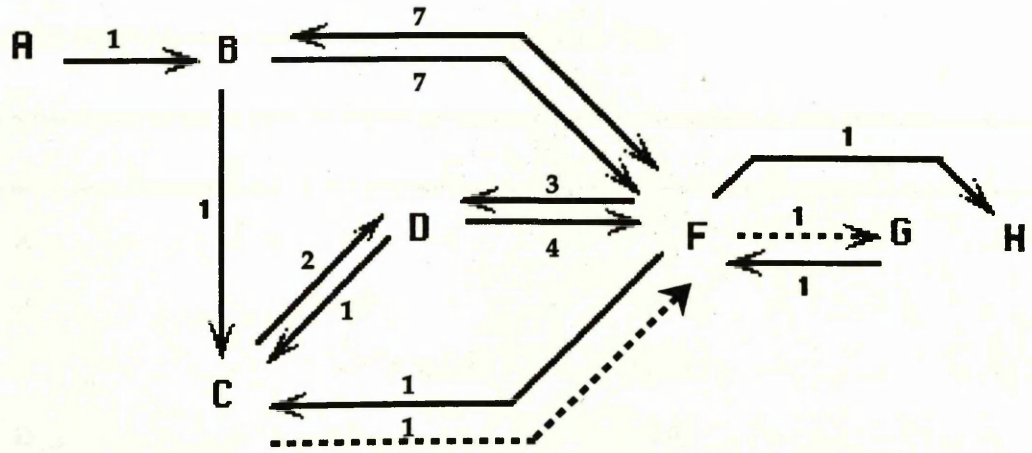

Figure. 3.2C Facies relationship diagram of the facies sequence in well A13 – NC7A . Numbers indicate how many times a particular upward transition occurs. Solid lines indicate sharp transitions between facies and dotted lines indicate gradational transitions.

	A	B	C	D	E	F	G	H	I	R-T
A	-	1	-	-	-	-	-	-	--	1
B	-	-	1	-	-	7	-	-	—	8
C	-	-	-	2	-	1	-	-	—	3
D	-	-	1	-	-	4	-	-	—	5
E	—	—	—	—	—	—	—	—	--	--
F	-	7	1	3	-	-	1	1	—	13
G	-	-	-	-	-	1	-	-	--	1
H	-	-	-	-	-	-	-	-	--	0
I	--	--	--	--	--	--	--	--	--	--
CL-T	0	8	3	5	--	13	1	0	--	31

Table. 3.1C Observed number of transitions between facies (transition count matrix) in well A13–NC7A. The numbers to the the right of the matrix indicate the total number of transitions in each row (R - T = Row Total); and those below the matrix indicate the number of transitions in each column (CL-T = Column Total)

	A	B	C	D	E	F	G	H	I
A	-	1	-	-	--	-	-	-	--
B	-	-	0.125	-	--	0.875	-	-	--
C	-	-	-	0.666	--	0.333	-	-	--
D	-	-	0.2	-	--	0.8	-	-	--
E	-	-	-	-	-	-	-	-	--
F	-	0.538	0.076	0.230	--	-	0.076	0.076	--
G	-	-	-	-	--	1	-	-	--
H	-	-	-	-	--	-	-	-	--
I	--	--	--	--	--	--	--	--	--

Table. 3.2C observed transition probability matrix in well A13–NC7A.

	A	B	C	D	E	F	G	H	I
A	-	0.266	0.100	0.166	--	0.433	0.033	0.033	--
B	-	-	0.130	0.217	--	0.565	0.043	0.043	--
C	-	0.285	-	0.178	--	0.464	0.036	0.036	--
D	-	0.307	0.115	-	--	0.500	0.038	0.038	--
E	-	-	-	-	--	-	–	-	--
F	-	0.615	0.230	0.384	--	-	0.077	0.077	--
G	-	0.266	0.100	0..166	--	0.433	-	0.033	--
H	-	0.258	0.096	0.161	--	0.419	0.032	-	--
I	-	--	--	--	--	--	--	--	--

Table. 3.3C Transition probabilities for random sequence matrix in well A13–NC7A.

	A	B	C	D	E	F	G	H	I
A	-	+ 0.734	- 0.100	- 0.166	--	- 0.433	- 0.033	- 0.033	--
B	-	-	- 0.005	- 0.217	--	+ 0.310	- 0.043	- 0.043	--
C	-	- 0.285	-	+ 0.488	--	- 0.131	- 0.036	- 0.036	--
D	-	- 0.307	+ 0.085	-	--	+ 0.300	- 0.038	- 0.038	--
E	-	-	-	---	--	-	-	-	--
F	-	- 0.077	- 0.160	- 0.154	--	-	0.001	+ 0.001	--
G	-	- 0.266	- 0.100	- 0.166	--	+ 0.567	-	- 0.033	--
H	-	- 0.258	- 0.096	- 0.161	--	- 0.419	- 0.032	-	--
I	-	--	--	--	--	--	--	--	--

Table. 3.4C Observed minus random transition probabilities matrix in well A13–NC7A.

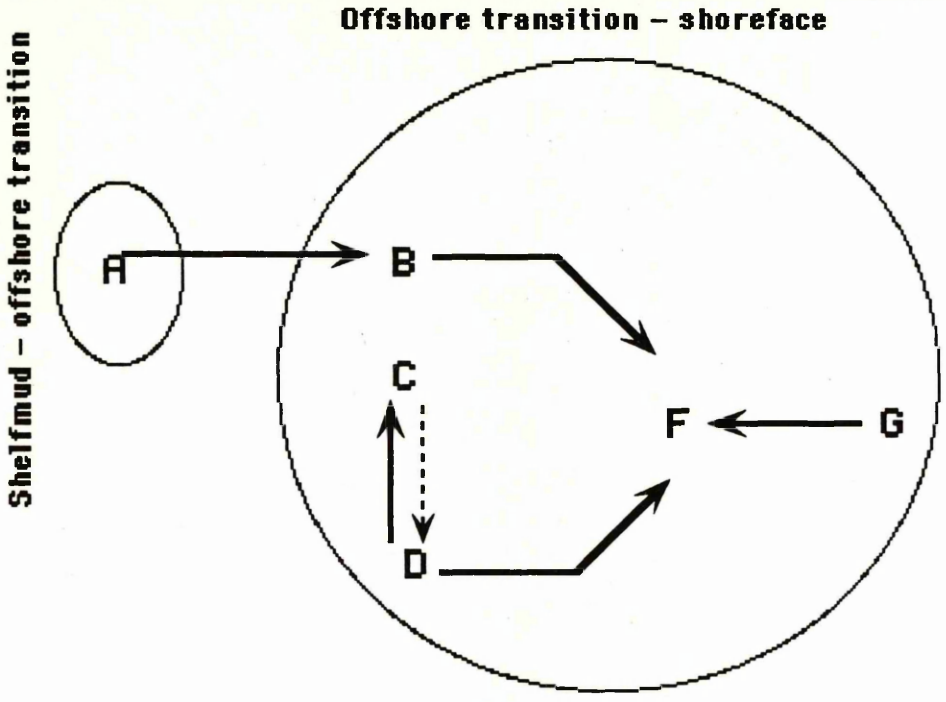

Figure 3.3C Facies relationship diagram showing facies transitions which occur more commonly than random in well A13–NC7A. The diagram is derived from data in Figure 3E , and only shows transitions whose observed - random transition probability exceeds 0.050 ; dotted arrows show probability between 0.050 & 0.1 ; light solid arrows 0.10 to 0. 20; heavy solid arrows probabilities > 0. 20 . Three interpreted facies associations are shown on the diagram.

CHAPTER 4

CHAPTER 4

GEOLOGICAL HISTORY OF THE AREA

The tectonic stability of cratonic basins such as the Hamada Basin, have provided them with a sensitive monitor in which the sea level history is viewed in the form of well defined and widely spread sedimentary cycles. The Hamada basin however, seem to consist of several cycles of sea level change reflected in the stacking pattern of unconformity bounded sedimentary sequences (see enclosure I). A cycle of relative change in sea level consists of a gradual relative rise, a period of still stand, and a rapid relative fall (Vail *et al.*, 1977). Under these conditions, an unconformity bounded sedimentary sequence usually forms (Vail *et al.*, 1977). During a cycle of relative sea level change the overall cumulative rise is interrupted by a number of smaller scale rapid rises and still stands (Vail *et al.*, 1977) during one of which the Tahara Formation is thought to have been deposited. The Tahara regressive sequence is one of several stacked regressive sequences formed as part of the transgressive-regressive cyclic fill of the Hamada intracratonic basin. In sequence stratigraphic terms the Tahara Formation is a progradational parasequence set which forms part of a sedimentary sequence (see enclosure I) and is characterised by a special position within that sequence. Relating the Tahara formation to a particular system tract within the sequence is not possible on the scale of the study, although the progradational nature of the set might suggest it to be of highstand system tract when compared to the ideal sequence of Van Wagoner (1990). During the overall regression of the Tahara formation, however, the sequence was interrupted by episodic pulses of of sea-level rise which resulted in the cyclic deposition of shelf to shore

face progradational parasequences. This fluctuating, but overall regressive, movement was terminated by a major marine transgression (Marar shale) which resulted in the formation of a parasequence set boundary that ended the underlaying stacking pattern.

The Tahara Formation provides a typical example of a storm dominated shelf to shoreface siliciclastic sequence (Fig. 4.1). Deposition probably took place in the proximity of a fine-grained coast line, within or adjacent to a deltaic system, which supplied enough sediment to overcome the effects of subsidence and cause the shoreline to migrate under conditions of stationary or falling sea level. The absence of coarse- or even medium-grained sands in the sequence can be attributed to more than one cause. One explanation suggests that deposition was adjacent to rather than within a deltaic system (see Fig. 4.1), in which the fine portion of coarse sediments brought to the shoreline by rivers was dispersed along the shoreline and away from the source by longshore currents. It was probably later transported offshore by winter storms, and here further sorting occurred. The extent of marine sands onto the shelf indicates that the hydraulic processes were adequate to move sand to considerable distances. The absence of coarse grained sands might alternatively be attributed to a complex paleogeography in which coarse material was trapped in lakes or lagoons and only the fine portion released to the shelf. Another explanation suggests that deposition was in-front of a delta system which only supplied fine sands to the shoreline.

The regional paleogeography of the Hamada basin during the deposition of the Tahara Formation is poorly understood. However, the

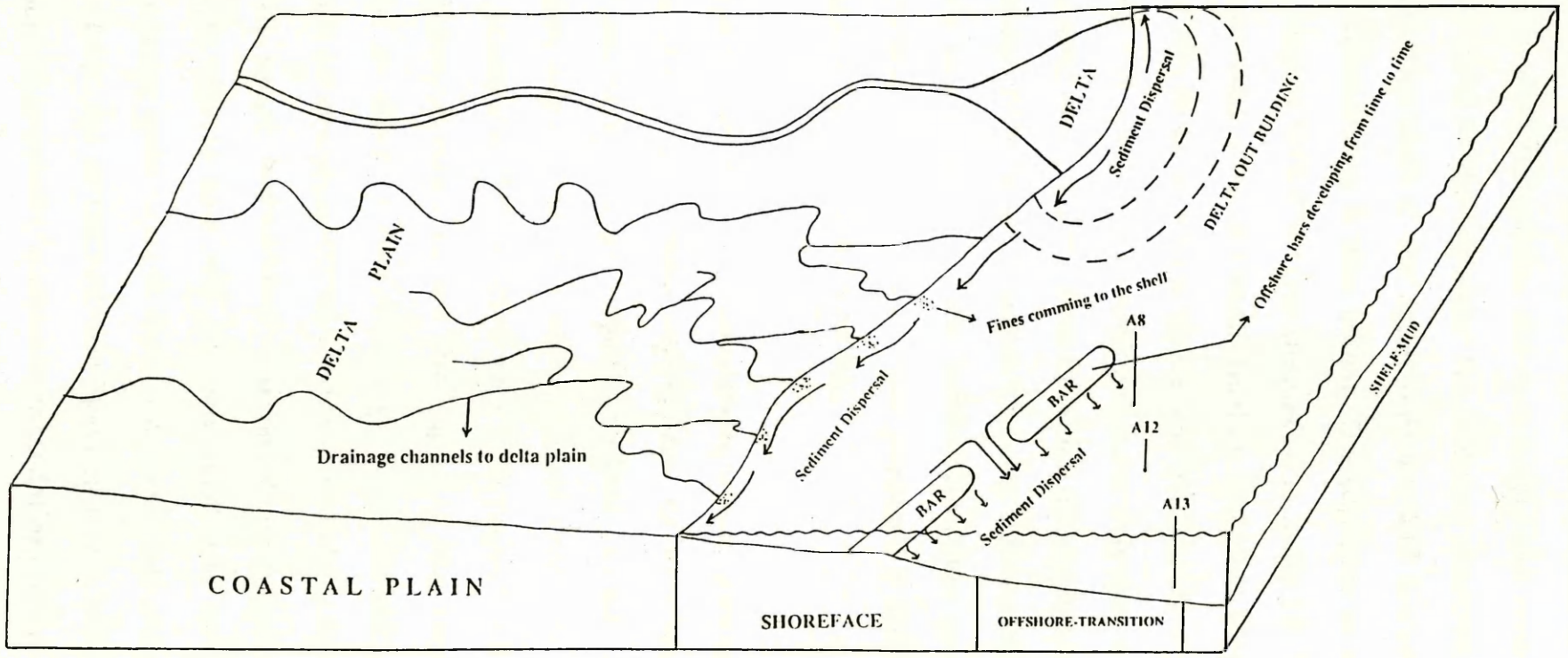

Fig. 4.1 Diagram illustrating the depositional system, dispersal of sediment and possible location of wells with respect to the suggested paleogeography (A8, A12 & A13)

reconstruction of paleogeography in the El-Gullebi area (see Fig. 4.1) is based on facies interpretations and their lateral and vertical relationships and distribution in the sequence. No evidence of exposure or shoreline deposition is present in the cored sections, and evidence to precisely position the shoreline is thus absent. The shoreline is inferred to have trended roughly ENE-WSW (see discussion in facies H). The extension of sandstone units onto the shelf further suggests that the shoreline migrated NW from its former (unknown) position to a position not far from well A13 (see Fig. 4.1). Regional facies mapping suggests that the source of sand was probably from the south and southeast corners of the basin (Beicip, 1973: internal company report). Cross-sections constructed from core data indicate that the Tahara Formation consists of several sandstone bodies, two of which have produced hydrocarbons to date (parasequence 14 & 15, well-A8-NC7A).

Deposition in the Tahara Formation reflects the operation of numerous variables including sediment supply, rate of subsidence and rate of eustatic sea level change. Other variables include local sediment compaction, slope, duration of parasequences, configuration of the coast, and the orientation of the studied wells with respect to the shoreline (see interpretation of facies H, see also Fig. 4.1) The above factors have interacted at different rats and magnitudes, resulting in the cyclic deposition of asymmetrical parasequences which differ in thickness, sand-shale ratios, bioturbation and facies arrangements. Where the subsidence rate is low and the sea level rise is low or falling, accommodation space is small. In contrast with high subsidence rate and high sea level rise accommodation space is large. More sediments can accumulate in situations where accommodation is large; shoaling and

shoreface progradation will thus occur over thick fine units (Brenchley et al., 1993) (eg. parasequences Nos. 6 & 11). On the other hand with small accommodation space there is a rapid seaward migration of shallow-water facies over more offshore ones producing parasequences with sharp facies transitions (Brenchley et al., 1993) (eg. parasequences Nos. 1 & 15). A sharp facies transition may also occur when a major river is diverted to a more distant part of the coastal plain while the abandoned muddy shelf continues to subside. This sudden and temporary change in sediment supply will result in the formation of a parasequence boundary above which near-shore shallow marine muds are deposited (assuming a slow rate of subsidence) (eg. facies E & G). These are later succeeded by sand, with renewed detrital influx creating a relatively sharp facies transition within parasequences (eg. parasequences Nos. 4 & 5). This idea has been proposed by Walker (1971) to explain coarsening-upwards sequences. However, "Parasequences that are formed on gently dipping coastlines commonly show upwards-coarsening and thickening sequences capped by shoreface sandstone" (Brenchley et al., 1993) if enough time is permitted. The poorly developed nature of facies within parsequences in the Tahara may thus suggest a relatively steep slope during the deposition of this formation. The orientation of the wells with respect to the shoreline is probably another major influence on the architecture of parasequences in the El-Gullebi area. Another location on the same shoreline a few miles away may at the same time have a quite different local rate of subsidence and deposition. Thus the position of the studied wells relative to the shoreline have made them effectively three separate areas (Fig. 4.1) which probably experienced different rates of sediment supply and were probably undergoing different rates of subsidence, and hence generated parasequences of different thickness and facies

architecture. Nevertheless, these wells have shown reasonable correlation with each other, indicating that, although their positioning was different, they were probably under the same set of environmental and tectonic conditions and were probably receiving sediments from the same source. Finally, local compaction of underlying sediments is another controlling factor which may cause subsidence of the coastline. Most parasequences in the Tahara Formation show upward-shallowing into shoreface facies, indicating a lack of accommodation space, although some parasequence are incomplete and have ended in the offshore-transitional environment, indicating either a large accommodation space, a short time duration, a variation in sediment supply or all these together. Variations among parasequences cannot be attributed to one particular process, although some predictions could be made. Based on the understanding of depositional dynamics, facies G in parasequence 7, for example, shows a real reduction in sediment supply but at the same time it shows no evidence of basin deepening. This suggests that the deposition of the sideritic mudstone beds was not the result of a large accommodation space created by basin subsidence, or a sea level rise more than it was the result of a change in sediment supply. Parasequences in the upper part of the Tahara Formation (eg. parasequence No. 15) have shown an increased rate of deposition and progradation compared with parasequences in the lower part, indicating a lack of accommodation space probably resulting from progressive basin filling and the proximity to active zones of sediment supply as the parasequence set shoals.

In the context of sequence stratigraphy the following geological history for the Tahara Formation is suggested (Fig. 4.2): At the end of the Aouinet-Ouenine deposition sea level rose, resulting in the formation of a

parasequence set boundary. Initially the rise rate was so fast that sediment input rate was no longer sufficient to fill the accommodation space created probably by the interaction of eustatic sea level change and basin subsidence. Depths were grater than storm wave base, and the shoreline was driven back over (probably) a complex paleogeography which outside the area of study could well have trapped fluvial sediments temporarily, increasing the overall declining sediment input rate to the shelf. A thick sequence of marine shale was deposited above the lower parasequence set boundary. Part of that shale is observed at the base of the cored sections in the three studied wells (see Fig. 2.27). In view of this, and on the basis of the predictions possible from sequence-stratigraphic analysis, the base of the Tahara Formation should be lowered to the base of this shale unit. However, as sea level approached its maximum value and the rise rate slowed, sediment input was once more able to cause the shoreline to prograde and regressive shelf sediments downlap over the shale unit.

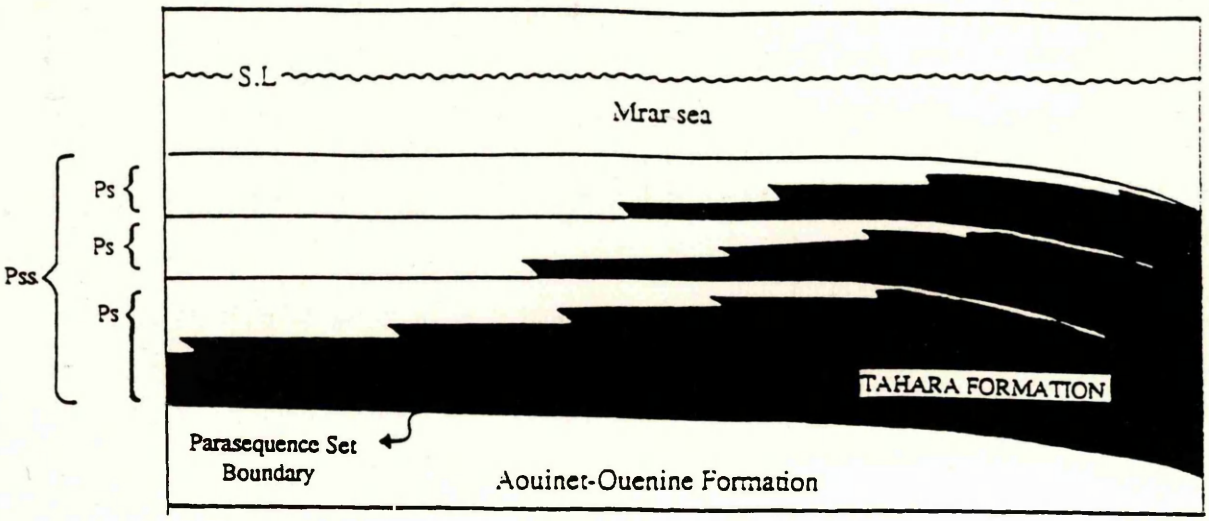

Stage 3

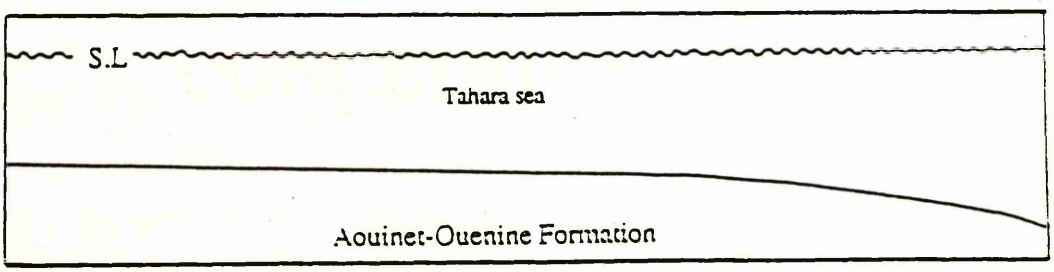

Stage 2

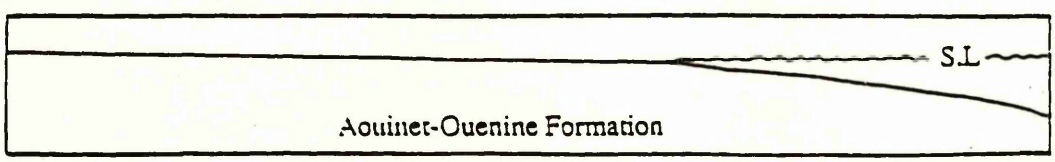

Stage 1

Fig. 4.2 Stages in the development of the Tahara Formation. Stage 1. Initial surface exposing Aounet Ouenin Fm. ; stage 2. the initial transgression which began the Tahara Fm. sequence. Stage 3. the basin fill which formed the present sequence.

CONCLUSION

CONCLUSION

-1- The Tahara Formation is a storm dominated siliciclastic shelf-shoreface sequence deposited on the eastern margin of the intracratonic Hamada basin in Libya.

-2- In sequence stratigraphic terms it is a progradational parasequence set bounded by two major marine flooding events (flooding surfaces). The parasequence set is thought to have been controlled by subsidence and sea level fluctuations working on a variable sediment supply.

-3- The Tahara formation consists of sixteen coarsening-thickening-and shallowing-upward parasequences stacked in a parasequence set separated by minor marine flooding surfaces.

-4- Parasequences grade to become less well defined when traced towards the basin centre.

-5- On the basis of grain size, bed thickness percentage of sandstone, percentage of bioturbation and facies interpretations, the series of studied wells is thought to have been oriented at an angle to the shoreline and are thought to reflect a transition to an increasingly offshore distal position.

-6- The deposition and distribution of facies was controlled by several factors of which the most important were: the rate of subsidence, rate of sediment supply, eustatic sea level change and the orientation of the wells with respect to the shoreline.

-7- The area was never below storm wave base after the deposition of facies (A), the deepest water facies in the sequence.

-8- The highest zone of biological activity is between the fair-weather and storm wave base

-9- Body fossils are rare and mainly restricted to the upper part of the sequence while trace fossils occur throughout the succession.

-10- There is a positive relationship between grain size, bed thickness and percentage of sandstone. There is a negative correlation between percentage of bioturbation and all the properties of the sandstone (see above)

-11- The sequences were deposited in the shoreface to offshore area of a coastline fed by one or more major rivers. However, the sequences studied here are thought to have been deposited some distance away from the main areas of sediment out-fall.

-12- In spite of the different approaches of the sequence stratigraphic, and the statistical techniques the results of analysis were similar.

REFERENCES

Aigner, T. (1982) Calcareous Tempestites: Storm dominated stratification in Upper Muschelkalk Limestones (Middle Trias, SW Germany): *In Einsele, G. and Seilacher, A., eds.*, Cyclic and Event Stratification: Springer-Verlag, Berlin, P. 180–198.

Aigner, T. & Reineck, H. E. (1982). Proximality trends in modern storm sands from the Heligoland Bight (North Sea) and their implications fore basin analysis. *Senckenbergiana Maritima*, **14**, 183-215.

Aigner, T. (1985) *Lecture Notes in earth sciences*, 3, 174pp Springer Verlag, Berlin. **10. 4. 4.**

Allen, J. R. L. (1982b) Sedimentary structures: Their character and physical basis, vol. **2**: Amsterdam, Esevier, 633p

Allen, P. A. & Underhill, J. R. (1989) Swaley cross-stratification produced by unidirectional flows, Bencliff Grit (Upper Jurassic), Dorset, U.K. *Jour. Geol. Soc. London*, v. **146**, p. 241-252.

Arnott, R. W. C. & Southard, J. B. (1990) Exploratory flow- duct experiments on combined-flow bed configuration, and some implications for interpreting storm -event stratigraphy: *Jour. Sed. Petrology*, v. **60**, p. 211-219.

Bartsch, W. S. & Schmoll, H. R. (1984) Bedding types in Holocene tidal channel sequences, Knik Amr, upper Cook Inlet, Alaska. *Jour. Sed. Petrology*, v. **54**, p. 1239-1250

Bayer, U. (1989) Stratigraphic and environmental patterns of ironstone deposits: *In Young T. P. & Taylor, W. E., eds.*, Phanerozoic Ironstones: *Geological Society of London Special Publication* **46**, P. 105–117

Bellini, E & Massa, D. (1980) A stratigraphic contribution to the Paleozoic of the southern basins of Libya. *In the Geology of Libya, M. J. Salem & M. T. Busrewil (eds).* Academic Press, Tripoli 1: 3

Bhattacharyya, D. P., & Kakimoto, P. K. (1982) Origin of ferriferous ooids: An SEM study of ironstone ooids and bauxite pisoids. *Journal of Sedimentary Petrology*, **52**, 849–857

Bless, M J M. & Massa D. (1982) Carboniferous Ostracodes in the Rhadames basin of western Libya - Paleoecological implications and comparisons with north-America, Europe and USSR: *Revue De L 'Institut Francais Du Petrole*, V. **37**, No. 1, pp. 19-61

Boersma, J. R.(1970) Distinguishing features of wave-ripple cross-stratification and morphology. Unpublished Ph.D. Thesis, university of Utrecht, 65pp.

Borghi, P. (1940) Fossili Paleozoici marini della Serie dell Uadi Ubarracat. *Ann. Mus. Libico Storia Nat.*, V. **2**, pp. 93-122

Bourgeois, J. (1980) A transgressive sequence exhibiting hummocky cross-stratification: the Cape Sebastian sandstone (Upper Cretaceous), southwestern Oregone: *Jour. Sed. Petrology*, v. **50**, p. 681-702.

Brenchley, P. J., G. Newall & I. G. Stanisteet (1979) A storm surge origin for sandstone beds in an epicontinantal platform sequence, Ordovician, Norway: *Sedimentary Geol.*, v.**22**, p. 185-217.

Brenchley, P. J. & G. Newall (1982) Storm influenced inner-shelf sand lobes in the Caradoc (Ordovician) of Shropshire, England. *J. Sediment. Petrol.* v, **52**, p. 1257–1269

Brenchley, P.J. (1985) Storm influenced sandstone beds: *Modern Geol.*, v. **9**,pp. 369-396

Brenchley, P. J., & Pickerill, R. K. (1991) Animal sediment relations in the Ordovician and Silurian of the Welsh Basin: *Proceedings of the Geological Association*, V. **110**,

Brenchley, P. J., Flint, S. S. & Stromberg, S. G. (1993) Quantitative facies discrimination and the application of sequence srtatigraphy to bed length modelling of shallow marine hetrolithic facies. *In. Subsurface Reservoir Characterisation from Outcrop Observation, Montadert, M & Eschard, R (eds).* **Editions Technip**

Brenchley, P. J., Pickerill, R. K. & Stromberg, S. G. (1993) The role of wave reworking on the architecture of storm sandstone facies, Bell Island Group (Lower Ordovician), eastern Newfoundland. *Sedimentology,* **40,** 2.

Brett, C. E., & Speyer, S. E. (1990) Taphofacies, in Briggs, D.E.G. and Crowther, P. R., eds., Paleobiology, A Synthesis: *Blackwell Scientific Publications, London,* p. 258–263.

Brett, C. E., & Baird, G. C. (1986) Comparative taphonomy: a key to paleoenvironmental interpretation based on fossil preservation: *Palaios,* V. **1,** P. 207–227

Bromley, R. G. & Ekdale, A. A. (1984) Chondrites: a trace fossil indicator of anoxia in sediments. *Sceince* **224,** 872–874

Bromley, R. G. (1990) Trace fossils: biology and taphonomy: *Unwin Hyman Ltd* P. 5-21

Bromley, R. G. & Asgaard, U. (1991) Ichnofacies: a mixture of taphofacies and biofacies. *Lethaia,* vol. **24,** pp. 153 – 163

Brown, L. F., & W. L. Fisher. (1977) Seismic-stratigraphy interpretation of depositional systems: examples from Brazil rift and pull-apart basins: *In C.E. Payton, ed., Seismic stratigraphy applications to hydrocarbon exploration: AAPG Memoir* **26,** p. 213-248

Bruce M. S., (1984) . High energy shelf-deposit: Early Proterozoic Wishart Formation, Northwestern Canada: *In Siliciclastic Shelf Sediments, Tillman, R. W and Siemers, C. T. (eds) Special Publication* No. **34** Tulsa

Buret, MB. & Moreau-Benoit, A. (1986) New information given by a palynoplanctological study of the sandy/shaly formation (Upper Silurian of Libya, Rhadames basin): *Comptes Rendus De l 'Academie Des Sciences Serie 11-Mecanique Physique Chimie Sciences De L 'Univers Sciences De La Terre* V. **302,** No. 16 p. 1009

Burollet, P. F. & Magnier, P. (1960) Remarques Sur la limite Cretace-Tertiaire en Tunisie et en Libya. *Proc. 21st Int. Geol. Congr., Pt.* **5,** pp. 136-144, 2 Cartes, Eng. Sum., Cophenhagen.

Burollet, P. F. (1963a) Reconnaissance geologique dans le sudest du bassin de Kufra. *Rev. Inst. Fr Petrole,* **18,** 1537-1545

Burollet, P. F. & Manderscheid, G. (1967) Le Devonien en Libya et en Tunisie. *Int. Symp. Devonian Syst.* (Calgary), 285-302.

Burollet, P. F. & Bryamjee, R. (1969) Sedimentological remarks on Lower Paleozoic sandstones of south Libya. In: Geology, Archaeology and Prehistory of the Southwestern Fazzan, Libya (ed. W. H. Kanes) *Petrol. Explor. Soc. Libya, 11th Annu. Field Conf.,* 91-101

Campbell, C. V. (1966) Truncated wave ripple laminae. *Jour. Sed. Petrology,* v. **36,** p. 825-828.

Carstens, M.R. Neilson, F. M. & Altinbilek, H. D. (1969) Bed forms generated in the laboratory under an oscillatory flow: anylatical and experimental study: *U.S Army Coastal engineering Research Centre Technical Memorandum no.* **28, 39** p. (plus 2 appendices).

Cheel, R.J. (1991) Grain fabric in hummocky cross-stratified storm beds: genetic implication, *Jour. Sed. Petrology,* v. **61,** p. 102-110.

Clifton, H. E. (1969) Beach lamination. *Marine Geol.,* **7**: 553–559

Clifton, H. E., Hunter, R. E. & Phillips, R. L., (1971) Depositional structures and processes in the non-barred high-energy nearshore. *J. Sedim. Petrol.,* **41,** 651–670

Clifton, H. E. (1972) Miocene marine to nonmarine transition in southern coast ranges of California [abs]: *Am. Assoc. Petroleum Geologists Bull.*, v. **56**, 28–39

Collinson, J. D. & Thompson, D. B. (1987) Sedimentary structures, George Allen & Unwin (publishers) Ltd.

Conant, L. C. & Goudarzi, G. H. (1967) Stratigraphic and tectonic framework of Libya. *Bull. Am. Assoc. Petrol. Geol.*, V. **51**, No. 5, pp. 719-730, 5 fig., Tulsa, Oklahoma.

Coquel, R., Doubinger, J. & Massa, D. (1988) New palynological data on the Visean Moscovian Carboniferous interval in the Ghadames basin (Libya)-Comparison with Saharan basins assessment of the Gondwanian and Euramerican influences: *Revue De L Institut Francais Du Petrole*, V. **43**, No. 1 pp. 3-16

Curray, J. R., (1960) Sediments and history of the Holocene transgression, continental shelf, Gulf of Mexico. *In: Recent Sediments Northwest Gulf of Mexico (Ed. by F. P. Shepherd, F. B. Phleger & Tj. H. Van Andel)*,pp. 221–266. *Bull. Am. Ass. Petrol. Geol.*

Curtis, C. D. (1985) Clay mineral precipitation and transformation during burial diagenesis. *Philosophical Transactions of the Royal Society of London* A **315**, 91–105

Davies, D. J., Powell, E. N., & Stanton, R. J., Jr. (1989) Taphonomic signature as a function of taphonomic process: shells and shell beds in a hurricane influenced inlet on the Texas coast: *Palaeogeography, Palaeoclimatology, Palaeoecology*, v. **72**, p. 317–356.

Davidson-Arnott, R. G. D., & Greenwood, B. (1974) Bedforms and structures associated with bar topography in the shallow water wave environment, Kouchibouguac Bay, New Bruniswick, Canada. *J. Sedim. Petrol.* v. **44**, 698–704

Davidson-Arnott, R. G. D., & Greenwood, B. (1976) Facies relationships on a barred coast, Kouchibouguac Bay, New Bruniswick, Canada. *In: Beach and neareshore sedimentation (Ed. by Davis, Jr., R. A. & Ethington, R. L.) pp 149–168 Spec. Publ. Soc. Econ. Paleont. Miner.*, **24** Tulsa.

De Raaf, J. F. M; Reading, H. G. & Walker R.G. (1965) Cyclic sedimentation in the lower Westphalian of North Devon, England. *Sedimentology*, V. **4**, P. 1-52

Desio, A. (1936a) Riassunto sulla Costituzione geolgica, del Fazzan. *Boll. Soc. Geol. Ital.*, V. **55**, No. 2, pp. 319-356, 3 fig.., 1 carta geol. scala 1: 3,000,000, Roma

Desio, A. (1936b) Prime notizie sulla presenza del Silurico fossilifero nel Fazzan. *Boll. Soc. Geol. Ital.*, V. **55**, No 1, pp. 116-120 Roma.

Dott, R. H., JR. & Bourgeois, J., 1982, Hummocky stratification: significance of its variable bedding sequences: *Geol. Soc. Am. Bull.*, v. **93**, p. 663-680.

Duke, W.L. (1982b) The 'type locality ' of hummocky cross-stratification: the storm-dominated Sillurian Medina Formation in the Niagara Gorge, New York and Ontario. *Proc. Ont. Petrol. Inst.* v. **21**, 2.1-2.31

Duke, W.L. (1985) Hummocky cross-stratification, tropical hurricanes and intense winter storms. *Sedimentology*, v. **32**, p. 167-194.

Duke, W.L. (1990) Geostrophic circulation or shallow marine turbidity currents? The dilemma of paleoflow patterns in storm-influenced prograding shore-line systems: *Jour. Sed. Petrology*, v. **60**, p. 870-883.

Evans, K. O. (1941) The classification of wave formed ripple marks: *Jour. Sed. Petrology*, v. **11**, 37–41

Eisma, Doeke, (1968) Composition origin and distribution of Dutch coastal sands between Hoek van Holland and the island of Vlieland: Netherlands. *Jour. Sed.*, v. **4**, 123–267

Ekdale, A. A. (1985) Paleoecology of the marine endobenthos. *Paleogeography., Paleoclimatology., Paleoecology.*, **50**, 63–81

Ekdale, A. A. (1988) Pitfalls of paleobathymetric interpretations based on trace fossil assemblages. *Palaios*, **3**, 464–472.

Elliott, T. (1986) Sliciclaclastic shore-line. *In: Sedimentary Environments and Facies (Ed by Reading, H.G):* Blackwell Scientific Publication, Oxford London Edinburgh Boston Mebourne

Fairchild, H. L. (1901) Beach structures in Medina sandstone. *Bull. Geol. Soc. Am.* v. **28**, p. 9-14.

Fabre, J. (1970a) Le Paleozoique terminal a facies gres rouge au Sahara central et occidental. C. R. *6eme Congr. Int. Stratigr. Geol. Carbonifere* (Sheffield, 1967), **2**, 737-744

Field, M. E., & Roy, P. S. (1984) Off-shore transport and sand-body formation: evidence from steep, high-energy shore-face, northeastern Australia. *Jour. Sed. Petrology,* v. **54**, 1292–1302

Fisher, W. L., & J. H. McGowen. (1967) Depositional systems in the Wilcox Group of the Texas and their relationship to occurences of oil and gas: *Transactions of the Gulf Coast Association of Geological Societies,* V. **17**, p. 105-125

Frey, R. W., Pemberton, S. G. & Saunders, T. d. A. (1990) Ichnofacies and bathymetry: a passive relationship. *Journal of Paleontology* **64**, 155–158

Fritz,W. J. & Moore, J. N. (1988) Basics of physical stratigraphy and sedimentology. *John Wiley & Sons*

George, T. N; Johnson, G. A. L; Mitchell, M; Prentice, J. E.; Ramsbottom, W. H. G; Sevastopulo, G. D. & Wilson, R. B. (1976) Dinatian: A correlation of Dinantian rocks in the British Isles: *Geol. Soc. Lond., Special Report* No. 7

Gilbert, G.K. (1899) Ripple marks and cross-bedding. *Bull. Geol. Soc. Am.* v. **10**, p. 135-140.

Godring, R. & Bridges, P. (1973) Sublittoral sheet sandstones: *Jour. Sed. Petrology*, v. **43**, p. 736- 747.

Gouadarzi, G. H. (1980) Structure of Libya. *In the Geology of Libya, M. J. Salem & M. T. Busrewil* (eds). Acadimic Press, Tripoli, **3**: 879

Greenwood, B. & Sherman, D. J. (1986) Hummocky cross-stratification in the surf zone: flow parameters and bedding genesis: *Sedimentology*, v. **33**, p. 33-45.

Greenwood, B. (1984) Hummocky lamination in the surf zone (abs.). *Soc. Econ. Paleo. Miner., Ann. Midyr Mg*, p36

Hamblin, A. P. & Walker, R. G., (1979) Storm-dominated shallow marine deposits: the Fernie-Kootenayn (Jurassic) transition, southern Rocky Mountains. *Can. J. Earth Sci.*, **16**, 1673-1690

Hammuda, O. S. (1980) Geological factors controlling fluid trapping and anomalous freshwater occurences in the Tadrart sandstone, Al-Hamadah -al Hamra area, Ghadames basin:*In the Geology of Libya, M. J. Salem & M. T. Busrewil* (eds). Acadimic Press, Tripoli, **2**: 509

Harland, W. B; Armstrong, R. L; Cox, A. V; Craig, L. E. & Smith, D. G (1990) A geological time scale 1989: *Cambridge University Press.*

Harms, J. C., Southard, J. B., Spearing, D. R. & Walker, R. G. (1975) Depositional environments as interpreted from primary sedimentary structures and stratification sequences: *Soc. Econ. Paleont. Mineral.* Tulsa, Short Course No. **2**, 161pp.

Howard, J. D. (1972) Trace fossils as Criteria for recognizing shore-lines in Stratigraphic Record: *Soc. Econ. Paleontologist Minerologists* Spec. Pub. No. **16**, p. 215-225.

Howard, J. D. (1975) The sedimentological significance of trace fossils. *In the study of trace fossils. R. W., Frey (ed),* 131-46 Berlin: Springer

Howard, J. D., & Reineck, H. E., (1981) Depositional facies of high energy beach to off-shore sequence, comparison with low energy sequence. *Bull. Am. Ass. petrol. Geol.,* **65,** 807-830

Hunter, R. E. & H. E. Clifton. (1982) Cyclic deposits and hummocky cross-stratification of probably storm origin in Cretaceous rocks of Cape Sebastian area, southwestern Oregon. *Jour. Sed. Petrology,* v. **52,** p. 127-144

Hunter, R. E., Thor, D. R., & Swisher, M. L. (1982) Depositional and erosional features of the inner shelf, Northeastern Bering Sea: *Geologie en Mijnbouw,* v. **61,** 49–62

Iijima, A. & Matsumoto, R. (1982) Berthierine and chamosite in coal measures of Japan. *Clays and clay Mineral,* **30,** 264-274

Ingrame, R. L., (1953) Fissilty of mud rocks: *Bull. Geol. Soc. Amer.* v. **64,** 869–878

Inman, D. L. (1957). Wave - generated ripples in neareshore sands: *Dept. Army Corps of Engineers, Beach Erosion Board Tech.* Mem **100,** 65pp

Ingle, J. C. (1966) The movement of beach sand: *New Your, Elsevier,* 221P

Jervey, M. T. (1988) Quantitative geological modeling of siliciclastic rock sequences and their seismic expression: *In , Sea level changes: an integrated approach, C. K. Wilgus et al., eds.: Society of Economic Paleontologists and Mineralogists Special Publication* **42,** P. 47-69

Jonson, H. D. & Buldwin, C. T. (1986) Shallow siliciclastic seas. *In: Sedimentary Environment and Facies (Ed. by Reading, H.G).* Blackwell Scientific Publication, Oxford, London, Edinburgh, Boston, Mesbourne

Kiltzsch, E. (1963) Geology of northeast flank of the Murzuq basin (Djebal Ben-Ghnema Dor el Gussa area): *Ints. Francais Petrole. Rev.* **18,** 1411-1427

Kiltzsch, E. (1965) Ein Profil aus dem Typusgebiet Gotland disher and devonischer Schichten der Zentralsahara (westrand Murzubecken, Libyen). *Erdol u. Kohle, Deusch.,* V. **18,** No. 8. pp. 605-603, 3 fig., Hamburg.

Kiltzsch, E. (1970) Problems of continental Mesozoic strata of southwestern Libya (with discussion). In Proc. Conf. African Geology (Dec., 1970): Regional Geology, pp. 483-494 Univ. Ibadan. Dept. Geol., Ibadan Nigeria.

Kirmani, KU. & Elhaj, F. (1988) Geology and hydrocarbon potential of the Hamada and Murzuq basins in western Libya: *Bull. Am. Assoc. Petrol. Geol.* V. **72,** No. 8 P 1010

Komar, P. D. Noeudeck, R. H. & Kulm, L. D. (1972) Observation and significance of deep water oscillatory ripple marks on the oragon continental shelf. *In: Shelf sediment transport: process and pattern (Ed. by D.J.P Swift, D.B. Duane & O.H. Pilkey)*

Komar, P. D., & Inman D. L. (1970) longshore sand transport on beaches. *J. Geophys. Res.* v. **75,** 5914–5927

Komar, P. D., Kulm, L. D. & Harlett,J. C., (1974) Observation and analysis of nepheloid layers on the Oregon continental shelf. *J. Geol.,* **82,** 104–111

Kulm, L. D., Roush, R. C., Harlett, J. C., Neudeck, R. H., Chambers, D. M. & Leckie D. A. & Walker, R. G. (1982) Storm-and tide-dominated shore-lines in Cretaceous Moosebar-Lower gates interval– outcrop equivalents of deep basin gas trap in western Canada. *Bull. Am. Ass. petrol. Geol.,* **66,** 138–157

Leckie, D. A. & Krystinik, L.F. (1989) Is there evidence for geostrophic currents preserved in the sedimentary record of inner to middle shelf deposits?: *Jour. Sed. Petrology,* v. **59,** p. 862-870.

Lelubre, M. (1946a) Sur la Paleozoique du Fezzan. *C. R. Hebd. Seanc. Accad. Sci.,* V. **222,** No. 24, pp. 1403-1404, Paris

Lelubre, M. (1948) Le Paleozoique du Fezzan sud-oriental. *C. R. Soc. Geol. Fr.,* V. **18,** No. 4, pp. 79-81, Paris

Lelubre, M. (1952a) Apercu sur la geolgie du Fezzan. *Bull. Serv. Carte Geol. d' Algerie, Travaux Recents Collaborateurs,* No. **3,** pp 109-148, 4 fig., biblio., Alger.

Levell, B. K. (1980) Evidence for current association with waves in late Precambrian shelf deposits from Finnmark, North Norway: *Sedimentology,* v. **27** p. 153-166

Lindholm, R. C. (1987) A practical approach to sedimentology: *Allen and Unwin, London* P. 1-38

Lobiziak, S. & Streel, M. (1989) Middle-Upper Devonian miospores from the Ghadamis basin (Tunisia-Libya) Systematics and Stratigraphy: *Review of Paleobotany and Paleontology,* V. **58,** No.2-4 pp. 173-196

Madon Mazlan, B. HJ. (1992). Depositional setting and origin of the berthierine oolitic ironstones in the lower Miocene Terengganu shale, Tenggol arch, off-shore Peninsular. Malaysia. *J. of Sedimentary Petrology,* v. No. **5,** P. 899-916

Massa, D. Collomb, G. R. (1960) Observations nouvelles sur la regiond Aouinet Ouenine et du Djebel Fazzan (Libye). *21st Int. Geol. Congr. Report., Pt.* **12,** pp. 65-73, 2 fig., Eng. Sum., Copenhagen.

Massa, D., Termier, G. & Termier, H. (1974) Le Carbonifere de Libye Occiental. Comp. *Fr. de Petrole, Notes et Mem.,* No. **11,** pp . 139-206, 5 + 11 fig., 2 table., 7 text-Pl.h.t., Paris

Massa, D. & Moreau-Benoit, A. (1976) Essai de Synthese Stratigraphique et palynologique du systeme Devonien en Libye Occidental. *Rev. Inst. Fr. Petrole,* V. **31,** No. 2, pp. 287-333, 5 fig., 8pl., Paris

Matthews, R.K. (1974, 1984) Dynamic stratigraphy.5 *Prentice-Hall, Inc., Englewood Cliffs, New Jersey*

McCave, I. N. (1971a) Wave effectiveness at the sea bed and its relationship to bed-forms and deposition of mud. *J. Sedim. Petrol.,* v. **41,** 89-96

McCave, I. N. (1985) Recent shelf clastic sediments. *In: Sedimentology: Recent Developments & Applied Aspects (Ed. by. Brenchley & B. P. J. Williams),* pp. 49-65. *Spec. Publ. geol. Soc, Lond.,* **18,** 49-65.

Middleton, G. V. (1973) Johannes Walter's law of the correlation of facies: *Geological Society Of American Bulletin,* V. **84,** p. 979-988

Mitchum, R. M. (1977) Seismic stratigraphy and global changes of sea level, Part 1: Glossary of terms used in seismic stratigraphy: *In C.E. Payton, ed., Seismic stratigraphy applications to hydrocarbon exploration: AAPG Memoir* **26,** p. 205-212

Moore, D. G. & Scruton, P. C. (1975) Minor internal structures of some recent unconsolidated sediments. *Bull. Am. Ass. Petrol. Geol.* **41.** 2723–51

Morang, A., & McMaster, R. L.,(1980) Nearshore bedform patterns along Rhode Island from side-scan sonar surveys: *Jour. Sed. Petrology,* v. **50,** 831–839

Moreau-Benoit, A. (1988) New reflections on palynozonation of the Middle and Upper Devonian in the Ghadames basin western Libya: *Comptes Rendus De l 'Academie Des Sciences Serie 11-Mecanique Physique Chimie Sciences De L Univers Sciences De La Terre* V. **307,** No. 7 pp. 863-869

Moreau-Benoit, A., & Massa D. (1988) Palynology and stratigraphy of a Lower Devonian type section of eastern Sahara (Ghadames basin, Libya):*Comptes Rendus De l 'Academie Des Sciences Serie 11-Mecanique Physique Chimie Sciences De L 'Univers Sciences De La Terre* V. **306,** No. 7 pp. 451-454

McKenzie, P. (1958) Rip-current systems: *Jour. Geology* v. **66,** 103–113

Nahon, D. Carozzi, A. V. & Parron, C. (1980) Lateritic weathering as a mechanism for generation of ferruginous ooids: *Journal of Sedimentary Petrology* V. **50,** P. 1287-1298

Norris, R. D. (1986) Taphonomic gradients in shelf fossil assemblages: Pliocene Purisima Formation, California: *Palaios,* v. **28,** p256–270.

Nelson, C. H. (1982) Modern shallow water graded sand layers from storm surges, Bering Shelf: a mimic of Bouma sequences and turbidite systems. *Jour. Sed. Petrology,* v. **52,** p. 537-545.

Pemberton, S. G. & Frey, R. W. (1984a) Ichnology of storm-influenced shallow marine sequence: Cardium Formation (Upper Cretaceous) at Seebe, Alberta. *In Stott, D. F., ed., The Mesozoic of middle North America. Canadian Society of Petroleum Geologists,* Memoir **9,** in press.

Pickerill, R. K., & Hurst, J. M. (1983) Sedimentary facies, depositional environment sand faunal association of the lower Llandovery (Silurian) Beechill Cove Formation, Arisaig, Nova Scotia: *Canadian Journal of Earth Sciences,* v. **29,** p. 1761–1779.

Pickerill, R. K., & Brenchley, P. J. (1991) Benthic macrofossils as paleoenvironmental indicators in marine siliciclastic facies. *Geoscience Canada* v. **18,** No. 3, P. 119-138

Posamentier, H. W. & Vail, P. R. (1988) Eustatic controls on clastic deposition II-sequence and system tract models in, C. K. Wilgus et al., eds., Sea-level change: an integrated approach: *Society of Economic Paleontologists and Mineralogists Special Publication* **42,** P. 125-154

Purdy, E G. (1964) Sediment as substrates. *In J. N. D. Newell (eds.), Approaches to paleoecology. New York, John Wiley, P. 238-271.*

Reading H. G. (1986) Sedimentary Environment and Facies: *Blackwell Scientific Publication,* Oxford London Edinburgh Boston Mebourne P. 4-19

Reineck, H. E. & Singh, I. B. (1971) Der Golf von Gaeta (Tyrrhenisches Meer) III. Die Gefuge von Vorstrand and Schelfsedimenten. *Senckenberg.* Mar. **3,** 185-201

Reineck, H. E. & Singh, I. B. (1972) Genesis of laminated sand and graded rhythmites in storm sand layers of shelf mud. *Sedimentology,* v.**18** : 123-128.

Reineck, H. E. & Singh, I. B. (1980) Depositional Sedimentary Environments: *Springer-Verlag Berlin Heidelberg*

Reimnitz, E. (1971) Surf-beat origin for pulsating bottom currents in the Rio Balsas Submarine Canyon: *Geol. Soc. Am Bull.,* **v.** 82, 81–90

Reimnitz, E., Toimil, L. J., Shepard, F. P., & Gutierrez-Estrada, M.(1976) Possible rip current origin for bottom ripple zones to 30m depth: *Geology,* v. **4,** 395–4

Rude, P. D. & Aller, R. C. (1989) Early diagenetic alteration of lateritic particle coatings in Amazon continental shelf sediments; *Journal of Sedimentary Petrology,* V. **59,** P. 704-716

Runge, E. J., (1975) Oregon continental shelf sedimentation: interrelationship of facies distribution and sedimentary processes. *J. Geol.,* **83,** 145-176

Said, F. M. & Kanes, WH. (1985) Paleozoic producing sequences in Ghadames basin of Libya, Tunisia, and Algeria - New stratigraphic concepts for hydrocarbon exploration: *AAPG, Bull. Am. Assoc. Petrol. Geol.* V. **69,** No. 2 P. 260

Salaj, J. & Nairn, AEM. (1987) Depositional environment of the lower Tar Member of the Zimam Formation (Upper Senonian) in the northern Hamada Al-Hamra, Libya: *Paleogeography, Paleoclimatology, Paleoecology,* V. **61,** No. 1-2, pp. 121-143

Seilacher, A. (1964) Biogenic sedimentary structures. *In Imbrie, J. & Newell, N. (eds): Approaches to Paleoecology,* 296–316. Wiley, New York.

Selly, R. C. (1970) Ancient Sedimentary Environments: *Chapman & Hall,* London, 237 pp

Siehl, A & Thein, J. (1989) Minette-type ironstone, in Young T. P. & Taylor, W. E., eds., Phanerozoic Ironstones: *Geological Society of London Special Publication* **46,** P. 105–117

Southard J. B., Lambie, J. M., Federico, D. C., Pile, H. T. & Weidman, C. R. (1990) Experiments on bed configuration in fine sands under bidirectional purely oscillatory flow, and the origin of hummocky cross-stratification: *Jour. Sed. Petrology,* v. **60,** p. 1-17.

Speyer, S. E., & Brett, C. E. (1988) Taphofacies models for eperic sea environment: Middle Paleozoic examples: *Palaeogeography, Palaeoclimatology, Palaeoecology,* v. **63,** p. 225–262

Stanley, S. M. (1986) Earth and Life Through Time: *W. H. Freeman & Company*

Sundbarg , A. (1965) The River Klaralven: A study of fluvial processes. *Geogr. Annlr,* **38,** 127-316.

Swift, D. J. P., Figueiredo, A. G., Freeland F. L., & Oertel, G. F.(1983) Hummocky cross-stratification and megaripples: a geological double standard?: *Jour. Sed. Petrology,* v. **53,** p. 1295-1318.

Swift, D J. P., Hudelson P. M., Brenner, R. L. &Thompson P. (1987) Shelf construction in a foreland basin: storm beds, sandbodies, and shelf-slope depositional sequences in the Upper Cretaceous Mesaverde group, Book Cliffs, Utah: *Sedimentology*, v. **34**, p. 423-457.

Vail, P. R; Mitchum, R. M & Thompson, S. III (1977) Seismic stratigraphy and global changes of sea level, Part 3: relative changes of sea level from coastal onlap: *In: C. W. Payton ed., Seismic stratigraphy applications to hydrocarbon exploration: AAPG Memoir* **26,** P 63-97

Van Houten, F. B & Purucker, M. E. (1984) Glauconitic peloids and chamositic ooids - favorable factors, constraints and problems; *Earth-science Reviews* V. **20,** P.211-243

Van Wagoner, J. C; Mitchum , R. M; Campion , K. M &Rahmanian , V.D (1990), Siliciclastic Sequence Stratigraphy in Well Logs, Cores, and Outcrops: Concepts for High Resolution Correlation of Time and Facies. *AAPG Methods in Exploration* Series No. **7**

Van Wagoner, J. C. (1985) Reservoir facies distribution as controlled by sea-level change, Abstract: *Society of Economic Paleontologists and Mineralogists* Mid-yeare Meeting, Golden, Colorado August 11-14, P. 91-92

Vos, RG. (1981) Sedimentology of an Ordovician fan delta complex, western Libya: *Sedimentary Geology*, V. **29,** No. 2-3, pp. 153-170

Vossler, S. M. & Pemberton, S. G. (1988) Skolithos in the Upper Cretaceous Cardium formation: an ichnofacies example of opportunistic ecology. *Lethaia* **21,** 351–362

Walker, R. G. (1971) Nondeltaic depositional environments in the Catskill clastic wedge (upper Devonian) of central Pennsylvania: *Geol. Soc. America. Bull.*, v. **82,** P. 1305-1326

Walker, R. G. (1979, 1984) Shallow marine sands: *In Walker, R. G., ed., Facias*

models: Geoscience Canada Reprint Series **1**

Walker, R. G., Duke, W. L., & Leckie, D. A. (1983) Hummocky stratification: significance of its variable bedding sequence: Discussion: *G.S.A. Bull.*, v. **94**, p. 1245-1249.

Walley, CD. (1985) Depositional history of southern Tunisia and northwestern Libya in mid and late Jurassic times: *Geological Magazine,* V. **122,** No. 3 pp. 233-247

Whitbread, T. & Kelling, G. (1982) Marar Formation of western Libya-Evolution of an early Carboniferous delta system: *AAPG, Bull. Am. Assoc. Petrol. Geol.* V. **66,** No. 8, pp.1091-1107

Young, T. P. (1989) Phanerozoic ironstones; an introduction and review: *In: Young, T. P., and Taylor, W. E. G., eds., Pahanerozioc ironstones; Geological Society of London Special Publication* **46,** P. 1X – XXV

GLASGOW
UNIVERSITY
LIBRARY

(I)

GENERAL STRATIGRAPHIC COLUMN OF THE HAMADA BASIN

AGE			FORMATIONS	LITHOLOGIC LOG	THICKNESS IN FEET	BRIEF LITHOLOGICAL DESCRIPTION
MESOZOIC	CRETACEOUS	UPPER	MIZDA-GASRTIGRINA		600	CHALKY LIMESTONE AND CLAYS WITH DOLOMITE BEDS IN PLACES
			GARIAN		250	LIMESTONE, DOLOMITIC LIMESTONE
			SIDI - ASSID		320	GYPSUM, SILT YELLOW-GREEN WITH SOME SHALE AND LIMY BEDS
					300	LIMESTONE, DOLOMITIC LIMESTONE, OOLITIC IN PLACES
		LOWER	CHICLA		700	SANDSTONE, CONGLOMERITIC IN PLACES WITH INTERBEDS OF REDDISH YELLOW GREENISH CLAY
			AUSTRIAN UNCONFORMITY			
			CABAO		500	UNCONFORM SANDSTONE WITH SILTSTONE, CLAY AND CLAYSTONE ALTERNATIONS ESPECIALLY AT THE BASE
	JURASSIC	UPPER	SHAKSHUK		450	ALTERNATION LIMESTONE, DOLOMITIC LIMESTONE, CLAY OCCASIONAL SANDSTONE
		MIDDLE	LES ABREGHS		900	DOMINATELY GYPSUM AT THE TOP WITH YELLOW GREEN CLAY AND SOME LIMY BEDS. ANHYDRITE DOMINANT AT THE BASE
		LOWER	BIR - ELGHANEM		1500	ANHYDRITE WITH THIN DOLOMITIC LIMESTONE BANDS
	TRIASSIC	UPPER	BUSHEBA		550	RED YELLOW SANDSTONE WITH RED CLAY
		MIDDLE	AZIZIA		750	MASSIVE LIMESTONE OCCASSIONALLY WITH SOME CLAY OR SHALE ALTERATIONS
			RAS HAMIA		950	MICACEOUS SANDSTONE OCCASSIONALLY WITH SOME SHALE STREAKS
		LOWER	OULED CHEBBI		320	
PALEOZOIC	PERMIAN				60	DARK GREEN, GREY SHALE
	CARBONIFEROUS	UPPER	HERCYNIAN UNCONFORMITY			FOSSILIFEROUS LIMESTONE
			DEMBABA		1700	
			ASSID DEFAR			SHALE OCCASSIONALLY SANDY. LIMESTONE
		LOWER	MRAR		1250	ALTERNATING SILTY MICACEOUS SHALE AND MICA. FINE GRAIN SANDSTONE OFTEN FERRUGINOUS
			TAHARA		200	
	DEVONIAN	MIDDLE - UPPER	AOUINAT OUENINE		900	INTERBEDDED VARICOLOURED SILTY SHALE MEDIUM GRAIN, YELLOW GREEN SANDSTONE
			OUAN KASA		800	SILTY SHALE WITH SOME SANDSTONE. CALCAREOUS BEDS AT THE BASE
		LOWER	TADRART		600	COMPOSED OF SANDSTONE OCCASSIONALLY FERRUGINOUS AT THE BASE. INTERBEDS WITH SOME SHALE STREAKS
			CALEDONIAN UNCONFORMITY			
	SILURIAN	MIDDLE	ACACUS	U	2100	SHALE ALTERNATING WITH SOME SANDSTONE INTERBEDS
				M		DOMINANTLY COMPOSED OF SHALES OCCASSIONALLY SOME MICRON SANDSTONE INTERBEDS.
				L		DOMINANTLY COMPOSED OF SANDSTONE WITH SHALE
		LOWER	TANEZZUFT		1600	MAINLY SHALE WITH SOME SANDSTONE BEDS ESPECIALLY AT THE TOP
	CAMBRO-ORDOVICIAN		MEMOUNIAT		800	MASSIVE SANDSTONE, COARSE AND KAOLINTIC WITH SILTY SHALE BANDS INTERCALATIONS AND BANDS OF SHALES
			MELEZ CHOGRANE		2880	ARGILLACEOUS SEQUENCE
			HAOUAZ			FINE AND QUARTZ SANDSTONE WITH SILTY MICACEOUS SHALE
			HASSOUNA			BROWN, YELLOWISH BROWN, MASSIVE MICACEOUS SANDSTONE WITH ABUNDANT CONGLOMERATE LENSES AT THE BASE
			MOURIZIDE			RED, VIOLET- QUARTZITIC SANDSTONE
PRECAMBRIAN						FOLDED METAMORPHIC ROCK

LEGEND

- LIMESTONE
- DOLOMITE
- DOLOMITIC LIMESTONE
- SANDSTONE
- SHALE
- SILTSTONE
- CONGLOMERATE
- GYPSUM
- ANHYDRITE
- CLAY
- MARL
- METAMORPHIC ROCK
- SHARP CONTACT
- UNCONFORMITY

SCALE

3000
2250
1500
750
375

FIGURE NO. 4

شركة الخليج العربي للنفط
ARABIAN GULF OIL COMPANY

GENERAL STRATIGRAPHIC COLUMN OF THE HAMADA BASIN

Date JULY'90	Author O ELFIGHI DR SHAH Modified by H Elwarfali	Drawn by JESS	Drwg No.

STRATIGRAPHIC SECTION OF TAHARA FORMATION IN THE TYPE WELL A8—NC7A

GEOCHRONOLOGY: ERA — PALEOZOIC; PERIOD — DEVONIAN/CARBONIFEROUS; EPOCH — LATE DEVONIAN/TOURNAISIAN; AGE — FAMENNIAN/HASTARIAN; FORMATION — TAHARA

FACIES: I, H

SUB-FACIES: F, B, D, F3, F1, C, F2, G, A, E

CORE-NUMBER: 1, 2, 3, 4, 5

CORE-INTERNAL: 5700′, 5706′, 5712′, 5718′, 5724′, 5730′, 5736′, 5742′, 5748′, 5754′, 5760′, 5766′, 5772′, 5778′, 5784′, 5790′, 5796′, 5802′, 5808′, 5814′, 5820′, 5826′, 5832′, 5838′, 5844′

LITHOLOGY

SEDIMENTARY STRUCTURES

GRAIN SIZE: CLAY, SILT, SAND (V. FINE, FINE, MEDIUM, COARSE); 0·0312, 0·0625, 0·125, 0·250, 0·500

PARA SEQUENCES

PERCENTAGE OF SAND PER METER OF CORE: 25 50 75

PERCENTAGE OF BIOTURBATION PER METER OF CORE: 25 50 75

THICKNESS OF SANDSTONE UNITS (CM): 2 4 8 16 32

ANGULARITY: ANGULAR, SUB-ANGULAR, SUB-ROUNDED, ROUNDED, WELL-ROUNDED

SORTING: P, M, G

ENVIRONMENT: SHELF MUD; OFF SHORE — TRANSITION (L M U); SHORE-FACE (L M U)

LEGEND

LITHOLOGY

- SHALE
- SILTSTONE
- SANDSTONE
- SAND/SHALE INTERLAMINATION
- OOLITIC IRONSTONE
- MUDSTONE

CONTRACTS

- SHARP - Planer
- TRANSITIONAL
- EROSITIONAL
- COARSENING UP PARASEQUENCE
- FINING UP PARASEQUENCE

SEDIMENTARY STRUCTURES

- HORIZONTAL BEDS
- GRADED BEDS ALTERNATING WITH MASSIVE UNITS OF SHALE
- HUMMOCKY X-STRATIFICATION
- WAVY BEDS
- BIOTURBATED BED WITH REMNANT STRATIFICATION
- BIOTURBATED BEDS

Increasing Intensity

- LOAD STRUCTURE
- VERTICAL BURROWS
- SIDERITIC CONCRETION
- SHELL FRAGMENTS
- FLASER BEDDING
- RIPPLE BEDDING
- LAG DEPOSITS
- GRADED BEDDING
- ESTIMATED GRAIN SIZE

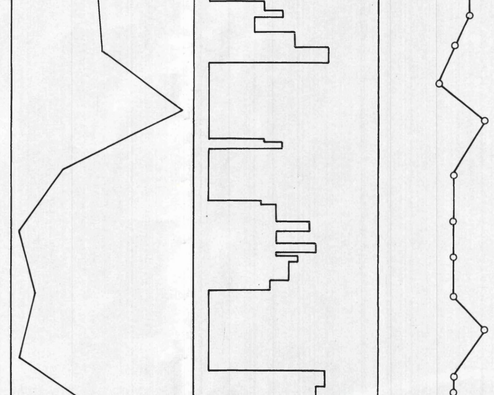

FACIES RELATIONSHIP DIAGRAM

(III)

STRATIGRAPHIC CROSS — SECTION

SW — NE

WELL A8-NC7A — 6·3 KM — WELL A12-NC7A — 27 KM — WELL A13-NC7A

DATUM: PARASEQUENCE SET BOUNDARY
(THE BASE OF THE MARAR SHALE)

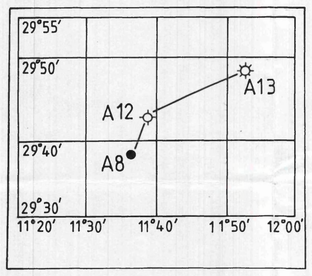

UNCORED INTERVAL

UNCORED INTERVAL

parasequence 14

parasequence 6

parasequence 1

VERTICAL SCALE 0 1 2 3 4m

HORIZONTAL SCALE ARBITRARY

LEGEND

A	SHALE SILTSTONE INTERLAMINATED FACIES	F	WAVY BEDDED FACIES		SANDSTONE
B	HUMMOCKY CROSS STRATIFIED SANDSTONE FACIES	G	OOLITIC IRONSTONE FACIES		SHALE
C	CHONDRITIC MUDSTONE FACIES	H	RIPPLE LAMINATED SANDSTONE FACIES		MUDSTONE
D	PARALLEL LAMINATED SANDSTONE FACIES	I	FOSSILEFEROUS SANDSTONE FACIES		OOLITIC IRONSTONE
E	SHALE SANDSTONE INTERLAMINATED FACIES		MISSING OR UNCORED INTERVAL		INTERFINGERING BOUNDARY
					CHANNEL

Ⓥ

CHRONOSTRATIGRAPHIC CROSS — SECTION

SW NE

A8 - NC7A 6·3 KM A12 - NC7A 27 KM A13 - NC7A

DATUM : PARASEQUENCE SET BOUNDARY
(THE BASE OF THE MARAR SHALE)

UNCORED INTERVAL

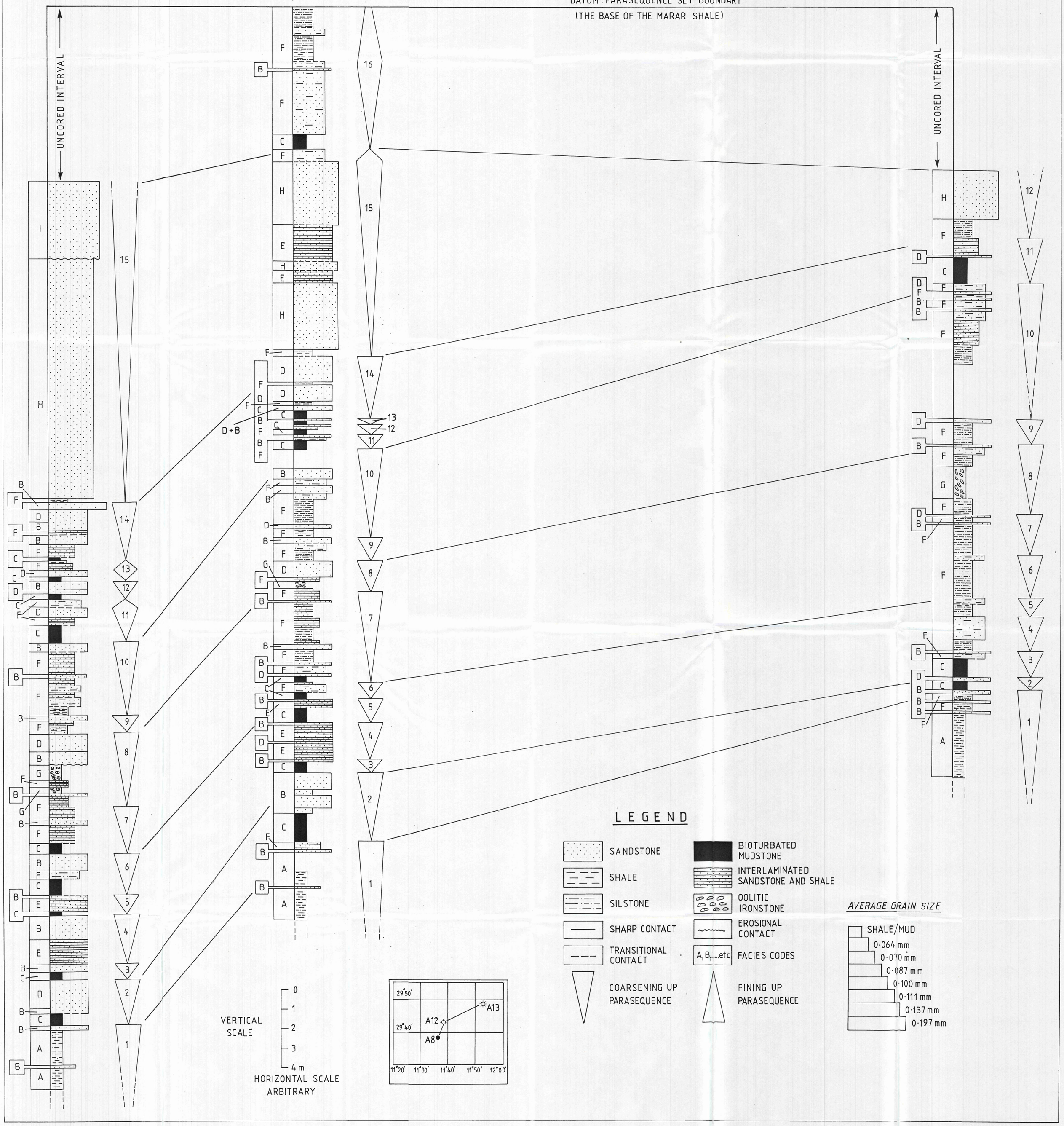

VERTICAL SCALE 0 1 2 3 4 m

HORIZONTAL SCALE ARBITRARY

LEGEND

- SANDSTONE
- SHALE
- SILTSTONE
- SHARP CONTACT
- TRANSITIONAL CONTACT
- COARSENING UP PARASEQUENCE
- BIOTURBATED MUDSTONE
- INTERLAMINATED SANDSTONE AND SHALE
- OOLITIC IRONSTONE
- EROSIONAL CONTACT
- A, B,....etc FACIES CODES
- FINING UP PARASEQUENCE

AVERAGE GRAIN SIZE

- SHALE/MUD
- 0·064 mm
- 0·070 mm
- 0·087 mm
- 0·100 mm
- 0·111 mm
- 0·137 mm
- 0·197 mm